COMPARATIVE BEHAVIOUR OF AN UNDISTURBED CLAY UNDER TRIAXIAL AND PLANE STRAIN CONDITIONS

by

Yoginder P. Vaid
B.Sc. Engineering, Panjab University, India, 1959
M.A.Sc., University of British Columbia, 1968

A THESIS SUBMITTED IN PARTIAL FULFILLMENT OF
THE REQUIREMENTS FOR THE DEGREE OF
DOCTOR OF PHILOSOPHY

in the Department
of
Civil Engineering

We accept this thesis as conforming to
the required standard

THE UNIVERSITY OF BRITISH COLUMBIA

April, 1971

In presenting this thesis in partial fulfilment of the requirements for an advanced degree at the University of British Columbia, I agree that the Library shall make it freely available for reference and study. I further agree that permission for extensive copying of this thesis for scholarly purposes may be granted by the Head of my Department or by his representatives. It is understood that copying or publication of this thesis for financial gain shall not be allowed without my written permission.

Department of Civil Engineering

The University of British Columbia
Vancouver 8, Canada

Date May 28, 1971

ABSTRACT

Many field problems in soils approximate plane strain conditions. Conventional laboratory practice, however, consistently uses triaxial compression testing for evaluating strength and deformation properties of soils. Possible differences between triaxial and plane strain behaviour of natural soils have so far received little attention.

New plane strain and K_o-triaxial apparatuses have been designed in which it is now possible to shear samples under various stress paths. A series of triaxial and plane strain tests were performed on identically K_o-consolidated samples of an undisturbed, sensitive, marine clay. Drained and undrained compression and extension tests under both increasing and decreasing stresses were carried out. Similar series of tests were also made on heavily overconsolidated specimens.

It is demonstrated that the use of triaxial test results where plane strain conditions prevail invariably leads to an overestimate of deformations and an

underestimate of strength. Methods to estimate strains in undrained plane strain shear from the results of triaxial tests under identical stress paths have been developed. Similarly, strains during drained plane strain shear of normally consolidated clay could be predicted from drained and undrained triaxial results, using an extended form of Rendulic's hypothesis.

TABLE OF CONTENTS

LIST OF FIGURES

LIST OF TABLES

LIST OF SYMBOLS

$\sigma_{x,y,z}$	Principal total stresses in x,y,z directions
$\sigma'_{x,y,z}$	Principal effective stresses in x,y,z directions
$\sigma'_{xc,yc,zc}$	Principal consolidation stresses in x,y,z directions.
$\sigma'_{1,2,3}$	Major, intermediate and minor principal effective stresses
σ_{oct}	Octahedral or mean principal total stress
p, σ'_{oct}	Mean principal effective stress
p_c	Mean principal consolidation stress
p_f	Mean principal effective stress at failure
p_e	Equivalent pressure
q	Deviator stress, $(\sigma_1-\sigma_3)$
τ_{oct}	Octahedral shear stress
$\Delta\tau_{oct}$	Cummulative change in octahedral component of shear stress
σ'_{1c},σ'_{zc}	Major principal consolidation stress
Δu	Change in pore pressure
$\Delta p'$	Increment of pressure in lateral fluid system
C_u	Undrained strength, $(\sigma_1-\sigma_3)_{max}/2$
$\varepsilon_{x,y,z}$	Principal strains in x,y,z directions
$\varepsilon_{1,2,3}$	Major, intermediate and minor principal strains
γ_{oct}	Octahedral shear strain
V	Volume of sample

v	Volumetric strain, $\Delta V/V$
ϕ'	Angle of shearing resistance
c'	Cohesion
c	Compliance of lateral fluid pressure system
M, α	Stress ratio, q/p at failure
η^*	Stress ratio, $\sqrt{3}\ \tau_{oct}/p$
η'	Stress ratio, $(\sigma_1-\sigma_3)/(\sigma_1+\sigma_3)$
η_T, η_p	Compliance factors
b	Stress ratio, $(\sigma_2-\sigma_3)/(\sigma_1-\sigma_3)$
K_o	Ratio of lateral to vertical effective stress during one dimensional consolidation
m_v	Compressibility with respect to mean principal effective stress
e	Void ratio
λ	Slope of virgin K_o-consolidation line
κ	Slope of isotropic swelling line
a	Henkel pore pressure parameter
A_f	Skempton pore pressure parameter at failure

ACKNOWLEDGEMENTS

Financial support for the investigations reported in this thesis was provided by The National Research Council of Canada and the University of British Columbia. Grateful acknowledgement is expressed for this support.

The author wishes to thank his research supervisor, Dr. R. G. Campanella, for his guidance, encouragement and advice. He would also like to thank Dr. W. D. Liam Finn for his interest and encouragement and Dr. P. M. Byrne for many helpful discussions.

The technical assistance of the staff of the civil engineering workshop in fabricating the testing equipments is gratefully acknowledged.

CHAPTER I

INTRODUCTION

In the design of foundations and earth structures the problems of greatest concern are deformation and stability. Soil parameters needed to tackle these problems are generally derived from the conventional triaxial compression test. The stress and strain conditions of this triaxial test, however, rarely prevail in practical problems. Even in the case of loading a circular footing, triaxial conditions arise only at points on the central axis beneath the footing. In contrast to this, there are many field problems in which conditions approximate those of plane strain. Soil problems relating to retaining walls, strip footings, slopes, embankments, long excavations etc. are familiar examples of the plane strain condition. When confronted with these practical problems, it is almost invariably found that the only data available on the properties of soil have been obtained from the triaxial compression test. Because of the scarcity of information concerning the behaviour of soils under plane strain conditions, the possible difference between the triaxial and

the plane strain stress conditions is usually neglected. This can hardly be justified since there is insufficient experimental evidence, particularly for clays, which shows that there are no important differences in soil behaviour under plane strain and triaxial stress systems. Very little has been done to properly correlate data from different types of tests in the triaxial and the plane strain apparatuses. It is clear that there is a great need for such a correlation if soil parameters derived from the triaxial tests are to be used to solve field problems approximating plane strain conditions.

Many apparent anomalies and differences may arise when an attempt is made to determine practical soil parameters from tests in different types of apparatuses, and even for different types of tests in the same apparatus. For a given consolidation history, the stress-strain and the strength behaviour of clays is known to depend on the manner in which stresses are changed to induce failure. The condition of no lateral strain during consolidation (K_o-consolidation) is often the starting point for most deformation problems of natural sedimentary deposits. The mechanical behaviour of these clays, in particular, is very sensitive to the variation of total stress path to failure (Henkel & Sowa, 1963; Ladd & Bailey, 1964;

Ladd, 1965; Henkel, 1970). The nature of this variation is likely to be a function of the overconsolidation ratio which directly affects the K_o value (the ratio between horizontal and vertical effective stresses during one-dimensional consolidation) in the deposit. In view of the importance of this problem in the field, it is essential that shear behaviour of K_o-consolidated clays be properly correlated from different types of tests in the same apparatus. No comprehensive study in this direction has so far been reported even under triaxial conditions. Comparison between plane strain and triaxial conditions under similar total stress paths to failure has rarely been attempted. Lambe (1964, 1967), in his stress path method, emphasises the great need for obtaining soil parameters from tests in which the consolidation history and subsequent stress changes duplicate those anticipated in the field.

At present, the idealised stress-strain theories for clay materials (e.g. the Cambridge theory: Roscoe & Burland, 1968) are not sufficiently advanced to enable prediction of strains in natural clays under a variety of stress paths and stress systems. Non-linear and path dependent stress-strain relationships, however, are finding increased use with advanced numerical techniques, like the finite element method, for solving deformation problems

in the field (Clough & Woodward, 1967; Mitchell, 1969). Most of the laboratories usually do not have access to the more complicated plane strain apparatus. Therefore, if it is possible to correlate data from the triaxial and the plane strain tests under similar stress paths, the easily executable triaxial test could be used to estimate soil behaviour under plane strain conditions. For plane deformation analysis by finite elements, stress-strain relationships would be needed under stress paths likely to be anticipated in the given field problem.

In this thesis the development of two pieces of apparatuses is described: a plane strain and a K_o-triaxial apparatus. In these apparatuses similar series of tests were performed on a saturated undisturbed clay using "identical end of one-dimensional consolidation conditions" and, following a variety of stress paths to failure. In Fig. 1.1, x,y,z axes denote the fixed directions of principal axes within the triaxial and the plane strain specimens. In both the apparatuses it was possible to follow any desired stress path to failure in the stress plane σ_z vs. σ_x. The stress paths actually studied consisted of both compression and extension modes of failure, with either increasing or decreasing one of these two stresses σ_x and σ_z, while the other was held constant. In this manner, four different stress paths were obtained. If z-direction is

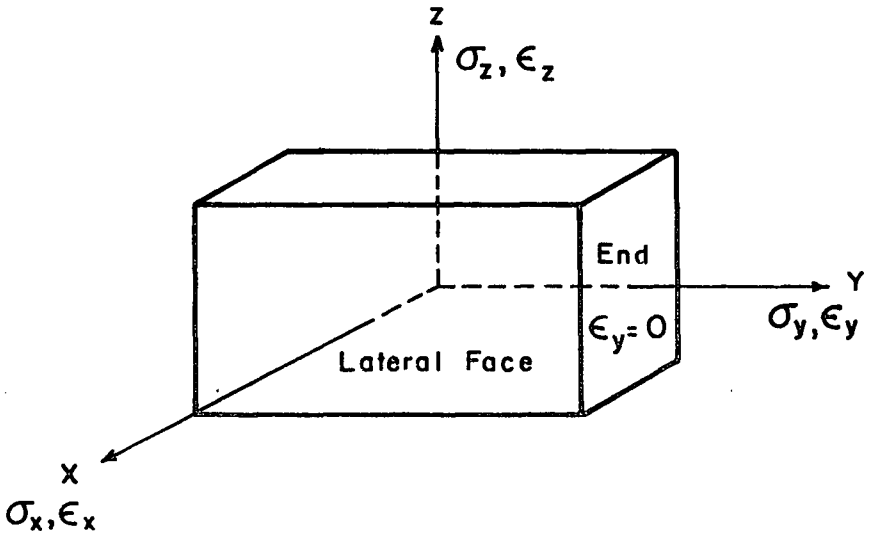

(a) Plane Strain Sample.

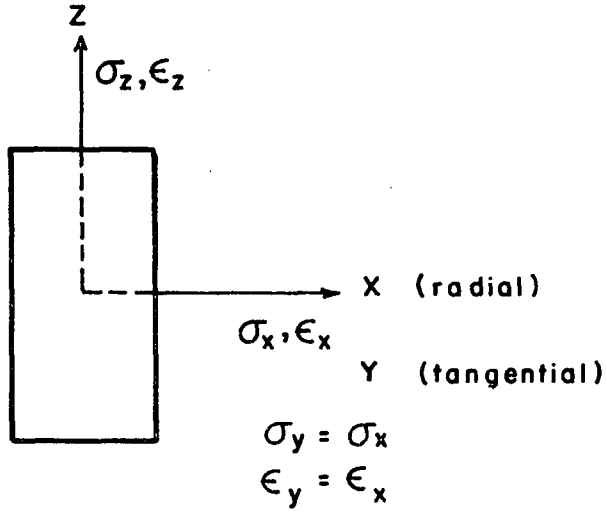

(b) Triaxial Sample.

Fig. 1·1 FIXED PRINCIPAL STRESS DIRECTIONS IN PLANE STRAIN AND TRIAXIAL SAMPLES.

taken to coincide with the axis of the specimen, these stress paths are:

1. Passive compression: σ_z increased, σ_x held constant
2. Active compression: σ_x decreased, σ_z held constant
3. Passive extension: σ_x increased, σ_z held constant
4. Active extension: σ_z decreased, σ_x held constant

For each of these stress paths consolidated undrained and drained tests were performed. Each type of test was made both under plane strain and triaxial stress conditions. The effect of consolidation history was studied by carrying out two series of tests - in the first series normal consolidation and in the second series heavy overconsolidation was used as the preshear condition.

Correlation of soil parameters has been attempted from different stress paths in the same test apparatus. Also a comparison and correlation of stress-strain-strength characteristics has been made for similar stress paths under plane strain and triaxial conditions. Estimation of soil parameters under plane strain conditions from results in the triaxial tests is then indicated.

CHAPTER II

LITERATURE REVIEW

There is a very limited amount of test data reported for clay materials which were consolidated under K_o-condition and in which subsequent stress changes corresponded to plane strain (Henkel and Wade, 1966; Duncan and Seed, 1966a; Hambly and Roscoe, 1969; Dickey et. al., 1968). The influence of varying the total stress path to failure on stress-strain-strength behaviour has generally been ignored not only under plane strain but also for the triaxial stress conditions. In particular, no information seems to exist on stress-strain-strength characteristics of heavily K_o-overconsolidated clays.

The following literature review will be considered under two separate sections. Under the first section are described studies, under the triaxial conditions, on the stress-strain-strength response of K_o-consolidated clays, and the influence of varying the total stress path to failure on this response. The second section deals with similar studies under plane strain conditions, along with comparison between plane strain and triaxial results wherever attempted.

2.1 Shear behaviour of K_o-consolidated clays under stress conditions of the triaxial test.

In all triaxial tests, including the K_o-triaxial, the directions of principal axes are fixed. Although an infinite variety of stress paths in σ_z vs. σ_x plane (see Fig. 1.1) can be followed during shear, the resulting strains give rise to either an axial compression or axial extension failure. The direction of major principal stress at failure, relative to its direction at the end of K_o-normal consolidation, remains unaltered in axial compression shear, whereas it is reoriented through 90° in axial extension shear. The reverse situation holds for heavily K_o-overconsolidated specimens, because the radial stress, σ_x, exceeds the vertical stress, σ_z, at the end of rebound or overconsolidation. Therefore, the stress system of the K_o-triaxial test permits study of strength mobilization under conditions of axial compression and extension with no reorientation or with 90° reorientation of principal stresses.

Hansen and Gibson (1949) showed that the undrained strength of K_o-consolidated clays having the same history of consolidation depends on the direction of the major principal stress at failure in relation to the direction

of major principal stress at consolidation. Assuming isotropy of effective strength parameters, c' and ϕ', and Skempton-pore pressure parameter, A_f, they showed that the undrained strength would be least for passive extension and maximum for active compression. This variation results from the fact that the changes in pore pressures, and thus the values of the undrained strength, depends on the degree of reorientation of the principal stresses which, in turn, depends on the orientation of the failure plane. c', ϕ' and A_f, however, are unlikely to be isotropic for most clays.

Many investigators have demonstrated the variation of undrained strength with orientation of the failure plane, by performing unconsolidated-undrained, (UU), triaxial tests on specimens trimmed with their axes at different angles to the plane on which major principal stress acted during one-dimensional consolidation (Ward, 1956; Ward et. al., 1959; Hvorslev, 1960; Lo, 1965; Bishop, 1966; Duncan & Seed, 1966; Lo & Milligan, 1967; Conlon et. al., 1970). Such specimens, however, differed from an element in the field in that the anisotropic stress system under which the specimens were consolidated had been released during sampling and replaced by an isotropic stress system sufficient to maintain constant volume. It has,

however, been shown (Skempton & Sowa, 1963; Ladd & Lambe, 1963; Noorany and Seed, 1965) that the undrained strength of a triaxial specimen from which the consolidation deviator stress has been unloaded without change in water content is almost equal to the undrained strength of an identical specimen tested with no release of the consolidation deviator stress (i.e. in-situ specimen), provided the direction of compressive strain to failure is the same in both cases. The strains resulting from the unloading of consolidation deviator stress are generally very small and cause little alteration in microstructure, which seems to be the reason for the two specimens giving the same undrained strength. In view of the foregoing observation, it seems likely that the nature of variation of undrained strength with orientation of failure plane, as determined from UU tests, would be similar to the in-situ strength for all orientations of the failure plane. For initially normally K_o-consolidated clays in which the major consolidation stress had acted in the vertical direction, UU strength of vertical specimen was found to be the greatest and the lowest UU strength was associated with failure plane oriented horizontally. Heavily overconsolidated clays (Ward et. al.), on the other hand, had horizontal specimens the strongest and vertical specimens the weakest.

Ladd and Bailey (1964) and Ladd (1964, 65, 67) performed undrained compression and extension tests on normally K_o-consolidated specimens of undisturbed Kawasaki and remolded Boston blue clays. For identical specimens, C_u/σ'_{1c} in extension was found to be approximately half of the value in compression for both types of clays. At maximum obliquity Kawasaki clay had a Coulomb ϕ' of 40° and 52° in axial compression and extension respectively. The corresponding values for Boston blue clay were 26° and 38°. Axial strain at failure in compression was generally less than 1/2% compared to more than 6% in extension. Axial compression and extension tests on Manglerud clay by Bjerrum and Kenny (1967) show similar differences in undrained strength of identical specimens. No data was given regarding ϕ' in compression and extension.

A correlation of drained and undrained conventional axial compression tests (cell pressure = constant) on 5 undisturbed Norwegian clays was done by Simons (1963). The same Coulomb ϕ' was found for both types of tests on initially K_o-consolidated specimens, provided $(\sigma'_1/\sigma'_3)_{max}$ was used for the failure condition. Bjerrum and Landva (1966) made similar conclusions for another Norwegian quick clay. Undrained ϕ' was in all cases less than drained ϕ' if maximum deviator stress was used as the failure

condition. This characteristic is typical of all sensitive clays.

Lewin and Burland (1970) performed a series of drained triaxial tests on anisotropically normally consolidated remolded slate dust, in order to demonstrate the dependence of strains on the direction of stress increment vector. The stress increment defined by $(\Delta\sigma_1'^2 + 2\Delta\sigma_3'^2)^{\frac{1}{2}}$ = constant, was imposed on identical samples which were consolidated to approximately K_o-condition. Both shear and volumetric strains were found to be the largest for the direction of stress increment vector corresponding to the greatest increase in deviator stress, $\sigma_1' - \sigma_3'$. For those directions of the stress increment vector which corresponded to the unloading of the consolidation deviator stress, both shear and volumetric strains were found to be practically insignificant. The size of the increment used was 5% of the length of the basic stress state vector, $(\sigma_1'^2 + 2\sigma_3'^2)^{\frac{1}{2}}$. These results, which were first of their kind, clearly demonstrated the dependence of strains on the applied stress path. The feature of particular interest was the extremely small strains associated with extension stress paths, when compared to those during compression stress paths. No information was presented on the failure conditions under the stress paths studied.

On the basis of the foregoing very limited data the following observations can be made regarding the behaviour of K_o-consolidated clays:

1. They are anisotropic with respect to their undrained strength. This variation of undrained strength may result from anisotropy with respect to the values of the effective strength parameters or anisotropy with respect to development of changes in pore pressure, or both; it may also result from reorientation of the principal stress directions.

2. In conventional triaxial compression the same effective strength parameters are reported for both undrained and drained shear using $(\sigma_1'/\sigma_3')_{max}$ as the failure condition.

3. ϕ' in undrained extension has been reported to be as much as 12° larger than the value during undrained compression.

4. Strains under drained conditions depend very much on the magnitude and the direction of the stress increment in the triaxial stress plane.

5. No information whatsoever is available on heavily overconsolidated clays when tested under the triaxial stress system. UU tests on these clays (with consolidation deviator stress removed), however, show that

the nature of anisotropy of undrained strength (horizontal samples strongest) is different from the type of anisotropy encountered in initially normally consolidated clays (vertical samples strongest).

6. Drained failure conditions in axial extension and active compression have not been studied. Consequently, no correlation of the different types of tests possible in the triaxial apparatus has been made.

2.2 Shear behaviour of K_o-consolidated clays under plane strain conditions.

Most plane strain equipments utilize rectangular test specimens. Consequently, directions of the principal stresses remain fixed as in the case of K_o-triaxial tests. Hence again, only axial compression or extension types of tests are possible. However, an infinite variety of stress paths in the plane normal to the direction of zero strain, i.e., σ_z, σ_x stress plane, can be followed to induce compression or extension failure.

Henkel and Wade (1966) reported comparison of undrained triaxial and plane strain passive compression tests on normally K_o-consolidated remolded Weald clay. It was shown that C_u/σ'_{1c} ratio in plane strain was about 8% higher when compared to the K_o-triaxial value. Axial

strain to failure in plane strain was 2% compared to 6% under K_o-triaxial conditions. However, at maximum obliquity, $(\sigma_1'/\sigma_3')_{max}$, Coulomb ϕ' was higher by only 1.2° in plane strain than the triaxial value. Effective stress paths in the two tests were uniquely defined in terms of octahedral stresses — the octahedral normal effective stress, σ'_{oct}, (This is also known as the mean normal effective stress and denoted by symbol p) and octahedral shear stress, τ_{oct}. In terms of principal stresses, σ_1, σ_2, σ_3, octahedral stresses are expressed as

$$\sigma'_{oct} = p = 1/3\ (\sigma_1' + \sigma_2' + \sigma_3') \tag{2.1}$$

$$\sigma_{oct} = 1/3\ (\sigma_1 + \sigma_2 + \sigma_3) \tag{2.2}$$

$$\tau_{oct} = 1/3 \sqrt{(\sigma_1-\sigma_2)^2 + (\sigma_2-\sigma_3)^2 + (\sigma_3-\sigma_1)^2} \tag{2.3}$$

The change in pore pressure, Δu, was shown to be controlled essentially by the changes in octahedral total normal stress, $\Delta\sigma_{oct}$, and octahedral shear stress, $\Delta\tau_{oct}$; i.e.

$$\Delta u = \Delta\sigma_{oct} + a\ \Delta\tau_{oct} \tag{2.4}$$

where

'a' is the Henkel pore pressure parameter. The value of the principal stress associated with zero strain direction was found to be intermediate between the other two principal effective stresses, and the ratio $\sigma_2'/(\sigma_1'+\sigma_3')$ stayed essentially constant during undrained shear. Ladanyi (1967) in discussion to Henkel and Wade's paper argued that part of the observed difference in strength and stress-strain behaviour in the two types of compression tests could be explained by using alternate stress-strain parameters. It was suggested that there might be a unique octahedral shear stress-strain (τ_{oct} vs. γ_{oct}) relationship, similar to the one in ductile materials which yield according to the von Mises yield condition. Octahedral shear strain, γ_{oct}, is defined in terms of principal strains ε_1, ε_2, ε_3 as

$$\gamma_{oct} = \frac{1}{3}\sqrt{(\varepsilon_1-\varepsilon_2)^2 + (\varepsilon_2-\varepsilon_3)^2 + (\varepsilon_3-\varepsilon_1)^2} \qquad (2.5)$$

Comparative triaxial and plane strain undrained compression tests, similar to those of Henkel and Wade, were reported by Shibata and Karube (1967) on remolded Osaka clay. Shibata and Karube also concluded that the undrained effective stress paths were essentially unique

in terms of octahedral stresses. At failure $(\sigma_1'/\sigma_3')_{max}$, however, the value of Coulomb ϕ' in plane strain was 39° to 47° when compared to ϕ' value of 35° to 38° under triaxial conditions.

Undrained plane strain axial compression and extension tests were performed by Duncan and Seed (1966) on undisturbed San Francisco Bay Mud. Similar tests were also reported by Dickey et. al. (1968) on samples of Boston Blue Clay. For identical end of K_o-consolidation condition both these clays showed undrained strength $((\sigma_1-\sigma_3)_{max}/2)$ in extension to be only 75% of the compression value. In Boston Blue Clay, peak deviator stress in compression was reached at 1.5% axial strain compared to 7% axial strain in extension. The corresponding values for Bay Mud were 3.5% and 10% respectively. At $(\sigma_1-\sigma_3)_{max}$, ϕ' for Boston Blue Clay was found to be 30° and 42° respectively in axial compression and extension shear. The corresponding values at $(\sigma_1'/\sigma_3')_{max}$ were 34° and 42°. For Bay Mud ϕ' value using $(\sigma_1-\sigma_3)_{max}$ or $(\sigma_1'/\sigma_3')_{max}$ as the failure condition was essentially the same and amounted to 38° in compression against 35° in extension.

Hambly and Roscoe (1969) performed a series of plane strain tests on K_o-consolidated specimens of remolded Kaoline. Drained and undrained tests were made using a

variety of stress paths to induce compression or extension failure. They too, found that extension undrained strength was slightly less than 2/3 of the compression value. However, ϕ' was found to be the same, irrespective of the stress path to failure, and equalled the value obtained from triaxial tests on the same clay. This seems to be in contradiction with all the previously quoted results. One rather surprising feature of the drained extension tests involving large unloading of the mean normal stress was, that there was no volume expansion at any stage of the test. Also irrespective of the stress path, $\sigma_y'/(\sigma_x' + \sigma_z')$ was found to be essentially constant during the test.

From the foregoing very limited data the following observations can be made regarding plane strain behaviour of clays:

1. No information exists on heavily K_o-over-consolidated specimens.

For K_o-normally consolidated samples,

2. Undrained strength in extension was about 66% to 75% of the compression value. Extension failure strain was 3 to 5 times larger than the strain required to compression failure.

3. Conclusions regarding the variations of Coulomb ϕ' are contradictory. Extension ϕ' was shown to be either larger by up to 12°, or smaller by 3°, or even equal to compression ϕ' according to the results of different investigators.

4. The ratio of the effective principal stress corresponding to the direction of zero strain to the sum of the other two principal effective stresses, stayed essentially constant during plane strain shear tests. The relationship was found to hold independent of the applied stress path.

The extremely limited data on comparison of triaxial and plane strain behaviour of normally K_o-consolidated clays showed that:

1. In undrained compression tests common effective stress paths were followed in terms of octahedral normal and shear stresses. Pore pressure changes were essentially controlled by changes in total octahedral normal and shear stresses.

2. Conflicting results existed on the relative values of ϕ' under triaxial and plane strain conditions. Plane strain compression ϕ' was shown to be larger by 1.2° to 9° or even equal to the triaxial ϕ' according to the results of different investigators. Results of only one

investigator showed extension ϕ' to be 4° larger in plane strain than the triaxial value (Ladd, 1967).

In view of the above mentioned limited and often contradictory data, this thesis is an attempt to study and compare the triaxial and plane strain behaviour of clays. The comparison is attempted under a number of applied stress paths, on both initially normally consolidated and heavily overconsolidated specimens. An understanding of the plane strain shear behaviour of clays is extremely important from the viewpoint of field application. In particular, correlation of the triaxial behaviour with the one under plane strain conditions would permit estimation of latter from the easily executable triaxial tests.

Most of the research summarized earlier in this chapter was done on remolded clays. In this study a natural, undisturbed, moderately sensitive clay was chosen, instead. In view of the important structural differences between remolded and natural clays, the conclusion derived from tests on remolded clays may not strictly hold for natural clays. This apparently was the reason for choosing a natural clay for the study reported herein.

CHAPTER III

THE APPARATUSES

3.1.0 Plane Strain Apparatus

Mark-I version of the plane strain apparatus has been described by Vaid (1968). Various modifications were proposed therin to be incorporated in the future design. In the following paragraphs only the general principle of the apparatus and the improvements made in Mark-I are described.

3.1.1 General Principle

The apparatus was designed to enable consolidation under K_o-condition and subsequent shear under plane strain condition. The rectangular specimen of soil is initially 4" long, 1" wide and 2¼" high. Fig. 1.1 defined the orientation of the plane strain specimen in relation to the reference cartesian co-ordinate system. Throughout this thesis the subscripts x,y,z will denote the fixed directions of the principal axes within the test specimen. When referring to principal stresses, or strains, the Arabic subscripts 1,2,3 will be used to

denote major, intermediate, and minor values of these quantities respectively. Vertical stress, σ_z, was transmitted to the specimen through a rigid loading cap, whereas flexible water filled rubber diaphrams sealed on stiff backing plates were employed to furnish the lateral principal stress, σ_x. The condition of zero strain in the longitudinal direction, y, was satisfied by confining the specimen length between a pair of rigid 'frictionless' end plates. The lateral pressure diaphrams and the rigid end plates were positioned around the specimen by clamping them together. An exploded view of the apparatus is shown in Fig. 3.1.

During K_o-consolidation the sample was prevented from experiencing any strain in the y-direction by the presence of rigid end plates and, in the x-direction by maintaining a constant volume of water in the lateral pressure diaphrams. The compliance of the lateral pressure diaphrams was small and did not seriously affect the K_o-value. The effect of magnitude of compliance on the measured K_o-value will be discussed later in this chapter.

3.1.2 Lateral Pressure Diaphrams

These diaphrams consisted of shallow, box shaped, water filled, thin rubber membranes sealed by rubber

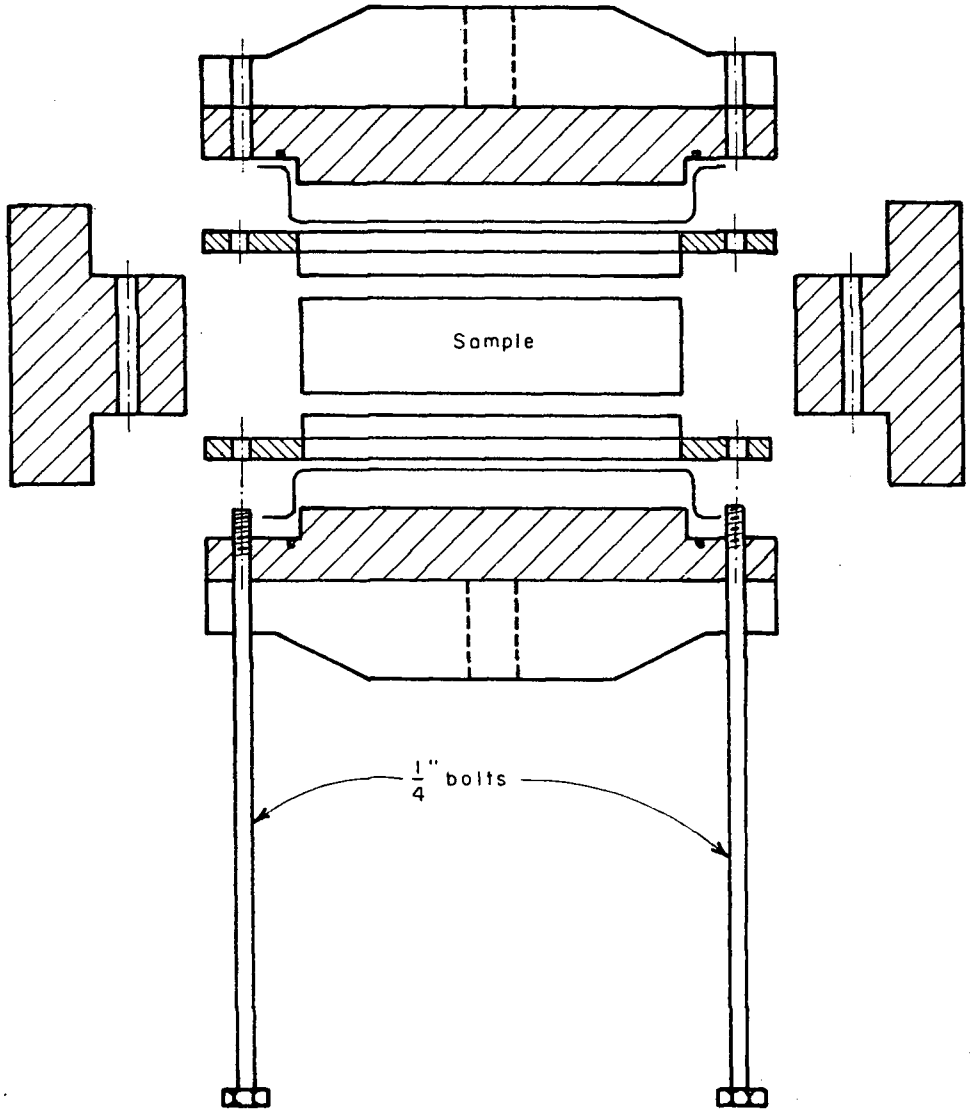

A - A

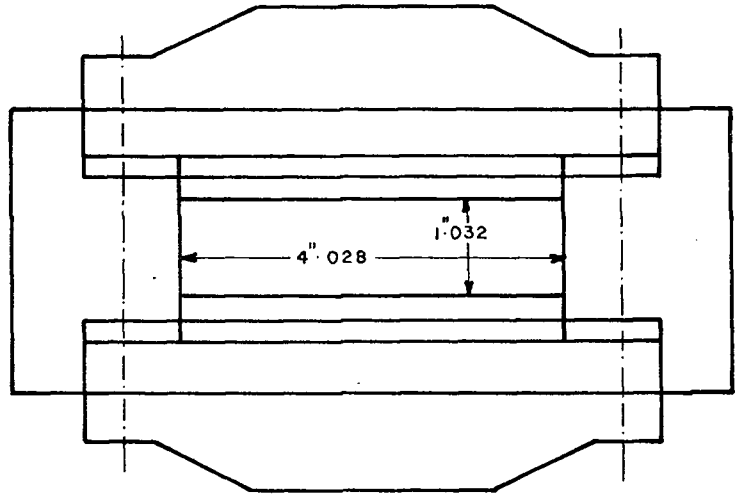

LATERAL PRESSURE DIAPHRAGMS AND END PLATES ASSEMBLY.

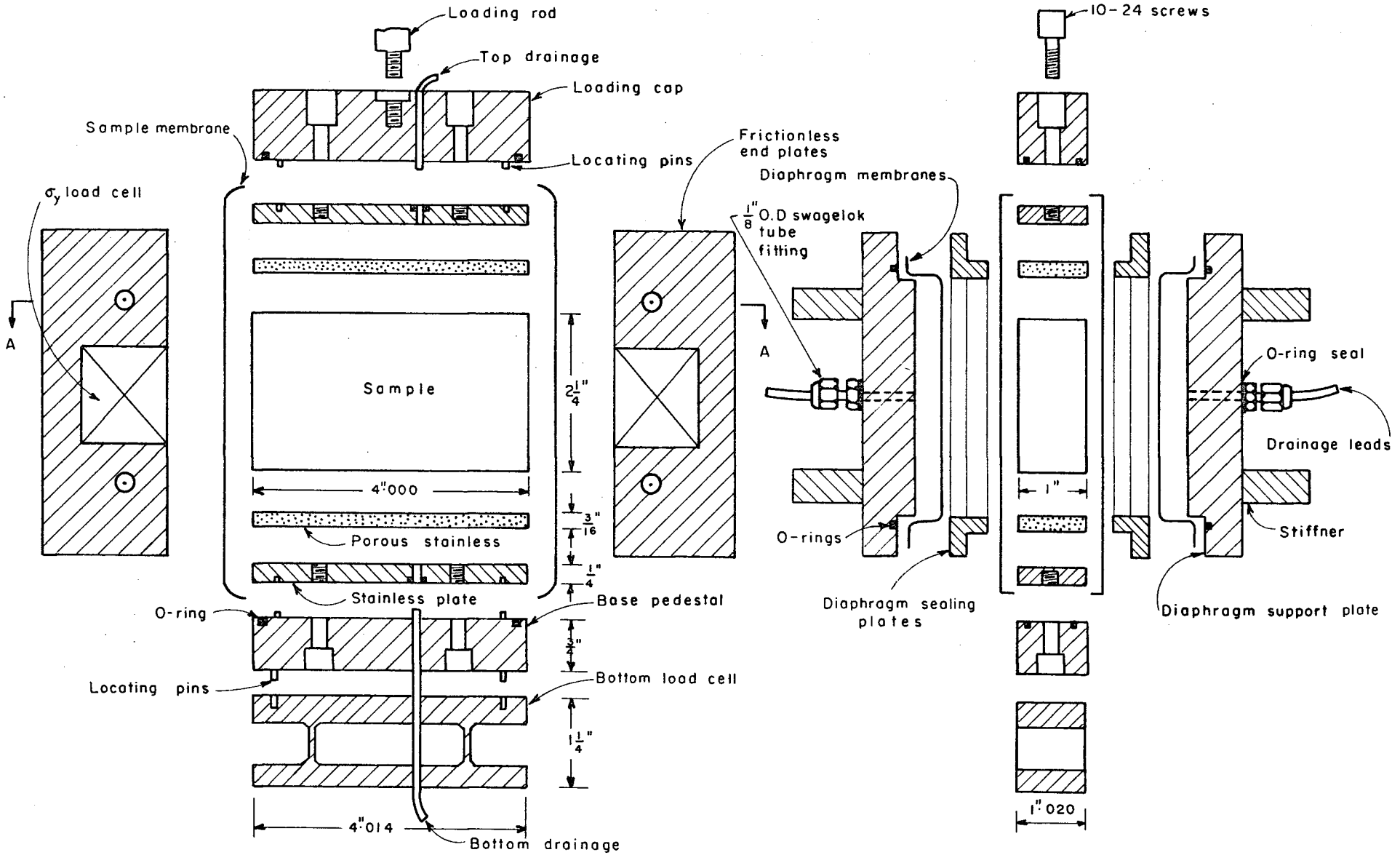

Fig.3·1 EXPLODED VIEW OF THE PLANE STRAIN APPARATUS.

O-rings on the faces of backing plates (Fig. 3.1). The backing plates were made out of 3/4" thick stainless, instead of perspex used in the earlier Mark-I, and were stiffened as before to keep the compliance of the lateral fluid pressure system to a minimum.

3.1.3 'Frictionless' End Plates

These plates were made out of aluminum instead of perspex used in the earlier Mark-I. The faces in contact with the specimen were highly polished. When assembling around the specimen, a thin layer of silicone grease was applied to this polished surface to keep the frictional drag between the sample and the plate to a minimum. These plates were instrumented with column type strain gaged aluminum load cells in order to measure the principal stress, σ_y (see Fig. 3.1). The area over which σ_y was measured amounted to at least 60% of the area of the specimen end at any time during the test.

3.1.4 Measurement of Side Friction

During the deformation of the specimen in the vertical direction, part of the vertical load is transferred through side friction to the rigid end plates and the lateral pressure diaphragms. The magnitude of this

frictional drag would depend on the effectiveness of lubrication between the moving and the stationary boundaries, and also on the intensity of normal pressure between them. Silicone grease was used as lubricant to keep the friction to a minimum value. In order to have a direct measure of the side friction, the base pedestal of the specimen was instrumented with an aluminum load cell (similar to those used to measure σ_y) which registered the vertical load transferred at the bottom of the specimen. With the knowledge of the load applied at the top and that transferred to the bottom a procedure was developed (Appendix A) to determine an average value of vertical stress, σ_z, which corrected for side friction effects.

3.2.0 K_o-Triaxial Apparatus

Details of the K_o-triaxial apparatus have been described elsewhere (Campanella & Vaid, 1971). Only a brief description of its important features is presented herein. Fig. 3.2 shows the apparatus with all essential details.

The apparatus is essentially a conventional triaxial cell with the difference that the area of the loading plunger is exactly equal to that of the soil specimen and, that stainless steel was used to build all

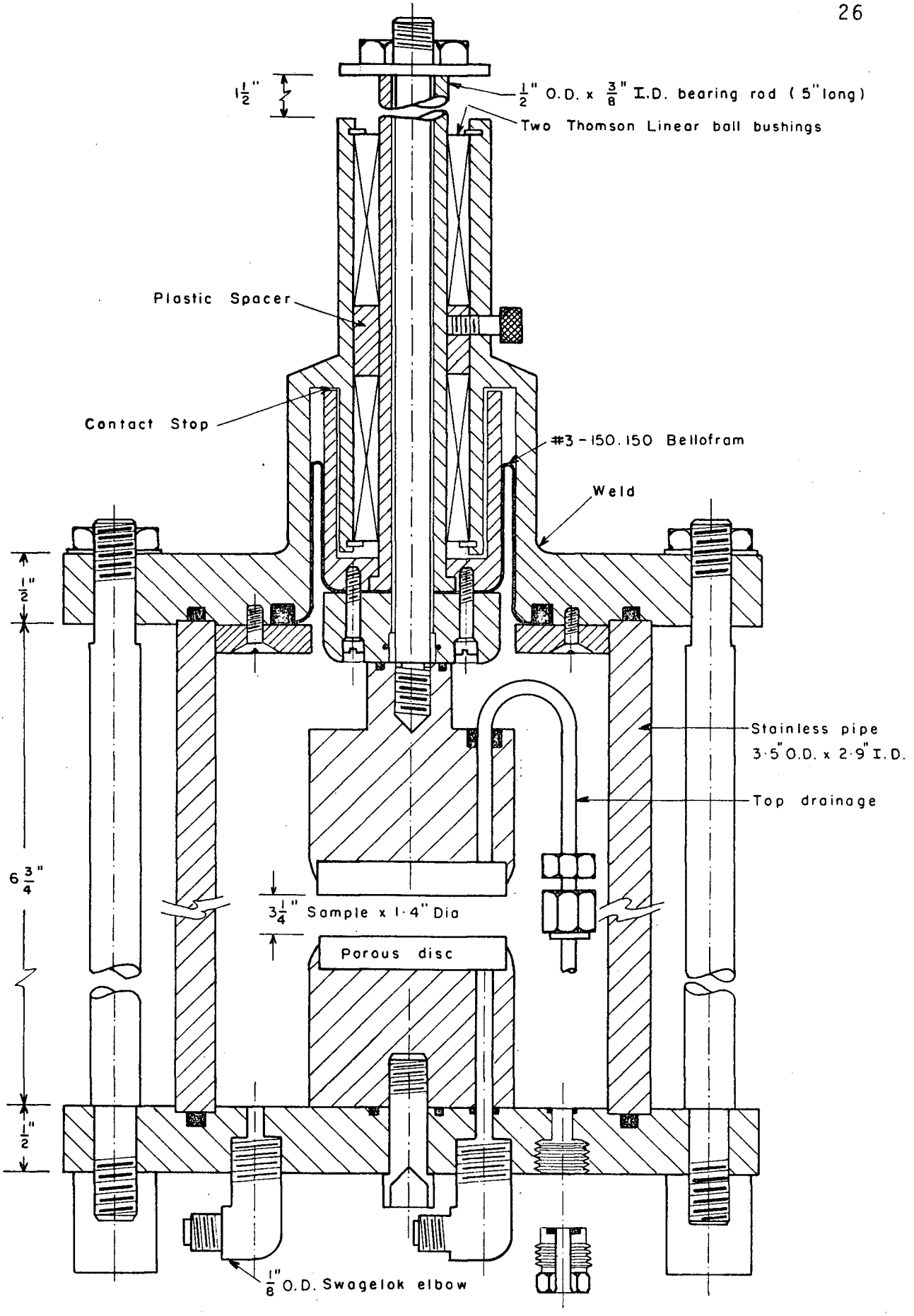

Fig. 3·2 k_o - TRIAXIAL APPARATUS.

its components. The loading plunger is guided in its vertical motion by a pair of linear Thompson Ball Bushings and is sealed to the head of the triaxial cell by a flexible rolling diaphram (see Fig. 3.2). In this manner a frictionless seal is obtained and the axial load measured outside this cell is precisely equal to that transferred to the soil specimen. Thus, a very undesirable characteristic of the conventional triaxial cells was eliminated. The thick stainless cylinder was used in order to keep the compliance of the cell to a minimum value. Thus when specimens were K_o-consolidated by shutting off the drainage lead to the cell, a condition of zero lateral strain was obtained due to the fact that the volume of water expelled from the specimen matched exactly with the volume of plunger moving in.

The cell, in fact, is suited to make both isotropically consolidated or K_o-consolidated triaxial tests. For isotropic consolidation the specimen cap is not screwed to the loading plunger. A very notable feature of the cell is the possibility it offers to make high pressure tests. The maximum cell pressure which can be used at present is about 500 psi, which happens to be the burst pressure for the type of rolling diaphram seal used.

3.3.0 Loading Equipment

A schematic layout of the loading system along with pressure and volume change measuring devices is shown in Fig. 3.3. The vertical load was applied by a rolling diaphram piston which was fully saturated with water on both sides. Each side of this piston was connected by means of 1/8" O.D. copper tubes to small water reservoirs through which air pressure could be applied, and also to a displacement plunger actuated by a constant rate strain drive. The lateral pressure system was similarly connected to an air pressure supply and to the same displacement plunger.

It was possible to perform all shear tests either under stress controlled or strain controlled loading. For stress controlled loading a particular stress was increased or decreased in discrete steps until failure under the chosen stress path occurred. This type of shear loading is unsuited to obtain post peak stress-strain behaviour of the soil. This may be a serious disadvantage particularly in case of sensitive soils which show maximum obliquity after the peak deviator stress is reached in consolidated undrained tests. Strength parameters with respect to effective stresses in such soils are found identical in C-U and C-D tests, provided maximum obliquity

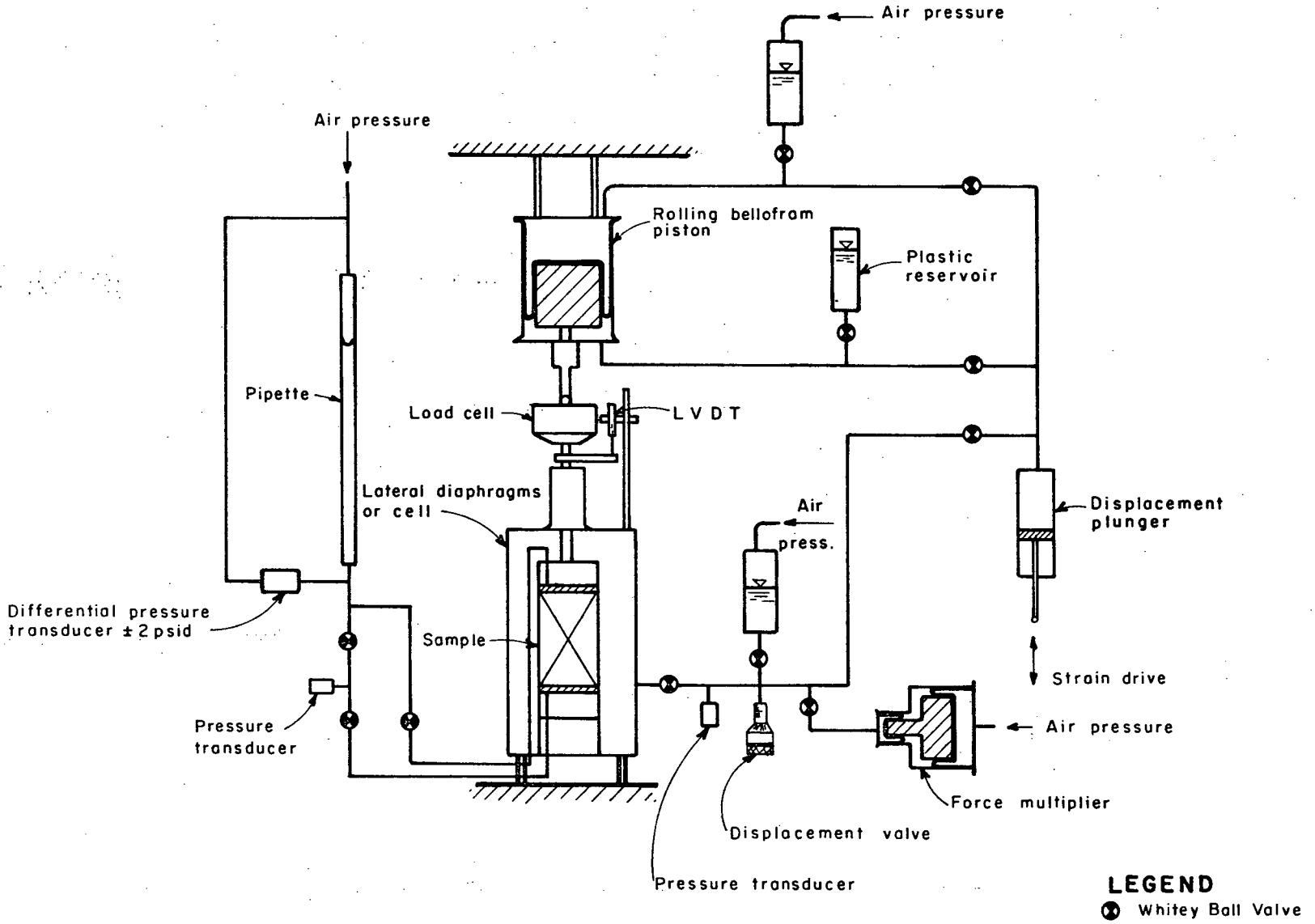

Fig.3·3 SCHEMATIC LAYOUT OF LOADING, DISPLACEMENT, VOLUME CHANGE AND PRESSURE MEASURING SYSTEM.

is used as the failure criterion. Stress controlled C-U tests, therefore, cannot be substituted for time consuming C-D tests to obtain drained strength parameters needed for long-term stability analyses.

Strain controlled tests could be made by displacing water at a constant rate into the loading piston or into or out of the lateral pressure system. Displacement of water at a constant rate was achieved with the strain drive moving the displacement plunger at a constant rate. For example, strain controlled axial compression tests with increasing σ_z could be made by the constant rate of water displacement into the top of the loading piston. Similar tests with decreasing σ_x could be made by removing water from the lateral pressure system at a constant rate. Similarly, strain controlled extension test with decreasing σ_z was possible by displacement plunger forcing water into the bottom of the loading piston whereas similar test with increasing σ_x could be made by forcing water at a constant rate into the lateral pressure system.

Air pressure was applied through 6' long saturated 1/8" O.D. saran tubings, in order to prevent diffusion of air into pore space or lateral water pressure system (Poulos, 1964). The line air pressure was limited to about 120 psi. Whenever high pressure was needed it

was generated through a pressure amplifier consisting of two double rolling diaphrams with an area ratio of 6 (see Fig. 3.3).

3.4.0 Data Aquisition

For tests in both apparatuses, loads were measured by load cells, fluid pressures by pressure transducers, displacements by linear differential transformers and volume changes by differential pressure transducers. Signals from all the transducers, load cells or transformers were fed into a Vidar Digital Data Aquisition System. Test data was acquired simultaneously on a magnetic tape and a printer. Magnetic tape was then used as input data file while reducing test data with the I.B.M. 360/67 computer at U.B.C. Data acquired on the printer helped to keep track of satisfactory progress of the experiments.

3.5.0 Important Characteristics Common to Both Apparatuses

3.5.1 K_o-Consolidation

Two different methods could be used for normal K_o-consolidation of the soil specimens. In the first method a state of hydrostatic stress, equal to the desired vertical consolidation stress, was built on the undrained specimen. The drainage valve on the lateral

fluid pressure system was then closed before commencement of consolidation. This ensured a constant volume of water in the lateral pressure system, thus preventing any strain in the x-direction. In the second method, again a state of hydrostatic stress was built, but now, equal to the desired back pressure during consolidation. The lateral pressure system was then made undrained and specimen consolidated under strain controlled loading with drainage permitted from top and pore pressure recorded at the bottom of the specimen.

In the first method very high gradients occur within the specimen in the initial stages of the consolidation process. This is sometimes considered objectionable. However, similar situations exist in conventional triaxial tests when isotropic consolidation is done in a single increment. In the single increment method of K_o-consolidation the lateral stress, σ_x, progressively decreased as consolidation progressed until equilibrium was reached at the end of consolidation. Forty-eight hours were allowed for normal consolidation. Since σ_x had decreased from its initial value, the lateral fluid pressure system under the final σ_x, contained an excess amount of water equal to the change in σ_x times the small compliance of the lateral pressure system. This, consequently, caused

the specimen to undergo a very small compressive lateral strain, thereby resulting in the final σ_x value not truly consistent with the actual K_o-value, but slightly larger. Compliance effects and observed K_o values are discussed later in this chapter.

In the K_o-consolidation by strain controlled loading, the use of slow rates of strain results in much smaller gradients during the entire consolidation process, thus overcoming the objection of one increment consolidation. However, as the consolidation progressed, lateral stress σ_x increased, but due to the small compliance of the system, fell slightly short of the value truly consistent with the actual K_o-condition. Thus, at the end of consolidation under the desired vertical stress, the specimen underwent a small extensional lateral strain, which was proportional to the product of change in σ_x from its initial to the final value and the compliance of the lateral pressure system.

During overconsolidation the measured equilibrium value of σ_x at the completion of swelling was, in both methods of consolidation, too large compared to that corresponding to true K_o-condition. This was because σ_x at the end of overconsolidation was in both cases smaller than the end of normal consolidation value from where the specimens were rebounded.

In all the tests described in this thesis incremental consolidation method was employed. One of the reasons for this decision was to avoid excessively large times required for strain controlled consolidation of the relatively long triaxial specimens. Due to the rather brittle nature of the clay used in this study, extremely slow rates would be needed for strain controlled consolidation in order to prevent undrained failure of the specimen. The compliance of the lateral pressure system did permit a very small lateral strain which would have caused undrained failure if the specimen could not drain as fast as it was being loaded. This situation did not arise in one increment K_o-consolidation where σ_x decreased rather than increased during the consolidation process, and the lateral pressure system contained at all times slight excess water corresponding to the instantaneous σ_x. This resulted in a small lateral compressive strain and therefore, there was no tendency for undrained failure during consolidation.

The effect of single increment and strain controlled consolidation on the K_o-value and subsequent undrained axial compression shear behaviour was studied for two Haney clay specimens. Both specimens were normally consolidated to the same vertical effective stress - one by a single increment and the other by strain controlled consolidation.

The K_o-value for incremental consolidation was found to be slightly larger (0.55 - 0.56) than the value under strain controlled consolidation (0.53 - 0.54). Thus the difference in the two K_o values was only about 5%. Additional comparative tests were performed and again the difference rarely exceeded the above mentioned value. The triaxial-undrained strength of these two specimens was found to be almost identical and so was the deviator stress and pore pressure vs. axial strain response. Since there was essentially no difference in the shear behaviour of the specimens consolidated in two different ways, the method involving one increment consolidation was used because of its simplicity and convenience.

3.5.2 Influence of Lateral Fluid Pressure System Compliance on Measured K_o

Both methods of K_o-consolidation imposed a small amount of lateral strain on the specimens during the consolidation process. As explained earlier, this was due to the small compliance of the lateral pressure systems. For both apparatuses this compliance was approximately 0.06 c.c/Kg/cm^2 and was sensibly linear with pressures larger than 1 Kg/cm^2 and up to about 10 Kg/cm^2. It can be shown that this small compliance did not

result in measured K_o-value of normally consolidated clay to be greatly in error from the true K_o-value. The magnitude of difference is a function of ratio of this compliance and the compressibility of the soil skeleton.

Assume a true K_o-normally consolidated clay specimen in equilibrium under a vertical effective stress, σ_z', and lateral effective stress $\sigma_x' = K_o\sigma_z'$.

Let V = volume of the soil specimen in c.c

c = compliance of the lateral pressure system in c.c/Kg/cm^2

m_v = compressibility of soil cm^2/ Kg - a function of mean normal effective stress, p, under K_o or approximate K_o-consolidation conditions.

$\Delta\sigma_z'$ = increment in vertical effective stress under fully drained conditions, and with lateral pressure system kept undrained.

Then if $c = 0$ (i.e. for the case of infinitely stiff system) the increase in lateral pressure

$$\Delta\sigma_x' = K_o\Delta\sigma_z' \tag{3.1}$$

Since $c \neq 0$, the change in pressure in lateral pressure system will not equal $K_o \Delta\sigma_z'$ but $\Delta p'$ where $\Delta p' < K_o \Delta\sigma_z'$. Change in volume of the specimen then is

$$\Delta V_1 = m_v V \frac{\Delta\sigma_z' + 2\Delta p'}{3} \tag{3.2}$$

In comparison changes in volume of the specimen in the presence of infinitely stiff lateral pressure system is

$$\Delta V_2 = m_v V \frac{\Delta\sigma_z' + 2K_o \Delta\sigma_z'}{3} \tag{3.3}$$

Expansion of the $c \neq 0$ lateral pressure system under increased pressure $\Delta p'$ is $\Delta V_3 = c\Delta p'$. Then it is obvious that the deficiency in volume change, $\Delta V_2 - \Delta V_1$, equals $c\Delta p'$, i.e. $c\Delta p' = 2/3\ m_v V(K_o \Delta\sigma_z' - \Delta p')$, or

$$\frac{\Delta p'}{\Delta\sigma_z'} = \frac{K_o}{1 + \frac{1.5}{V}\frac{c}{m_v}} \tag{3.4}$$

Substituting for V (= 150 c.c and 80 c.c respectively for plane strain and triaxial specimens) and c (= 0.06 c.c/Kg/cm^2 for both apparatuses),

$$\frac{\Delta p'}{\Delta \sigma_z'} = \frac{K_o}{1 + \frac{0.0006}{m_v}} = \frac{K_o}{\eta_p} \text{ for plane strain} \qquad (3.5)$$

$$\frac{\Delta p'}{\Delta \sigma_z'} = \frac{K_o}{1 + \frac{0.00114}{m_v}} = \frac{K_o}{\eta_T} \text{ for triaxial} \qquad (3.6)$$

where

$$\eta_p = 1 + \frac{0.0006}{m_v}$$

$$\eta_T = 1 + \frac{0.00114}{m_v}$$

The ratio of lateral to vertical effective stress after the vertical stress increment, $\Delta\sigma_z'$, is now

$$(K_o)_m = \frac{K_o \sigma_z' + \Delta p'}{\sigma_z' + \Delta \sigma_z'}$$

$$(K_o)_m = K_o \cdot \frac{\sigma_z' + \frac{1}{\eta}\Delta\sigma_z'}{\sigma_z' + \Delta\sigma_z'} \qquad (3.7)$$

Equation 3.7 shows that the error in the measured K_o value, $(K_o)_m$, depends on η which is a function of the compressibility of clay. For the clay tested, m_v was of the order of 0.05 cm^2/Kg in the normally consolidated range. Consequently the measured $(K_o)_m$ will not differ from the true K_o by more than 2%. Values of m_v during rebound of this clay from $\sigma_z' = 6$ Kg/cm^2 to $\sigma_z' = 0.3$ Kg/cm^2 were in the range of 0.004 to 0.045 cm^2/Kg. Using this range of values of m_v in Eqs. 3.5 to 3.7 it can be shown that the measured $(K_o)_m$ could be about 10% larger than the true K_o when the sample was rebounded from $\sigma_z' = 6$ to $\sigma_z' = 0.3$ Kg/cm^2. In order to obtain overconsolidated samples as near to the K_o-condition as possible, compliance of the lateral pressure system was artificially reduced by expanding the total volume of lateral pressure system. This was achieved by means of a displacement valve in which the plunger could move out to increase the total volume of the lateral pressure system (see Fig. 3.3).

3.6.0 Measured K_o-Values

Both the plane strain and the K_o triaxial equipments have the important capability of being used as one-dimensional oedometers with measurements of the lateral effective stresses. Thus the magnitude of $K_o = \sigma'_x/\sigma'_z$, the coefficient of lateral earth pressure at rest, can be determined as a function of the consolidation history. This is particularly interesting when K_o-consolidation is done under strain controlled conditions and a continuous variation of K_o values with overconsolidation ratio is obtained.

A cyclic K_o-consolidation test was performed on undisturbed Haney clay - the soil used in this study. The test was performed in the K_o triaxial apparatus but plane strain apparatus could be used likewise. The vertical effective stress, σ'_z, was built on the specimen to about 6 Kg/cm^2 during the first loading cycle, which was followed by a rebound to $\sigma'_z \sim 0.6$ Kg/cm^2. During the second loading cycle σ'_z was built up to about 16.5 Kg/cm^2 (235 psi) which was followed by second rebound to $\sigma'_z \sim 0.5$ Kg/cm^2.

Fig. 3.4 shows e-log σ' relationships for the entire history of consolidation. The stresses represented are both, σ'_z and p. e-log σ'_z and e-log p are parallel in the normally consolidated range

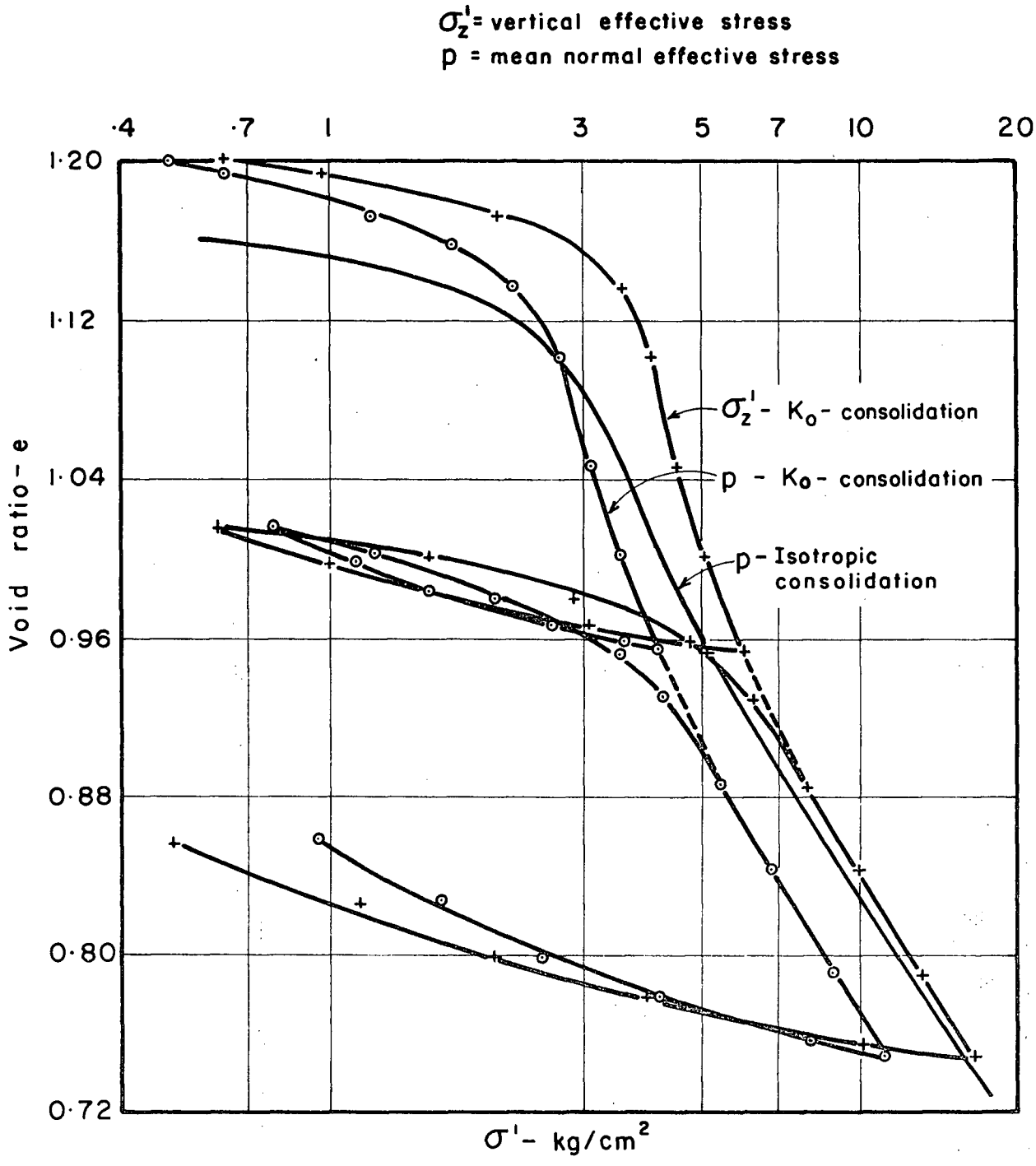

Fig.3·4 e - logσ' RELATIONSHIPS - UNDISTURBED HANEY CLAY.

($\sigma_z' > 4$ Kg/cm^2) and are typical of a sensitive clay. The normally consolidated branch of the e-log σ' curve for second loading cycle was precisely along the extension of the normally consolidated branch of the curve for the first loading cycle.

Also shown in Fig. 3.4 is the e vs. log p relationship for a strain controlled isotropic consolidation test on the same clay and in the same apparatus. The specimen used for the isotropic consolidation test had a slightly lower initial void ratio compared to the specimen used in K_o consolidation test. This results in initial part of e vs. log p relationship for isotropic consolidation to lie below the similar relationship for K_o consolidation. However, for $p > 5$ Kg/cm^2, i.e., in the normally consolidated range, the e-log p relationships for the two types of consolidation are parallel. For a given p, K_o consolidation results in lower void ratio when compared to that under isotropic consolidation. These results are similar to those reported by Khera and Krizek (1966) and Lewin and Burland (1970). However, for a given p, the difference in void ratio for the two types of consolidation is very pronounced in the clay tested, apparently because of the sensitive nature.

Fig. 3.5 shows the relationship between lateral effective stress, σ_x', and vertical effective stress, σ_z'.

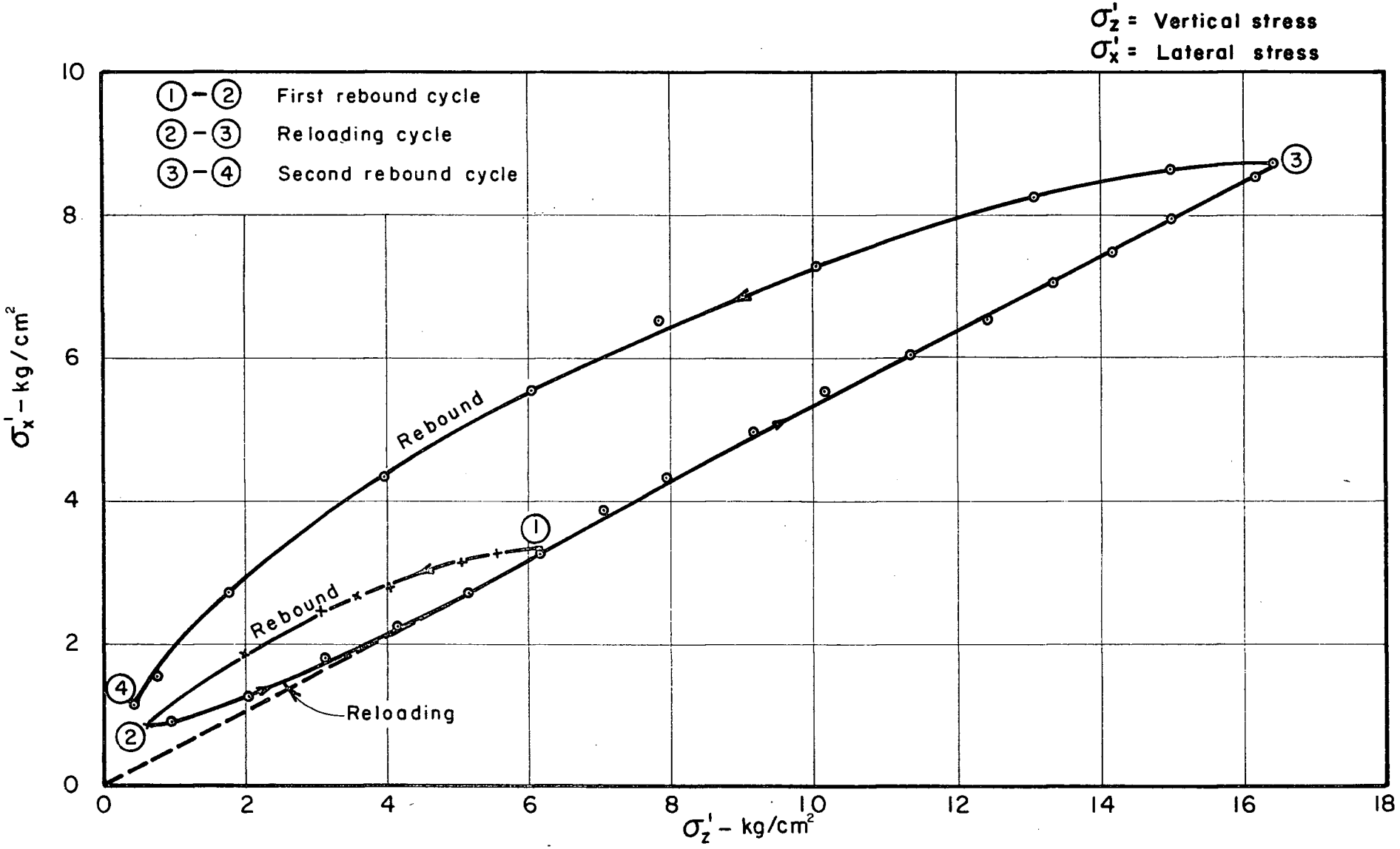

Fig.3·5 RELATIONSHIP BETWEEN VERTICAL AND LATERAL EFFECTIVE STRESSES DURING ONE DIMENSIONAL CONSOLIDATION-UNDISTURBED HANEY CLAY.

It is seen that the relationship is linear for the normally consolidated clay and is not altered by an interrupted unloading and reloading sequence. The slope of this straight line is 0.54, which is thus the average value of K_o under the condition of normal consolidation.

Variation of K_o with overconsolidation ratio, (O.C.R.) = $\sigma'_{z_{max}}/\sigma'_z$ is shown in Fig. 3.6. K_o increases as the clay is rebounded from its normally consolidated state. It achieves a value of about 2.0 for overconsolidation ratio of 20. For the same overconsolidation ratio, K_o seems to be independent of the magnitude of σ'_z from which the rebound cycle is initiated. The relationship, K_o vs. overconsolidation ratio during reloading cycle, is different when compared to the similar relationship during rebound. For a given O.C.R., K_o during reloading is smaller than during rebound.

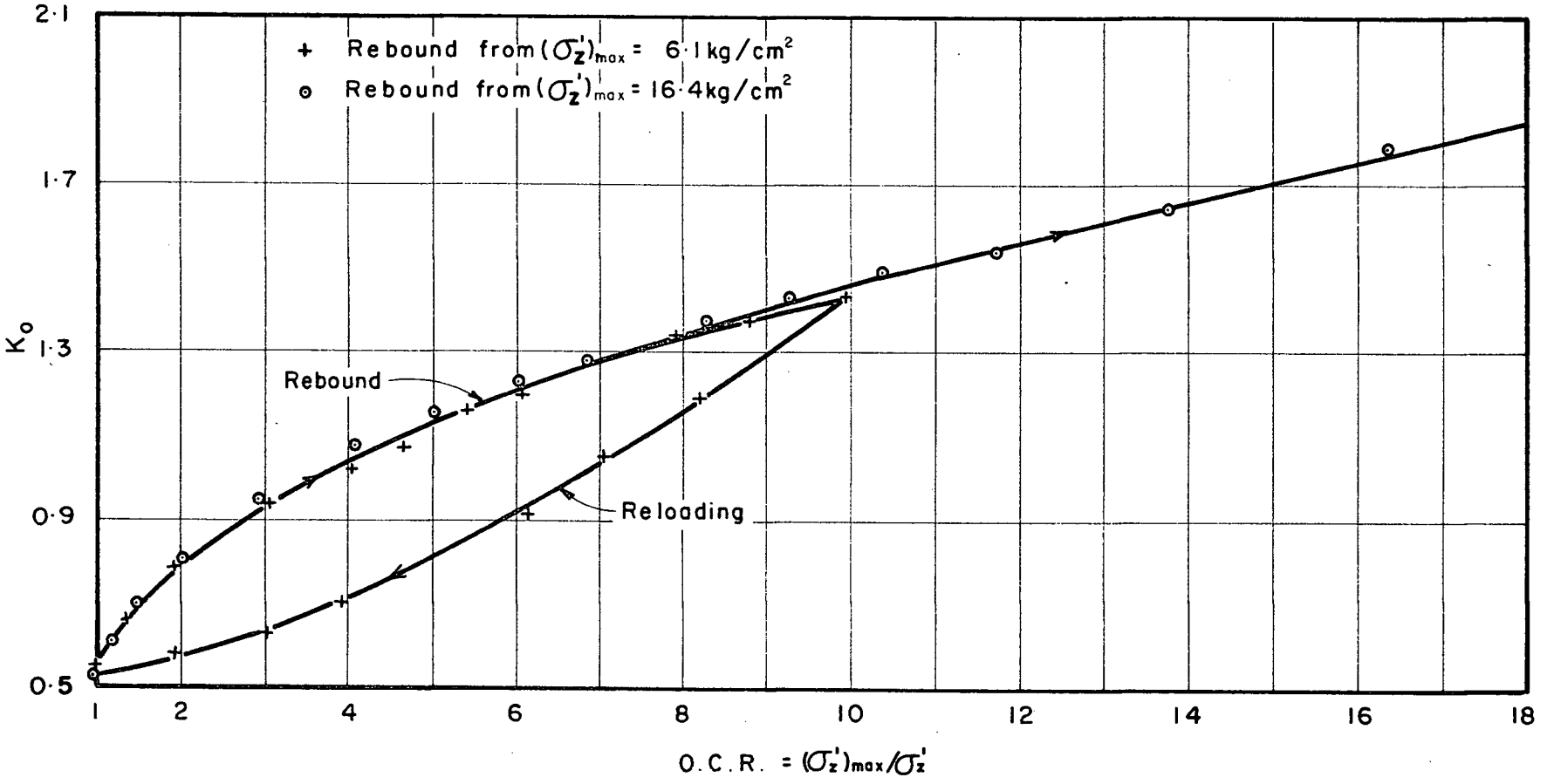

Fig.3·6 VARIATION OF K_o WITH OVER CONSOLIDATION RATIO-UNDISTURBED HANEY CLAY.

CHAPTER IV

LABORATORY TESTING

4.1.0 Description of Clay Tested

The clay used in this study was taken from an open pit belonging to the Haney Brick and Tile Co., Haney, B.C. This pit is located about 30 miles east of U.B.C. on the north bank of the Fraser River. Block samples of this clay, which will be referred to as Haney clay, were obtained in June, 1967. A three-foot deep trench was dug around an area about three feet square, thus isolating a large block of soil. The top one foot or so of disturbed clay was removed, and approximately nine inches cube blocks were trimmed using a fine piano wire. The blocks were carefully wrapped in the field with Saran wrap. After transportation to the laboratory, they were sealed with several coatings of wax. The blocks were stored in a moist room until required. No noticeable change in water content of these blocks was observed, even for storage period of up to three years.

Haney clay is thought to have been deposited in a marine environment (Armstrong, 1957). Subsequent uplift of the land relative to the sea caused the deposit to be exposed, and over the ensuing years percolating rain water has leached out most of the salt. Haney clay thus possesses a sensitive structure. Table 1 shows its typical physical properties.

4.2.0 Experimental Procedures

4.2.1 Installing Specimens in Apparatuses

Detailed procedures to install clay specimens has been described by Vaid (1968) for the plane strain tests and by Campanella and Vaid (1971) for the K_o-triaxial tests.

4.2.2 K_o-consolidation

All specimens were first normally consolidated to the same vertical effective stress of approximately 6 Kg/cm^2. Consolidation was done against a back pressure of 1 Kg/cm^2, starting from a hydrostatic total stress state of approximately 7.5 Kg/cm^2 for plane strain and 7 Kg/cm^2 for K_o-triaxial tests. Larger initial stress was used for plane strain tests in order to compensate for some of the vertical load being transferred through side friction; thus resulting in

Table 1

PHYSICAL PROPERTIES OF UNDISTURBED HANEY CLAY

Liquid Limit	46 %
Plastic Limit	26 %
Plasticity Index	20 %
Natural water content	41-44%
Degree of saturation	100 %
Specific gravity of solids	2.80
Percent finer than 2 microns	46 %
Unconfined compressive strength	~ 1 Kg/cm^2
Sensitivity	~ 6 - 10
Activity - P.I/%<2μ	0.44
Maximum past pressure (from K_o-consolidation tests)	~ 4 Kg/cm^2
Predominant clay mineral	Chlorite

lower vertical stress at the sample bottom, but giving the desired vertical effective stress of 6 Kg/cm^2 as the average value. The lateral fluid pressure systems were kept undrained during the consolidation process and no allowance was made for their small flexibility. A period of 48 hours was allowed for consolidation for tests involving normally consolidated samples.

Overconsolidated specimens were obtained by unloading the vertical stress to get the desired overconsolidation ratio, which is defined herein as the ratio of the maximum past to the final vertical effective stress under which the specimen was allowed to swell. As before, vertical stress was taken off while keeping the lateral fluid pressure systems undrained. As pointed out in Chapter III, large changes in stresses are associated with very small strains during rebound of clays, because of their greatly reduced compressibility. To achieve overconsolidation as close to the K_o-condition as feasible, adjustments were made for the compliance of the lateral pressure system by means of the displacement valve (see Fig. 3.3). The amount of adjustment would depend on the decrease in lateral pressure while unloading the vertical stress during overconsolidation. Twenty-four hours

were allowed for swelling under the reduced vertical stress before the samples were subjected to shear testing.

4.2.3 Shear Testing

All tests were made using strain controlled loading or pressure change, with the exception of a few drained tests on overconsolidated specimens, which were load controlled. These tests required very small strains to failure which, in turn, necessitated extremely slow testing rates. Such slow rates could not be selected on the strain drive. Time to failure for consolidated undrained tests was estimated using recommendations of Bishop and Henkel (1962) and Blight (1963). Sufficiently slow testing rates were used, so as to result in time to failure far in excess of the calculated value. Drained tests were made by permitting drainage from the top only while pore pressure was measured at the bottom of the specimen. Testing rates used were such, that at no time the difference between the pore pressures at the top and the bottom of the specimen amounted to more than 4% of the current vertical effective stress. The distribution of this excess pore pressure over the height of the specimen was assumed to be parabolic when calculating the effective stresses

(Byrne, 1966; Smith & Wahls, 1969). This testing technique enabled evaluation of effective stresses in the sample at all stages of the test with confidence. The range of axial strain rates used for most of the tests were between 0.1 to 0.15 % per hour. Similar testing rates were used for plane strain and K_o-triaxial tests, in order to eliminate any rate effects on the shear behaviour of clays.

At the end of the shear test, specimens were allowed to swell under a small effective stress of about 0.1 Kg/cm^2 before removal for final water content determination (Henkel and Sowa, 1963).

4.3.0 Development of the Testing Program

The main aim of this thesis was to compare, for the identical end of K_o-consolidation state, the plane strain and triaxial behaviour of Haney clay under similar total stress paths to failure. The comparison was to be made for both normally and heavily overconsolidated initial states.

Normally consolidated specimens were obtained by K_o-consolidation to a vertical effective stress of approximately 6 Kg/cm^2 (maximum past pressure for the clay was approximately 4 Kg/cm^2). Heavily overconsolidated specimens were obtained by allowing the normally

consolidated specimens swell under a reduced vertical effective stress of 0.3 Kg/cm^2, thus giving an over-consolidation ratio of about 20. The overconsolidation ratios actually obtained were in the range of 15 to 19. This was because of the inability to estimate the final average vertical stress, which depends on side friction in the plane strain apparatus. Variations in over-consolidation ratio, from the desired value of 20, occurred in the K_o-triaxial tests, because of the difficulty in adjusting the precision pressure regulators to hold constant pressure in the loading piston while operating in the very low pressure range.

4.3.1 Stress Paths Investigated

The axes of principal stress (and strain) are fixed by both apparatuses, but it was possible to interchange the relative magnitude of the principal stresses, σ_z and σ_x, at any stage of the test. In this way it was possible to make either axial compression or extension tests with any desired stress path in σ_z vs. σ_x stress plane. However, the investigation was restricted to the study of the following stress paths:

Axial Compression

Passive - The vertical stress, σ_z, was increased while holding the lateral stress, σ_x, constant at end of consolidation value.

Active - The lateral stress, σ_x, was decreased while holding the vertical stress, σ_z, constant at the end of consolidation value.

Axial Extension

Active - The vertical stress, σ_z, was decreased while holding the lateral stress, σ_x, at the end of consolidation value.

Passive - The lateral stress, σ_x, was increased while holding the vertical stress, σ_z, at the end of consolidation value.

For each of these stress paths, consolidated undrained and drained tests were made. One series of tests were made on normally consolidated specimens and the second series consisted of heavily overconsolidated specimens. Each type of test was made both under plane strain and triaxial stress conditions.

CHAPTER V

PLANE STRAIN TEST RESULTS ON NORMALLY CONSOLIDATED HANEY CLAY

In this chapter results of tests on normally consolidated Haney clay under plane strain conditions are described. The results are presented in a manner which would demonstrate the influence of applied stress path on the plane strain response of 'identically' K_o-consolidated specimens. Undrained behaviour under different consolidation stresses can usually be derived by using normalised stress parameters. The existence of a normalised stress stress-strain behaviour for a normally consolidated clay is well known (Hvorslev, 1960; Henkel, 1960; Roscoe and Poorooshasb, 1963). This was found to be true for Haney clay also. Three passive compression undrained tests, each consolidated to different vertical consolidation stress σ_z', yielded essentially identical normalised deviator stress, $(\sigma_z-\sigma_x)/\sigma_{zc}'$, vs. axial strain, ε_z, relationship. Similarly, other normalised plots, e.g., change in pore pressure, $\Delta u/\sigma_{zc}'$ vs. ε_z were found to be identical for tests with different values of σ_{zc}'.

When comparing the plane strain behaviour under different stress paths, variations of specific stress or strain parameters are plotted against axial strain, ε_z. Compressive strains and volume decreases are considered positive.

5.1.0 Undrained Test Results

5.1.1 Stress-Strain Relationships

Fig. 5.1 shows normalised deviator stress, $|\sigma_z - \sigma_x|/\sigma_{zc}'$ vs. axial strain, ε_z, for identically consolidated samples, under the four undrained stress paths - active and passive compressions and extensions. The relationship is identical for the two compression stress paths. This result was as expected, because in undrained tests the effective stress path is predetermined by the pore water pressure characteristics of the sample. In spite of the variations in the applied total stress, for a specimen with a given consolidation history, only one effective stress path can be obtained during compression shear. The deviator stress-strain response depends on the variations of the effective stresses within the specimen and, therefore, should be the same if different systems of total stresses give rise to the same effective stress path. Similarly,

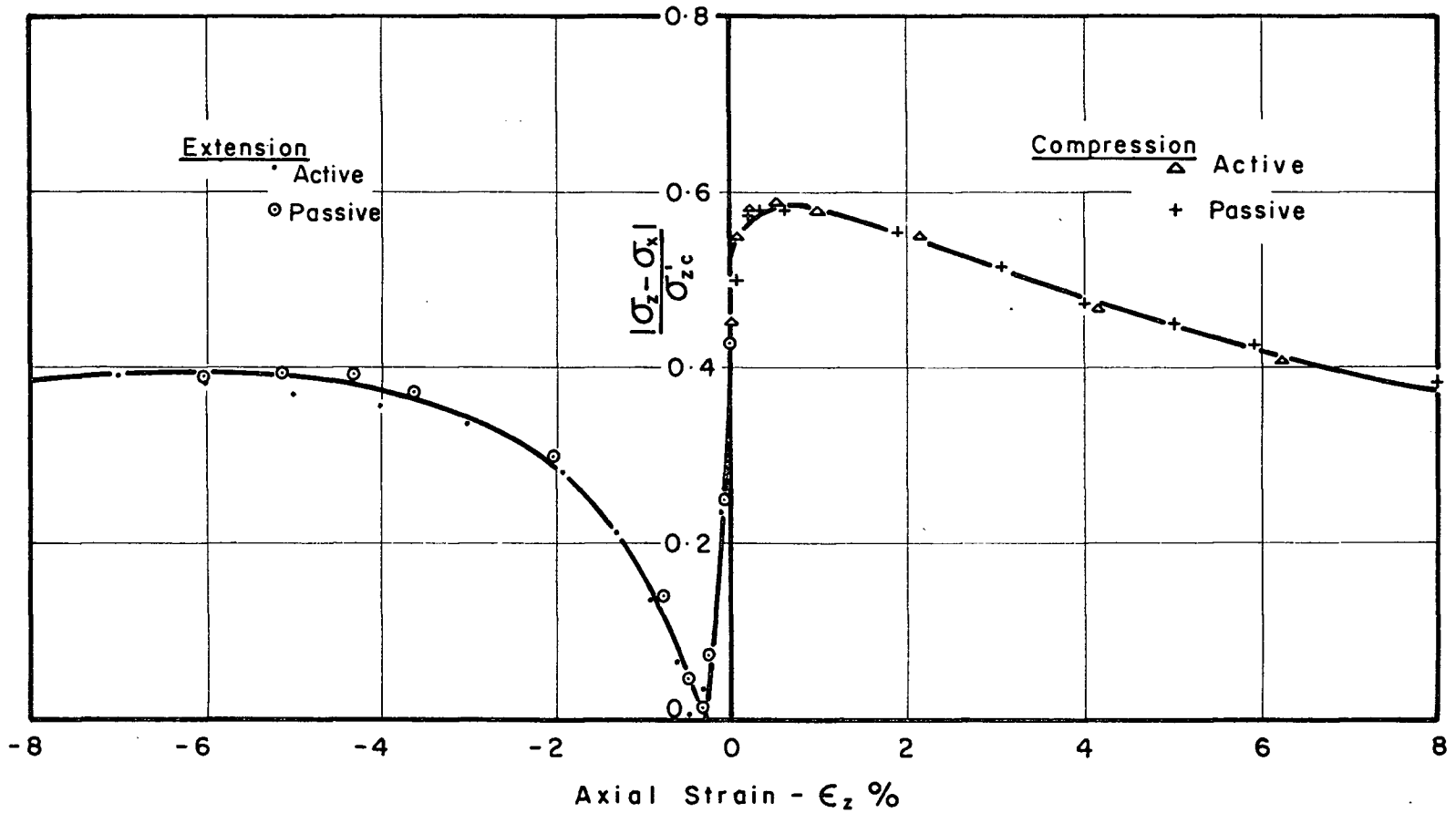

Fig. 5·1 DEVIATOR STRESS-STRAIN RELATIONSHIPS DURING UNDRAINED PLANE STRAIN SHEAR-N.C. HANEY CLAY.

$|\sigma_z - \sigma_x|/\sigma_{zc}'$ vs. ε_z relationship is identical for the two extension tests for the same reasoning that any system of total stresses leading to extension shear results in the same effective stress path.

Haney clay was very brittle in compression failure ($|\sigma_z - \sigma_x|_{max}$); the axial strain at failure was only 0.4%. On the other hand the extension failure was of a plastic type with failure strain around 7%. The undrained strength, ($|\sigma_z - \sigma_x|_{max}/2$), in extension was only 70% of the compression value. It was interesting to note that at large strains the deviator stress in compression dropped below the value the specimens carried at the end of consolidation, and the peak deviator stress in extension was even smaller than the end of consolidation value. Compression tests were carried to about 18% axial strain. The deviator stress then had dropped to 40% of the peak value and was still decreasing. Thus, no approach to a residual strength was apparent.

In axial compression shear, the condition of maximum obliquity, $(\sigma_1'/\sigma_3')_{max}$ was reached at a much larger strain than the maximum deviator stress (Fig. 5.2). This is a well known characteristic of sensitive clays and is due to a progressive rise of pore pressure

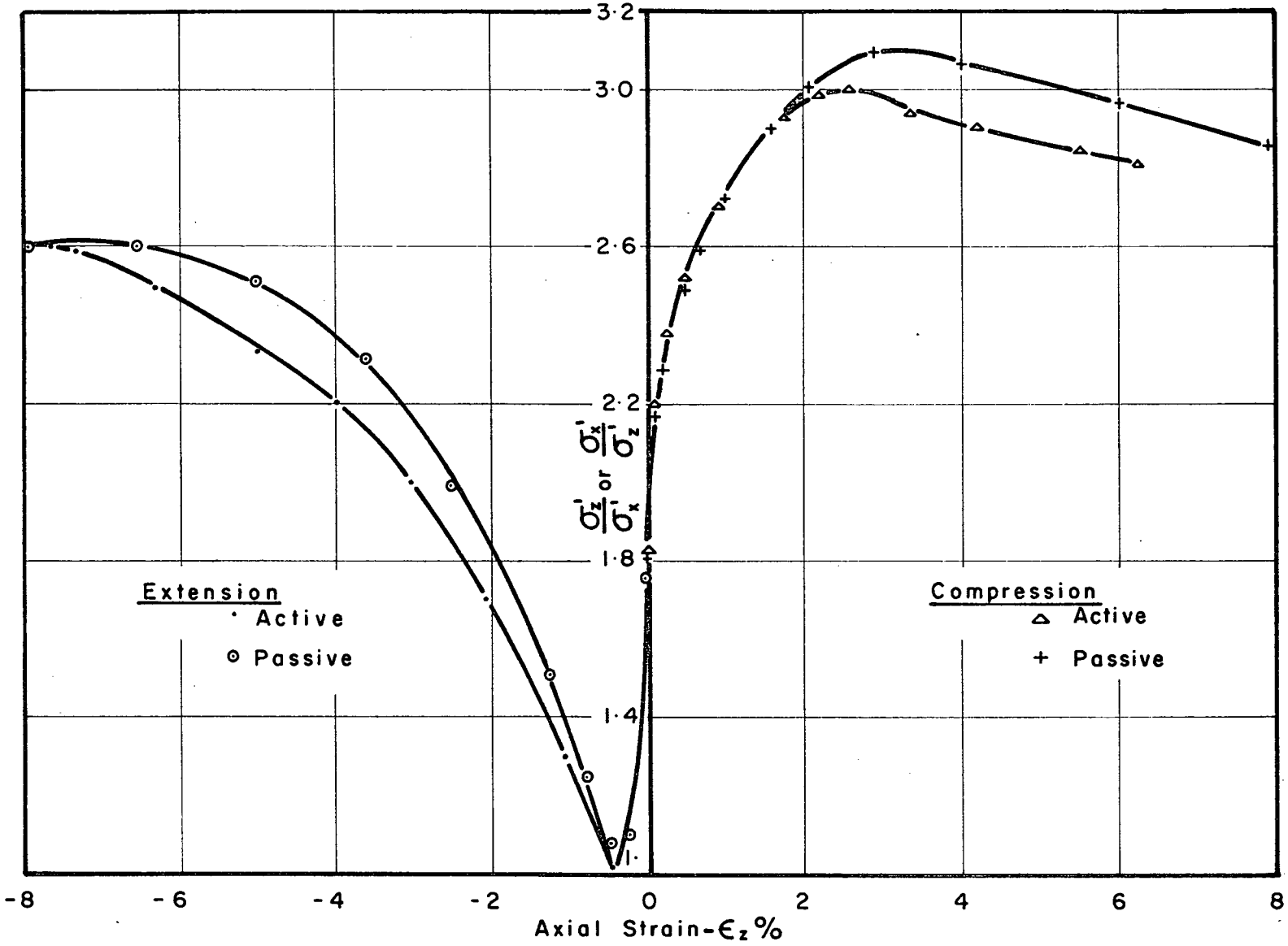

Fig.5·2 PRINCIPAL EFFECTIVE STRESS RATIO- STRAIN RELATIONSHIP DURING UNDRAINED SHEAR IN PLANE STRAIN- N.C. HANEY CLAY.

after the maximum deviator stress is reached (Crawford, 1959; Bjerrum & Simons, 1960). In extension shear, however, points of $|\sigma_z - \sigma_x|_{max}$ and $(\sigma_1'/\sigma_3')_{max}$ coincided. Mobilization of Coulomb friction, as characterised by the effective stress ratio, σ_z'/σ_x' or σ_x'/σ_z', was practically identical for the two compression stress paths and also for the two extension paths.

Fig. 5.3 shows the variation of effective stresses σ_x', σ_y', σ_z' during shear. The stresses have been normalised by dividing them by σ_{zc}', the vertical consolidation stress. The variation of each stress was essentially the same for both compression tests and also for the two extension tests. Therefore, results from only one compression and one extension tests are shown. In compression shear, σ_y', the stress associated with zero strain direction was always intermediate between the other two stresses σ_x' and σ_z'. In contrast, during extension shear, σ_y' was the minor principal effective stress until about 2% axial extensional strain. This seems contrary to the familiar concept that stress in the direction of zero strain has always an intermediate value relative to the other two stresses. However, assuming linear elastic behaviour at small strains it can be shown that σ_y' must be the minor principal effective stress in the initial stages of the extension shear. A

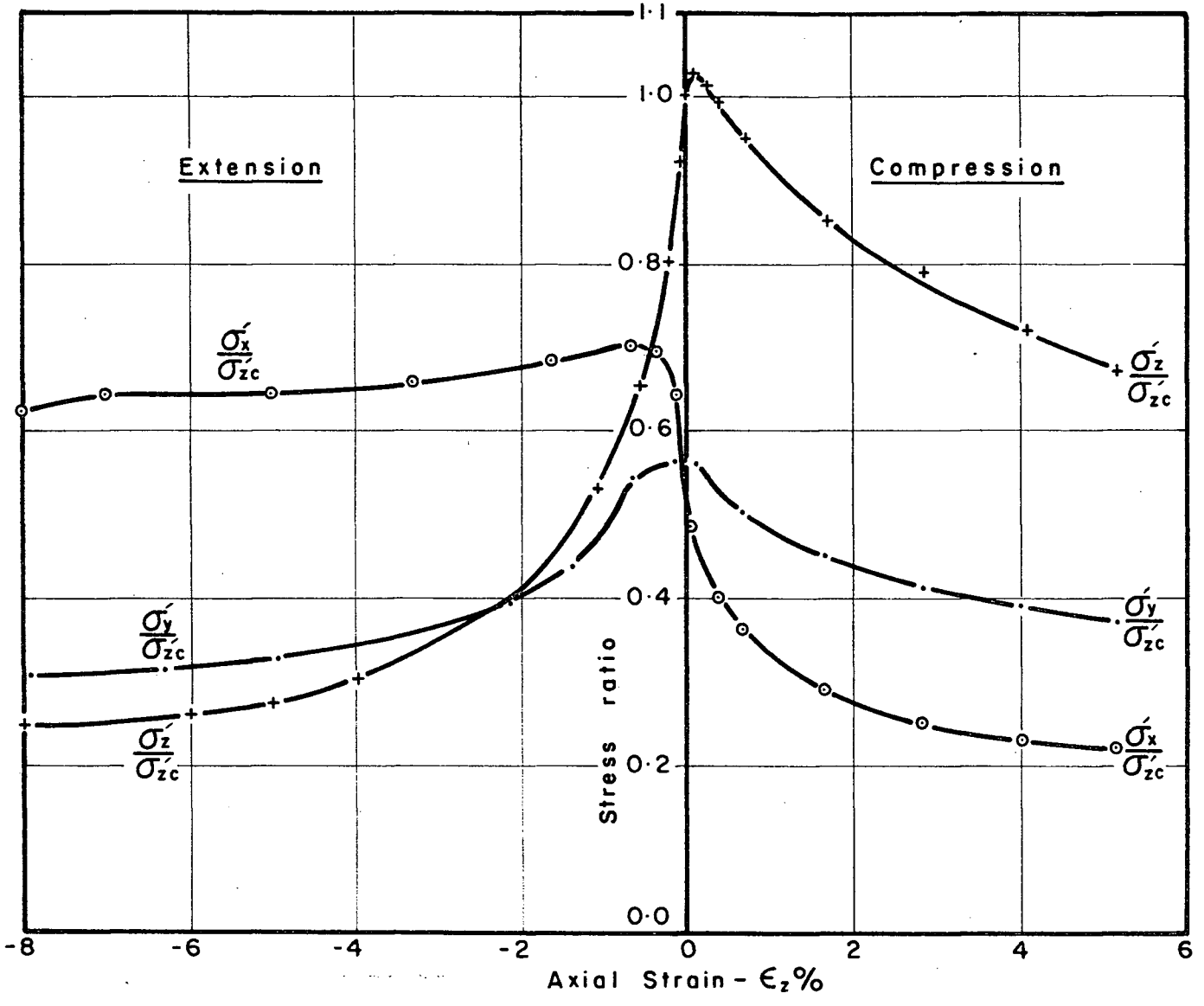

Fig. 5·3 EFFECTIVE STRESS-STRAIN RELATIONSHIPS DURING UNDRAINED PLANE STRAIN SHEAR-N.C. HANEY CLAY.

similar situation can be shown to exist in the results of Hambly and Roscoe (1969). At failure, σ_y' was, as usual, the intermediate principal stress. Irrespective of the relative magnitude of σ_y', the ratio $\sigma_y'/(\sigma_x'+\sigma_z')$ stayed essentially constant (Fig. 5.4) at 0.37 ± 0.02 during undrained shear. This is similar to the results of Hambly & Roscoe (1969) and Henkel and Wade (1966).

5.1.2 Pore Pressures

Fig. 5.5 shows the change in pore pressure, Δu, for the four identical specimens under the imposed stress paths. For the passive compression and extension paths the pore pressure rises continuously during tests, due partly to increase in mean normal stress and partly to changes in shear stresses. It is interesting to note that there was a substantial rise of pore pressure after a small initial drop in active compression, despite the test involved decreasing mean normal stress. This behaviour is associated with structural collapse of sensitive soil skeleton. Only active extension shear resulted in net negative change in pore pressures. Note the wide variations in Δu during active and passive extension.

Since undrained effective stress paths are known to be identical under similar strain paths, it should

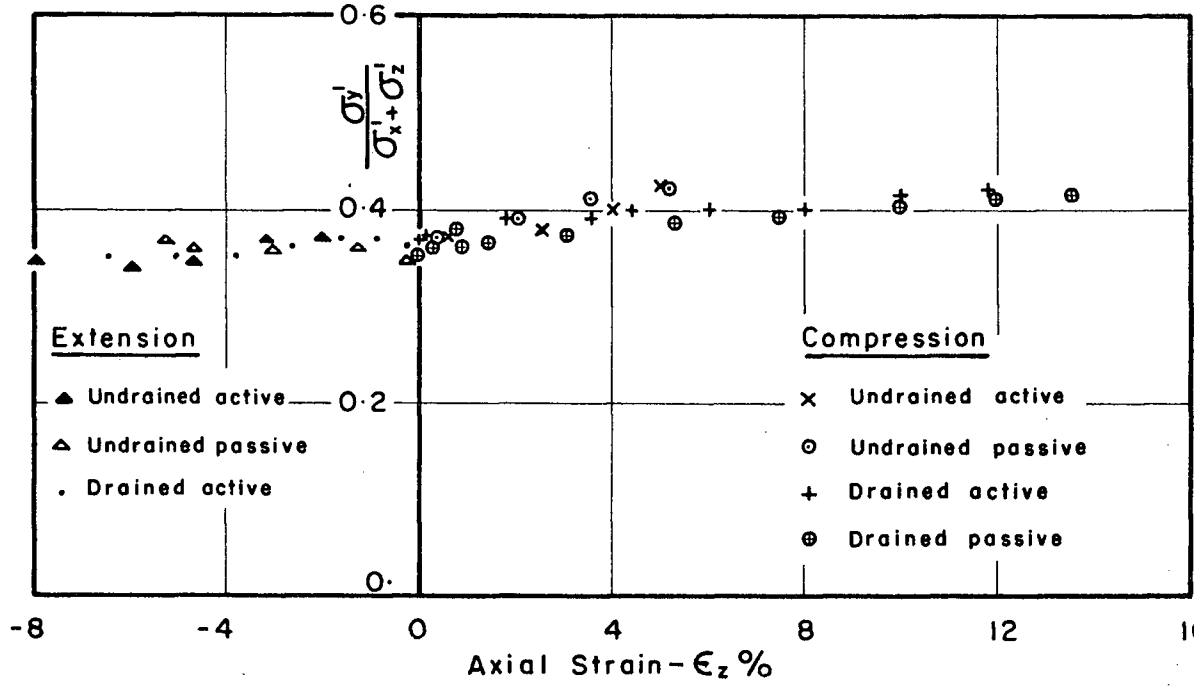

Fig. 5·4 STRESS RATIO $\frac{\sigma_y'}{\sigma_x'+\sigma_z'}$ - STRAIN RELATIONSHIP DURING PLANE STRAIN SHEAR - N.C. HANEY CLAY.

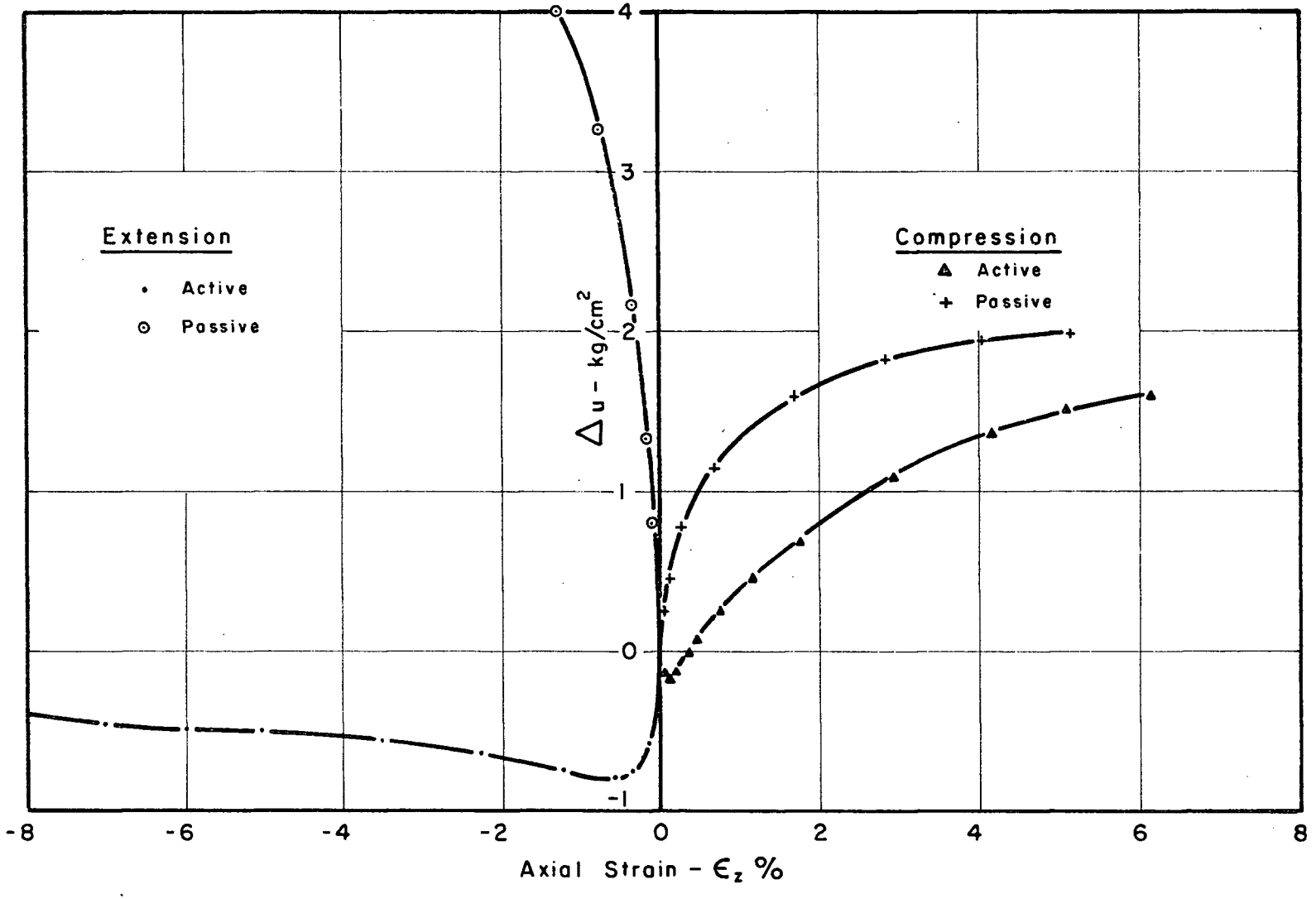

Fig. 5·5 PORE PRESSURE CHANGE - STRAIN RELATIONSHIPS DURING UNDRAINED PLANE STRAIN SHEAR - N.C. HANEY CLAY.

be possible to characterise uniquely the changes in pore pressure in terms of stress changes during either compression or extension shear. This is accomplished by the use of pore pressure parameters. For states of stress which are not axially symmetric, changes in pore pressures are better expressed by Henkel's Equation 2.4, than in Skempton's (1954):

$$\Delta u = \Delta\sigma_{oct} + a\ \Delta\ \tau_{oct} \tag{2.4}$$

Earlier, Henkel (1960) proposed a variation of Eq. 2.4 which was expressed as

$$\Delta u = \Delta\sigma_{oct} + \frac{a}{3}\sqrt{(\Delta\sigma_1-\Delta\sigma_2)^2 + (\Delta\sigma_2-\Delta\sigma_3)^2 + (\Delta\sigma_3-\Delta\sigma_1)^2} \tag{5.1}$$

Both Eqs. 2.4 and 5.1 relate the shear induced pore pressure linearly to some measure of change in shear stresses; however, Eq. 2.4 relates the shear induced pore pressure to change in octahedral shear stress, whereas Eq. 5.1 relates the shear induced pore pressure to octahedral component of change in shear stress. Eq. 5.1 seems to be of a more general nature, because it predicts a definite change in pore pressure even if stress changes are such that τ_{oct} and

σ_{oct} stay constant. Eq. 2.4 during such a stress change will incorrectly predict a zero change in pore pressure. Even so, Eq. 5.1 proves insensitive to the pronounced effect of rotation or reorientation of principal stresses on the induced pore pressures, as demonstrated by Duncan and Seed (1966) and Dickey et. al. (1968). An expression similar to Eq. 5.1 but with stresses referred to fixed axes, x,y,z will take account, in a simple way, of pore pressure induced by changes in mean normal stress and those induced in a cumulative way by changes in shear stresses, including rotation or reorientation of principal axes. The desired expression is

$$\Delta u = \frac{\Delta\sigma_x + \Delta\sigma_y + \Delta\sigma_z}{3} + \frac{a}{3}\sqrt{(\Delta\sigma_x-\Delta\sigma_y)^2 + (\Delta\sigma_y-\Delta\sigma_z)^2 + (\Delta\sigma_z-\Delta\sigma_x)^2} \qquad (5.2)$$

A similar equation was suggested by Baker and Krizek (1969).

In Fig. 5.6 is shown the variation of pore pressure parameter 'a' (as defined in equation 5.2) with axial strain, for the different stress paths. Both compression tests lie on a single curve and so do the two extension tests,

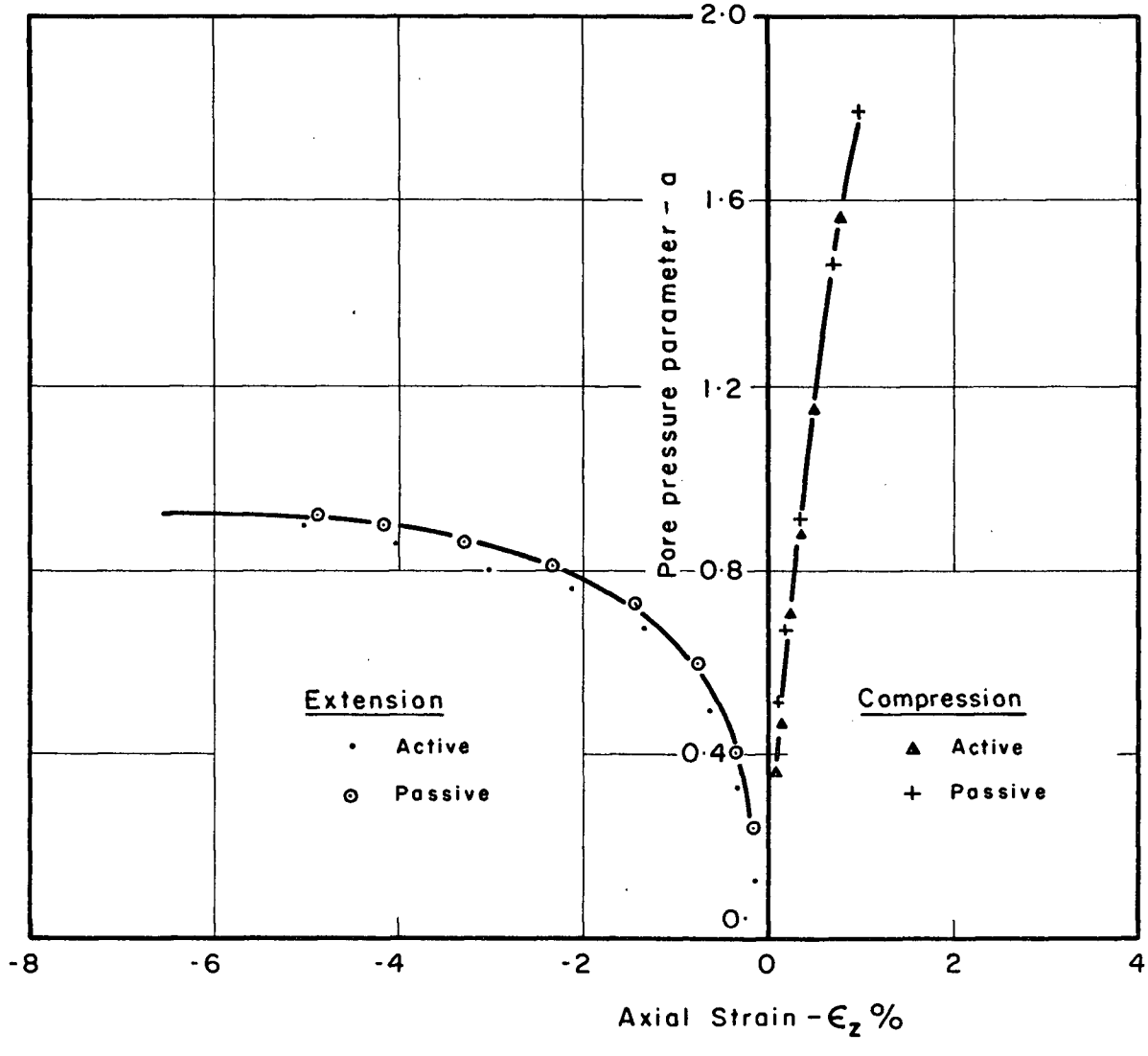

Fig.5·6 VARIATION OF PORE PRESSURE PARAMETER 'a' WITH AXIAL STRAIN DURING UNDRAINED PLANE STRAIN SHEAR- N.C. HANEY CLAY.

but the nature of variation of 'a' with strain bears no resemblance in the two groups of tests. Average value of 'a' at failure ($|\sigma_z-\sigma_x|_{max}$) in compression was 1.2 compared to 0.9 in extension. The value of pore pressure parameter 'a' is a function of the compressibility of clay due to changes in shear stresses. Because of the irreversible nature of clay behaviour, this compressibility is bound to be larger under increasing shear stresses when compared to that under decreasing shear stresses. This difference is likely to be more pronounced in Haney clay which has a sensitive structure to further compression following one-dimensional consolidation.

5.1.3 Effective Stress Paths

Full implications of the differences between compression and extension modes of deformation become evident when the effective stress paths followed in two types of tests are considered. Stress paths have been used in the study of undrained tests by many researchers (Rendulic, 1936; Roscoe et. al., 1958; Henkel, 1960; Lambe, 1964, 1967), and a wide variety of stress spaces have been used. A simple stress space in which the coordinates are σ_z' and σ_x' is used herein to represent

undrained plane strain tests. Fig. 5.7 shows the stress paths followed in the four plane strain tests. Since the two compression and the two extension paths are identical, only passive compression and active extension results are presented in this figure. Both σ_z' and σ_x', as before, have been divided by σ_{zc}'. The two stress paths start from the same point P in stress space, which represents identical end of consolidation state. During compression test the stress path follows the curve labelled PQ, while in the extension test the stress path followed is PR. Axial strains in percent have been indicated in the stress space and the effective stress failure envelopes $(\sigma_1'/\sigma_3'_{max})$ for both compression and extension states have also been shown.

As was shown in Fig. 5.1 the maximum value of deviator stress, $|\sigma_z-\sigma_x|$, in compression occurred at 0.4% axial strain but, it will be seen in Fig. 5.7, this point is reached before the stress path becomes tangential to the effective stress failure envelope. The point of tangency corresponds to an axial strain of about 3%. In the extension test a very large reduction of the value of σ_z' took place during shear, and both the point of tangency to the effective stress failure envelope and the peak deviator stress were reached at a

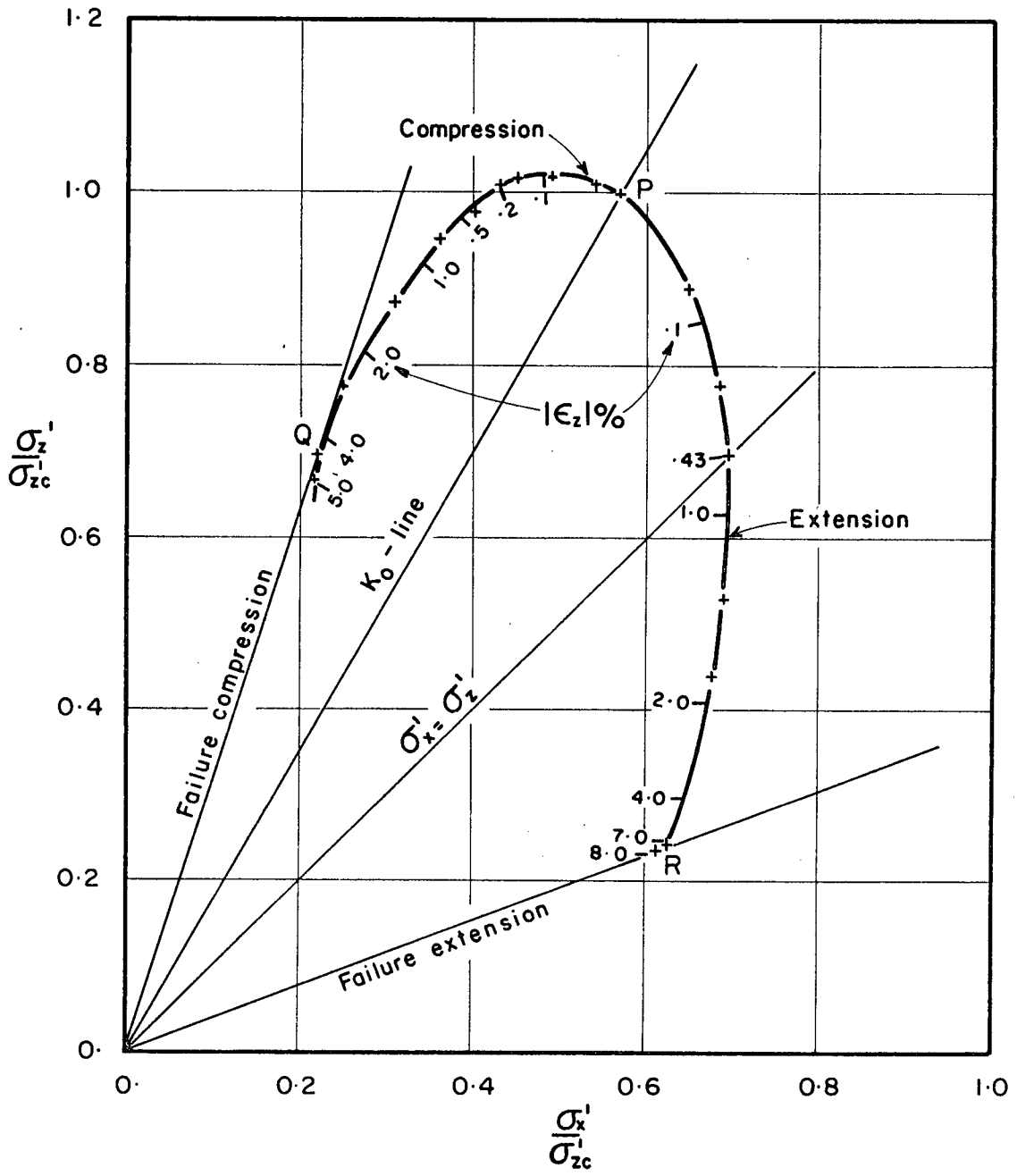

Fig. 5·7 UNDRAINED EFFECTIVE STRESS PATHS DURING PLANE STRAIN SHEAR - N.C. HANEY CLAY.

strain, $|\varepsilon_z|$, of about 7%. In both compression and extension paths, the strains increase rapidly as the failure envelopes are approached and, if deformations in the field are to be limited, the imposed stresses must be controlled so that the stress paths will not get too close to the failure envelopes. The average value of ϕ' was 30.4° in compression and 26.1° in extension. These relative values are similar to those reported by Duncan and Seed (1966) for the Bay mud, which implies that Haney clay is anisotropic with respect to its effective strength parameters. The large increase in extension ϕ' over the compression value reported by Dickey et. al. (1968) is likely to be the result of neglecting friction on the vertical boundaries of the specimen. This neglect results in an underestimate of the minor principal stress and consequently a substantial error in the ratio $(\sigma_1'/\sigma_3')_f$ for a small error in σ_3'. During compression test the neglect of friction causes the major principal stress, σ_1', to be overestimated and, therefore, the ratio $(\sigma_1'/\sigma_3')_f$ is influenced only to a small degree.

5.2.0 Drained Test Results

Only three stress paths, active and passive compression and active extension, were studied for drained

plane strain conditions. Passive extension test could not be performed due to limitations of the plane strain apparatus; i.e. the capacity of the lateral pressure diaphragms was around 12 Kg/cm^2. The value of σ_x required to cause passive extension failure would have been around 18 Kg/cm^2.

5.2.1 Stress-Strain Relationships

Fig. 5.8 shows the variation of deviator stress, $|\sigma_z-\sigma_x|$, and Fig. 5.9 represents the variation of σ_z'/σ_x' or σ_x'/σ_z' with axial strain, ε_z, in the three types of tests. Among the compression paths, the specimen subjected to passive compression had higher $|\sigma_z-\sigma_x|_{max}$ because of higher effective stresses at failure when compared to specimen subjected to active compression. As shown in Fig. 5.9 both these specimens attained almost the same peak effective stress ratio, σ_1'/σ_3' and, therefore, had the same limiting angle of friction ϕ'. But the axial strain required to develop this ϕ' was about 12% in passive compression compared to only about 4% in active compression. While analysing stability in soils where the ultimate or residual strength is lower than the peak strength (such as the clay considered herein), the assumption of a constant

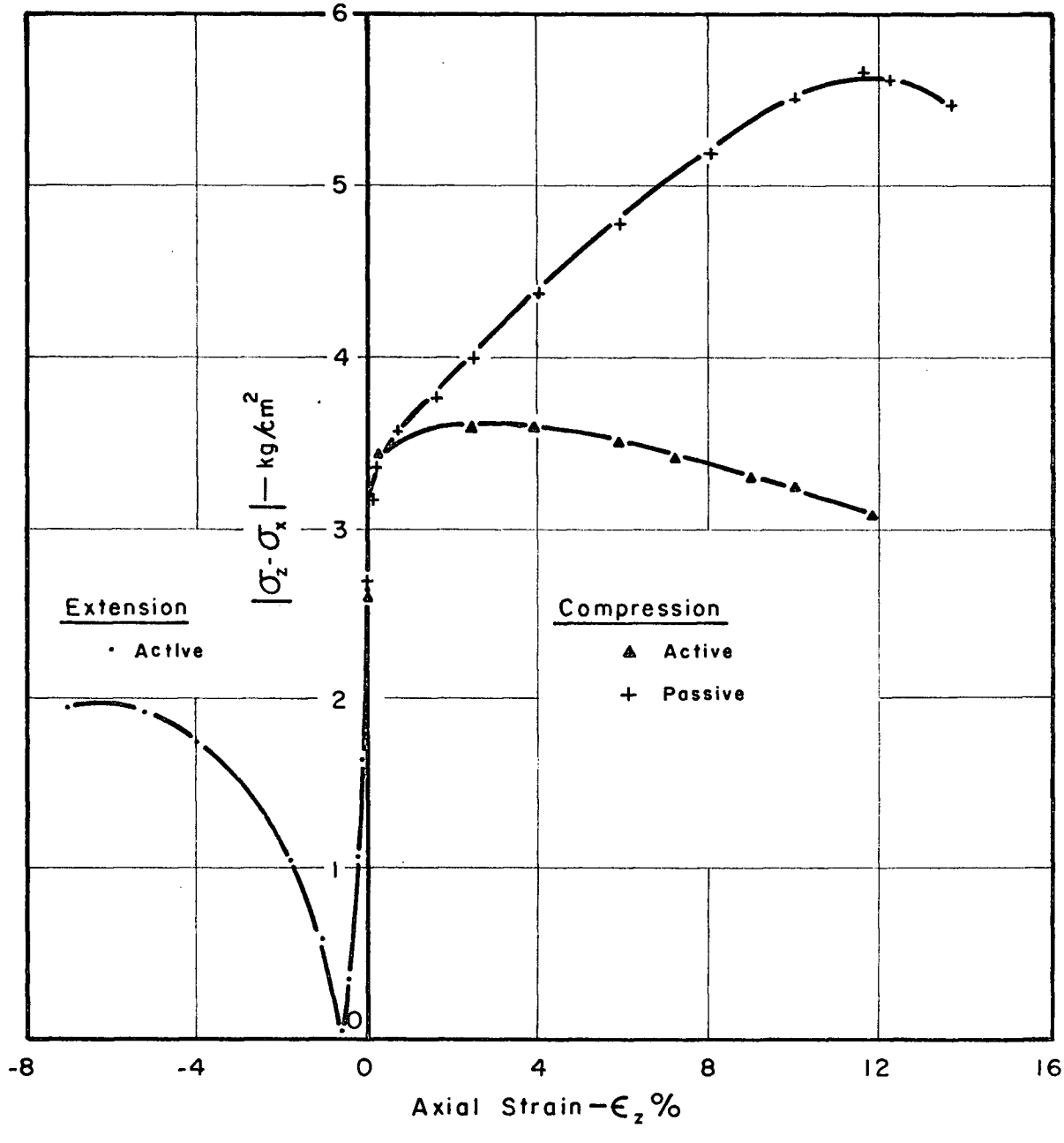

Fig.5·8 DEVIATOR STRESS-STRAIN RELATIONSHIPS DURING DRAINED PLANE STRAIN SHEAR- N.C.HANEY CLAY.

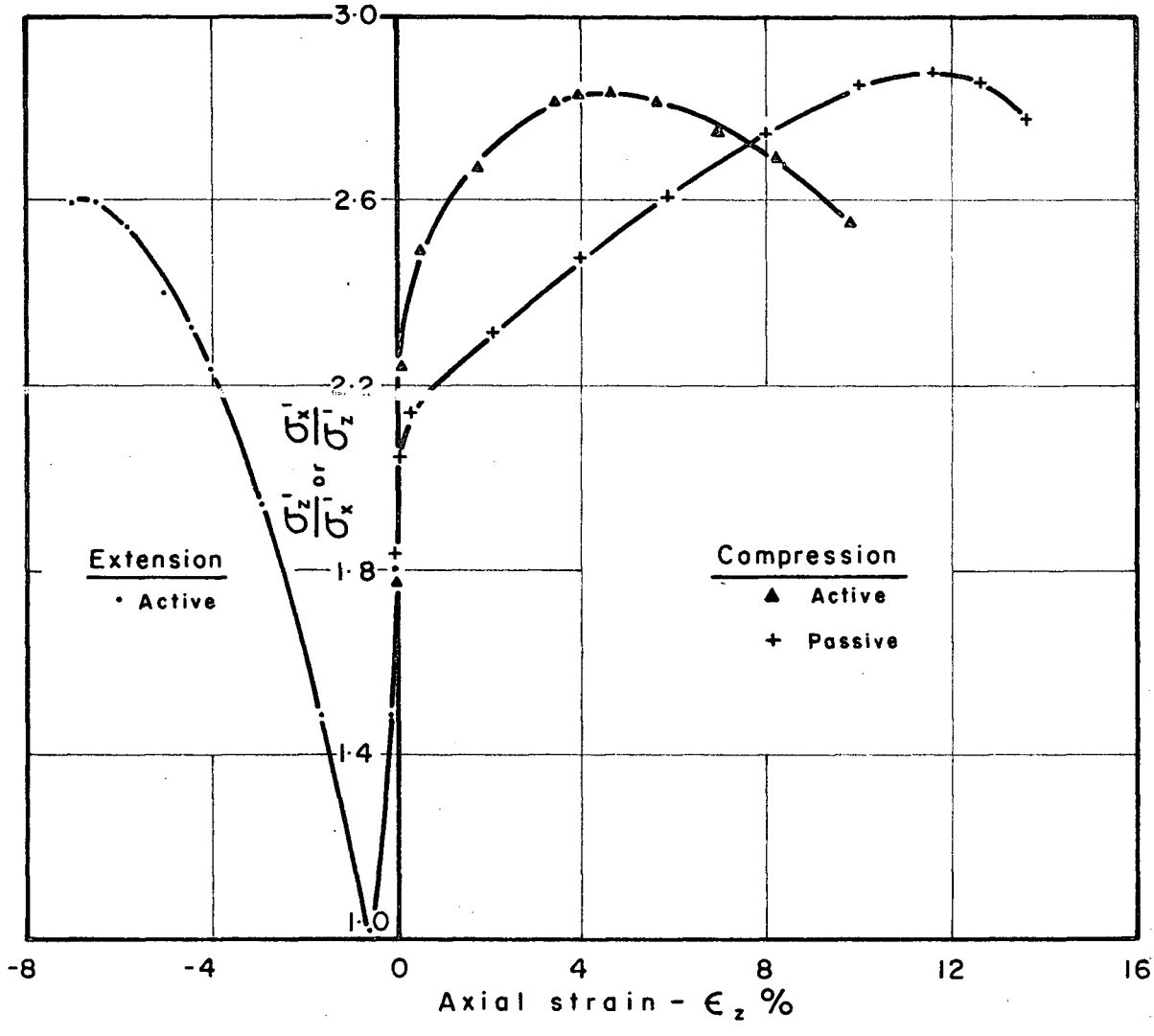

Fig.5·9 EFFECTIVE STRESS RATIO-STRAIN RELATIONSHIPS DURING DRAINED PLANE STRAIN SHEAR- N.C. HANEY CLAY.

compression ϕ' will, therefore, lead to an estimate on the unsafe side.

Failure during active extension occurred with a low peak deviator stress (about 55% of the active compression value). This was due to smaller effective stresses on the sample at failure. Also the associated ϕ' for extension was lower than for compression failure by an amount of about 3°. The axial strain at failure was around 7%.

Previously, Fig. 5.3 showed that during undrained extension σ'_y was the minor and not the intermediate principal stress during early stages of the shear. A similar situation was found to exist for drained active extension shear, where σ'_y remained the minor principal stress until about 2% axial strain. Thereafter, σ'_y, assumed a value intermediate between σ'_x and σ'_z. However, the stress ratio, $\sigma'_y/(\sigma'_x+\sigma'_z)$, was found to stay essentially constant during drained shear also and, the magnitude of this ratio (0.37 ± 0.02) was found to be independent of the applied stress path (see Fig. 5.4). This ratio had the same constant magnitude during undrained shear.

5.2.2 Volume Changes

Fig. 5.10 shows volumetric strains, v, during drained shear as a function of axial strain, ε_z, for the three tests. A comparison of Fig. 5.10 with Fig. 5.5 will show the similarity of the volumetric strains with pore pressure changes for the corresponding stress paths. Passive compression shear was associated with very large volume decreases and the rate of volume change is seen to be considerable at peak deviator stress. This implies that not all the input energy was being dissipated in overcoming shear stresses, but a part of it was utilized in doing work against the confining pressure. A similar situation existed for active compression, but to a lesser degree. This volume decrease behaviour is due in part to breakdown of structural framework of particles in the sensitive marine clay, which is brought about by applied shear stresses. The clay structure as a result is rendered more compressible. During active extension shear, a very small volume increase occurred. This would imply that the active extension response during drained shear will be very close to that during undrained shear.

5.2.3 Failure Conditions

As shown in Fig. 5.9 the peak effective stress ratio, σ_1'/σ_3', in both types of axial compression was

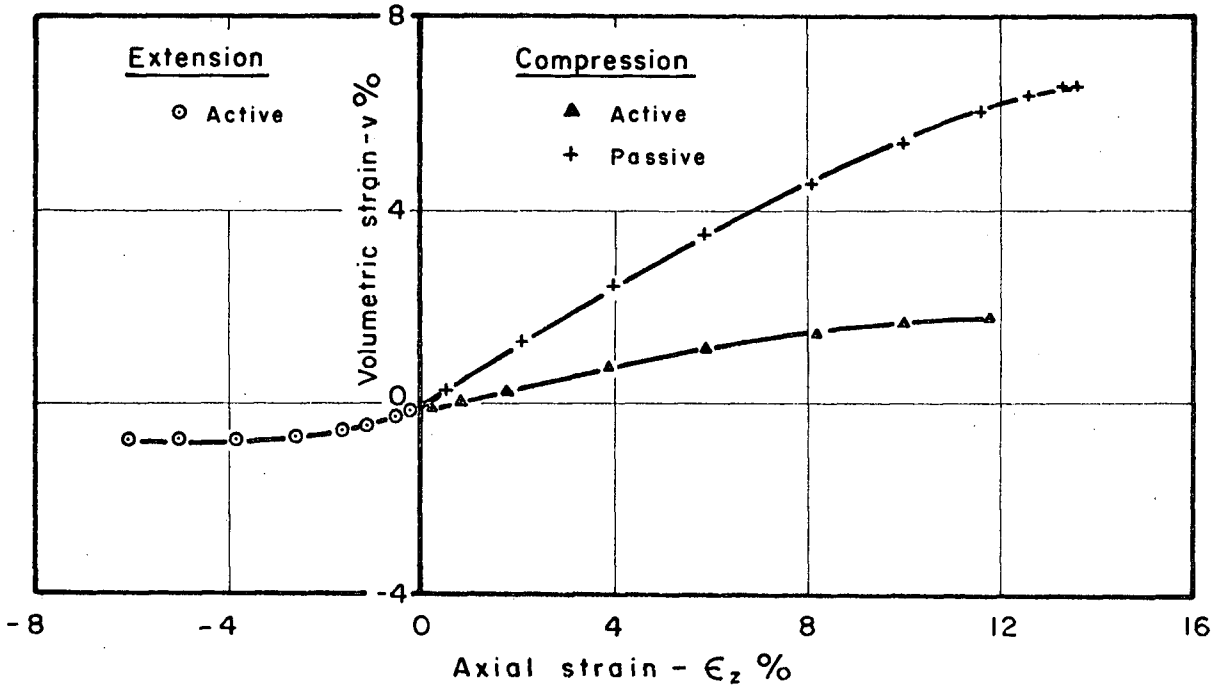

Fig. 5·10 VOLUMETRIC STRAIN - AXIAL STRAIN RELATIONSHIPS DURING DRAINED PLANE STRAIN SHEAR- N.C. HANEY CLAY.

approximately the same and corresponds to an average $\phi' = 28.8°$. On the other hand ϕ' in extension was 26.5°. This result is different from that reported by Hambly and Roscoe (1969), who found the same ϕ' for drained plane strain compression and extension; however, their result was for a remolded clay as opposed to undisturbed natural sensitive clay reported herein.

5.3.0 Comparison and Correlation of Drained and Undrained Test Results

There seems to be no similarity between the compression and extension plane strain behaviour of Haney clay. Thus, a comparison between drained and undrained tests will be considered separately for axial compression and axial extension modes of shear.

5.3.1 Drained and Undrained Stress-Strain Characteristics

The hypothesis that a unique relationship exists between void ratio and effective stresses for a saturated normally consolidated remolded clay was first proposed by Rendulic (1937), who argued that the new void ratio after a change in effective stresses is not dependent on the stress path but is exclusively determined by the new principal effective stresses.

His tests consisted of conventional load increasing drained and undrained triaxial tests on samples which were initially isotropically consolidated. Rendulic also suggested the anisotropically consolidated specimens would fall into the same pattern. Later, Henkel (1960) verified and amplified Rendulic's hypothesis using tests with more elaborate stress paths. Investigations by Whitman et. al. (1960), Skempton and Sowa (1963) and further results of Henkel and Sowa (1963), however, demonstrated that anisotropically consolidated specimens do not fit in the pattern of unique void ratio effective stress relationship for isotropically consolidated specimens. The reason advanced for this disagreement was the presumably different microstructure built up during dissimilar consolidation histories of the specimens, resulting in different properties, even if the effective stresses were the same.

Roscoe et. al's (1958) concept of a unique state boundary surface is an alternate statement of Rendulic's concept of uniqueness of void ratio and effective stresses for the triaxial tests. Roscoe and Poorooshasb (1963) proposed a two-dimensional plot of the entire state boundary surface by using p/p_e and q/p_e as axes. Where

$p = 1/3\ (\sigma_1' + \sigma_2' + \sigma_3')$

$q = (\sigma_1' - \sigma_3')$

p_e = equivalent pressure - which is the pressure on the virgin consolidation line corresponding to the current void ratio of the specimen.

The stress parameter p and q specify completely the current stress state in the triaxial tests. Rendulic's uniqueness concept then implies that isotropically normally consolidated remolded clay when tested in load increasing drained or undrained compression possesses a unique surface in (p,q,e) space.

No attempt appears to have been made to investigate the possibility that Rendulic's hypothesis may also hold for a normally consolidated clay with a given type of anisotropic consolidation history, e.g., K_o-consolidation history. Since K_o-consolidation is believed to impart to the clay a microstructure different from that obtained under isotropic consolidation, the unique surface in (p,q,e) space for K_o-consolidated clay, (called the anisotropic yield or state boundary surface hereinafter) in case such a surface exists, will be different from the isotropic yield surface in the same space. The possibility that a unique anisotropic yield surface may exist for

normally K_o-consolidated Haney clay will now be examined. If such a surface does exist, the implications thereof can then be used to correlate drained and undrained tests.

A unique yield surface in (p,q,e) space suggests that void ratio is a function of mean normal stress, p, and of an appropriate measure of shear stress, which is q in the triaxial tests. During plane strain deformation $\sigma_2' \neq \sigma_1'$ or σ_3' and, therefore, τ_{oct} will be the more appropriate measure of shear stress in preference to q. It is, therefore, postulated that a unique yield surface in (p, τ_{oct}, e) space might exist for load increasing compression tests on K_o-consolidated Haney clay. The corresponding two-dimensional plot of this surface would then be with p/p_e and τ_{oct}/p_e as axes. Since only K_o-consolidation conditions are considered, p_e will be referred to the virgin K_o-consolidation line (Fig. 3.4) as opposed to virgin isotropic consolidation line considered by Roscoe and Poorooshasb (1963) for treating isotropically consolidated clays.

Fig. 5.11 shows all drained and undrained compression tests plotted with p/p_e and τ_{oct}/p_e as axes. It can be seen that except for the small initial deviations the load increasing drained passive compression test results lie on the state boundary surface curve determined by the

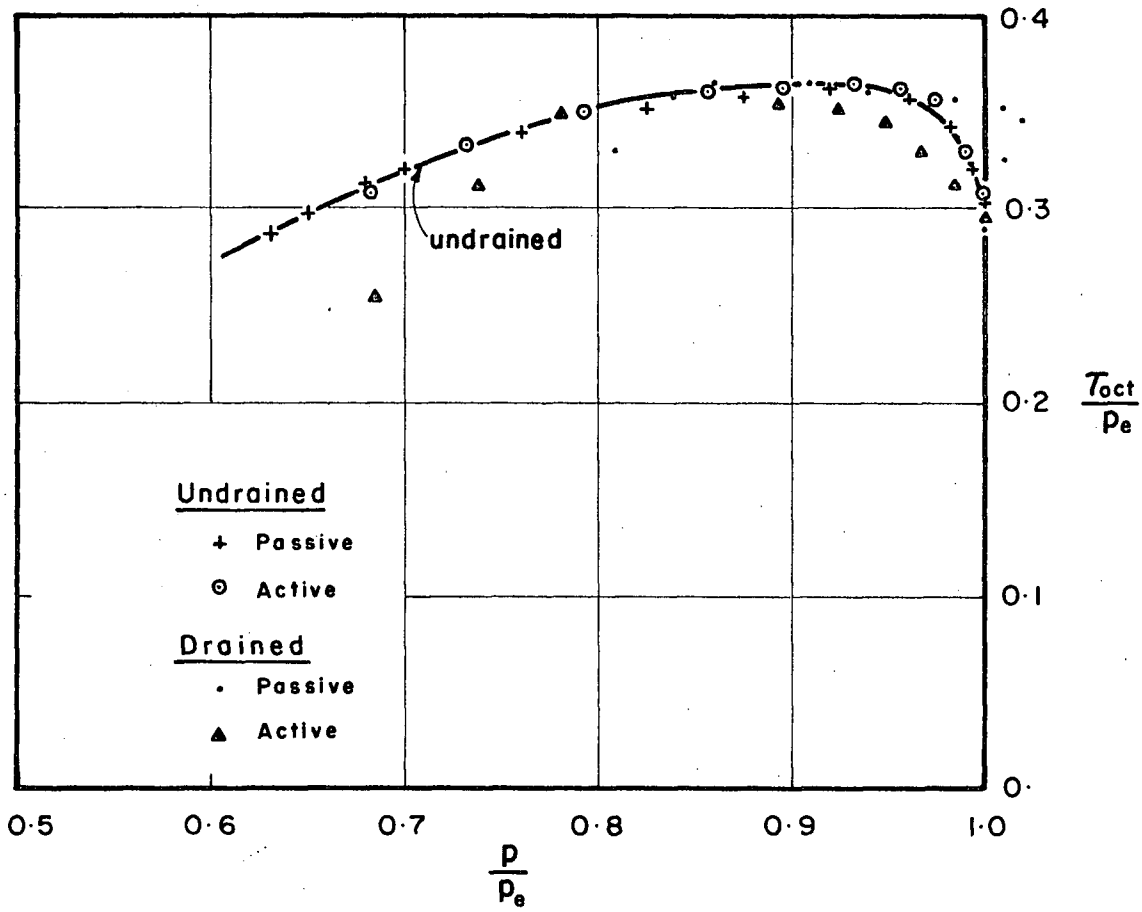

Fig.5·11 STATE BOUNDARY SURFACE CURVE FOR PLANE STRAIN COMPRESSION TESTS- N.C. HANEY CLAY.

undrained tests. The initial departure from the undrained state boundary surface curve is believed to be due to an incomplete dissipation of excess pore pressures at small strains of the order of 1/2% ε_z. This discrepancy, which arises as a result of strain controlled loading, could possibly be eliminated in a stress controlled type of test. Results of unloading drained active compression test, however, fall slightly below the state boundary surface curve for the undrained tests. This is in accordance with Rendulic's restriction on the uniqueness concept, which was considered valid for only those stress paths which resulted in consolidation or volume decrease of the specimen. Plane strain specimens, when sheared under drained active compression, underwent a small initial increase in void ratio. If as a first approximation the undrained state boundary surface curve can be considered to be applicable for load increasing drained compression stress paths, then it is possible to predict change in void ratio due to the addition of a stress increment in drained plane strain tests by reversing the procedure used to construct Fig. 5.11. For example, for the current state of stress $(p, \tau_{oct})_1$, the ratio τ_{oct}/p can be determined and then from Fig. 5.11 the point where this τ_{oct}/p ratio cuts the undrained state boundary surface curve is found

and the value of p/p_e is read. Since p is known, this gives p_e which is the point on the virgin K_o-consolidation line having the same void ratio as the stress state $(p, \tau_{oct})_1$. After the stress increment is applied the new value of p_e is found in the same manner for the new state of stress $(p, \tau_{oct})_2$. Knowing the compression index, λ, ($\lambda = e_1-e_2/\ln p_2-\ln p_1 = .252$ from Fig. 3.4) the difference in void ratio for the two states of stress can be determined, which can be expressed as a volumetric strain.

τ_{oct}/p vs. volumetric strain relationship predicted by the above mentioned technique for the drained passive compression test is shown in Fig. 5.12 by the soild curve. The observed τ_{oct}/p vs. volumetric strain relation is also shown. Except for the small overprediction in the initial stages, there is an excellent agreement between the predicted and observed volumetric strains. As already pointed out, the discrepancy in the initial stages of the test could be the result of only incomplete dissipation of excess pore pressures during the strain controlled type of drained shear.

Predicted and observed volumetric strains during drained active compression are shown in Fig. 5.12a. For values of $\tau_{oct}/p < 0.41$ the predicted strains are zero. Thereafter, the observed strains tend to be larger than predicted.

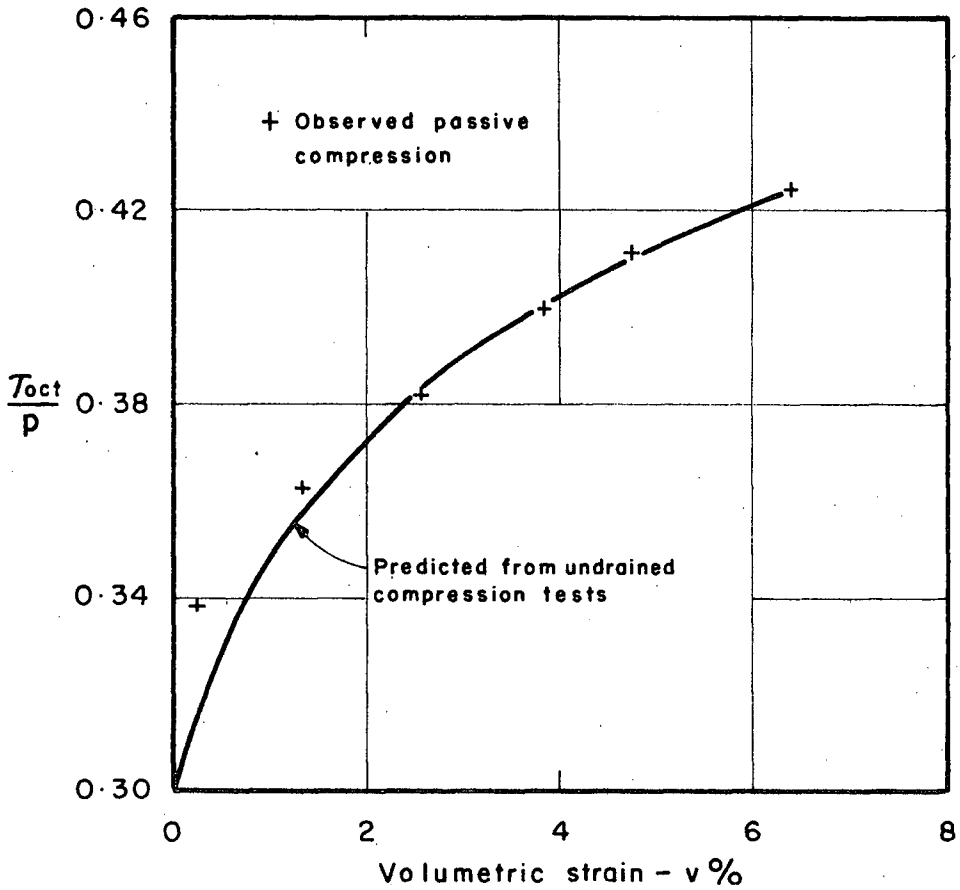

Fig.5·12 COMPARISON OF PREDICTED AND OBSERVED VOLUMETRIC STRAINS DURING DRAINED PLANE STRAIN PASSIVE COMPRESSION- N.C. HANEY CLAY.

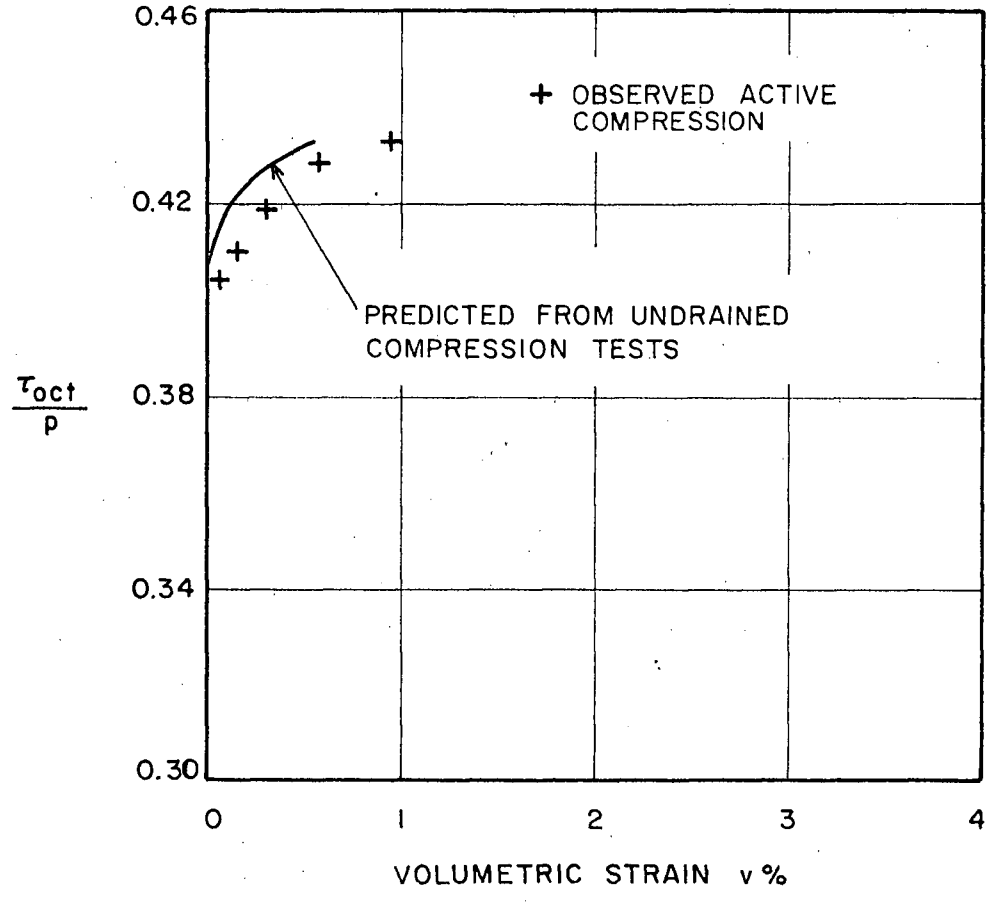

FIG. 5.12a COMPARISON OF OBSERVED AND PREDICTED VOLUMETRIC STRAINS DURING DRAINED PLANE STRAIN ACTIVE COMPRESSION – N.C. HANEY CLAY.

It is therefore suggested, that the Rendulic approach can be extended to predict volumetric strains in load increasing drained compression tests from the results of undrained compression tests, provided the specimens considered have the same consolidation history. Alternatively, pore pressures could be predicted during undrained tests from the results of drained tests.

Rendulic's hypothesis was limited to cases where deviator stress was being increased and the clay underwent consolidation. Roscoe and Schofield (1963) considered the situation which involved unloading of shear stresses. According to their suggestion, the volumetric strains during drained active extension triaxial shear (which involves unloading of both q and p) would be determined solely by the changes in p. The increase in void ratio, Δe, due to a reduction in p from p_1 to p_2 was proposed to be governed by $\Delta e = \kappa \ln p_1/p_2$ where κ is the slope of isotropic swelling curve. If the same criterion is used to estimate volumetric strains in plane strain drained active extension shear, the observed strains were found to be in close agreement with prediction. Volumetric strains in this active extension test were very small (< 0.75% at failure) and, therefore, their prediction seems to be of hardly any importance.

In the drained tests volumetric strains alone, however, are insufficient to describe the complete state of

strain. Consideration has been given to the prediction of shear strains in drained test on the assumption that normally consolidated saturated clays can be assumed to yield according to the work hardening theory of plasticity (as done in Cambridge stress-strain theory). A prediction of shear strains in the drained passive compression test, from the results of undrained compression tests, can be attempted using normality condition of the plasticity theory, if the following assumptions are made:

1. The empirical stress-void ratio surface of the Rendulic type can be regarded as the yield surface which is assumed to be symmetric about p axis in (p, τ_{oct}) space. Irrecoverable or plastic strains occur only for states of the sample on this yield surface.

2. The current yield locus can be considered to be identical with the undrained stress path corresponding to the current void ratio state of this specimen. In the Cambridge theory this is equivalent to the assumption, $\kappa = 0$.

3. All strains are considered irrecoverable.

In Fig. 5.13 a typical current yield locus is shown in (p, τ_{oct}) axes. This locus is the undrained stress path corresponding to the current void ratio of the sample. If a stress increment is now applied on the stress state at P, the normality condition requires

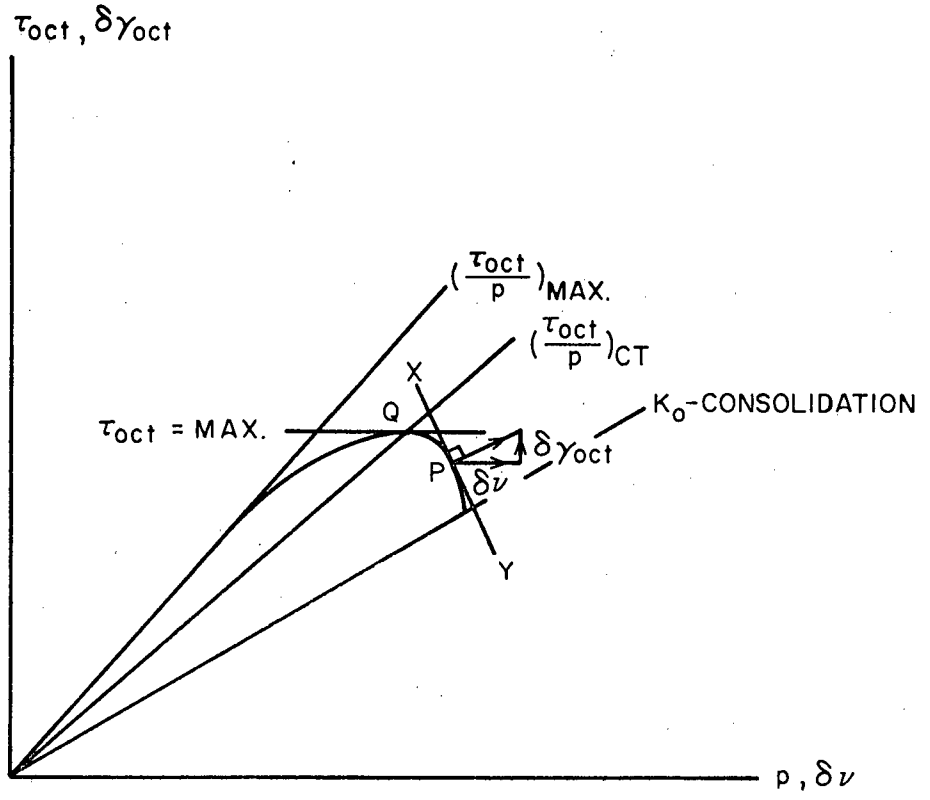

FIG. 5.13 TYPICAL UNDRAINED STRESS PATH AND ASSUMED CURRENT YIELD LOCUS FOR N.C. HANEY CLAY.

$$\frac{\delta \gamma_{oct}}{\delta v} = - \frac{1}{\frac{d\tau_{oct}}{dp}} \tag{5.3}$$

where

$$\delta\gamma_{oct} = \frac{1}{3}\sqrt{(\delta\varepsilon_1-\delta\varepsilon_2)^2 + (\delta\varepsilon_2-\delta\varepsilon_3)^2 + (\delta\varepsilon_3-\delta\varepsilon_1)^2} \tag{5.4}$$

$$\delta v = \delta\varepsilon_1 + \delta\varepsilon_2 + \delta\varepsilon_3 \tag{5.5}$$

Consider a soil element in equilibrium under a state $(p, \tau_{oct}, e)_1$ and let a stress increment be applied resulting in the new equilibrium state, $(p, \tau_{oct}, e)_2$. Restricting the stress changes to the stress path corresponding to drained passive compression, increment in δv due to the applied stress increment can be determined from the extended Rendulic anisotropic yield surface, using the procedure described earlier in this section. The current yield locus corresponding to the state $(p, \tau_{oct}, e)_1$ will be the undrained stress path with $e = e_1$. A graphical evaluation of the slope of this

yield locus at the basic stress state $(p, \tau_{oct})_1$ gives the magnitude of the strain increment ratio, $\delta\gamma_{oct}/\delta v$, and hence $\delta\gamma_{oct}$ can be determined as δv is already known. Repetition of this incremental procedure in small steps of increments in stress ratio, τ_{oct}/p, determines the desired predicted shear stress-strain relationship. It may be mentioned here, that for any stress state (p, τ_{oct}), the slope of current yield loci is a function of stress ratio τ_{oct}/p only and can be determined from the single undrained state boundary surface curve of Fig. 5.11.

The predicted τ_{oct}/p vs. $\int\delta\gamma_{oct}$ relationship for the drained passive compression test is shown in Fig. 5.14, along with the observed relationship. The prediction of shear strains cannot be made for τ_{oct}/p values ≥ 0.38 which is the critical stress ratio, $(\tau_{oct}/p)_{CT}$, at which the tangent to the undrained stress paths (or yield loci) becomes horizontal (see Fig. 5.13). From the normality condition this implies unlimited shear distortion, $\delta\gamma_{oct}$, without any volume change, i.e. $\delta\gamma_{oct}/\delta v \rightarrow \infty$. However, the predicted stress-strain relationship for values of $\tau_{oct}/p < (\tau_{oct}/p)_{CT}$ is in satisfactory agreement with the observed relationship up to $\int\delta\gamma_{oct} \sim 1.5\%$, which corresponds to an axial strain $\varepsilon_z \sim 2.5\%$. The axial strain at failure in drained passive compression was around 12% and, therefore, normality condition of plasticity theory can, at best,

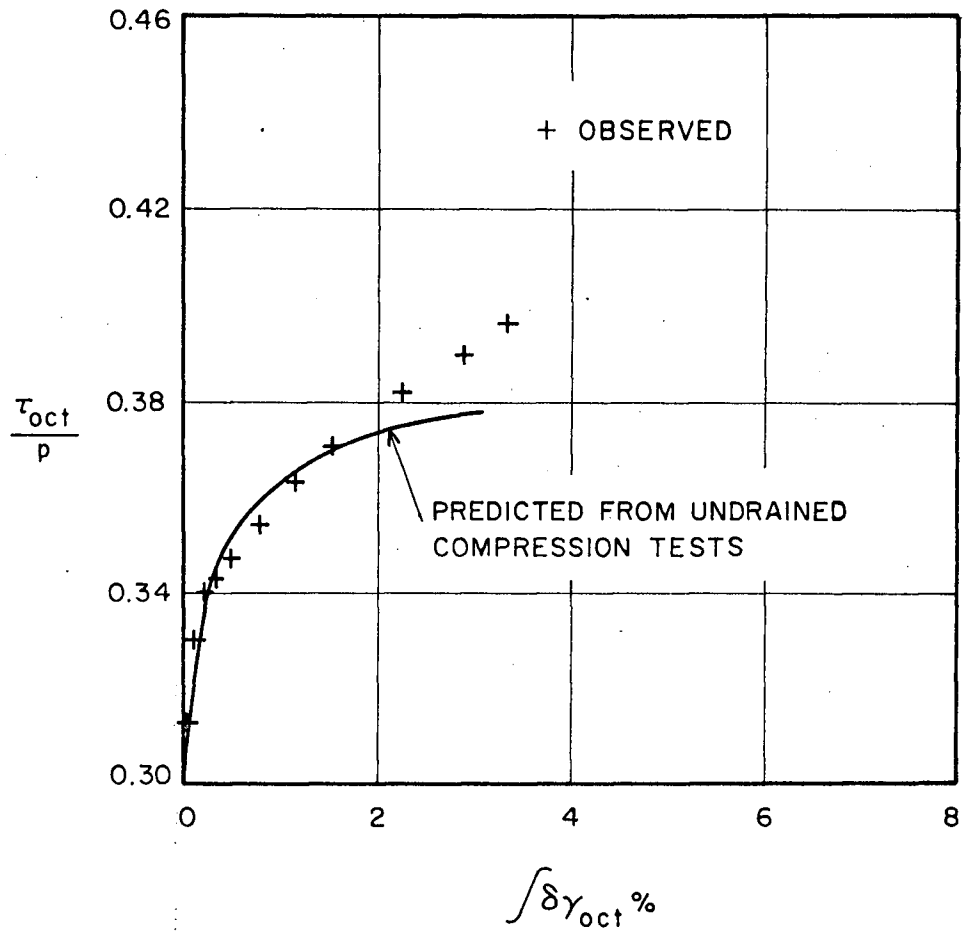

FIG. 5.14 COMPARISON OF OBSERVED AND PREDICTED SHEAR STRAINS DURING DRAINED PLANE STRAIN PASSIVE COMPRESSION - N.C. HANEY CLAY.

provide reasonable prediction of shear strains until about 20% of the failure strains. For clays in which the condition of τ_{oct} = max is identical with the condition of τ_{oct}/p = max (such as in remolded clays), shear strain predictions could be attempted for the entire drained stress path.

During drained active compression shear, the applied stress increments are such that the stress increment vector at the stress point P is directed to the left of the tangent to the yield locus (see Fig. 5.13). Such stress changes imply unloading, i.e. they do not cause plastic distortion. Because all strains were assumed irrecoverable, the clay would remain rigid with respect to shear strains during the imposed active compression drained shear. Stress changes during drained active extension shear also correspond to unloading and this would again imply rigid behaviour in shear. Roscoe and Burland (1968) used the concept of a double yield locus to determine irrecoverable shear distortion for state paths below the yield surface. For $\kappa = 0$ clays, their concept implies that the τ_{oct}/p vs. γ_{oct} relationship for those drained tests whose state paths lie entirely below the yield surface is identical to the τ_{oct}/p vs. γ_{oct} relationship for the corresponding undrained test. In the active compression undrained test,

$(\tau_{oct}/p)_{CT}$ = 0.38 was reached at γ_{oct} = 0.1% and, therefore, the identity of τ_{oct}/p vs. shear strains relation in undrained and drained tests cannot even be attempted by Roscoe and Burland's method for γ_{oct} > 0.1%. For drained active extension test, however, their method correctly predicts an almost identical τ_{oct}/p vs. γ_{oct} relationship to that of the corresponding undrained test (Fig. 5.15).

5.3.2 Stress σ'_y

One common feature of all the undrained and drained plane strain test was the nature of variation of principal stress σ'_y, associated with the direction of zero strain. Similar to the observation of Hambly and Roscoe (1969) for a remolded Kaolin, the ratio $\sigma'_y/(\sigma'_x+\sigma'_z)$ stayed essentially constant during plane strain shear of Haney clay (Fig. 5.4). It is interesting to note that the magnitude of this ratio, which resembles Poisson's ratio for an elastic material, was very nearly equal to $K_o/(1+K_o)$. The latter expression also equals Poisson's ratio if linear elastic behaviour is assumed during one-dimensional (K_o) consolidation. Similar relationships i.e. $\sigma'_y/(\sigma'_x + \sigma'_z) \sim K_o/(1+K_o)$ can be shown to exist in the results of Henkel and Wade (1966) and Hambly and Roscoe

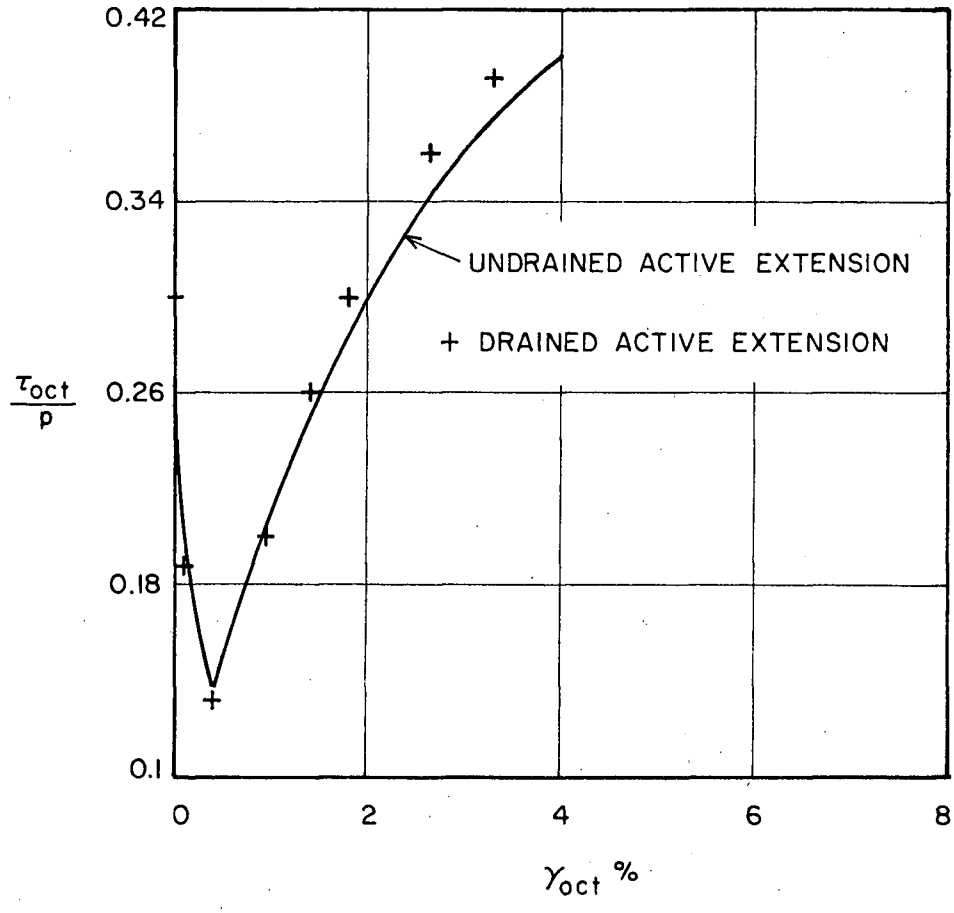

FIG. 5.15 COMPARISON OF SHEAR STRESS - STRAIN RELATIONSHIP DURING PLANE STRAIN DRAINED AND UNDRAINED ACTIVE EXTENSION _ N.C. HANEY CLAY.

(1969). Such a relationship can prove very useful for estimating σ_y' in plane strain, if K_o value of the normally consolidated clay is known.

5.4.0 Drained and Undrained Strength Characteristics

The results of all the plane strain tests are summarized in Table II. For the same type of drained and undrained tests the relative strength, as characterised by $|\sigma_z-\sigma_x|_{max}/2$, depends on the nature and the amount of volume change in the drained test. Passive compression tests are the conventional types of compression test, in which drained strength is much larger than the undrained strength. Haney clay, because of its sensitive nature, underwent a volume decrease in active drained compression despite decreasing mean normal stresses; this resulted in drained strength being higher than the undrained strength of an identical specimen. This is contrary to the usual concept that active drained strength is always smaller than the undrained value (Bishop and Henkel, 1962). During active axial extension the specimen underwent a small swelling, and therefore drained strength mobilized was smaller than the corresponding undrained value. It is surprising that the remolded clay used by Hambly and Roscoe (1969) showed a

TABLE II

Summary of Plane Strain Test Results on N.C. Haney Clay

	End of Consolidation		Failure Condition									
			$(\sigma_1-\sigma_3)_{max}$						$(\sigma_1'-\sigma_3')_{max}$			
	σ'_{zc}	K_o	Axial Strain %	$\frac{\sigma_1-\sigma_3}{\sigma'_{zc}}$	a	v%	σ_1'/σ_3'	ϕ'	Axial Strain %	σ_1'/σ_3'	ϕ'_m	ϕ'_c
Undrained Tests												
Passive compression	6.01	.55	.4	.582	1.2	0	2.49	25.3°	2.9	3.10	30.8°	30.8°
Active compression	5.93	.55	.5	.59	1.15	0	2.52	25.6°	2.6	3.00	30.0°	30.0°
Active extension	5.90	.56	-7.1	.392	.91	0	2.59	26.3°	-7.1	2.59	26.3°	26.3°
Passive extension	5.87	.57	-5.2	.394	.90	0	2.56	26.0°	-5.2	2.56	26.0°	26.0°
Drained Tests												
Passive compression	5.96	.54	12.0	.95	—	6.0	2.88	29.0°	12.0	2.88	29.0°	32°
Active compression	5.98	.56	4.5	.605	—	0.9	2.85	28.7°	4.5	2.85	28.7°	31°
Active extension	5.87	.55	-7.0	.341	—	-0.8	2.61	26.5°	-7.0	2.61	26.5°	26.5°

Stresses in Kg/cm^2

ϕ'_m = ϕ' measured

ϕ'_c = ϕ' corrected for volume change

volume decrease in the drained active extension shear, and a highly flocculated marine clay used in this study underwent swelling. Considerations of the differences in soil structure of a remolded and an undisturbed marine clay would predict larger swelling during unloading type shear of a remolded clay (Scott, 1963).

A comparison of the measured effective strength parameter, ϕ', during drained and undrained shear is also presented in Table II for both failure conditions - $|\sigma_z-\sigma_x|_{max}$ and $(\sigma_1'/\sigma_3')_{max}$. During drained shear the two failure conditions coincide. At $|\sigma_z-\sigma_x|_{max}$, ϕ' was essentially the same (25.9° ± 0.6°) for all stress paths excepting drained compression. At $(\sigma_1'/\sigma_3')_{max}$, the measured ϕ' in drained compression was about 1.5° smaller than the corresponding undrained compression value, whereas the drained and undrained extension ϕ' were essentially the same. However, a fundamental comparison between drained and undrained ϕ' at $(\sigma_1'/\sigma_3')_{max}$ can only be made if drained tests are corrected for energy expended in volume change at failure. This is particularly essential for tests on Haney clay in which significant volume changes were taking place near drained compression failure. The correction to measured peak deviator stress was applied as recommended by Bishop (1953, 1964). Thus for the drained tests

$$(\sigma_z-\sigma_x)_{corrected} = (\sigma_z-\sigma_x)_{measured} + \sigma'_x \cdot \frac{dv}{d\varepsilon_z} \qquad (5.6)$$

where $dv/d\varepsilon_z$ is the slope of volumetric strain vs. axial strain plot at $|\sigma_z-\sigma_x|_{max}$. The corrected ϕ' is then calculated by

$$\sin \phi'_{corrected} = \frac{(\sigma_z-\sigma_x)_{corrected}}{(\sigma_z-\sigma_x)_{corrected} + 2\,\sigma'_x} \qquad (5.7)$$

In Table II both measured ϕ' and ϕ' corrected for volume change component in drained test are shown. It can be seen that ϕ' was practically the same for all compression tests - drained or undrained. This result for plane strain tests is similar to the reslt on clays from the conventional isotropically consolidated triaxial tests. Similarly ϕ' in undrained and drained extension was the same (there is no energy component in drained active extension test, since $dv/d\varepsilon_z = 0$). But ϕ' associated with compression failure was on the average 5° larger than ϕ' associated with extension failure.

CHAPTER VI

RESULTS OF TRIAXIAL TESTS ON NORMALLY CONSOLIDATED HANEY CLAY

In this chapter the results of triaxial tests on normally consolidated Haney clay are described. For the same total stress path the triaxial behaviour was found to be qualitatively very similar to the behaviour under plane strain conditions. The reasons advanced for a particular kind of observed plane strain behaviour, under a given total stress path, therefore, apply to triaxial conditions also. The triaxial results are discussed only briefly. Details are presented for those triaxial tests only which deviate in a marked way from their plane strain counterparts.

6.1.0 Undrained Test Results

For identical K_o-consolidated specimens the results of tests under the four total stress paths are shown in Fig. 6.1 through Fig. 6.6. The following characteristics of the results can be noted from these figures.

1. The two compression stress paths resulted in identical $|\sigma_z-\sigma_x|/\sigma'_{zc}$ vs. ε_z relationship and so did the two extension stress paths (Fig. 6.1). However, the relationship was different for compression and extension stress paths. Compression failure ($|\sigma_z-\sigma_x|_{max}$) occurred at only 0.4% axial strain compared to about 7% axial strain required to induce extension failure.

2. The extension undrained strength, $|\sigma_z-\sigma_x|_{max}/2$, was slightly less than half of the compression value (Fig. 6.1). This result is similar to those reported by Ladd (1965, 67) and Bjerrum and Kenny (1967). The peak deviator stress in extension was even smaller than the value of deviator stress the specimen could sustain at the end of K_o-consolidation. There was a very large post peak drop in deviator stress during compression shear.

3. The condition of $(\sigma'_1/\sigma'_3)_{max}$ was reached at about 6% axial strain during axial compression shear (Fig. 6.2). During axial extension shear the maximum deviator stress and the maximum stress ratio, $(\sigma'_1/\sigma'_3)_{max}$, occurred at the same strain.

4. During active extension stress path, despite a very large unloading of mean normal stresses, the net change in pore pressure at failure was positive (Fig. 6.3). This is indicative of the pronounced increase in compressibility

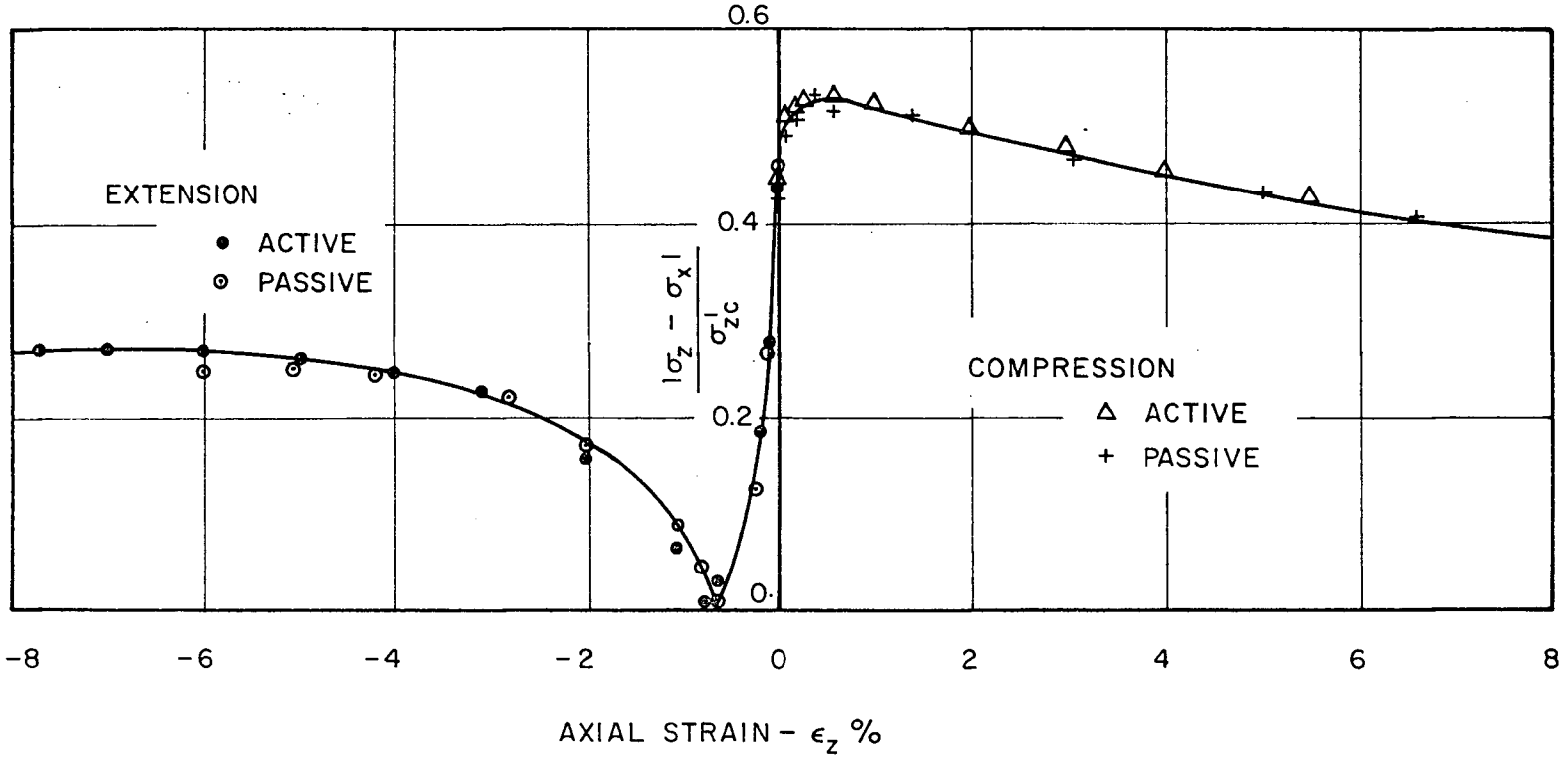

FIG. 6.1 DEVIATOR STRESS-STRAIN RELATIONSHIP DURING UNDRAINED TRIAXIAL SHEAR - N.C. HANEY CLAY.

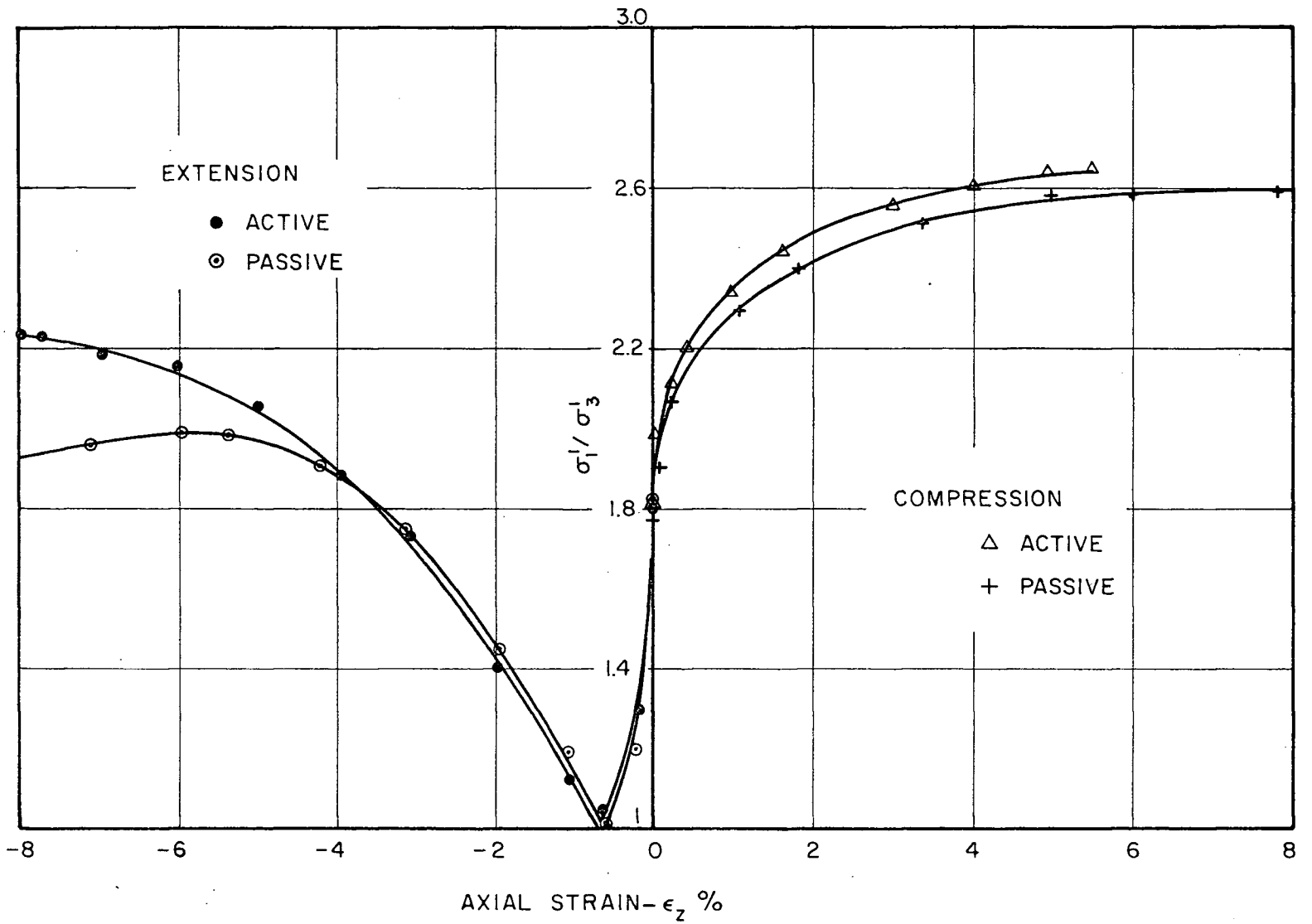

FIG. 6.2 PRINCIPAL EFFECTIVE STRESS RATIO - STRAIN RELATIONSHIPS DURING UNDRAINED TRIAXIAL SHEAR - N.C. HANEY CLAY.

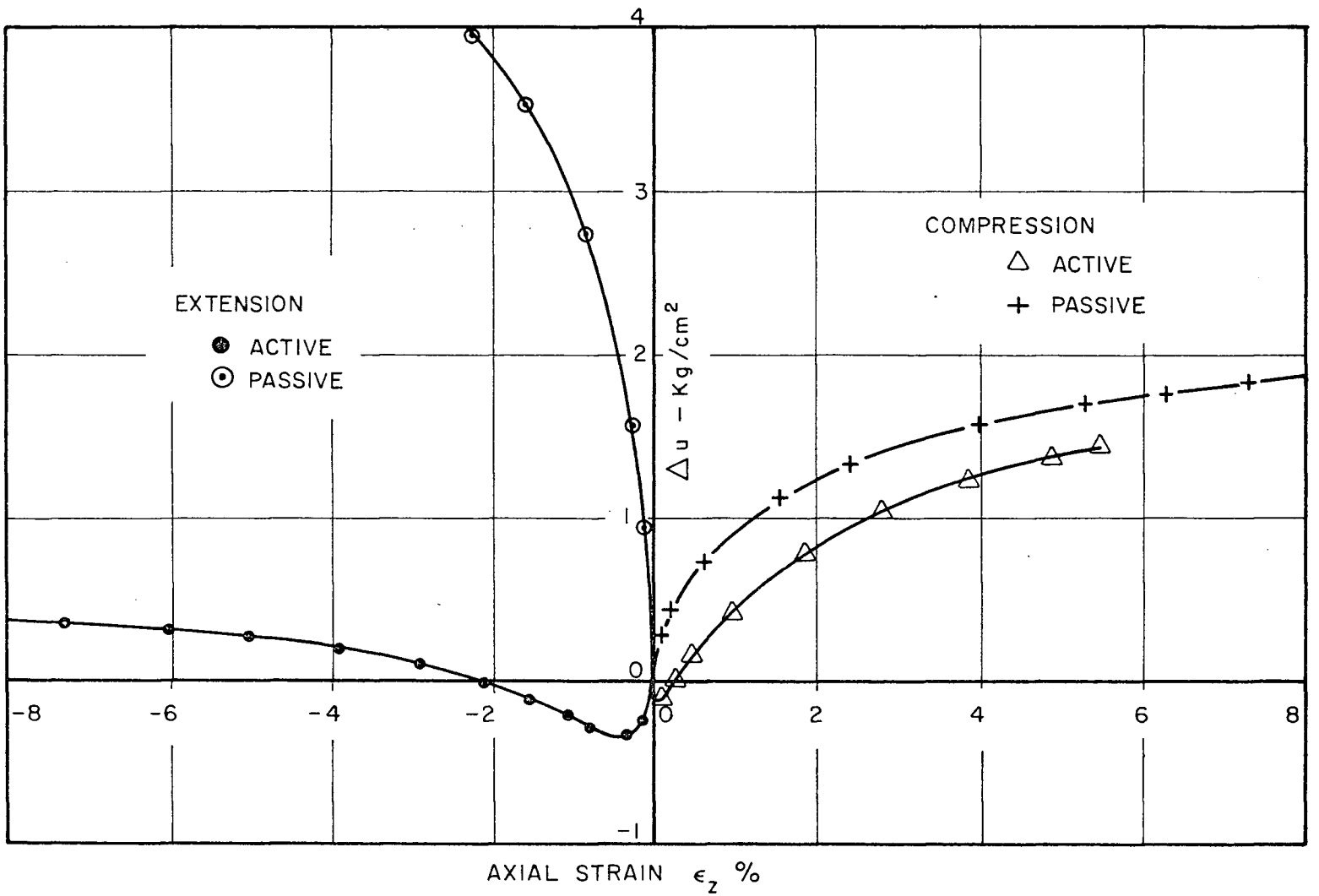

FIG. 6.3 PORE PRESSURE CHANGE - STRAIN RELATIONSHIPS DURING UNDRAINED TRIAXIAL SHEAR - N.C. HANEY CLAY.

of the sensitive clay skeleton due to imposed shearing stresses. Pore pressure parameter 'a' vs. axial strain 'ε_z' relationship is practically identical for similar strain paths (Fig. 6.4). However, the relationships for axial compression and axial extension stress paths have no similarity with each other.

5. Effective stress paths followed in σ_z'/σ_{zc}' vs. σ_x'/σ_{zc}' stress space were practically identical for similar strain paths (Fig. 6.5). The average value of ϕ' at $(\sigma_1'/\sigma_3')_{max}$ for axial compression shear was found to be 26.6° compared to 21° during axial extension shear. This result is opposite to those reported by Ladd and Bailey (1964) and Ladd (1967), who reported $\phi'_{extension} = \phi'_{compression}$ + 8 to 10° for one natural and one remolded clay. In the conventional type of triaxial apparatus, discounting of even a very small ram friction can result in gross overestimates of the ratio $(\sigma_1'/\sigma_3')_f$ in extension tests. For the active extension test the axial stress is the minor principal stress at failure and its magnitude is generally small, considering the usual range of pressures for laboratory testing of clays. For a given amount of error in σ_3', the ratio $(\sigma_1'/\sigma_3')_f$ is affected more severely, particularly when σ_3' is relatively small. The K_o-triaxial apparatus used in this study was equipped with a frictionless ram and,

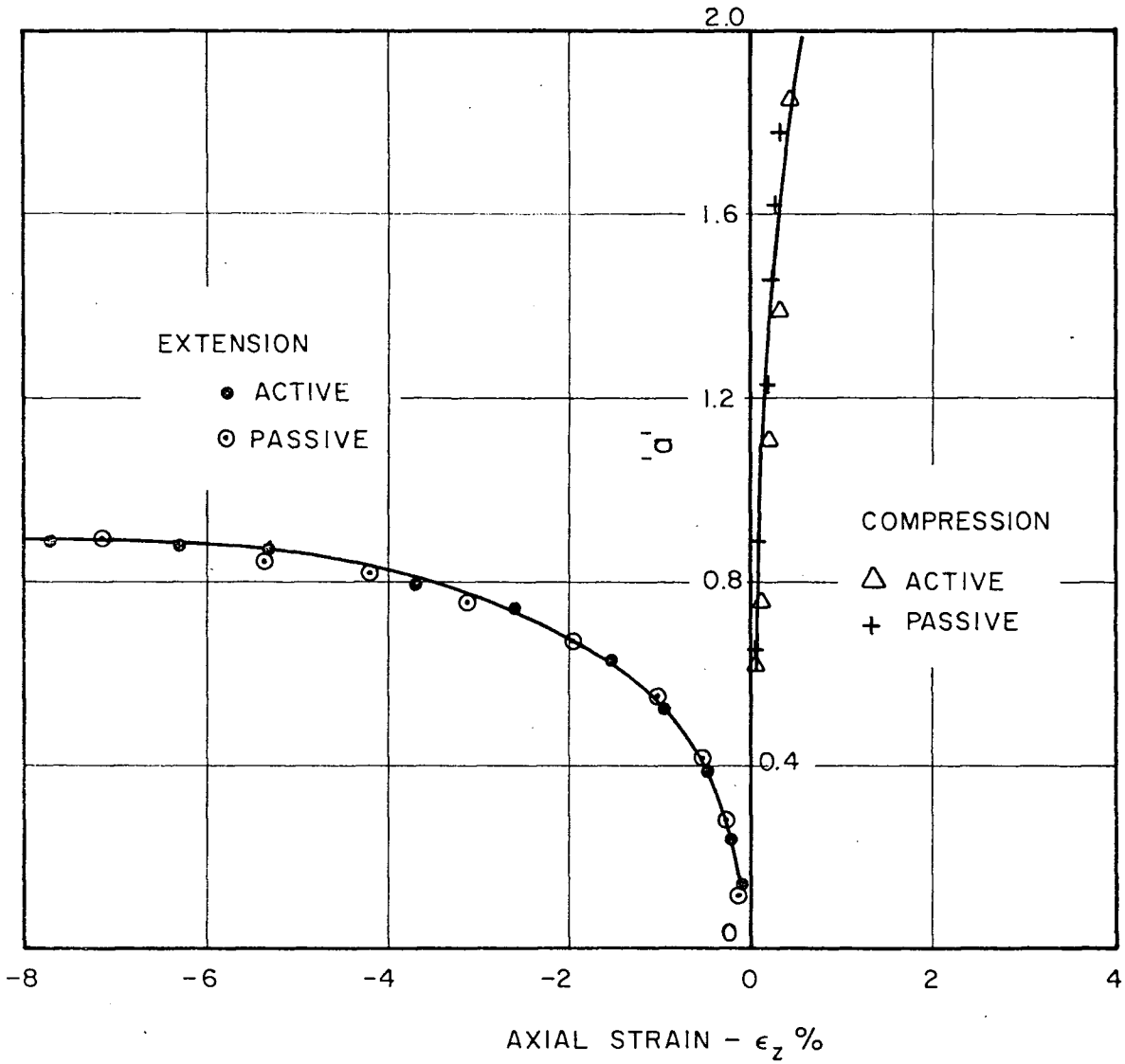

FIG. 6.4 PORE PRESSURE PARAMETER 'a' - STRAIN RELATIONSHIPS DURING UNDRAINED TRIAXIAL SHEAR - N.C. HANEY CLAY.

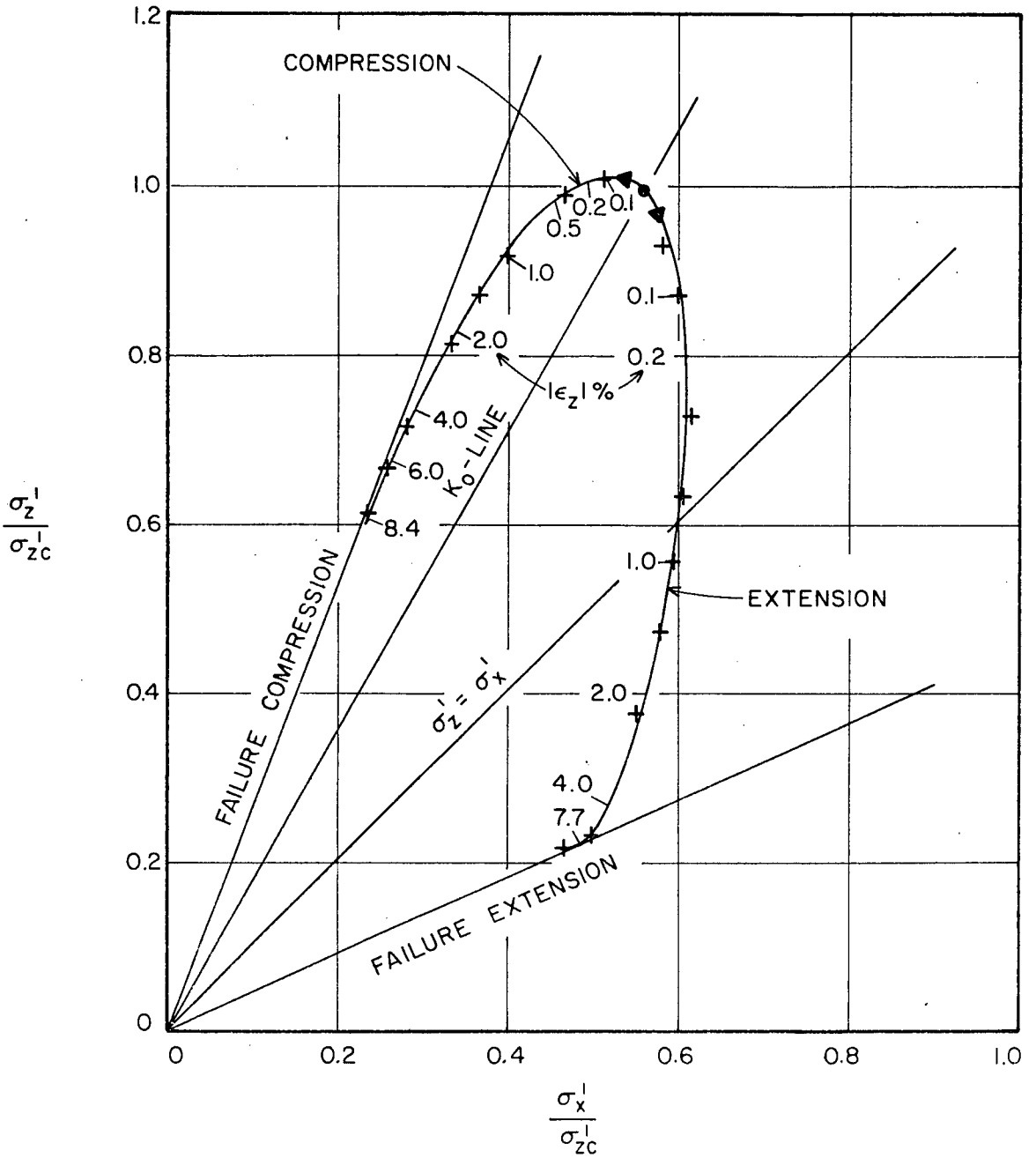

FIG. 6.5 EFFECTIVE STRESS PATHS DURING UNDRAINED TRIAXIAL SHEAR - N.C. HANEY CLAY.

therefore, no errors should arise in estimating axial stress acting on the specimen.

6.2.0 Drained Test Results

Fig. 6.6 and 6.7 show, respectively, the deviator stress and effective stress ratio vs. axial strain relationships for the four drained triaxial tests on initially identical specimens. In axial compression the maximum strength, $(\sigma_z-\sigma_x)_{max}/2$, mobilised was under the passive compression stress path, because the specimen had higher effective stresses at failure. Both compression specimens, however, attained approximately the same peak effective stress ratio $(\sigma_1'/\sigma_3')_{max}$. Similarly, drained passive extension stress path resulted in larger peak deviator stress due to large effective stresses on the specimen at failure when compared to specimen subjected to active extension stress path. The peak effective stress ratio and hence the value of ϕ' associated with passive extension, however, was much smaller than the value of effective stress ratio associated with active extension shear, although practically the same strain was needed to mobilise it. The reason for this discrepancy is obvious from Fig. 6.8, which shows the extremely large volumetric strain rates in the specimen subjected to passive extension when compared

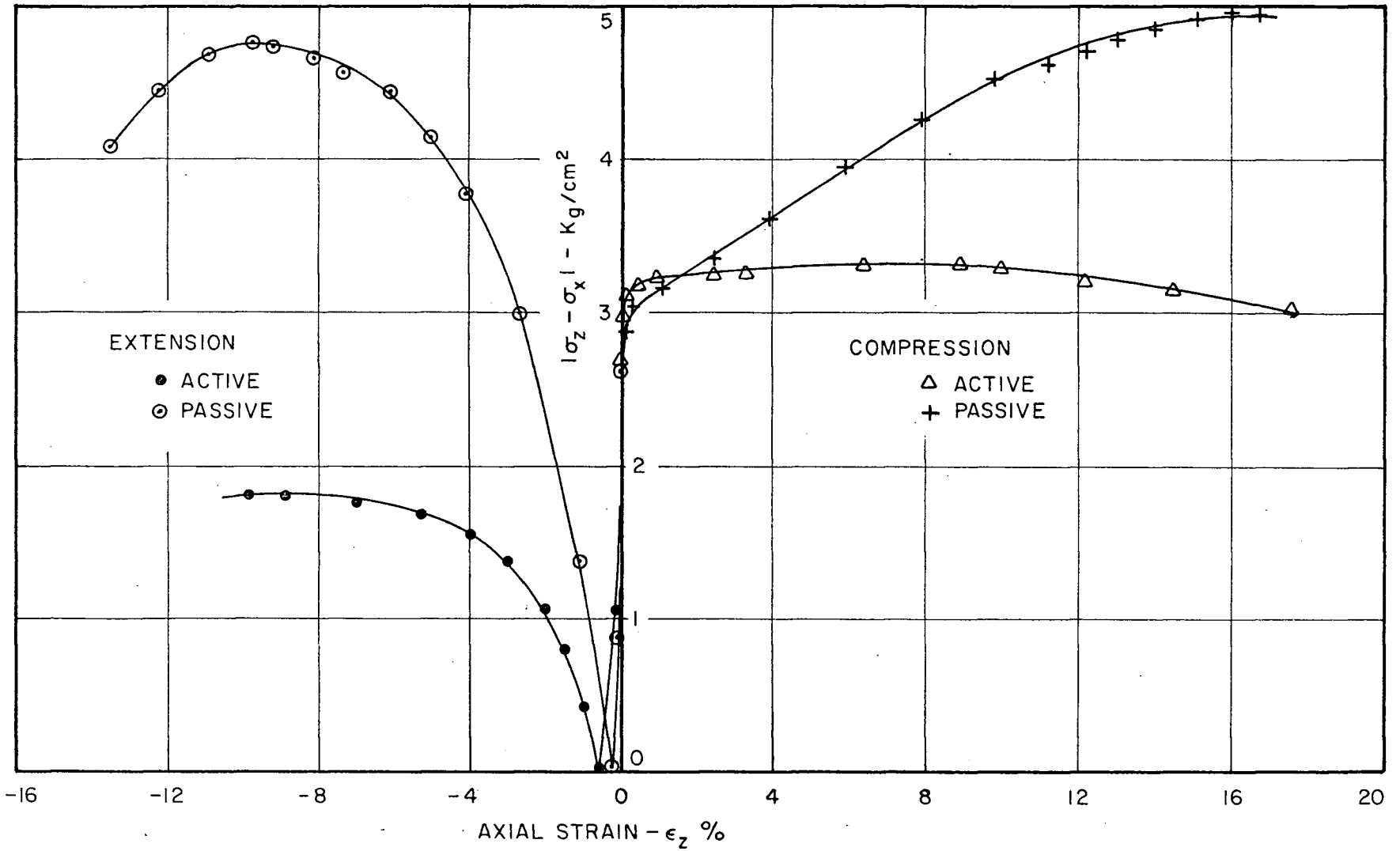

FIG.6.6 DEVIATOR STRESS - STRAIN RELATIONSHIPS DURING DRAINED TRIAXIAL SHEAR- N.C. HANEY CLAY.

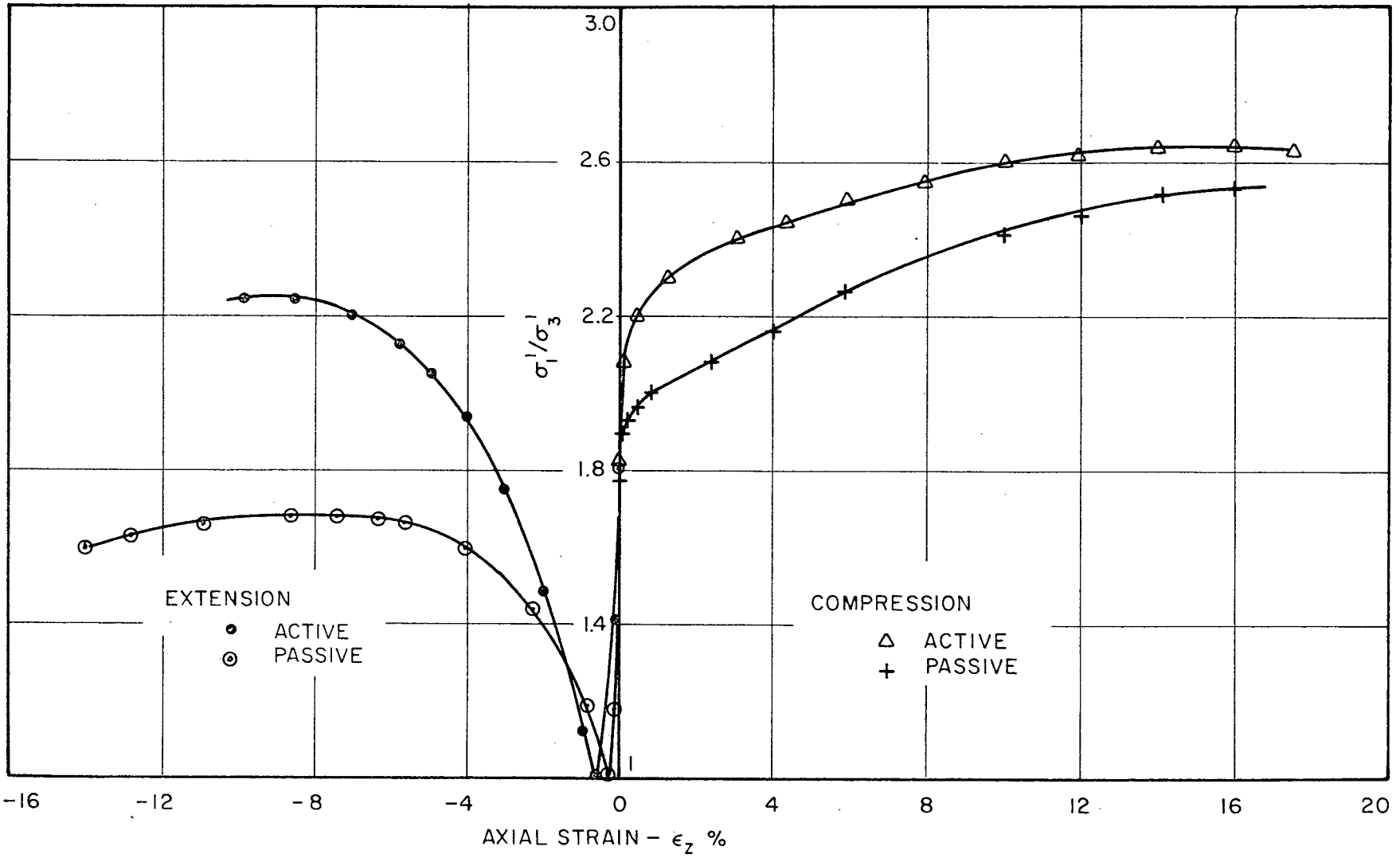

FIG. 6.7 PRINCIPAL EFFECTIVE STRESS RATIO – STRAIN RELATIONSHIPS DURING DRAINED TRIAXIAL SHEAR – N.C. HANEY CLAY.

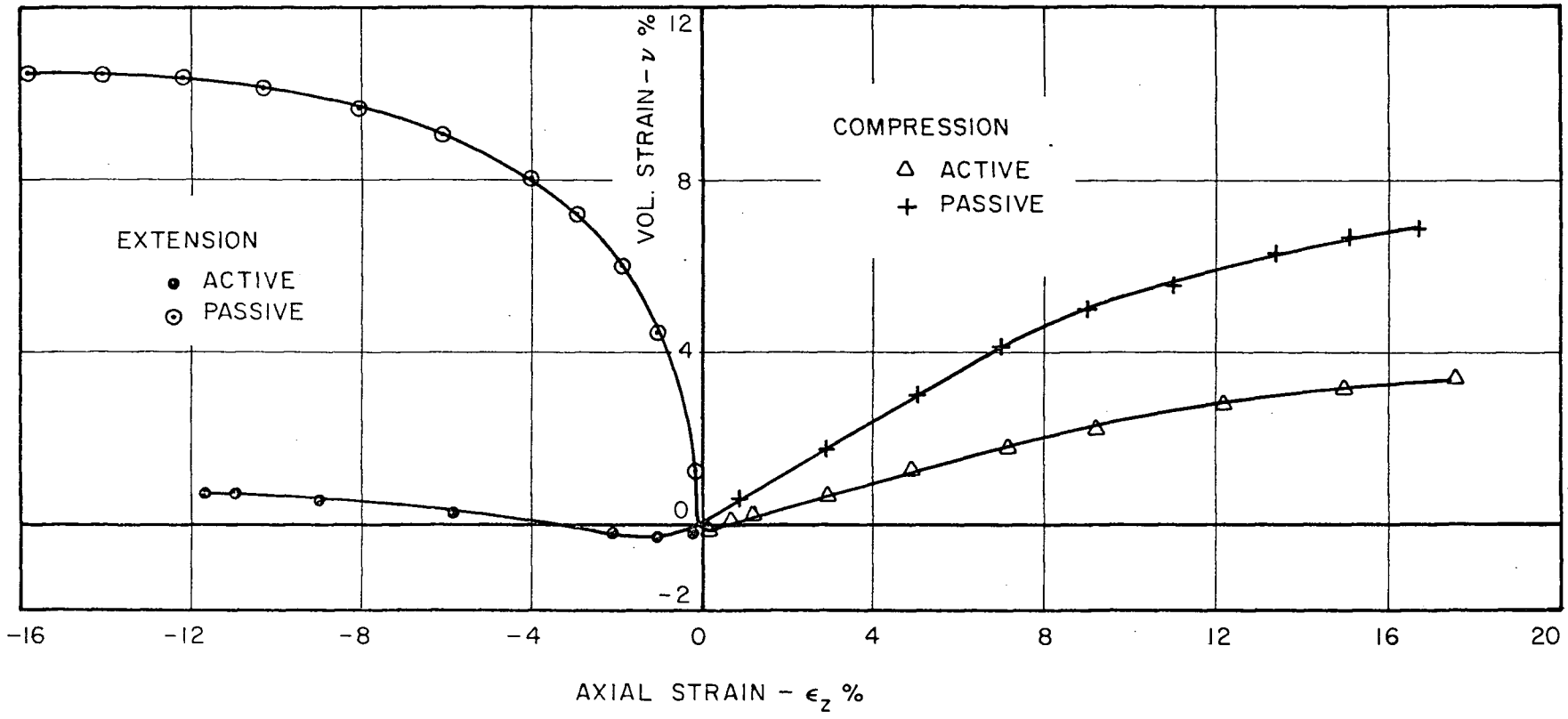

FIG. 6.8 AXIAL STRAIN - VOLUMETRIC STRAIN RELATIONSHIPS DURING DRAINED TRIAXIAL SHEAR - N.C. HANEY CLAY.

to the specimen under active extension. It will be shown later in this chapter that $(\sigma_1'/\sigma_3')_{max}$ when corrected for energy due to volume change was almost the same in the two extension tests.

All specimens underwent volume decrease at failure irrespective of the type of stress path followed (Fig. 6.8). This is interesting, especially for the specimen subjected to active extension stress path, where even the very large unloading of mean normal stress resulted in net volume compression until failure.

The peak effective stress ratio, $(\sigma_1'/\sigma_3')_{max}$, during axial compression shear corresponds to an average measured $\phi' = 25.8°$. During axial extension shear the measured $\phi' = 21.8°$ and $14.5°$ respectively for the active and passive conditions.

6.3.0 Comparison and Correlation of Drained and Undrained Test Results

6.3.1 Stress-Strain Relationships

Rendulic's hypothesis of uniqueness of void ratio and effective stress was seen to hold reasonably well for load increasing axial compression shear of K_o-consolidated triaxial specimens. This is shown in the plot of τ_{oct}/p_e vs. p/p_e in Fig. 6.9 where the results from all

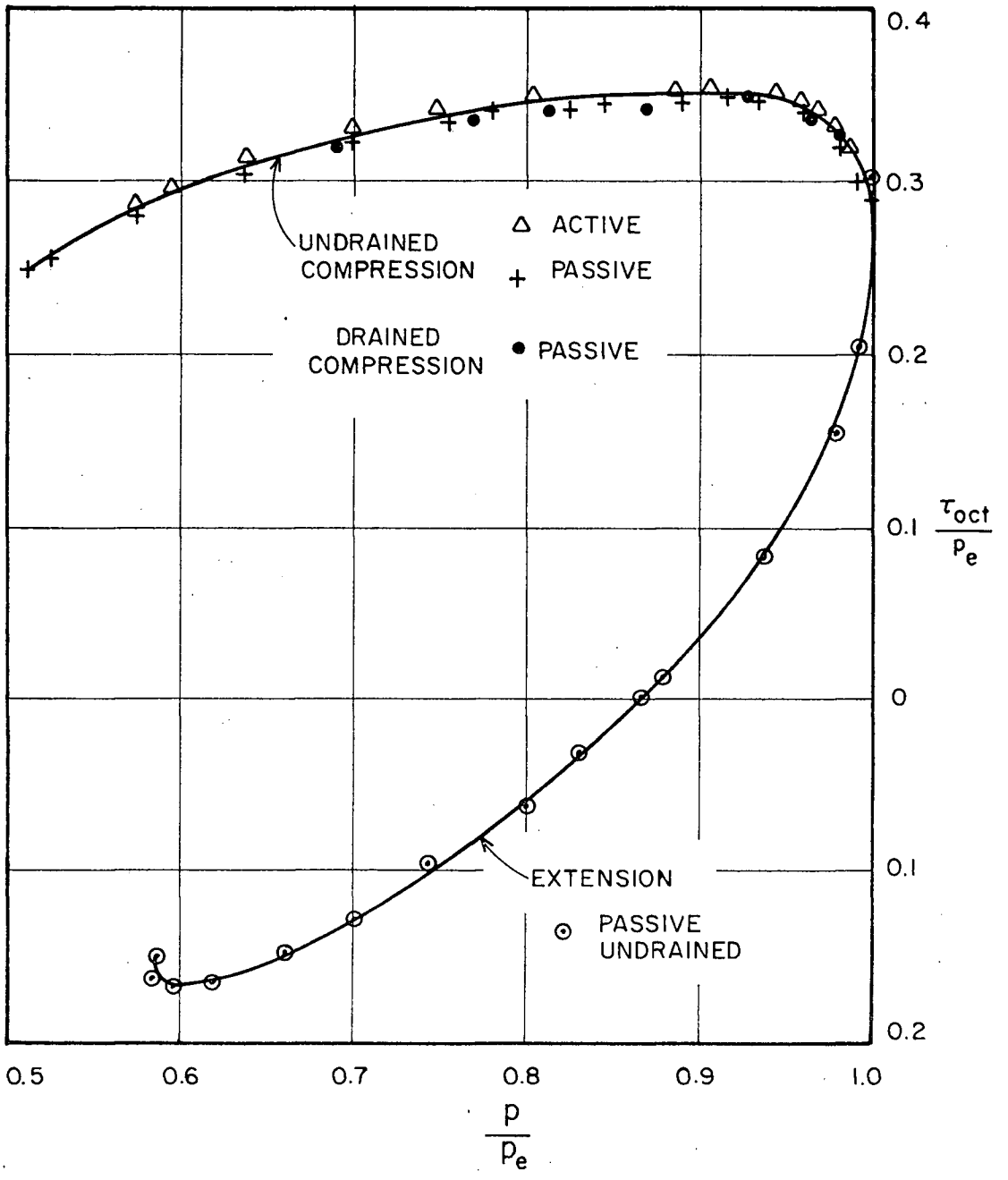

FIG. 6.9 COMPRESSION AND EXTENSION STATE BOUNDARY SURFACES FOR TRIAXIAL TESTS - N.C. HANEY CLAY.

such tests fall essentially on the same curve - the Rendulic triaxial yield surface curve. It, therefore, implies that volume changes in drained passive compression K_o-triaxial test could be predicted from Rendulic yield surface curve determined from the undrained test on similarly consolidated specimens. Such a predicted curve of τ_{oct}/p vs. volumetric strain, v, is shown in Fig. 6.10 along with the observed relationship. A very good agreement is obtained between predictions and observations. For the triaxial test results, however, the shear stress parameter $q = (\sigma_1-\sigma_3)$ could be used instead of, τ_{oct}, as done by Roscoe et. al. (1958) for representing Rendulic's uniqueness relationship. But for the sake of consistency with presentation of plane strain results, τ_{oct} has been used herein. For triaxial stress condition, τ_{oct} is a constant multiple of q.

Volumetric strains predicted for drained active compression shear from undrained yield surface are shown in Fig. 6.11 where the observed τ_{oct}/p vs. v relationship is also shown. The predicted strains are, in general, smaller than the observed, except in the earlier stages of the test.

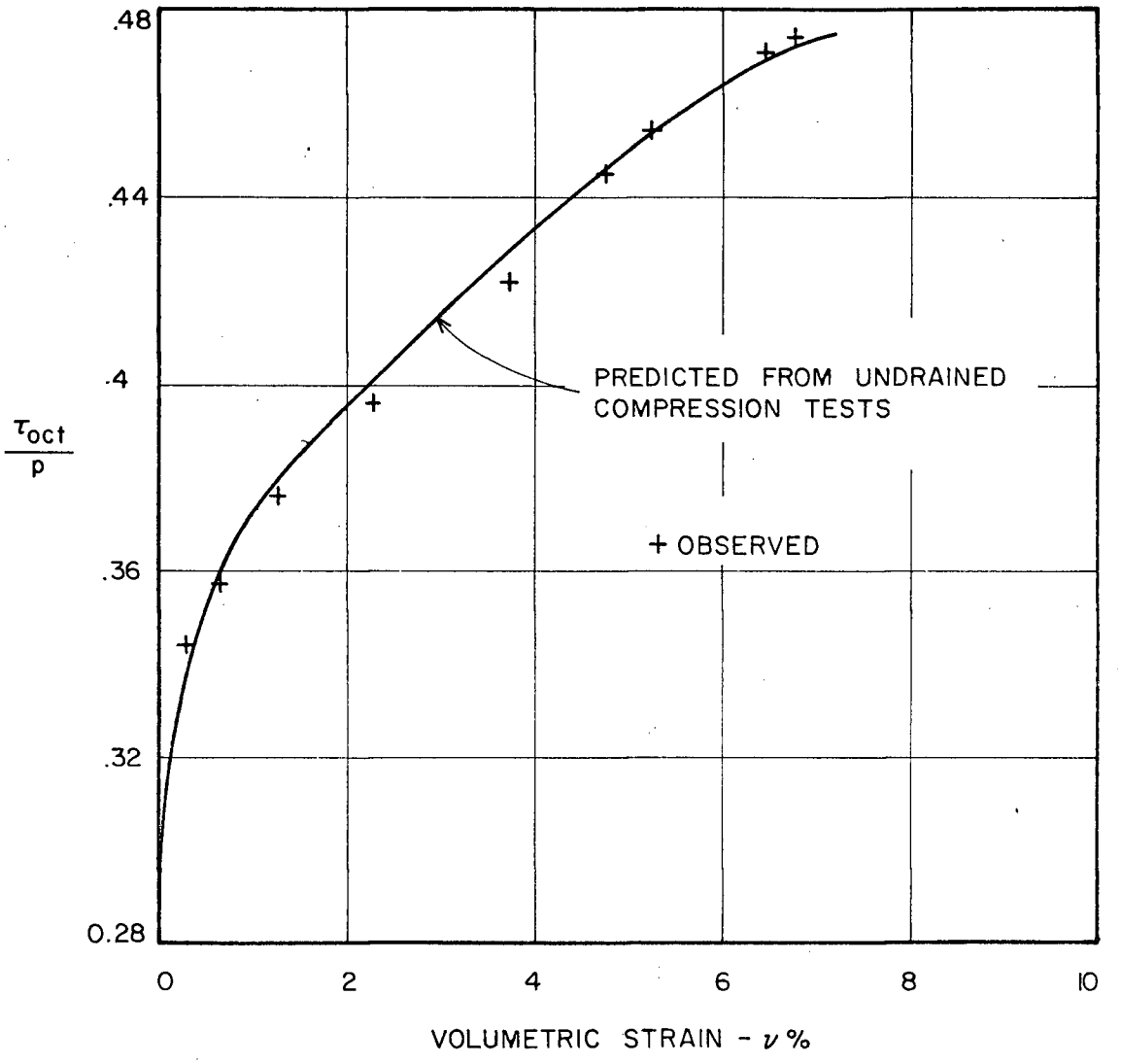

FIG. 6.10 COMPARISON OF OBSERVED AND PREDICTED VOLUMETRIC STRAINS DURING TRIAXIAL DRAINED PASSIVE COMPRESSION - N.C. HANEY CLAY.

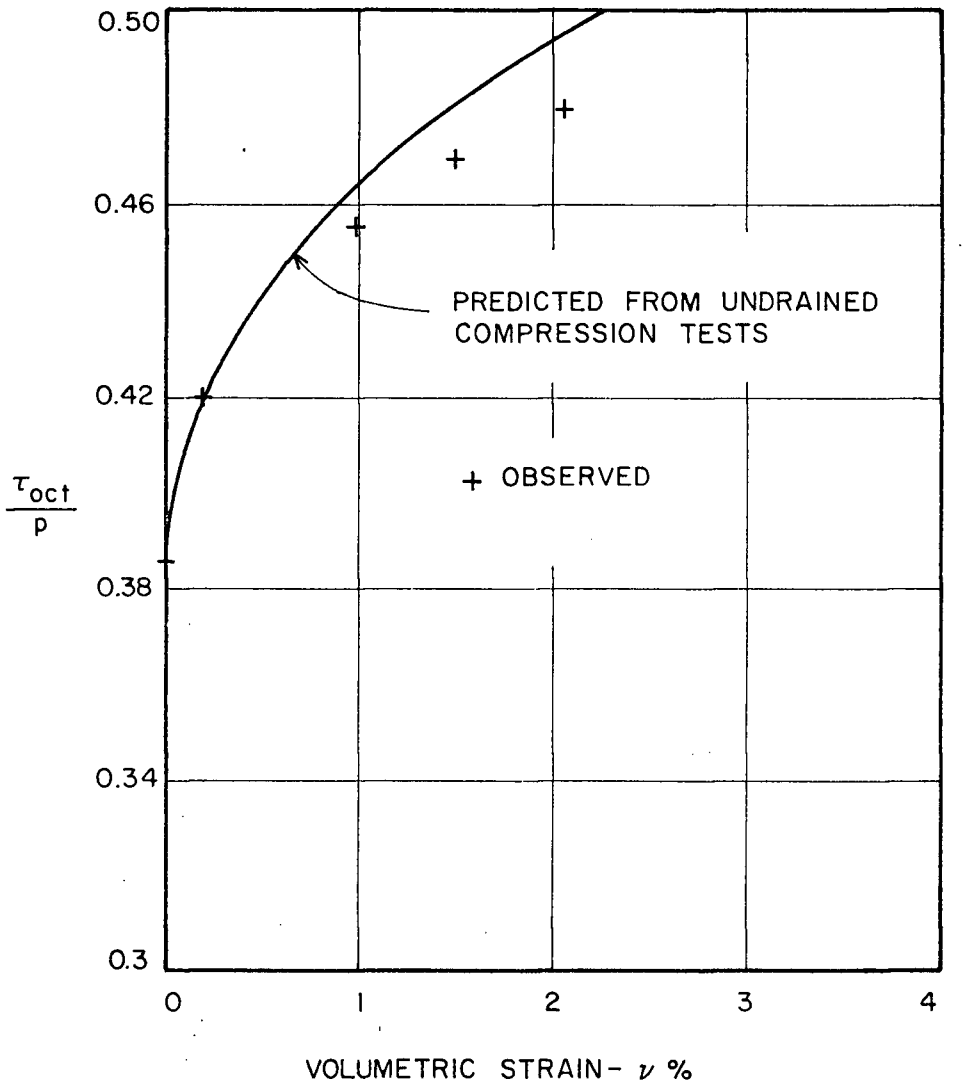

FIG. 6.11 COMPARISON OF OBSERVED AND PREDICTED VOLUMETRIC STRAINS DURING TRIAXIAL DRAINED ACTIVE COMPRESSION – N.C. HANEY CLAY.

The existence of a unique yield surface for undrained and load increasing drained compression tests suggests, that the undrained and load increasing drained extension test may also lie on a common yield surface, which may be called the extension yield surface. If this was true, then volume changes in drained passive extension test could be predicted from the results of undrained extension tests by the same technique as employed for compression tests. Fig. 6.12 shows the comparison between the predicted and the observed volumetric strains. For the part of the stress path which involves decreasing stress ratio, τ_{oct}/p, predicted strains are too large. However, for the part of the stress path which involves increasing stress ratio, increments of predicted volumetric strains are close to the observed increments.

The limitations regarding predictions of shear strains in drained compression tests from results of undrained compression tests are the same as explained for plane strain tests. Methods based on theory of plasticity can, at best, be applied until stress ratio τ_{oct}/p reaches a value corresponding to the condition of τ_{oct} = maximum in the undrained tests. This corresponds to shear strains in drained test which, for Haney clay, are less than 20% of the failure strains. Comparison between observed and

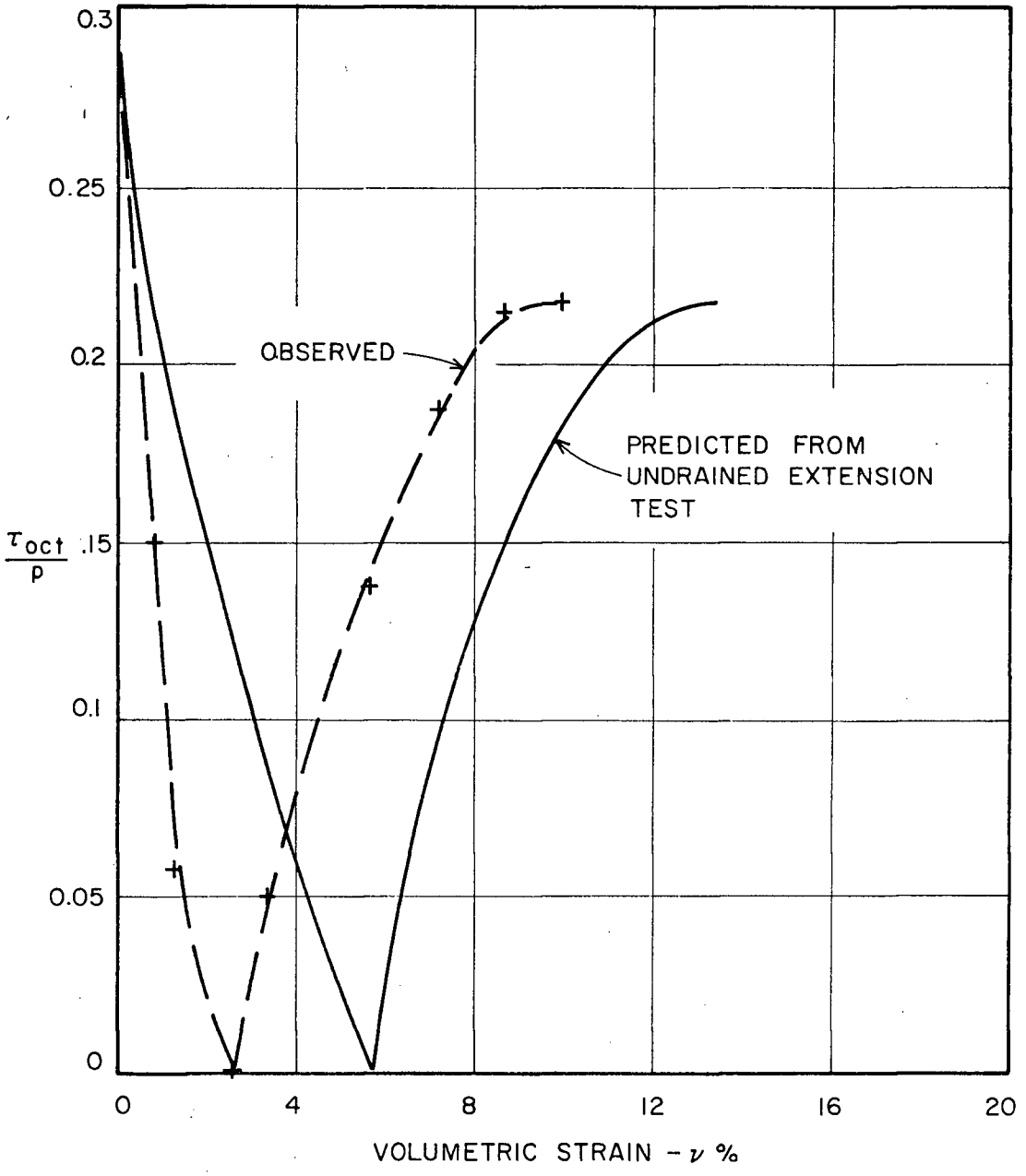

FIG. 6.12 COMPARISON OF OBSERVED AND PREDICTED VOLUMETRIC STRAINS DURING TRIAXIAL DRAINED PASSIVE EXTENSION - N.C. HANEY CLAY.

predicted strains for τ_{oct}/p values below the limiting value was found to be of the same type as demonstrated for plane strain tests (see Fig. 5.14).

The stress ratio, τ_{oct}/p, vs. shear strain, γ_{oct}, relationship for drained active extension test was almost identical to the relationship for the corresponding undrained test (Fig. 6.13). This was to be expected, since volume changes associated with drained active extension were very small, and therefore, the situation was close to that of the undrained extension. A similar result was pointed out for the plane strain conditions in Fig. 5.15. Prediction of shear strains during drained passive extension could not be attempted. This was so because, during extension shear no unique stress-void ratio relationship common to undrained and load increasing drained tests could be established.

6.3.2 Failure Conditions

The results of all triaxial tests are summarized in Table III. The peak deviator stress in each drained test was found to be larger than the peak deviator stress in the corresponding undrained test. The reason for this was the net volume compression experienced by all the specimens until failure. This seems to be an unusual

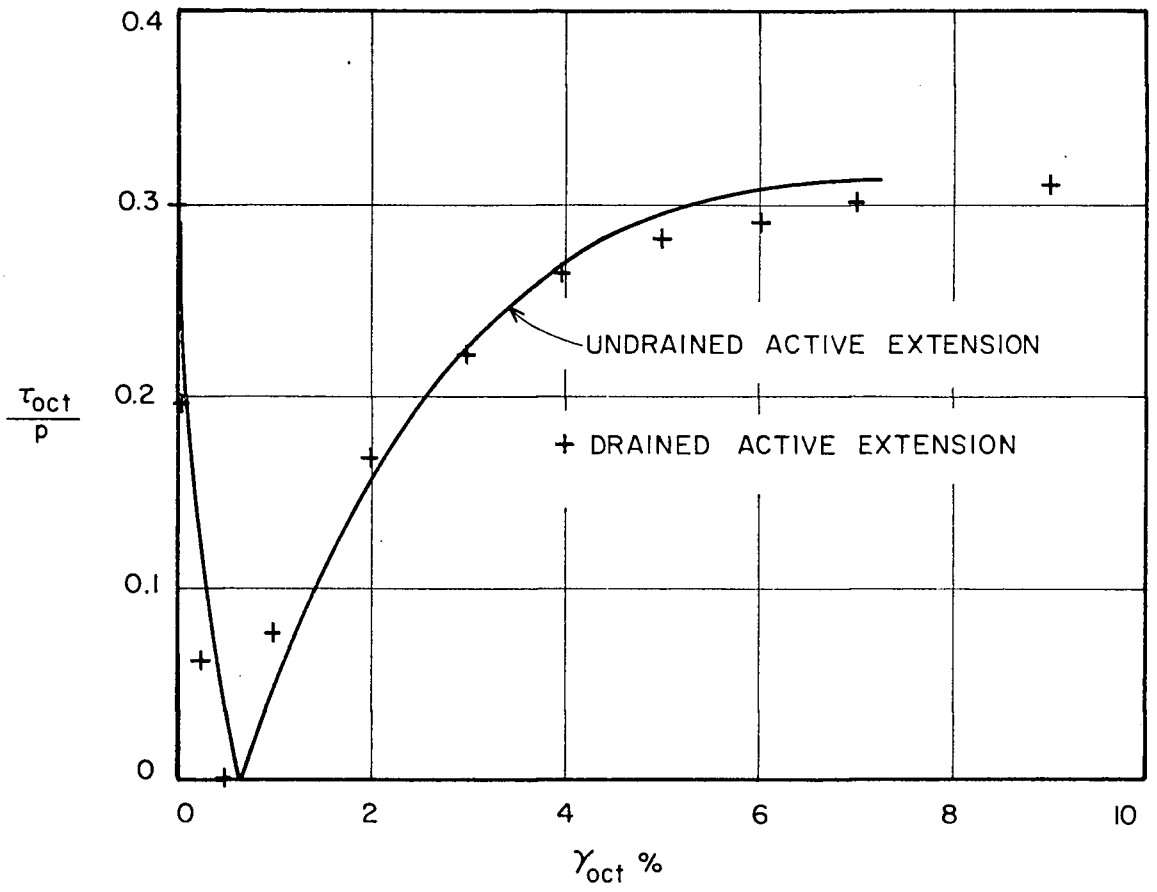

FIG. 6.13 COMPARISON OF SHEAR STRESS - STRAIN RELATIONSHIP DURING TRIAXIAL DRAINED AND UNDRAINED EXTENSION - N.C. HANEY CLAY.

TABLE III

Summary of Triaxial Test Results on N.C. Haney Clay

	End of Consolidation		Failure Condition									
			$(\sigma_1-\sigma_3)_{max}$						$(\sigma'_1/\sigma'_3)_{max}$			
	σ'_{zc}	K_o	Axial Strain %	$\frac{\sigma_1-\sigma_3}{\sigma'_{zc}}$	a	v%	σ'_1/σ'_3	ϕ'	Axial Strain %	σ'_1/σ'_3	ϕ'_m	ϕ'_c
Undrained Tests												
Passive compression	5.84	.56	.4	.528	1.39	0	2.11	20.9°	8.0	2.60	26.4°	26.4°
Active compression	5.91	.55	.45	.534	1.50	0	2.14	21.2°	6.0	2.65	26.8°	26.8°
Active extension	5.91	.56	-7.7	.272	.89	0	2.23	22.4°	-7.7	2.23	22.4°	22.4°
Passive extension	5.92	.55	-5.8	.25	.85	0	1.99	19.4°	-5.8	1.99	19.4°	19.4°
Drained Tests												
Passive compression	5.96	.56	16.0	.834	—	6.8	2.54	25.8°	16.0	2.54	25.8°	27.2°
Active compression	5.97	.55	7.0	.555	—	1.8	2.54	25.8°	7.0	2.54	25.8°	27.8°
Active extension	5.94	.56	-9.0	.306	—	0.7	2.18	21.8°	-9.0	2.25	21.8°	21.8°
Passive extension	5.91	.55	-9.2	.808	—	9.8	1.69	14.5°	-9.2	1.69	14.5°	20.0°

Stress in Kg/cm^2

ϕ'_m = ϕ' measured

ϕ'_c ϕ' corrected for volume change

result when looked in the light of existing data on remolded clays (Bishop & Henkel, 1962). But considering the sensitive nature of the clay used in this study, this behaviour can be regarded as the result of increased compressibility due to imposed shear stresses. This induces tendency to volume decrease more than the tendency to volume increase during stress paths associated with unloading of mean normal stresses.

Effective strength parameter ϕ' is shown tabulated for all the triaxial tests in Table III. For drained tests, both the measured ϕ' value and the ϕ' value corrected for volumetric strain rates at failure (as explained in Chapter V) are shown. At maximum deviator stress failure condition, ϕ' was essentially same (21° ± 1.5°) for all stress paths except drained compression and drained passive extension. At $(\sigma_1'/\sigma_3')_{max}$, the measured ϕ' in drained compression was about 0.6° smaller than the corresponding undrained compression value; whereas passive extension drained ϕ' was as much as 5° to 6° smaller than the corresponding undrained and drained active extension values. However, when drained ϕ' was corrected for volumetric strain rates, essentially the same ϕ' was found for drained and undrained compression failure. Similarly, corrected drained ϕ' and undrained ϕ' during extension

failure was found to be essentially the same. But ϕ' during compression failure was on the average 5° larger than ϕ' during extension failure.

CHAPTER VII

COMPARISON OF PLANE STRAIN AND TRIAXIAL RESULTS

N. C. HANEY CLAY

In this chapter the stress-strain and the strength behaviour of normally consolidated Haney clay is compared and correlated for triaxial and plane strain conditions. The end of K_o-consolidation was identical for all samples. Conventional comparison of the stress-strain behaviour and of effective strength parameter, ϕ', is considered first. This is done to point out the essential differences between the triaxial and plane strain response, and the possible errors involved while solving a plane strain problem using triaxial test results. In later sections attempts are made to correlate triaxial and plane strain behaviour, i.e., to predict plane strain behaviour from triaxial test results. Two approaches are examined for correlating stress strain behaviour. The first is an empirical approach, which follows along the lines of suggestions made by Newmark (1960) and Rendulic (1937). The second is related to concepts proposed by Roscoe and Burland (1968), whose 'revised' and 'modified' Cambridge stress-strain

theories enable prediction of drained plane strain behaviour from soil parameters determined from isotropically consolidated triaxial tests. Lastly, the various failure theories considered applicable to soils are examined to correlate triaxial and plane strain strength behaviour.

7.1.0 Conventional Comparison

This consists of comparing the triaxial and plane strain behaviour in terms of stress parameters which are functions of the major and minor principal effective stresses only. Comparisons including the intermediate principal stress will be considered in later sections. The strain parameters used in conventional comparison are the axial strain, ε_z, associated with axial stress, σ_z, and volumetric strain, v.

7.1.1 Undrained Tests

It has previously been shown (Chapters V and VI) that the undrained behaviour of Haney clay was independent of the total stress path, provided compression and extension modes of shear were considered separately. For example, the behaviour of decreasing lateral stress tests (active compression) was the same as increasing axial stress tests (passive compression). Thus, in comparison of triaxial

and plane strain results no distinction will be made between active and passive compression, or active and passive extension, and they will be simply termed undrained compression and undrained extension respectively.

Figure 7.1 shows the normalised deviator stress, $|\sigma_z-\sigma_x|/\sigma'_{zc}$, vs. axial strain, ε_z, relationships during undrained compression and extension under triaxial and plane strain conditions. The similarity of the triaxial and plane strain results for both compression and extension may be noted. It is interesting that undrained compression failure, $(|\sigma_z-\sigma_x|_{max})$, took place at a relatively small value of axial strain, or about 1/2%, and was the same for both plane strain and triaxial conditions. This small strain at failure is different from that reported by Henkel and Wade (1966) for a remolded clay, initially K_o-consolidated. They reported 2% axial strain to failure under plane strain compression and 6% axial strain to failure under triaxial compression. In contrast to the compression behaviour, the extension deviator stress-strain relationship was plastic in character for both triaxial and plane strain conditions. Again it is interesting to note that the large axial strain for extension failure, about 7%, was the same for both triaxial and plane strain conditions. It is, therefore, concluded that for undisturbed Haney clay, plane

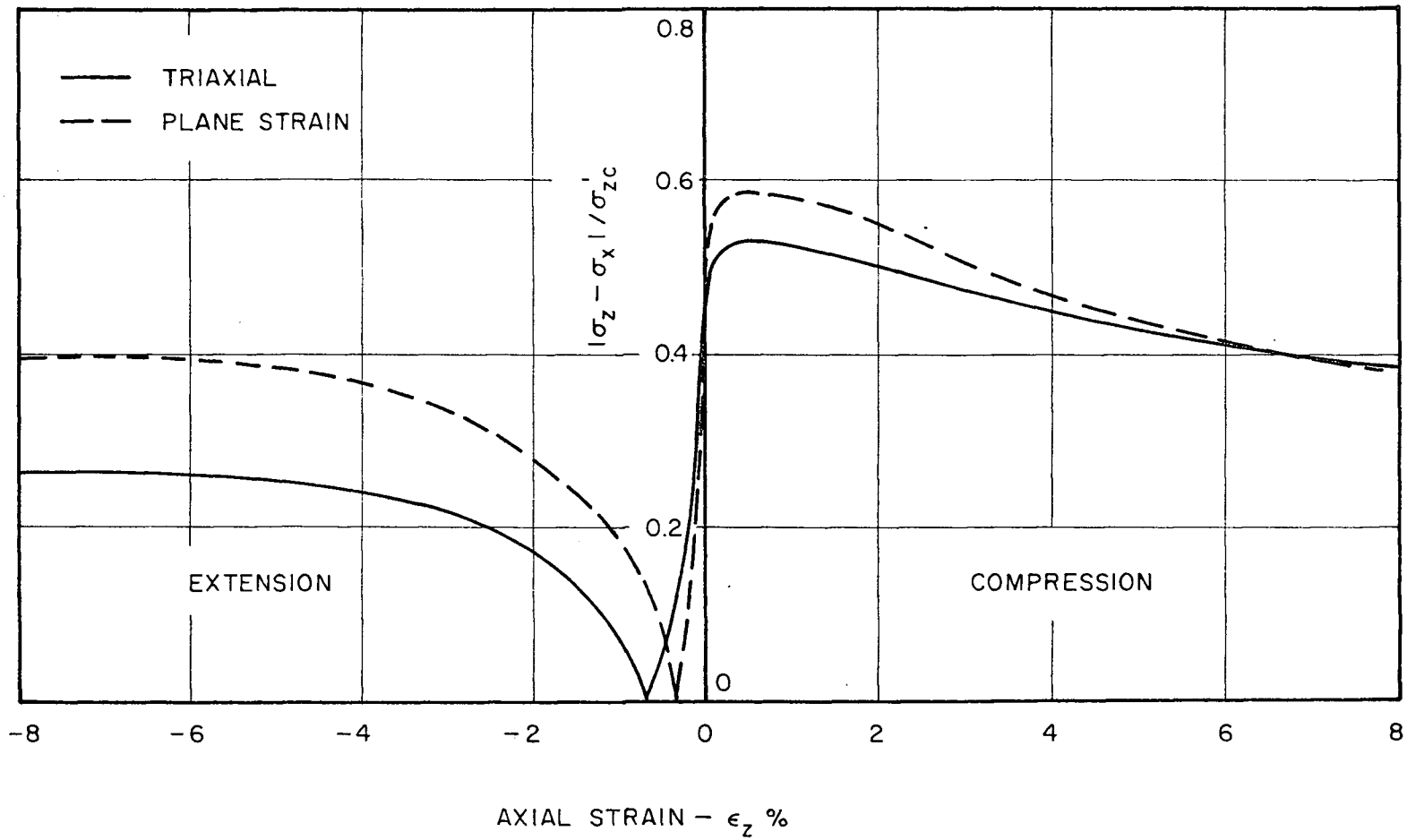

FIG.7.1 COMPARISON OF DEVIATOR STRESS-STRAIN RELATIONSHIPS UNDER UNDRAINED TRIAXIAL AND PLANE STRAIN SHEAR – N.C. HANEY CLAY.

strain conditions do not result in failure strains which are different from those under the corresponding triaxial conditions.

C_u/σ'_{1c}, the ratio of undrained strength, $|\sigma_z-\sigma_x|_{max}/2$, to the major principal consolidation stress, σ'_{zc}, during undrained compression was 0.293 for plane strain and 0.265 for triaxial conditions. Thus, the plane strain undrained strength was about 11% higher than the triaxial value. Similar differences between plane strain and triaxial compression strength were reported by Henkel and Wade (1966) for a remolded clay, and by Ladd (1967) for Boston Blue clay. There was a significant loss in strength once the peak was passed for both triaxial and plane strain compression shear. At an axial strain of 5% the deviator stress had fallen below the value at the end of consolidation for both types of test and, the deviator stress-strain curves merged together thereafter. It therefore appears that post peak strength behaviour of the clay tested at relatively large strains is the same under both triaxial and plane strain conditions. Compression tests, which were carried to strains up to 15%, possessed identical deviator stress-strain relationships in triaxial and plane strain once the axial strain exceeded 5%.

C_u/σ'_{1c} ratio during plane strain extension was found to be 0.197 compared to the triaxial value of 0.13. Thus, undrained strength in plane strain extension was as much as 50% higher than the triaxial value. Similar results were quoted by Ladd (1967) for Boston Blue clay, which had 67% higher undrained extension strength in plane strain than under triaxial conditions.

The rate at which friction was mobilized, as represented by the ratio of the major to minor principal effective stresses, was higher in plane strain than under triaxial conditions, for both compression and extension modes of shear (Fig. 7.2). During both triaxial and plane strain compression, pore pressures were still increasing when the maximum deviator stress condition occurred and, in consequence, the peak values of the effective stress ratio, $(\sigma'_1/\sigma'_3)_{max}$, was reached at larger strains. However, in plane strain the peak stress ratio occurred at 3% axial strain and showed a marked drop thereafter, whereas under triaxial conditon 6% axial strain was required until $(\sigma'_1/\sigma'_3)_{max}$, which stayed essentially constant with further strain. During extension shear the peak deviator stress and peak effective stress ratio were reached at the same strain of about 7% for both triaxial and plane strain conditions.

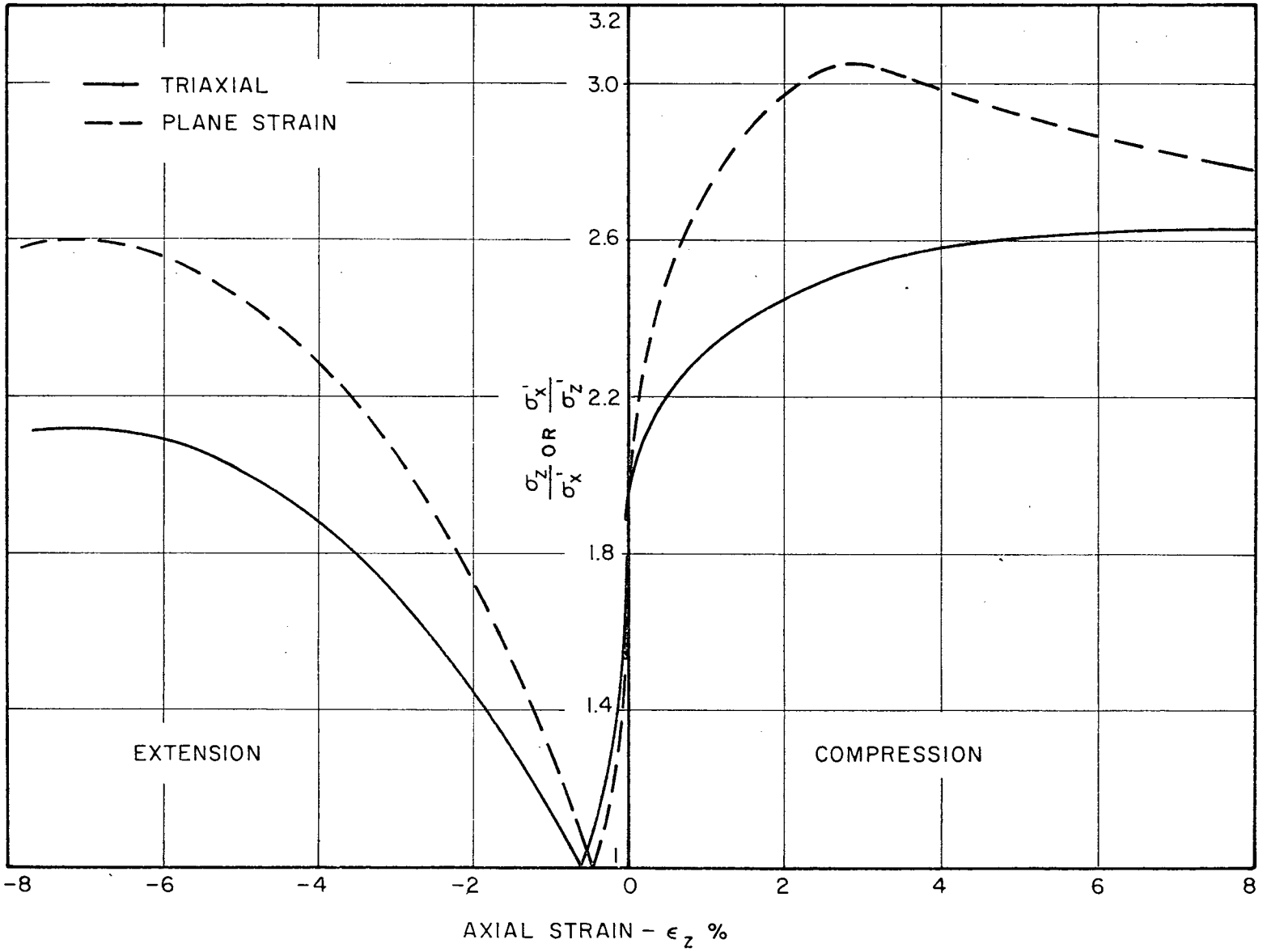

FIG. 7.2 COMPARISON OF EFFECTIVE STRESS RATIO - STRAIN RELATIONSHIPS DURING UNDRAINED TRIAXIAL AND PLANE STRAIN SHEAR - N.C. HANEY CLAY.

The undrained plane strain and triaxial compression and extension effective stress paths in σ'_x/σ'_{zc}, σ'_z/σ'_{zc} stress space are shown in Fig. 7.3. The remarkable similarity of the triaxial and plane strain compression and also the extension paths may be noted. As was shown in Fig. 7.1 the maximum value of deviator stress in compression occurred at about 0.5% axial strain for both triaxial and plane strain condition but, it can be seen in Fig. 7.3, this point was reached before the stress paths become tangential to the failure envelopes. The point of tangency corresponds to about 3% axial strain for plane strain and 6% axial strain for triaxial conditions. The value of ϕ' corresponding to the effective stress failure envelopes ($\sigma'_1/\sigma'_{3_{max}}$) are 30.4° in plane strain and 26.6° under triaxial conditions. This is consistent with results on remolded clay reported by Henkel and Wade (1966) and also by Shibata and Karube (1967), who showed compression ϕ' in plane strain to be 1.2° and 5° larger respectively. It is interesting to note here that the values of ϕ' at maximum deviator stress were about 5° lower than those at peak effective stress ratio for both plane strain and triaxial tests. The extension stress paths become tangent to the effective stress failure envelopes at the same strain at which the maximum deviator stress was reached. The

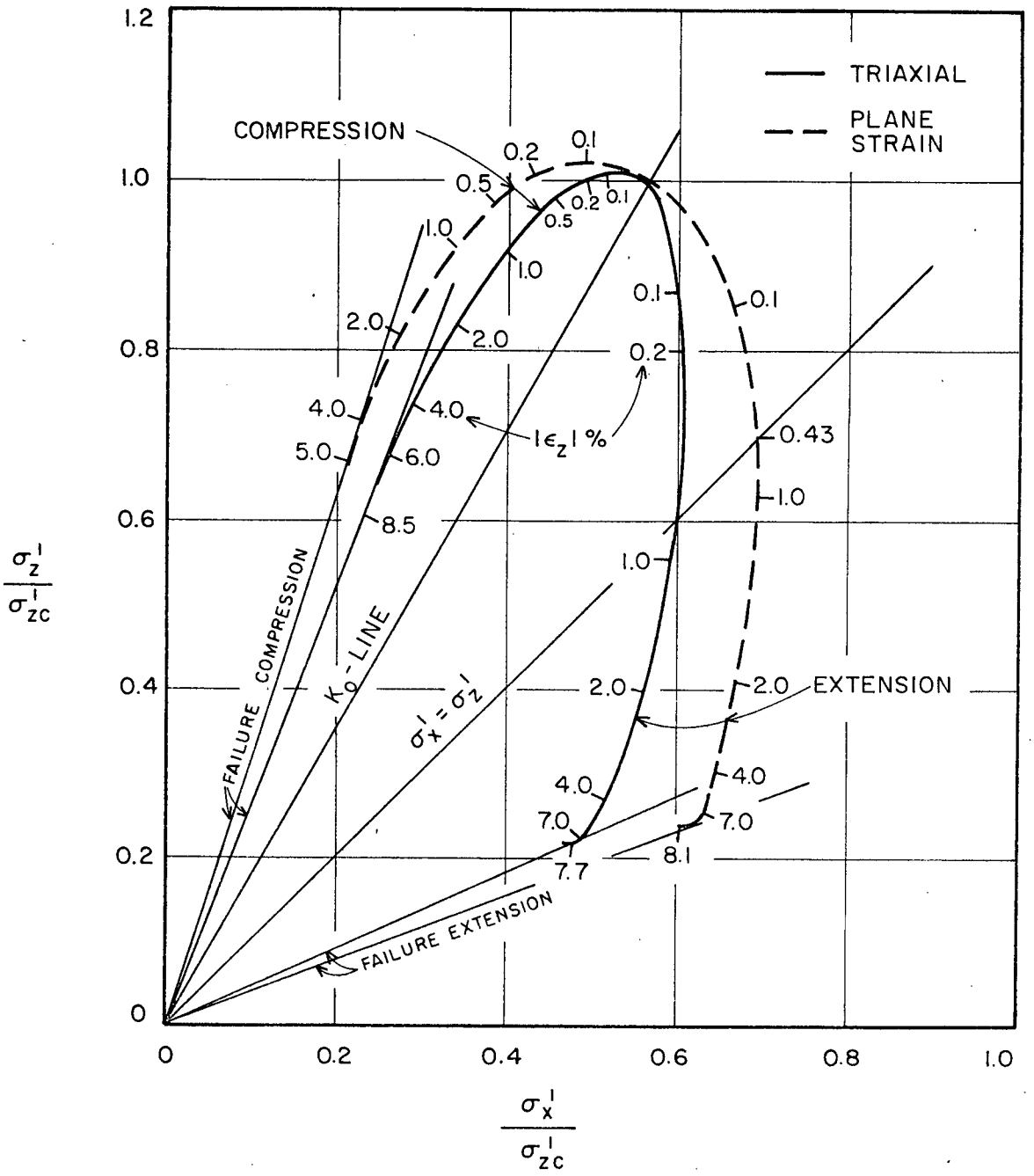

FIG. 7.3 COMPARISON OF EFFECTIVE STRESS PATHS IN UNDRAINED TRIAXIAL AND PLANE STRAIN SHEAR – N.C. HANEY CLAY.

values of ϕ' during extension failure are 26.1° for plane strain and 21° for triaxial conditions. For Boston Blue clay, Ladd (1967) reported plane strain extension ϕ' to be 42° compared to 38° under triaxial conditions. It is, therefore, concluded that ϕ' at $(\sigma_1'/\sigma_3')_{max}$ is larger in plane strain than under triaxial conditions by about 4° to 5° in undisturbed Haney clay; the conclusion applies to both compression and extension modes of shear.

A summary of undrained failure characteristics under triaxial and plane strain conditions is presented in Table IV. Both, maximum deviator stress and maximum stress ratio failure conditions are considered for comparison of triaxial and plane strain behaviour. The shear strength, C_u, of any particular undrained specimen depends on the effective stresses acting at the time of failure and on the shear strength parameters. Since the effective stresses used during consolidation process were identical, the strength difference between triaxial and plane strain conditions must be explained in the pore pressure changes after consolidation, and in the shear strength parameters, ϕ'. During compression shear under identical stress paths, the change in pore pressure at failure was almost the same under both triaxial and plane strain conditions and, therefore, higher strength

TABLE IV

Comparison of Failure under Undrained Triaxial and Plane Strain Conditions

	Failure Condition						
	$(\sigma_1-\sigma_3)_{max}$				$(\sigma_1'/\sigma_3')_{max}$		
	Axial Strain %	C_u/σ_{1c}'	σ_1'/σ_3'	ϕ'	Axial Strain %	σ_1'/σ_3'	ϕ'
Undrained Compression							
Plane strain	0.5	0.293	2.50	25.4°	3	3.05	30.4°
Triaxial	0.45	0.265	2.12	21.0°	6	2.62	26.6°
Undrained Extension							
Plane strain	-7.1	0.197	2.57	26.1°	-7.1	2.57	26.1°
Triaxial	-7.5	0.13	2.1	21.0°	-7.5	2.1	21.0°

$C_u = (\sigma_1-\sigma_3)_{max}/2$

σ_{1c}' = major consolidation stress

in plane strain was associated with larger ϕ' in plane strain. During extension shear under identical stress paths, the change in pore pressure at failure was smaller in plane strain than under triaxial condition and, therefore, higher strength in plane strain was associated with not only larger ϕ' but also smaller pore pressures in plane strain.

7.1.2 Drained Tests

During drained shear the total stress path is the same as the effective stress path. Active and passive shear modes give rise to different effective stress paths, and since soil reponse is a function of effective stresses, drained active and passive behaviour is not identical. Comparison between triaxial and plane strain behaviour is presented for identical stress paths to failure. A passive compression plane strain test could not be performed and, therefore, no comparison with triaxial results can be made.

Fig. 7.4 shows deviator stress-strain relationships during drained plane strain and triaxial compression and extension. Plane strain curves, for all the tests, lie above the corresponding curves for triaxial conditions. Thus, the plane strain test always gives

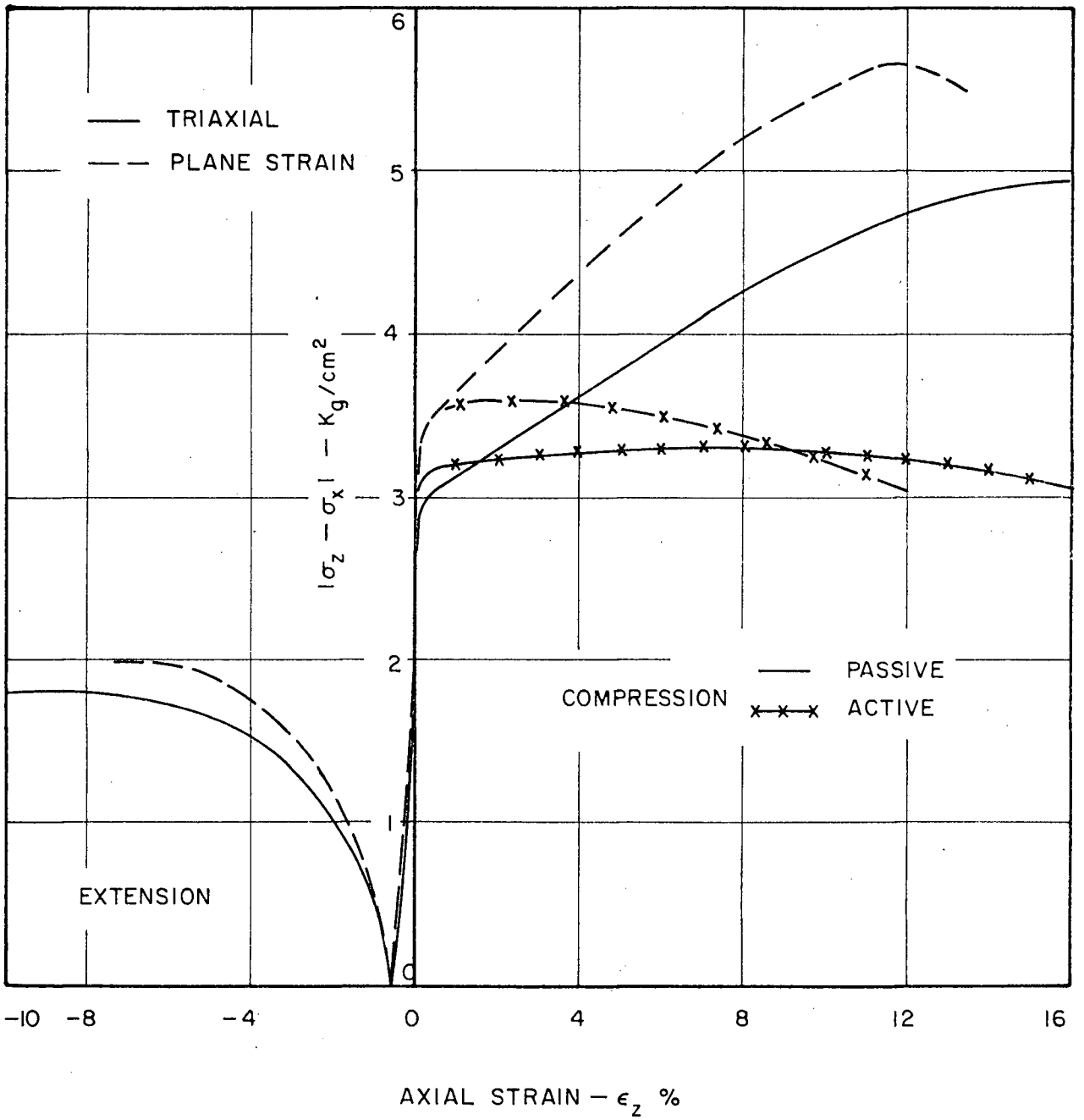

FIG. 7.4 COMPARISON OF DEVIATOR STRESS-STRAIN RELATIONSHIPS DURING DRAINED TRIAXIAL AND PLANE STRAIN SHEAR - N.C. HANEY CLAY.

a higher strength than the corresponding triaxial test. Drained failure in passive compression was reached at 12% axial strain in plane strain compared to 16% axial strain under triaxial conditions. Plane strain relationship showed a characteristic peak, whereas the triaxial relationship did not. Drained failure in active compression occurred at smaller axial strains - 4.5% in plane strain and about 7% under triaxial conditions. Again, the post peak loss in strength was more marked for plane strain than under triaxial conditions. During drained active extension, failure was reached at 7% axial strain for plane strain and about 9% axial strain for triaxial conditions. It is, therefore, concluded that for a given stress path the axial strains to drained failure in plane strain was always somewhat less than those for triaxial, but the general behaviour was not very different.

The change in pore pressure during drained shear is zero. Therefore, the deviator stress mobilized at any strain under a given stress path depends only on the mobilized friction (as reflected in the principal effective stress ratio). The stress ratio-strain relationships are shown in Fig. 7.5. For all the stress paths studied, the plane strain test always had higher stress ratios at a given strain than the corresponding triaxial test. The

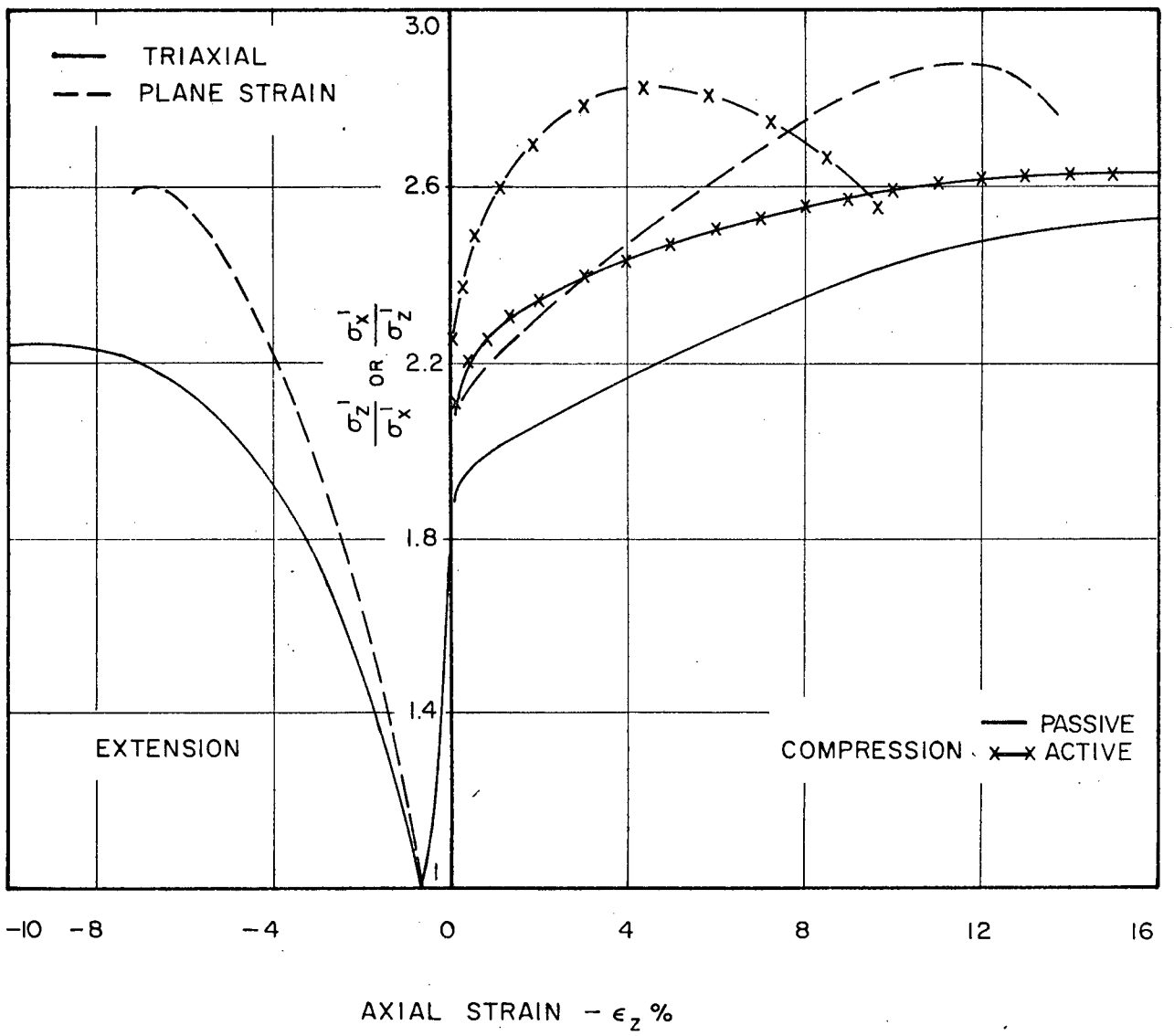

FIG. 7.5 COMPARISON OF EFFECTIVE STRESS RATIO – STRAIN RELATIONSHIPS DURING DRAINED TRIAXIAL AND PLANE STRAIN SHEAR – N.C. HANEY CLAY.

preceding conclusions regarding relative strains to peak deviator stress during drained plane strain and triaxial shear, under any given stress path, apply to the occurrence of peak stress ratios as well.

Comparison of volumetric strains, v, under triaxial and plane strain conditions, for all the stress paths studied, is presented in Fig. 7.6. During active and passive compression, volumetric strain - axial strain relationships are essentially identical until failure. This implies identical rates of volumetric strain during triaxial and plane strain shear under the same applied stress path. However, during drained active extension shear, the plane strain specimen showed swelling until failure, whereas the triaxial specimen showed a net compression at failure after slight swelling in the initial stages.

For a given type of test there is no difference between values of ϕ' for the active or the passive case. This was the behaviour observed in undrained tests. Also the ϕ' values in drained tests are not too different to those in undrained tests for $(\sigma_1'/\sigma_3')_{max}$ condition of failure under similar strain paths. A summary of drained failure characteristics under triaxial and plane strain conditions is given in Table V. ϕ' for drained compression in plane

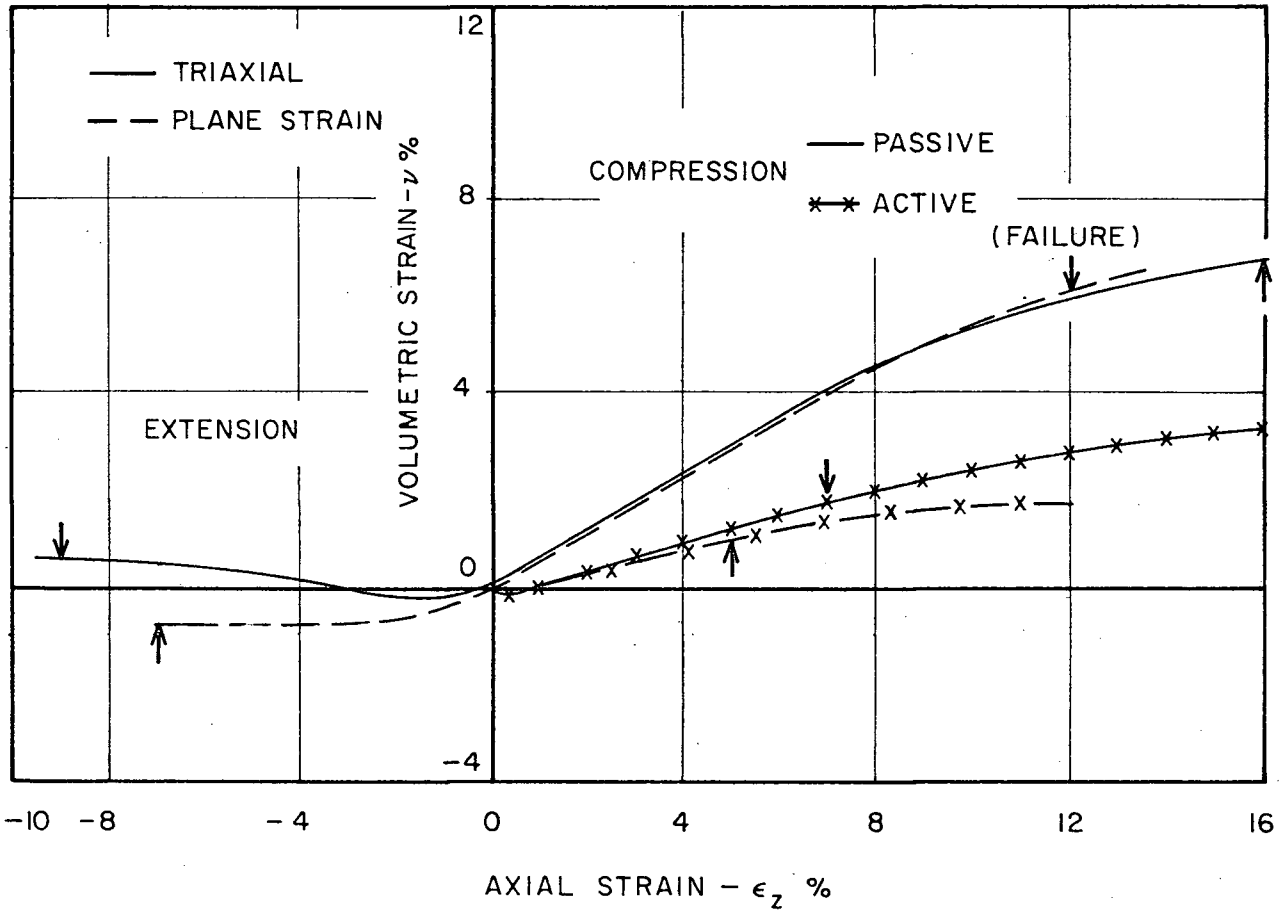

FIG. 7.6 VOLUMETRIC STRAIN - AXIAL STRAIN RELATIONSHIPS DURING DRAINED TRIAXIAL AND PLANE STRAIN SHEAR - N.C. HANEY CLAY.

TABLE V

Comparison of Failure under Drained Triaxial and Plane Strain Conditions

	End of Consolidation			Failure Condition $(\sigma_1-\sigma_3)_{max}$ or $(\sigma_1'/\sigma_3')_{max}$						
	σ'_{zc}	σ'_{xc}	K_o	Axial Strain %	v%	σ'_z	σ'_x	$\sigma_1-\sigma_3$	σ_1'/σ_3'	ϕ'
Passive Compression										
Plane strain	5.96	3.23	0.54	12	6.0	8.67	3.01	5.66	2.88	29°
Triaxial	5.96	3.33	0.56	16	6.8	8.21	3.24	4.97	2.54	25.8°
Active Compression										
Plane strain	5.98	3.36	0.56	4.5	0.9	5.55	1.95	3.60	2.85	28.7°
Triaxial	5.97	3.28	0.55	7	1.8	5.46	2.15	3.31	2.54	25.8°
Active Extension										
Plane strain	5.87	3.24	0.55	-7	-0.8	1.25	3.25	2.00	2.61	26.5°
Triaxial	5.94	3.30	0.56	-9	0.7	1.49	3.25	1.76	2.18	21.8°

Stresses in Kg/cm^2

strain was 3° higher than that under triaxial conditions. This result is different from that of Hambly and Roscoe (1969), who reported the same ϕ' for triaxial and plane strain drained compression of a remolded clay. ϕ' in drained extension was 5° higher in plane strain than under triaxial conditions. Thus, ϕ' for compression in plane strain was 3 to 4° higher than that for triaxial, and for extension was 5° higher in plane strain, regardless of drained or undrained, peak deviator stress or peak σ_1'/σ_3' failure conditions.

The drained strength of any particular specimen depends on the effective stresses acting at the time of failure and on the angle of shear resistance ϕ'. If the effective stresses used during the consolidation process are the same and one of the principal stresses, σ_z' or σ_x', is held constant during shear, the strength differences can arise only due to differences in ϕ'. For all the drained stress paths studied, either σ_x' or σ_z' was held constant. Hence under a given stress path, the triaxial or plane strain strength should be a predetermined quantity if the magnitude of ϕ' is known. For example, for the passive compression stress path in which σ_x' is held constant at σ_{xc}', the drained strength will be given by

$$(\sigma'_z-\sigma'_x)_{max} = \sigma'_{xc}\left[\frac{1+\sin\phi'}{1-\sin\phi'} - 1\right] \qquad (7.1)$$

For active compression, σ'_z is held constant at σ'_{zc} and, therefore,

$$(\sigma'_{zc}-\sigma'_x)_{max} = \sigma'_{zc}\left[1 - \frac{1-\sin\phi'}{1+\sin\phi'}\right] \qquad (7.1a)$$

Similarly, for active extension with σ'_x held constant at σ'_{xc}

$$(\sigma'_{xc}-\sigma'_z)_{max} = \sigma'_{xc}\left[1 - \frac{1-\sin\phi'}{1+\sin\phi'}\right] \qquad (7.1b)$$

Using Eqs. 7.1 to 7.1b and the measured values of ϕ' in Table V, the plane strain strength would be higher than the triaxial value by 22%, 7% and 12% respectively for passive compression, active compression and active extension stress paths. The measured increase in plane strain strength of only 14% in passive compression was due to smaller value of σ'_x at failure in plane strain compared to

that under triaxial condition. Small differences in σ_x' or σ_z' from their end of consolidation values occurred, partly from small excess pore pressures at failure and partly due to change in x-sectional area of the specimen with strain. In addition, specimens subjected to the same stress path under triaxial and plane strain condition had slight variations in the end of consolidation stresses, which directly influenced their drained strength.

7.2.0 Correlation of Triaxial and Plane Strain Behaviour: Stress-Strain Relations

For linear elastic materials which are isotropic the general stress-strain relationships involve only two independent constants - Young's modulus, E, and Poisson's ratio, ν. For nonlinear materials these relationships become more complex. Simple approximations which are adequate in many cases, including the plastic range, involve the concept of functional relationship between octahedral normal stress, σ_{oct}, and octahedral normal strain, v/3, and between octahedral shear stress, τ_{oct}, and octahedral shear strain, γ_{oct}. Each of these relations is, in many cases, independent of the other. In soils, however, shear stresses may cause volume increase or decrease at constant mean

normal stress. Consequently, the simpler relationships that might be applicable to many metals, in which volumetric strain is a function only of mean normal stress and not of octahedral shear stress, are not applicable to soils. In other words, there will be a coupling in the relationships connecting the four quantities, σ_{oct}, τ_{oct}, v, γ_{oct}.

Newmark (1960) suggested the following three dimensional stress-strain relationships for cohesive soil.

$$v = f_1 (p, \tau_{oct}) \tag{7.2}$$

$$\gamma_{oct} = f_2 (p, \tau_{oct}) \tag{7.3}$$

where

f_1 and f_2 are arbitrary functions. All other quantities have been defined previously. These relationships disregard any influence of the third stress invariant, $\sigma_1'\sigma_2'\sigma_3'$, on stress-strain behaviour, which may not be the case. For the case of undrained tests, v is zero and Eq. 7.2 reduces to $f_1(p, \tau_{oct}) = 0$ or

$$\tau_{oct} = f_3(p) \tag{7.4}$$

Eq. 7.4 implies that undrained stress paths on the octahedral stress plane will be unique for tests under different stress systems. The combination of Eqs. 7.3 and 7.4 yields

$$\gamma_{oct} = f_4(\tau_{oct}) \tag{7.5}$$

Equation 7.5 indicates that a unique relationships exists between octahedral shear stress and octahedral shear strain. Ladanyi (1967) also suggested the possibility of such a relationship.

7.2.1 Undrained Effective Stress Paths

Fig. 7.7 shows effective stress paths followed on the octahedral stress plane for all triaxial and plane strain tests. The stresses have been normalized by dividing them with p_c, the octahedral effective normal stress at the end of consolidation. It can be seen that the results from all the compression tests fall essentially on the same curve, thus verifying the uniqueness expressed by Eq. 7.4. Similar conclusions were reached by Henkel and Wade (1966) and Shibata and Karube (1967) but, only for passive compression tests on

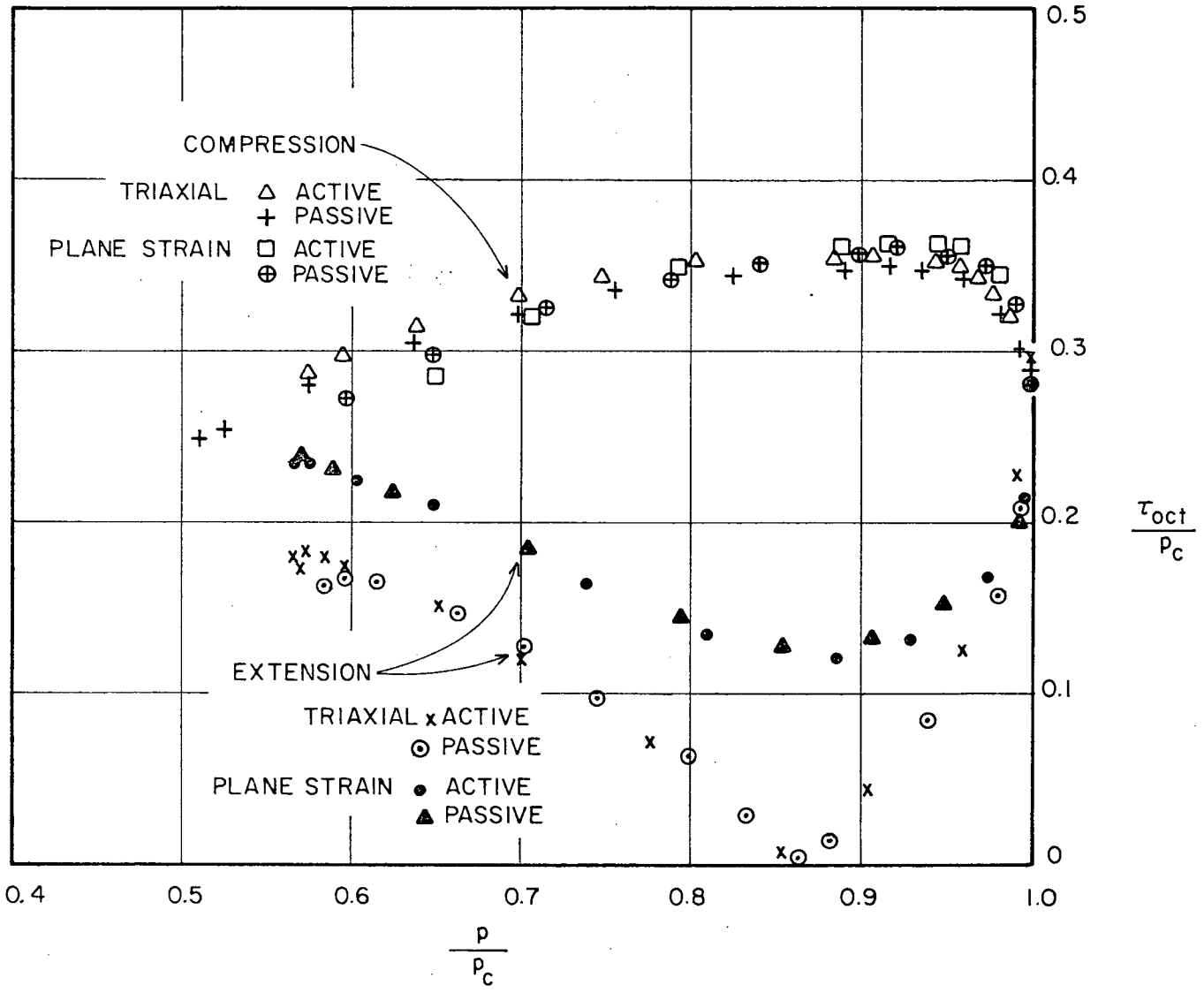

FIG. 7.7 OCTAHEDRAL EFFECTIVE STRESS PATHS DURING UNDRAINED TRIAXIAL AND PLANE STRAIN SHEAR – N.C. HANEY CLAY.

remolded clays. For Haney clay the triaxial and plane strain stress paths were found to be unique even after the peak deviator stress was reached. No appreciable divergence under the two stress systems was noticeable until the condition of maximum stress ratio, τ_{oct}/p, was approaching. During undrained extension, however, the stress paths followed were not found to be common to triaxial and plane strain conditions. In these tests a decrease occurs in both τ_{oct} and stress ratio, τ_{oct}/p. For triaxial stress conditions, since $\tau_{oct} \propto |\sigma_x-\sigma_z|$, this unloading process involves a reduction of τ_{oct} to zero when the stress state corresponds to $\sigma_z=\sigma_x$. However, under plane strain conditions τ_{oct} cannot reduce to zero, as the necessary condition for this to happen, i.e. $\sigma_x = \sigma_y = \sigma_z$, is never realized. Thus, in extension shear no agreement can be expected between the octahedral effective stress paths for triaxial and plane strain conditions.

7.2.2 Stress-Strain Comparisons

Undrained compression tests

Figure 7.8 shows the octahedral shear stress vs. octahedral shear strain relationships. Due to a small scatter in the K_o-values of the specimens, τ_{oct} at the

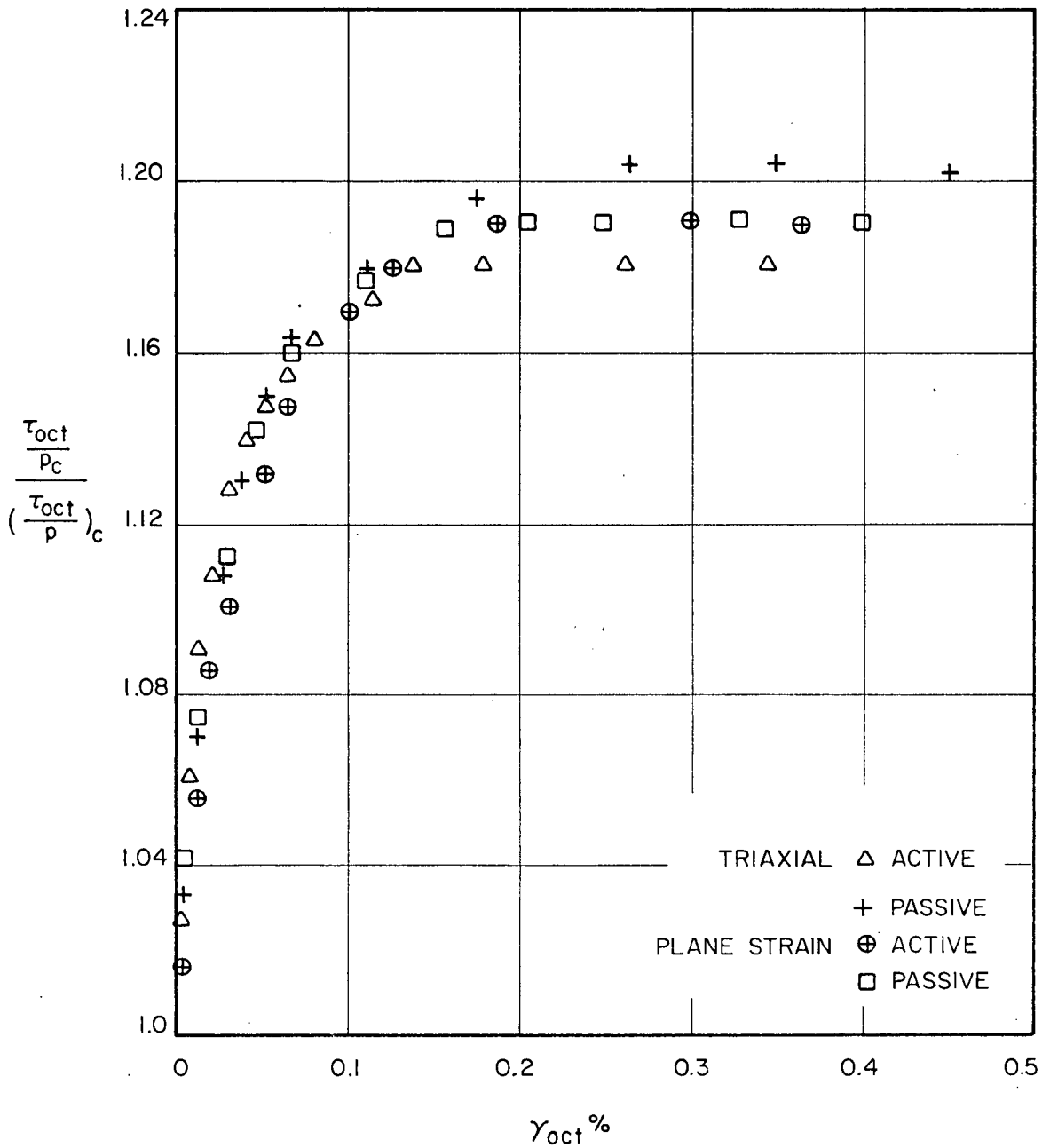

FIG. 7.8 OCTAHEDRAL SHEAR STRESS – STRAIN RELATION DURING UNDRAINED TRIAXIAL AND PLANE STRAIN COMPRESSION – N.C. HANEY CLAY.

end of consolidation was slightly different in each test. In order to have the same starting point for all stress-strain curves, the normalized octahedral shear stress, τ_{oct}/p_c, has been divided by the value of this variable at the end of consolidation. Thus, all stress-strain curves start with an ordinate of unity at zero shear strain. It can be seen from the figure that all the compression tests do obey extremely well the postulated unique octahedral shear stress-strain relation of Eq. 7.5. Compression failure ($|\sigma_z-\sigma_x|_{max}$) in both plane strain and triaxial tests occurred at strains below γ_{oct} = 0.3%. The octahedral stress-strain relationship, therefore, is seen to hold almost until failure condition is reached. Also, it was shown in Fig. 7.7 that octahedral effective stress paths were found to be identical even after the occurrence of $(\sigma_z-\sigma_x)_{max}$. This would suggest that the octahedral stress-strain relationship common to triaxial and plane strain should hold even beyond the condition of maximum deviator stress. Fig. 7.9 shows that such a post peak stress-strain relation does hold remarkably well until $\gamma_{oct} \sim 3\%$.

Undrained extension tests

As already mentioned, during undrained extension shear, τ_{oct} decreases to a minimum value before increasing to

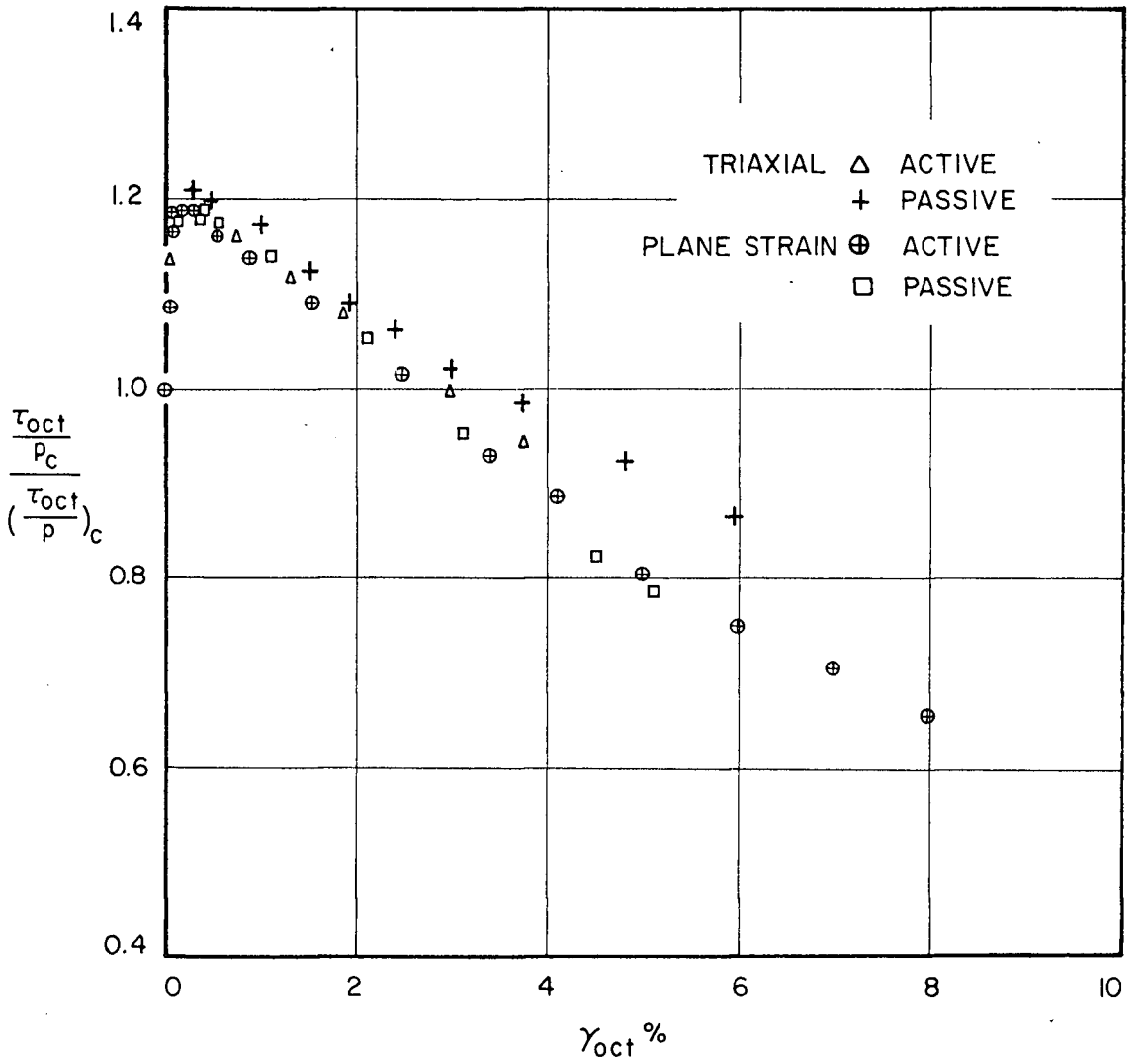

FIG. 7.9 POST PEAK OCTAHEDRAL SHEAR STRESS-STRAIN RELATION DURING UNDRAINED TRIAXIAL AND PLANE STRAIN COMPRESSION - N.C. HANEY CLAY.

cause failure. For triaxial tests, τ_{oct} attains the minimum value of zero in contrast to the plane strain tests where it reduces to about 50% of its value at the end of consolidation (Fig. 7.7). A relationship between τ_{oct}/p_c and γ_{oct} similar to that in compression tests cannot, therefore, exist for extension tests. However, if an alternative shear stress parameter, which can be considered as octahedral change of shear stress, is used instead of τ_{oct}, then both the plane strain and triaxial tests result in identical effective stress paths and, therefore, a unqiue octahedral stress strain relationship common to triaxial and plane strain conditions may exist. This shear stress parameter is expressed as

$$\Delta\tau_{oct} = \frac{1}{3}\sqrt{(\Delta\sigma_x-\Delta\sigma_y)^2 + (\Delta\sigma_y-\Delta\sigma_z)^2 + (\Delta\sigma_z-\Delta\sigma_x)^2} \qquad (7.6)$$

and is similar to that used in pore pressure Equation 5.2. $\Delta\tau_{oct}$ thus is a measure of cumulative change in octahedral component of shear stress. The relationship between $\Delta\tau_{oct}/p_c$ and octahedral shear strain is shown in Fig. 7.10 for all the triaxial and plane strain undrained tests. The remarkable uniqueness of the octahedral stress-strain relationship is clearly demonstrated in this figure. The very

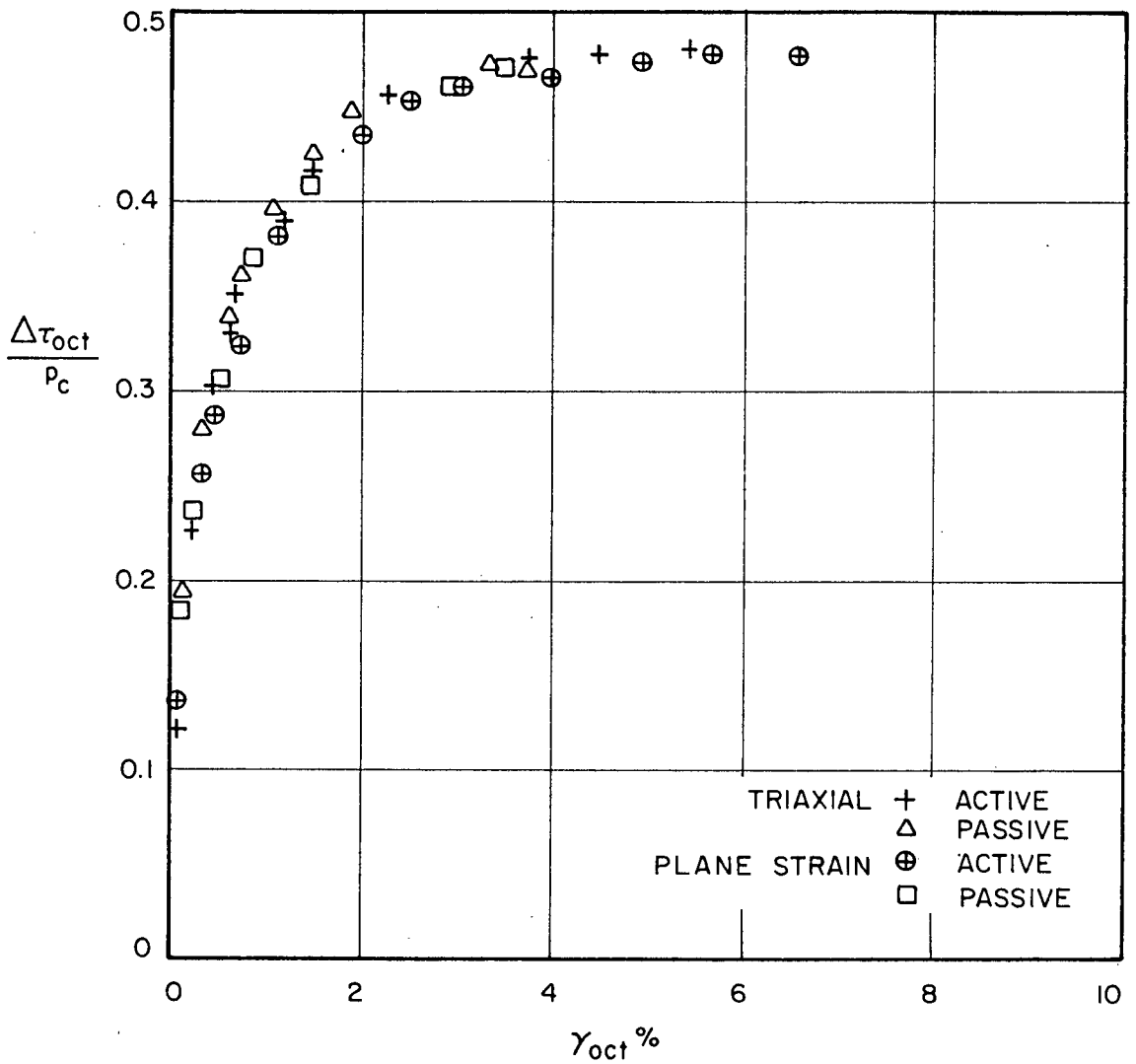

FIG. 7.10 OCTAHEDRAL SHEAR STRESS – STRAIN RELATION DURING UNDRAINED TRIAXIAL AND PLANE STRAIN EXTENSION – N.C. HANEY CLAY.

significant feature to be noted is the validity of this relation for all strains until failure.

Drained Stress-Strain Relationships:
Volumetric Strains: Compression Tests

It was shown in Chapter V and VI that an extended form of Rendulic's hypothesis of uniqueness of void ratio and effective stresses could be successfully used to predict volumetric strains in load increasing drained compression tests from the results of undrained compression tests. The hypothesis was shown to be valid for both triaxial and plane strain conditions separately. The uniqueness of effective stress paths on the τ_{oct} vs. p plane, for both plane strain and triaxial undrained compression tests (Fig. 7.7), now implies the existence of an undrained state boundary surface curve in τ_{oct}/p_e, p/p_e axes, which is common to triaxial and plane strain stress systems. It was also shown in Chapter V that excellent agreement was obtained between volumetric strains actually measured and those predicted from the undrained state boundary surface curve for the case of drained plane strain passive compression test. Since the undrained state boundary surface is the same for plane strain and triaxial undrained tests, precisely the same predictions of volume change in plane

strain test would be made from the results of undrained triaxial compression tests (see Fig. 7.11). It is, therefore, suggested that volumetric strains in load increasing drained plane strain compression tests can be predicted from the results of undrained triaxial test on an identical specimen, by applying extended Rendulic hypothesis in (p, τ_{oct}, e) space.

It was not found possible (Chapters V and VI) to make satisfactory predictions of volumetric strains in load decreasing drained active compression tests, by the application of Rendulic's hypothesis. This was due to the fact that τ_{oct}/p_e vs. p/p_e curve for such tests fell slightly below the similar curve for undrained or load increasing drained compression tests. This situation was common to both triaxial and plane strain stress systems. However, it is interesting to note that a common τ_{oct}/p_e, p/p_e curve is obtained for both plane strain and triaxial drained active compression tests. This is shown in Fig. 7.12. This amounts to saying that there can be assumed to exist a state boundary surface curve for drained unloading active compression tests, which is different from that for the undrained compression tests, but is common to triaxial and plane strain conditions. It, therefore, follows that the τ_{oct}/p_e vs. p/p_e relationship of the triaxial test

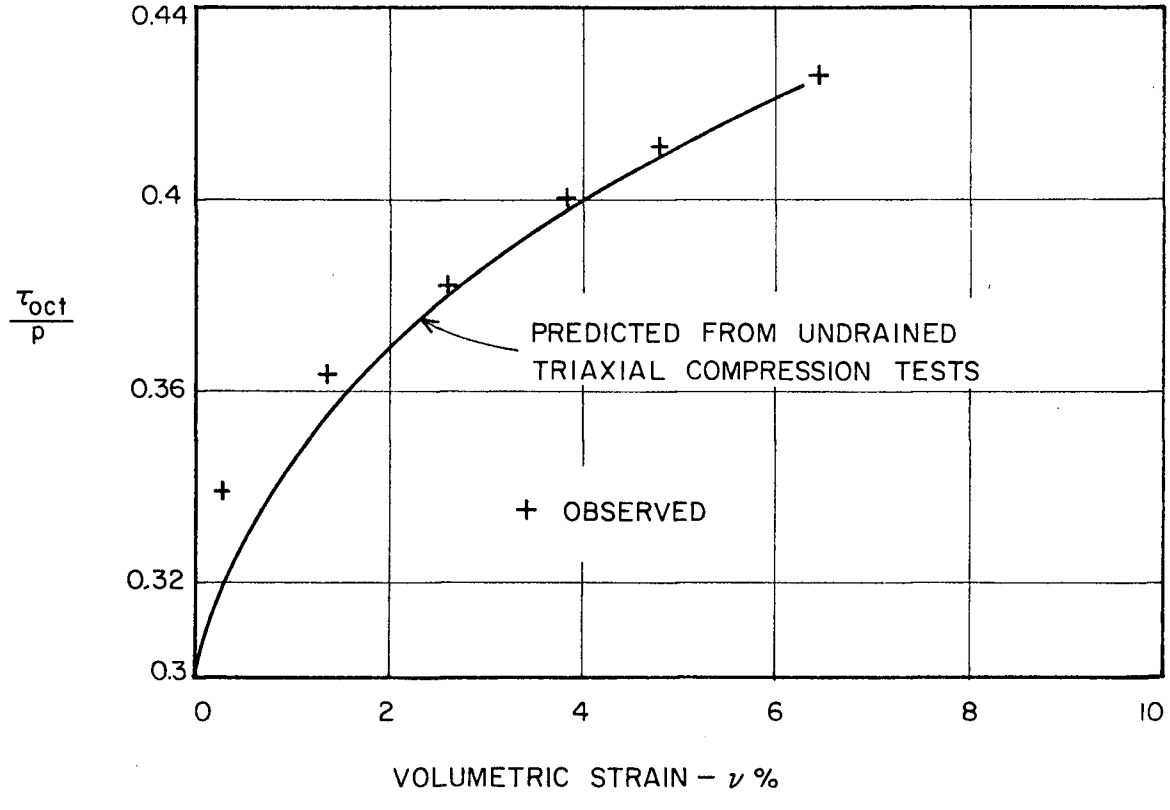

FIG. 7.11 COMPARISON OF OBSERVED AND PREDICTED VOLUMETRIC STRAINS DURING PLANE STRAIN DRAINED PASSIVE COMPRESSION – N.C. HANEY CLAY.

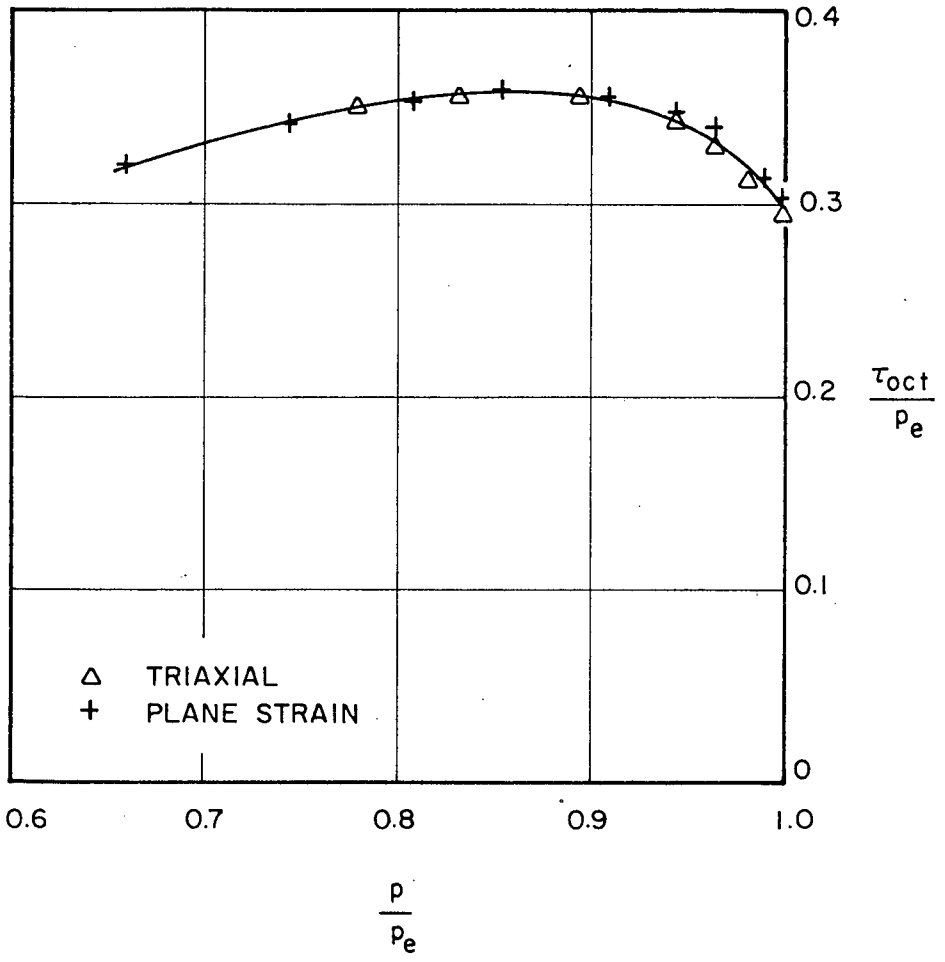

FIG. 7.12 COMMON STATE BOUNDARY SURFACE CURVE FOR DRAINED TRIAXIAL AND PLANE STRAIN ACTIVE COMPRESSION – N.C. HANEY CLAY.

could be used to predict volume changes in the plane strain test. Volumetric strains thus predicted for drained plane strain active compression test are shown in Fig. 7.13, along with the observed values. Keeping in view the small magnitude of volumetric strains, agreement between predictions and observations is good.

Volumetric Strains - Extension Tests

It was shown in Chapter V and VI that undrained and drained behaviour during active extension was virtually identical for both plane strain and triaxial stress systems. This is due to the very small volume changes associated with the drained tests, which renders the situation close to the undrained one. It was also shown earlier in this chapter that the undrained extension stress-strain relationship was unique in terms of $\Delta\tau_{oct}$ vs. γ_{oct} (Fig. 7.10). It, therefore, follows that drained active extension tests, because of being almost identical to their undrained counterparts, will also possess a unique $\Delta\tau_{oct}$ vs. γ_{oct} relationship. That this is very nearly true is shown in Fig. 7.14. From this relationship one can predict changes in mean normal effective stress, p, in plane strain from the results of triaxial tests. The volumetric strains in plane strain drained active extension test can then be evaluated from changes in mean normal stress, p, and the swelling index, κ, as was discussed in Chapter V. Changes in p under plane strain are found as follows: for a given γ_{oct},

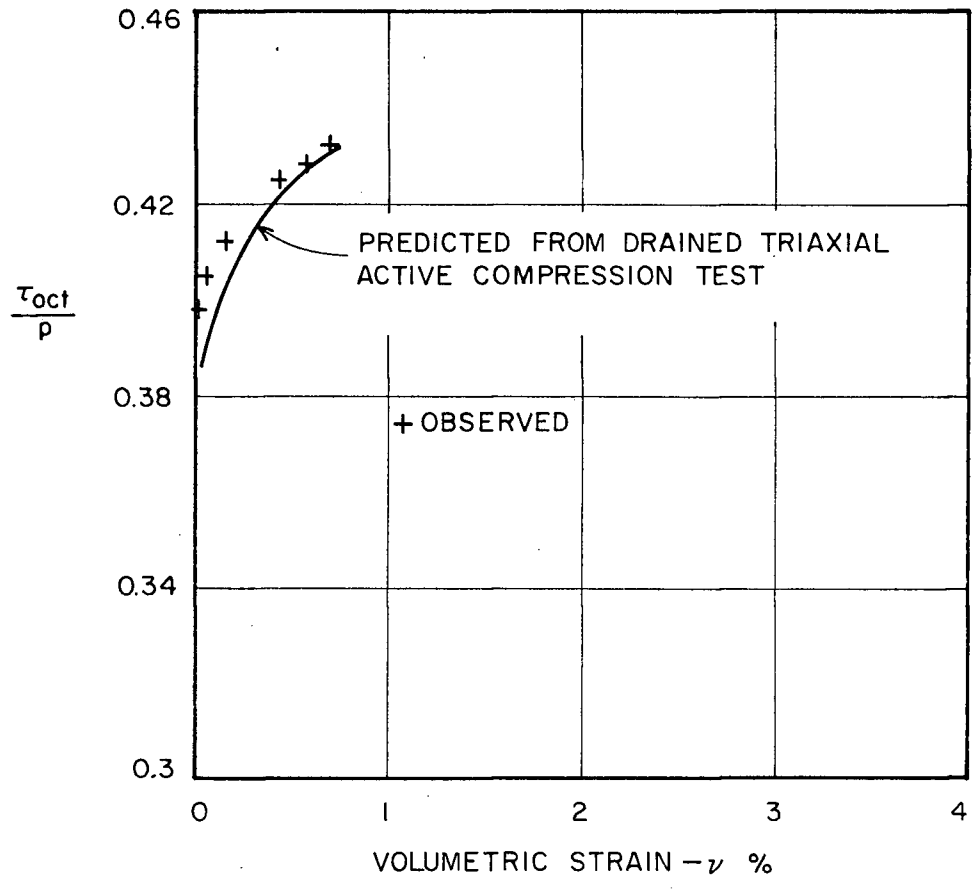

FIG. 7.13 COMPARISON OF OBSERVED AND PREDICTED VOLUMETRIC STRAINS DURING PLANE STRAIN DRAINED ACTIVE COMPRESSION – N.C. HANEY CLAY.

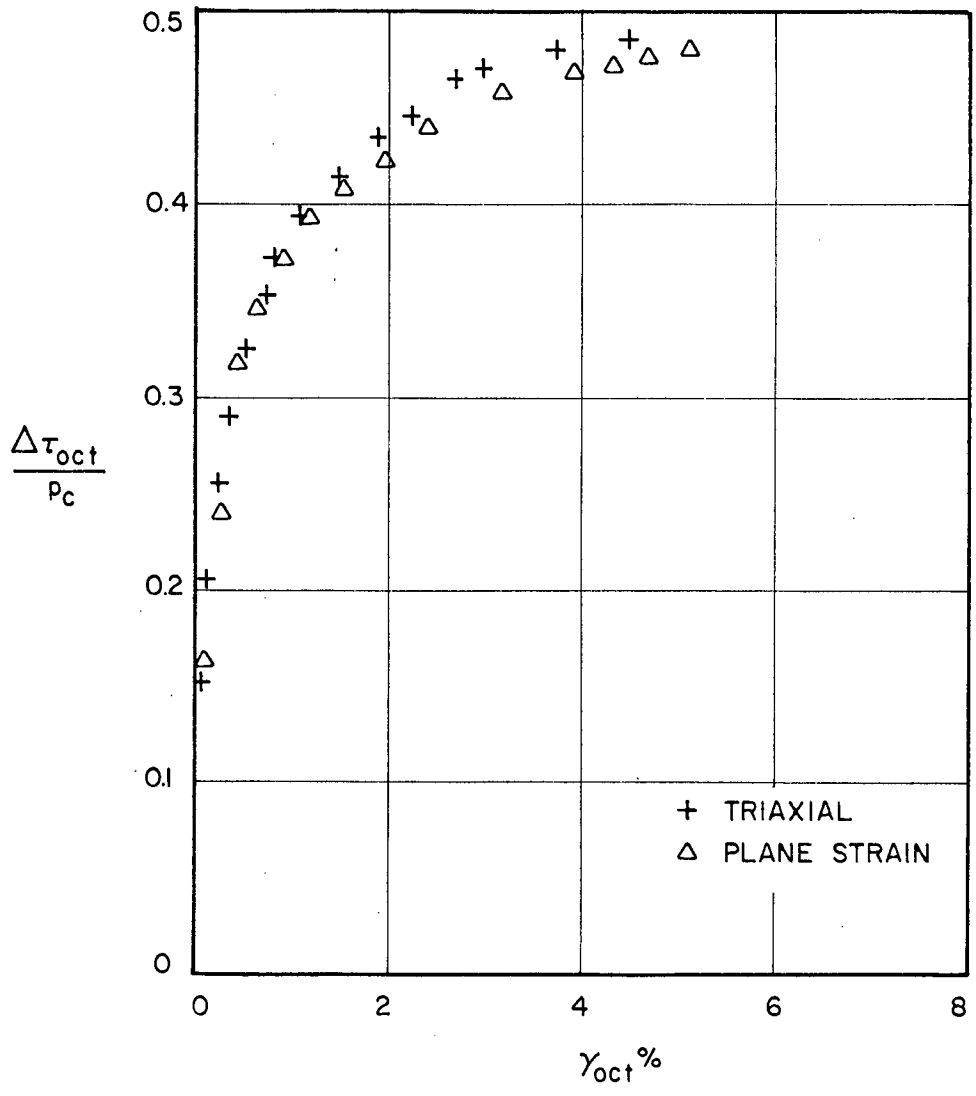

FIG. 7.14 OCTAHEDRAL SHEAR STRESS - STRAIN RELATION DURING TRIAXIAL AND PLANE STRAIN DRAINED ACTIVE EXTENSION - N.C. HANEY CLAY.

$(\Delta\tau_{oct})_{p.s} = (\Delta\tau_{oct})_T$ • • • where subscripts refer to plane strain and triaxial conditions respectively. During drained active extension stress path, σ'_x is held constant at σ'_{xc} and, therefore, $\Delta\sigma'_x = 0$. It was shown in Chapter V that in plane strain $\sigma'_y \sim 0.37(\sigma'_x + \sigma'_z)$, $\therefore (\Delta\sigma'_y)_{p.s} = 0.37(\Delta\sigma'_z + \Delta\sigma'_x)$ and then $(\Delta\tau_{oct})_{p.s} = (\Delta\tau_{oct})_T$ reduces to $0.877(\Delta\sigma'_z)_{p.s} = (\Delta\sigma'_z)_T$ and

$$(\Delta p)_{p.s} = \frac{1}{3}\left[\left(\Delta\sigma'_z\right)_{p.s} + 0.37\left(\Delta\sigma'_z\right)_{p.s}\right] \qquad (7.7)$$

Volumetric strains during drained extension tests, however, were very small (less than 0.75% in absolute magnitude) and, therefore, their prediction may not be very important.

Since load increasing drained passive extension test could not be performed in the plane strain apparatus, no attempt can be made to correlate plane strain and triaxial volume changes for this total stress path.

Shear Strains:

It was pointed out in both Chapters V and VI that normality condition of theory of plasticity could not be used for prediction of plastic strain increment ratio, $\delta\gamma_{oct}/\delta v$, for Haney clay when stress ratio τ_{oct}/p was ≥ 0.38. This corresponds to the point on the state boundary surface curve where tangent to this curve becomes horizontal and, therefore, implies unlimited shear strain, $\delta\gamma_{oct}$ without volume change. In load increasing drained compression tests on Haney clay, however, this stress ratio corresponded to a γ_{oct} value of about 20% of that at failure. Therefore, the normality condition coupled with empirical extended Rendulic stress-volume strain relationship is of limited use for prediction of shear strains in drained plane strain compression tests form the results of drained or undrained triaxial compression tests.

Equation 7.3 suggests that there may be a common τ_{oct}/p vs. γ_{oct} relationship for drained compression tests common to triaxial and plane strain conditions. Such relationships are shown plotted in Figures 7.15 and 7.16 for drained passive and active compression tests. Because of small differences in the intial values of τ_{oct}/p, the ratio, $(\tau_{oct}/p)/(\tau_{oct}/p)_c$, was used as the ordinate, where $(\tau_{oct}/p)_c$ is the value of (τ_{oct}/p) at tne end of consolidation.

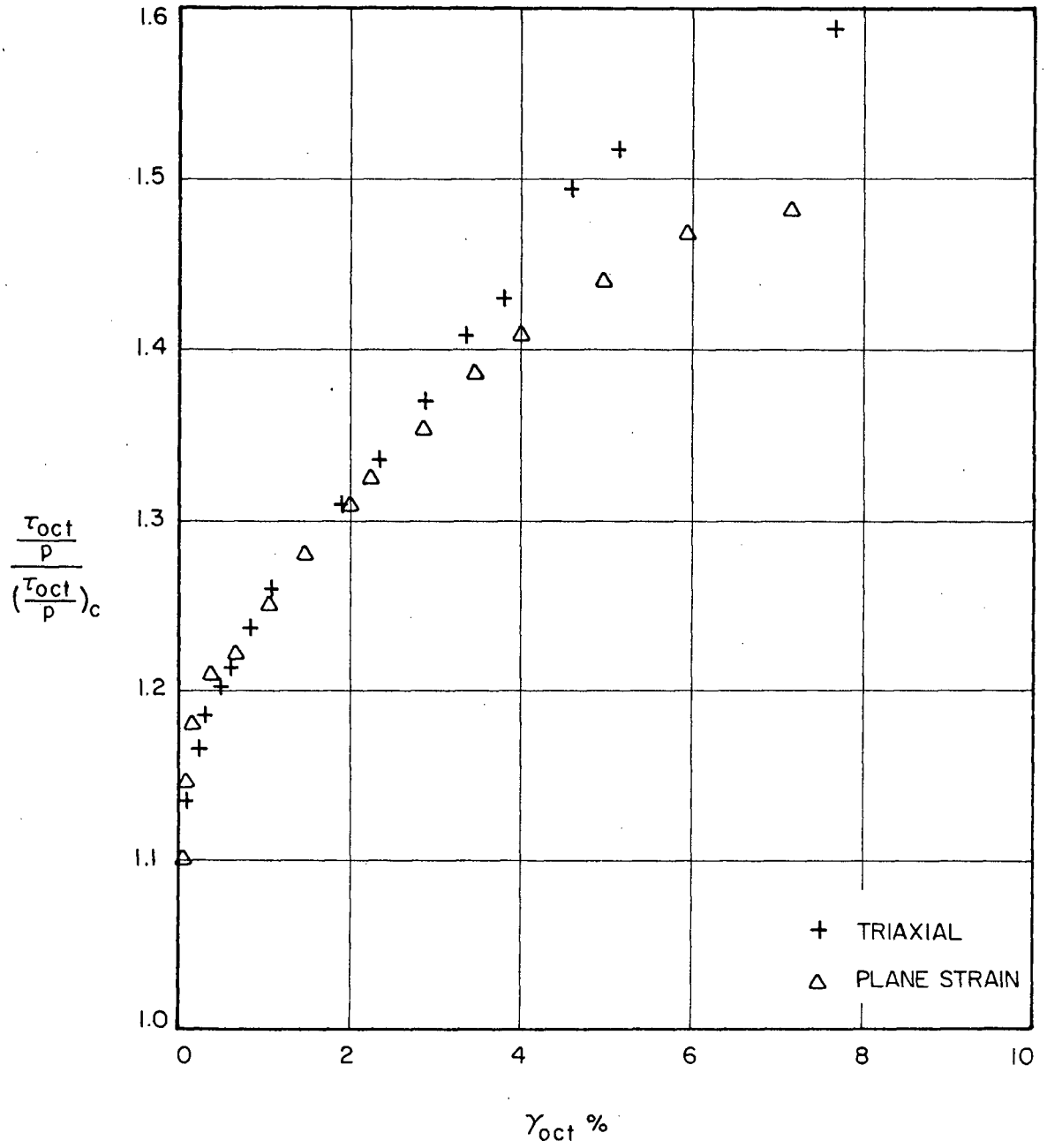

FIG. 7.15 OCTAHEDRAL STRESS RATIO - SHEAR STRAIN RELATION DURING DRAINED TRIAXIAL AND PLANE STRAIN PASSIVE COMPRESSION - N.C. HANEY CLAY.

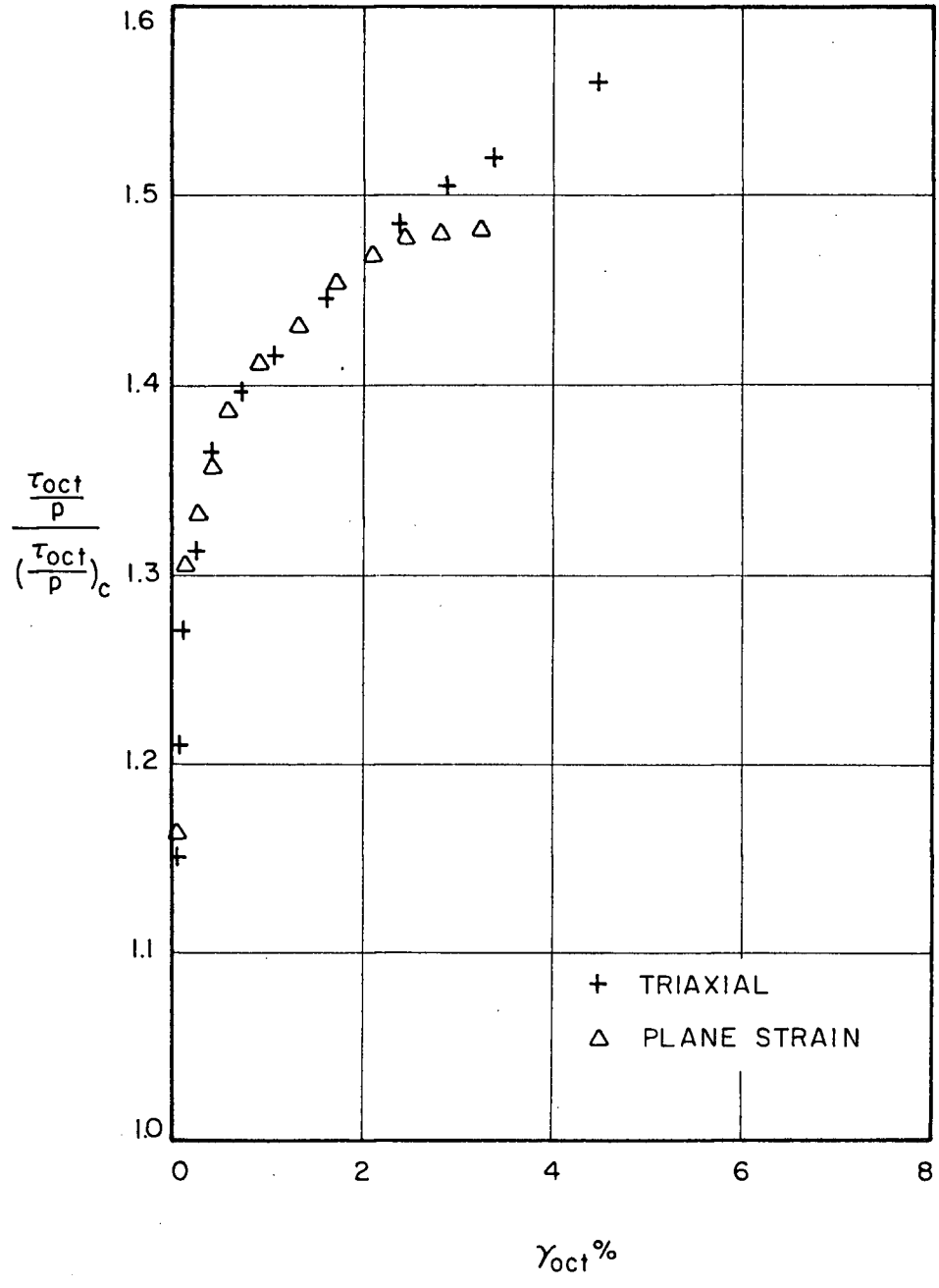

FIG. 7.16 OCTAHEDRAL STRESS RATIO – SHEAR STRAIN RELATION DURING DRAINED TRIAXIAL AND PLANE STRAIN ACTIVE COMPRESSION – N.C. HANEY CLAY.

It can be seen that the relationship postulated does hold quite well for shear strains which are about 60% of the failure value in plane strain passive compression. The agreement for active compression is seen to hold almost until failure in plane strain.

It was shown in Fig. 7.14 that during drained active extension $\Delta\tau_{oct}/p_c$ vs. γ_{oct} relationship was common to triaxial and plane strain conditions. This relationship, therefore, can be used to predict shear strains in plane strain drained active extension test from the results of similar test under triaxial conditions.

7.3.0 Prediction of Drained Plane Strain Behaviour From Soil Parameters Determined in Triaxial Compression by the Cambridge Stress-Strain Theory

Roscoe and Burland (1968) describe the extension of Cambridge stress-strain theory for predicting plane strain behaviour of a normally consolidated saturated remolded clay by using soil parameters determined from isotropically consolidated triaxial compression tests. In this theory it is assumed that both the state boundary surface and the yield locus for such a clay are symmetrical about the space diagonal, $\sigma_1'=\sigma_2'=\sigma_3'$, in the three-dimensional

principal effective stress space. The equation of the state boundary surface in $(p, \sqrt{3}\tau_{oct})$ three-dimensional stress space is

$$\frac{p}{p_e} = \left(\frac{M^{*2}}{M^{*2} + \eta^{*2}} \right)^{1-\frac{\kappa}{\lambda}} \tag{7.8}$$

where p_e, κ, λ refer to isotropic compression or swelling conditions and can be obtained from isotropic consolidation test. $\eta^* = \sqrt{3}\tau_{oct}/p$, $M^* = \sqrt{2/3}\, M$. M is the ratio between deviator stress, q, and p in triaxial compression test at the critical state. (An element of soil is assumed to have reached critical state if it continues to deform without change in e, p or q.) In triaxial compression tests on remolded clays, critical state is reached when q reaches a maximum, which occurs at the same time when q/p reaches a maximum.

Roscoe and Burland assume the clay to be an isotropic rigid work-hardening material. For this assumed condition $\kappa = 0$ and equation of state boundary surface curve becomes

$$\frac{p}{p_e} = \frac{M^{*2}}{M^{*2} + \eta^{*2}} \qquad (7.9)$$

An average value of ϕ' during triaxial compression of Haney clay was 27° (Chapter VI), which gives $M = 6\sin\phi'/3-\sin\phi' = 1.07$. Fig. 7.17 shows the predicted state boundary surface for Haney clay. Also shown in this figure are the results from undrained compression test in plane strain. It can be seen that the observed undrained stress path neither lies on nor bears any resemblance to the state boundary surface curve derived from triaxial test soil parameters. It, therefore, would appear that the strains predicted for drained plane strain passive compression test from the assumed state boundary surface (Eq. 7.9) are not likely to bear any relationship to the observed strains. For $\kappa = 0$ clays the undrained stress path is also the current yield locus. The shape of the predicted and the observed undrained stress paths then suggests (Fig. 7.17) that the shear strain increments for a given change $\delta\eta^*$ in η^*, calculated from the predicted yield locus will be too large when compared to those calculated from the observed yield locus. This is because, for a given value of η^* the slope of predicted yield locus is much flatter

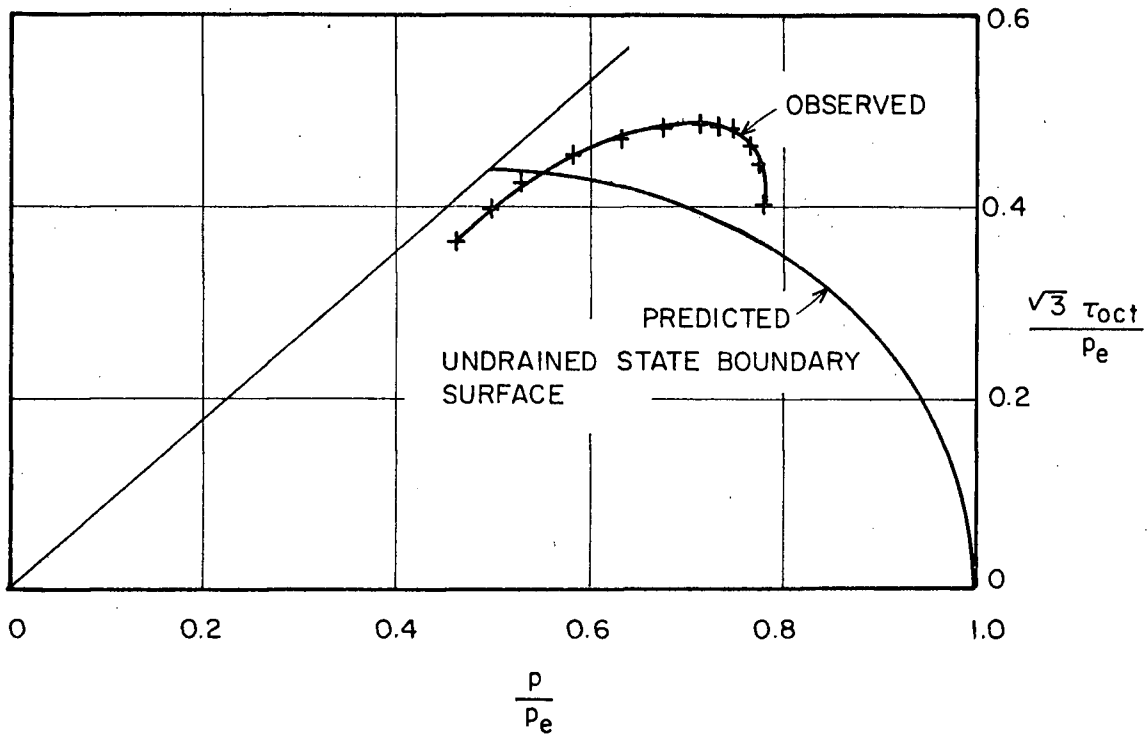

FIG. 7.17 COMPARISON OF OBSERVED STATE BOUNDARY SURFACE CURVE AND THE STATE BOUNDARY SURFACE CURVE PREDICTED BY THE CAMBRIDGE THEORY FOR UNDRAINED PLANE STRAIN COMPRESSION - N.C. HANEY CLAY.

than that of the observed yield locus. Consequently, the ratio $\delta\gamma_{oct}/\delta v$ is too large in the former case. That the Cambridge theory does overpredict strains will be demonstrated for the passive drained plane strain test.

Hambly and Roscoe (1969) gave the following equations for prediction of strains during plane strain yield, using triaxial parameters M and λ. These equations correspond to what is known as the 'modified' theory.

$$\delta\varepsilon_z + \delta\varepsilon_x = \frac{\lambda}{1+e}\left[\frac{2\eta' \delta\eta'}{\left(\frac{M}{\sqrt{3}}\right)^2 + \eta'^2} + \frac{\delta s}{s}\right] \tag{7.10}$$

$$\delta\varepsilon_z - \delta\varepsilon_x = \frac{\lambda}{1+e}\left[\frac{2\eta'\delta\eta'}{\left(\frac{M}{\sqrt{3}}\right)^2 + \eta'^2} + \frac{\delta s}{s}\right]\left[\frac{2\eta'}{\left(\frac{M}{\sqrt{3}}\right)^2 - \eta'^2}\right] \tag{7.10a}$$

where $\eta' = (\sigma_z'-\sigma_x')/(\sigma_z'+\sigma_x')$ and $s = (\sigma_z'+\sigma_x')/2$.

Figure 7.18 shows the predicted stress-strain relationships for the drained plane strain passive compression test according to Eqs. 7.10. Also shown in the figure

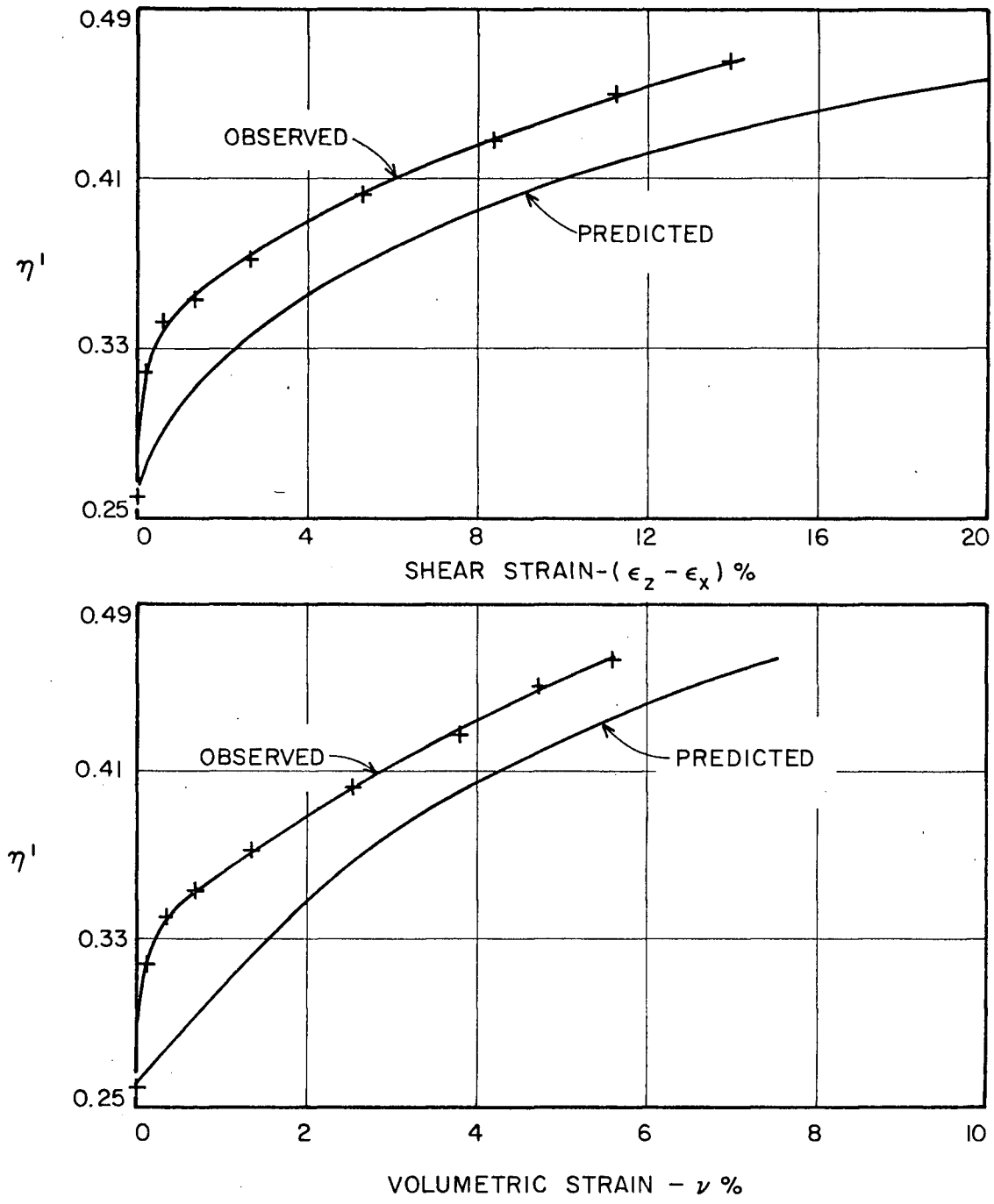

FIG. 7.18 COMPARISON OF OBSERVED STRESS-STRAIN RELATIONS AND THOSE PREDICTED BY CAMBRIDGE THEORY DURING DRAINED PLANE STRAIN PASSIVE COMPRESSION – N.C. HANEY CLAY.

are strains actually observed in this test. Both volumetric and shear strains predicted by the theory are too large. In particular, as would be expected from the shape of the predicted and the observed yield loci (Fig. 7.17), the predicted shear strains are excessively larger than the observed values. For undisturbed Haney clay, therefore, the Cambridge theory does not provide satisfactory prediction of strains in loading plane strain tests from the soil parameters determined in the triaxial tests. A similar statement would apply for the active drained plane strain tests. For the drained active extension test, the applied stress path always lies below the current yield locus. For such stress changes the 'modified' Cambridge theory predicts zero shear and volumetric strains. Roscoe and Burland (1968) also presented a 'revised' version of the 'modified' Cambridge theory. The 'revised' theory does predict shear strains in the drained active extension plane strain test. The magnitude of the shear strain at any value of η' would be equal to the shear strain for the same value of η' in the corresponding undrained test. In other words, the shear stress-strain relationship for the drained and undrained active extension plane strain tests would be identical. This was shown to be very nearly true in Fig. 5.15 where

drained and undrained plane strain active extension tests give essentially identical τ_{oct}/p vs. γ_{oct} relationships.

The Cambridge stress-strain theory, at present, is unable to predict strains in undrained plane strain tests using the results obtained in the triaxial tests.

7.4.0 Correlation of Triaxial and Plane Strain Failure Conditions

7.4.1 Undrained Strength

The conventional measure for undrained strength of soil is one-half the peak deviator stress $(\sigma_1-\sigma_3)_{max}/2$. It has previously been shown that for identical stress paths, $(\sigma_1-\sigma_3)_{max}/2\sigma'_{1c}$ was larger in plane strain than under triaxial conditions. These apparent differences in undrained strength can, however, be explained if the undrained strength is characterised by maximum octahedral shear stress, $(\tau_{oct})_{max}$. This follows from the observed uniqueness of octahedral effective stress paths and the octahedral stress-strain relationships. Table VI shows the values of τ_{oct}/p_c at $(\tau_{oct})_{max}$. (The condition of $(\tau_{oct})_{max}$ is reached at the same time as $(\sigma_1-\sigma_3)_{max}$.) It can be seen that the triaxial and plane strain compression failure occurs at essentially identical values of τ_{oct}/p_c. In axial extension,

TABLE VI

Co-relation of Undrained Strength under Triaxial and Plane Strain Conditions

	Failure Condition $(\sigma_1-\sigma_3)_{max}$ or $(\tau_{oct})_{max}$	
	$(\sigma_1-\sigma_3)/2\sigma'_{1c}$	τ_{oct}/p_c
Undrained Compression		
Plane strain	0.293	.363
Triaxial	0.265	.356

	$(\sigma_1-\sigma_3)/2\sigma'_{1c}$	τ_{oct}/p_c	$\Delta\tau_{oct}/p_c$
Undrained Extension			
Plane strain	0.193	0.242	0.479
Triaxial	0.130	0.175	0.476

σ'_{1c} - major consolidation stress

p_c - mean consolidation stress

however, unique effective stress paths and stress-strain relationships were found only if $\Delta\tau_{oct}$ was used as the shear stress parameter. Therefore, at failure condition $\Delta\tau_{oct}/p_c$ in place of τ_{oct}/p_c was found to be the same under both triaxial and plane strain stress systems.

7.4.2 Failure Criteria

A failure criterion expresses a functional relationship between effective stresses at failure. There are three failure criteria usually considered applicable to soils (Bishop, 1966). For normally consolidated clays (c=0) these criteria can be written as

Mohr-Coulomb:
$$\frac{\sigma_1'-\sigma_3'}{\sigma_1'+\sigma_3'} = \sin\phi' \tag{7.11}$$

Extended Tresca:
$$\sigma_1'-\sigma_3' = \alpha p \tag{7.12}$$

Extend von Mises:
$$\tau_{oct} = \frac{\sqrt{2}}{3}\alpha p \tag{7.13}$$

where α is a soil constant. Of these three criteria the Mohr-Coulomb does not recognize any influence of σ_2' on the angle of shearing resistance, ϕ'. It has

been previously shown, however, that Mohr-Coulomb ϕ' was, for all stress paths, larger in plane strain than under triaxial conditions. The Mohr-Coulomb criterion, therefore, underestimates the plane strain strength of Haney clay.

The other two criteria, the Extended Tresca and Extended von Mises, do account for the influence of σ_2' on failure conditions. Considering triaxial failure conditions as the reference at which all the three criteria are made to coincide, the ϕ' implied under plane strain conditions according to extended Tresca and von Mises criteria can be evaluated. Then a comparison of observed and predicted ϕ' would show if either of those failure criteria could be considered applicable to undisturbed Haney clay. If the value of σ_2' relative to σ_1' and σ_3' is expressed by

$$b = \frac{\sigma_2' - \sigma_3'}{\sigma_1' - \sigma_3'} \tag{7.14}$$

then the Tresca and von Mises criteria can be expressed as follows (Bishop, 1966):

Extended Tresca:

$$\frac{\sigma_1'-\sigma_3'}{\sigma_1'+\sigma_3'} = \frac{1}{\frac{1}{3} + \frac{2}{\alpha} - \frac{2}{3}b} \tag{7.15}$$

Extended von Mises:

$$\frac{\sigma_1'-\sigma_3'}{\sigma_1'+\sigma_3'} = \frac{1}{\frac{1}{3} + \frac{2}{\alpha}\sqrt{1-b+b^2} - \frac{2}{3}b} \tag{7.16}$$

For a given triaxial 'α' and the value of 'b' in plane strain, the left hand sides of Eqs. 7.15 and 7.16 express the values of $\sin\phi'$ implied by the Extended Tresca and Extended von Mises criteria.

Table VII shows the values of plane strain ϕ' predicted by Eqs. 7.15 and 7.16 along with observed values of ϕ'. Both $(\sigma_1-\sigma_3)_{max}$ and $(\sigma_1'/\sigma_3')_{max}$ failure conditions are considered for undrained compression failure. The observed ϕ' is closest to that predicted by the Extended von Mises criterion at the $(\sigma_1'-\sigma_3')_{max}$ undrained failure conditions. However, the comparison between the observed and predicted ϕ' values at $(\sigma_1'/\sigma_3')_{max}$ for both undrained and drained failure seems to favour the Extended Tresca criterion.

During triaxial extension failure b=1, and from Eqs. 7.15 and 7.16 this implies largest ϕ' for the

TABLE VII

Comparison Between Observed Plane Strain ϕ' and ϕ' Predicted from Triaxial Results by Different Failure Criteria

	Triaxial Failure		Plane Strain Failure			
	ϕ'	α	b	Observed ϕ'	Predicted ϕ'	
					Tresca	Von Mises
Undrained Compression						
at $(\sigma_1-\sigma_3)_{max}$	21.0°	0.814	0.22	25.4°	22.2°	24.4°
at $(\sigma'_1/\sigma'_3)_{max}$	26.6°	1.053	0.285	30.4°	29.4°	33.1°
Drained Compression						
Active & passive	25.8°	1.017	0.285	28.8°	28.2°	32.0°

triaxial state of stress, when compared to other states with $b<1$. During plane strain extension failure 'b' was typically around 0.15. Both Tresca and von Mises criteria then imply larger ϕ' for triaxial extension than for plane strain conditions. This is opposite to the observed plane strain ϕ' which was larger than triaxial ϕ' by about 5°. Thus, it must be concluded that none of the classical failure criteria, at least in the present form, satisfactorily predicts failure for all types of stress paths and stress systems.

CHAPTER VIII

TEST RESULTS ON HEAVILY OVERCONSOLIDATED HANEY CLAY

8.1.0 The Influence of Stress Path on Triaxial and Plane Strain Results

The effect of variation in applied stress path on the behaviour of Haney clay was essentially the same for both triaxial and plane strain conditions. Thus, the following discussion of results applies to both groups (triaxial and plane strain) of tests.

The end of consolidation stresses were slightly different from sample to sample in each group of tests (Tables VIII & IX), which may account for some of the observed difference in behaviour under the various applied stress paths. It may be mentioned here that in overconsolidated samples the end of consolidation condition was $\sigma_x' = \sigma_y' > \sigma_z'$, and therefore, compression stress paths were associated with an initial unloading of deviator stress and subsequent reorientation of principal stresses at failure. Tables VIII and IX will be discussed throughout section 8.1.

TABLE VIII

Summary of Drained and Undrained Triaxial Test Results on O.C. Haney Clay

	End of Consolidation					Failure Condition									
				O.C.R.		$(\sigma_1-\sigma_3)_{max}$					$(\sigma'_1/\sigma'_3)_{max}$				
	σ'_{zc}	K_o	p_c	$\frac{(\sigma'_z)_{max}}{\sigma'_{zc}}$	$\frac{(p_c)_{max}}{p_c}$	$\varepsilon_z\%$	$\sigma_1-\sigma_3$	σ'_1/σ'_3	v%	a	$\varepsilon_z\%$	$\sigma_1-\sigma_3$	σ'_1/σ'_3	v%	a
Undrained															
Compression	0.32	2.11	0.56	18.6	7.4	7.8	1.30	3.05	0	-.62	3.5	1.06	3.45	0	-0.36
Extension	0.31	2.2	0.55	19.2	7.6	-7.8	1.05	3.10	0	-1.9	-3.0	0.88	3.45	0	-1.68
Drained Compression															
Passive	0.33	1.74	0.50	18.1	8.3	6.0	1.48	3.35	0.7	—	6.0	1.48	3.35	0.7	—
Active	0.31	2.14	0.55	19.2	7.6	2.0	0.30	8.1	-4.6	—	2.0	0.30	8.1	-4.6	—
Drained Extension															
Active	0.31	2.15	0.54	19.1	7.7	-4.6	0.60	6.7	-2.1	—	-4.6	0.60	6.7	-2.1	—
Passive	0.31	1.98	0.52	19.1	8.0	-8.0	1.06	3.2	0.4	—	-8.0	1.06	3.2	0.4	—

Stresses in Kg/cm^2

TABLE IX

Summary of Drained and Undrained Plane Strain Test Results on O.C. Haney Clay

	End of Consolidation					Failure Condition									
				O.C.R.		$(\sigma_1-\sigma_3)_{max}$					$(\sigma_1'/\sigma_3')_{max}$				
	σ'_{zc}	K_o	p_c	$\frac{(\sigma'_z)_{max}}{\sigma'_{zc}}$	$\frac{(p_c)_{max}}{p_c}$	ε_z%	$\sigma_1-\sigma_3$	σ_1'/σ_3'	v%	a	ε_z%	$\sigma_1-\sigma_3$	σ_1'/σ_3'	v%	a
Undrained															
Compression	0.35	1.64	0.50	17.3	8.1	3.8	1.42	4.5	0	-0.48	2.5	1.16	4.8	0	-0.3
Extension	0.38	1.68	0.56	15.6	7.6	-4.0	1.14	3.1	0	-1.26	-2.1	1.01	3.3	0	-1.05
Drained															
Passive compression	0.35	1.59	0.56	16.6	8.5	4.8	1.66	4.2	2.2	—	4.8	1.66	4.2	2.2	—
Active extension	0.39	1.50	0.54	15.4	8.1	-4.0	0.99	5.0	-1.2	—	-4.0	0.99	5.0	-1.2	—
Passive extension	0.38	1.58	0.53	15.4	7.7	-4.0	1.18	3.4	0.2	—	-4.0	1.18	3.4	0.2	—

Stresses in Kg/cm^2

8.1.1 Undrained Test Results

The deviator stress-strain behaviour during undrained compression and extension was very similar (Fig. 8.1) and the axial strain at failure was essentially the same. The undrained strength, $(\sigma_1-\sigma_3)_{max}/2$, in extension was about 81% of that in compression (Tables VIII, IX).

Shear induced pore pressures, as reflected in the pore pressure parameter, 'a' (Eq. 5.2) were entirely negative during extension shear, thus indicating a dilatant structure (Fig. 8.2). Compression stress path, on the other hand, gave rise to shear induced pore pressures which were initially positive and pore pressures did not become negative until about 1% axial strain. This behaviour is in apparent contrast to that of familiar isotropically heavily overconsolidated soils, in which shear induced pore pressures are often found negative from the beginning of compression shear.

One of the reasons for this difference in pore pressure behaviour may lie in the manner in which overconsolidation ratio (O.C.R.) is defined for isotropically and K_o-consolidated samples. For isotropically consolidated samples, it makes no difference whether O.C.R. is defined as the ratio of maximum to rebound vertical

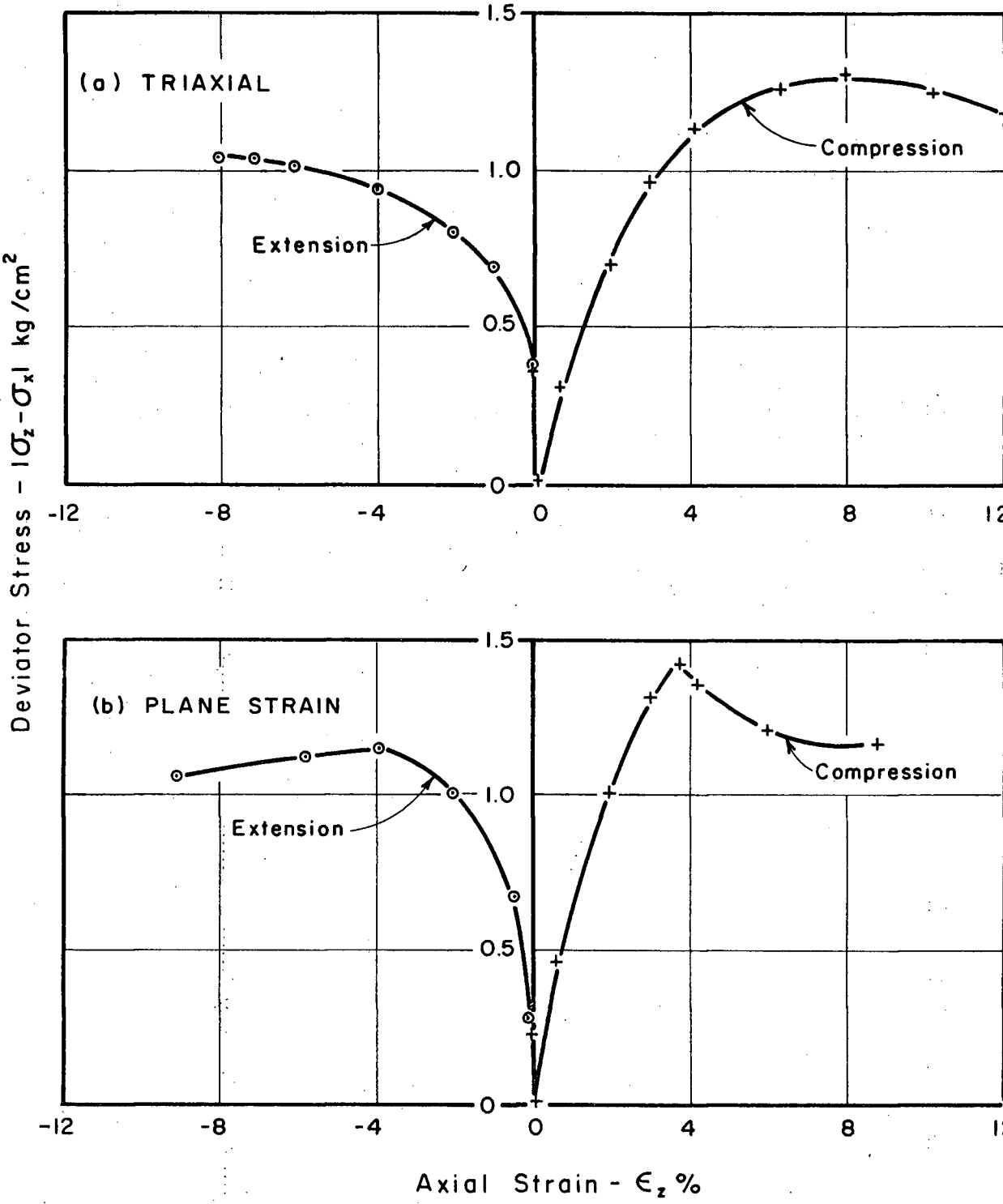

Fig.8.1 - DEVIATOR STRESS-STRAIN RELATIONSHIPS DURING UNDRAINED TRIAXIAL AND PLANE STRAIN SHEAR - O.C. HANEY CLAY.

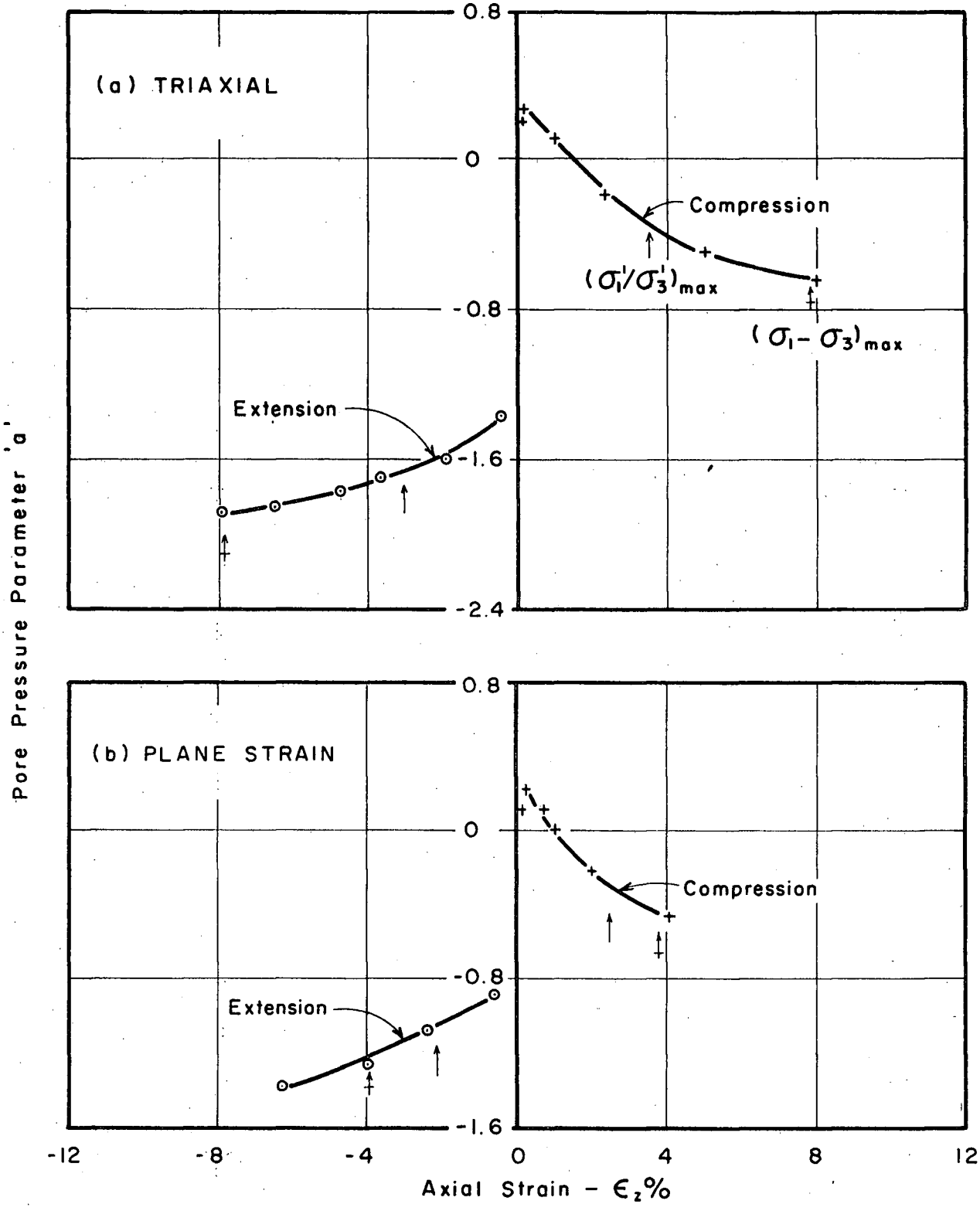

Fig.8.2 – VARIATION OF PORE PRESSURE PARAMETER 'a' WITH AXIAL STRAIN DURING UNDRAINED TRIAXIAL AND PLANE STRAIN SHEAR – O.C. HANEY CLAY.

effective stresses or maximum to rebound mean normal effective stresses. In contrast, O.C.R. defined by the two criteria are very different for K_o-consolidated clays. In the test series presented herein, O.C.R. by the usual definition, $(\sigma'_{zc})_{max}/\sigma'_{zc}$, was between 15.4 to 19.2, while the value of O.C.R. = $(p_c)_{max}/p_c$, with respect to mean effective stresses was only between 7.4 and 8.3 (see Tables VIII, IX). Consequently, the shear induced pore pressures in compression, after K_o-overconsolidation, may not be regarded as representative of 'heavy' overconsolidation if O.C.R. should be defined as $(p_c)_{max}/p_c$. It is, therefore, important to be clear about the proper definition of O.C.R. while dealing with K_o-overconsolidated clays, particularly when their behaviour is to be compared with isotropically overconsolidated clays.

Another factor which may be responsible for lack of dilatancy during compression is the initial unloading of shear stresses. The clay structure is known to be less dilatant to decreasing than to increasing shearing stresses. In addition, the sensitive clay used in this study need not be very dilatant in the overconsolidated state, particularly when the maximum past vertical effective stress was only 6 kg/cm^2; i.e.,

the overconsolidated structure may reflect to some extent the pronounced sensitivity of the normally consolidated clay structure by generating positive pore pressures due to shear.

For both compression and extension modes of shear, strains were found to increase rapidly as effective stress failure envelopes (tangents to the stress paths through the origin) were approached (Fig. 8.3) and, if deformations in the field are to be limited, the imposed stresses must be controlled so that the stress paths do not get too close to the failure envelopes. Extension tests, in particular, required very small loading before the effective stress paths got very close to the failure envelopes. Maximum deviator stress was reached at strains much larger than at which $(\sigma_1'/\sigma_3')_{max}$ occurred for both compression and extension stress paths. It is interesting to observe that the compression effective stress paths stayed to the left of the starting point, P, even until maximum deviator stress was reached. This implies that in the conventional passive compression test, in which σ_x is held constant, positive pore pressures are generated until failure, and hence a volume contraction will occur during drained shear of an identical sample.

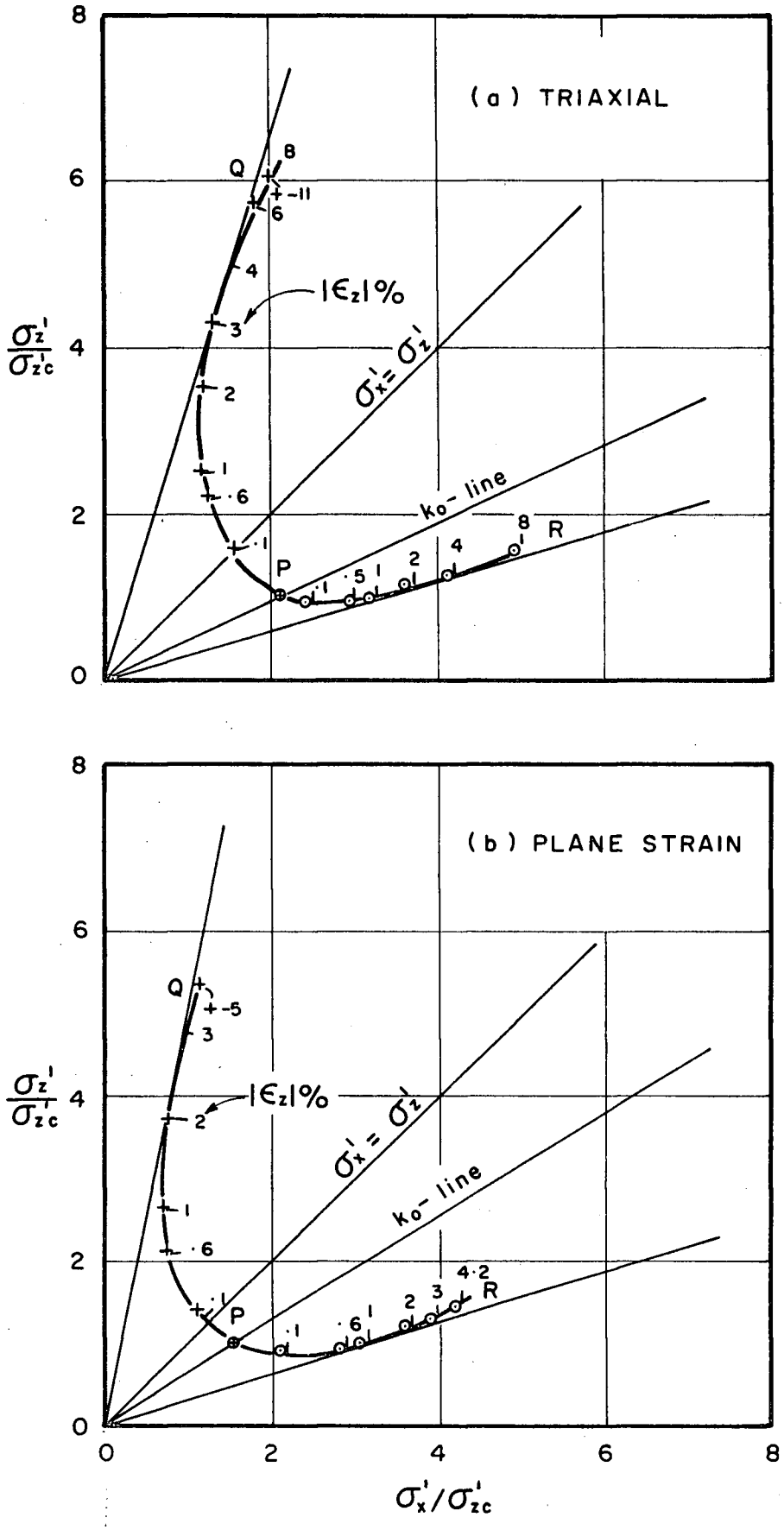

Fig. 8·3 — EFFECTIVE STRESS PATHS DURING UNDRAINED TRIAXIAL AND PLANE STRAIN SHEAR O.C. HANEY CLAY.

8.1.2 Drained Test Results

Although the deviator stress-strain behaviour was stiffer in passive compression when compared to passive extension (Fig. 8.4) the axial strains to failure were essentially the same (Table VIII, IX). It is interesting to note that the sample subjected to active compression did not fail even when the lateral effective stress was reduced to almost zero (plane strain test under the same stress path was not performed for this reason). Since the clay was overconsolidated, it is not surprising that its strength for the effective stress state, $\sigma'_z = \sigma'_{zc}$; $\sigma'_x \sim 0$, exceeded the maximum applied shear stress, $\sigma'_{zc}/2$. The sample was, therefore, caused to fail by increasing the vertical stress, while lateral stress was maintained at the reduced value of approximately zero. The discontinuity in the deviator stress-strain curve is a result of this change in the mode of loading. A similar discontinuity in the plane strain active extension stress-strain curve (Fig. 8.4b) is also due to the change over to the passive type extension loading after the vertical effective stress was reduced to almost zero with the sample undergoing no failure.

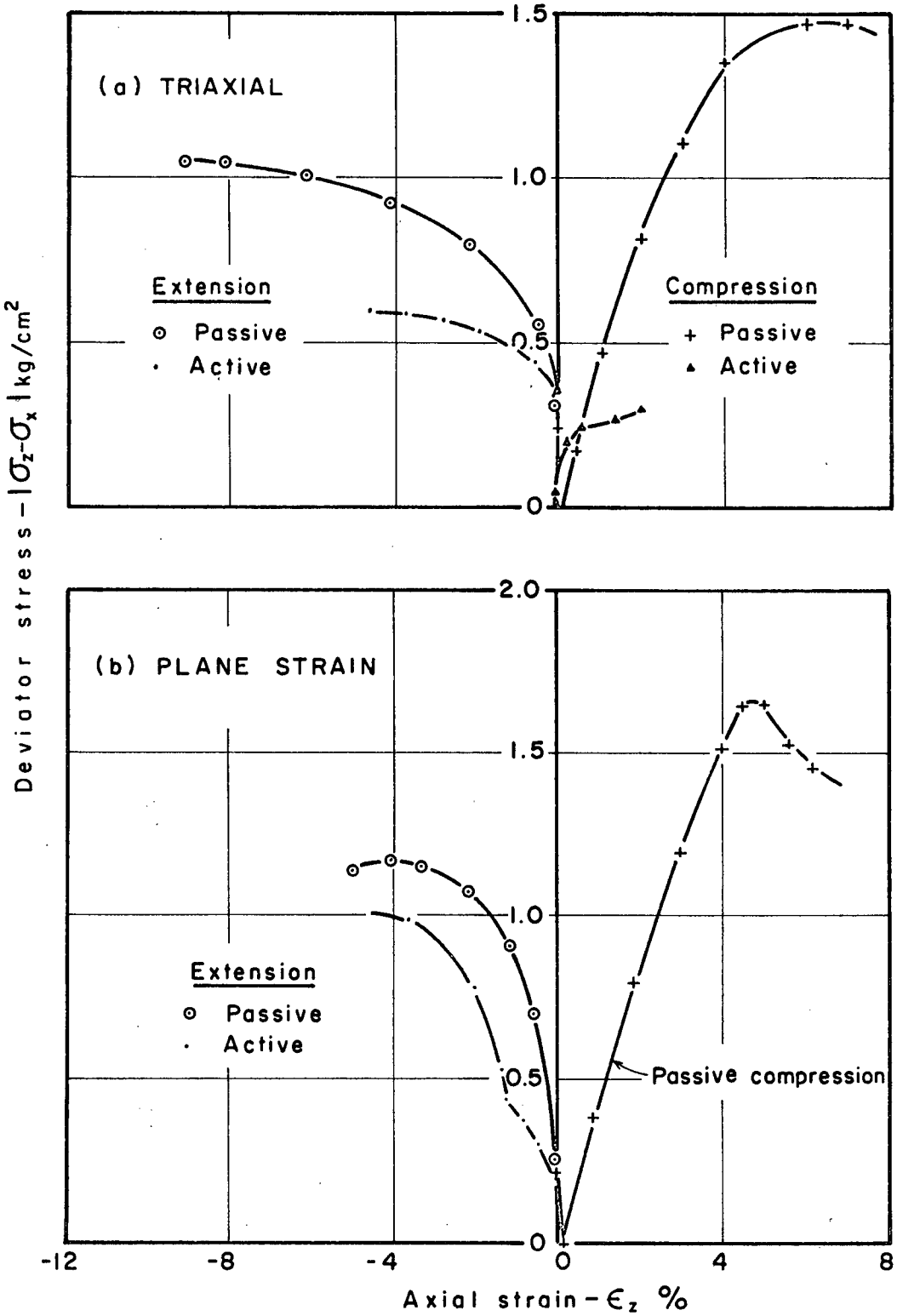

Fig.8.4 – DEVIATOR STRESS-STRAIN RELATIONSHIPS DURING DRAINED TRIAXIAL AND PLANE STRAIN SHEAR – O.C. HANEY CLAY .

Passive compression gave rise to a volume contraction until failure (Fig. 8.5), which is not typical for the compression of heavily overconsolidated clays. Possible reasons for such behaviour have already been considered in the previous section on undrained tests. There was also a volume decrease up to failure during passive extension. However, this volume decrease was very small and hence the shear behaviour was very close to that of corresponding undrained tests.

Due to reduction of effective stresses to very small values in active compression and extension, volume expansion was quite large. The discontinuity in the volumetric strain curve in Fig. 8.5b is due to the change over from active to passive extension shear, required to cause failure.

8.1.3 Comparison of Drained and Undrained Behaviour

The concepts of uniqueness of void ratio and effective stresses during drained and undrained shear have not generally been extended to heavily overconsolidated clays, and in particular for clays with one-dimensional consolidation history. Therefore, no attempt was made to correlate volume changes in drained

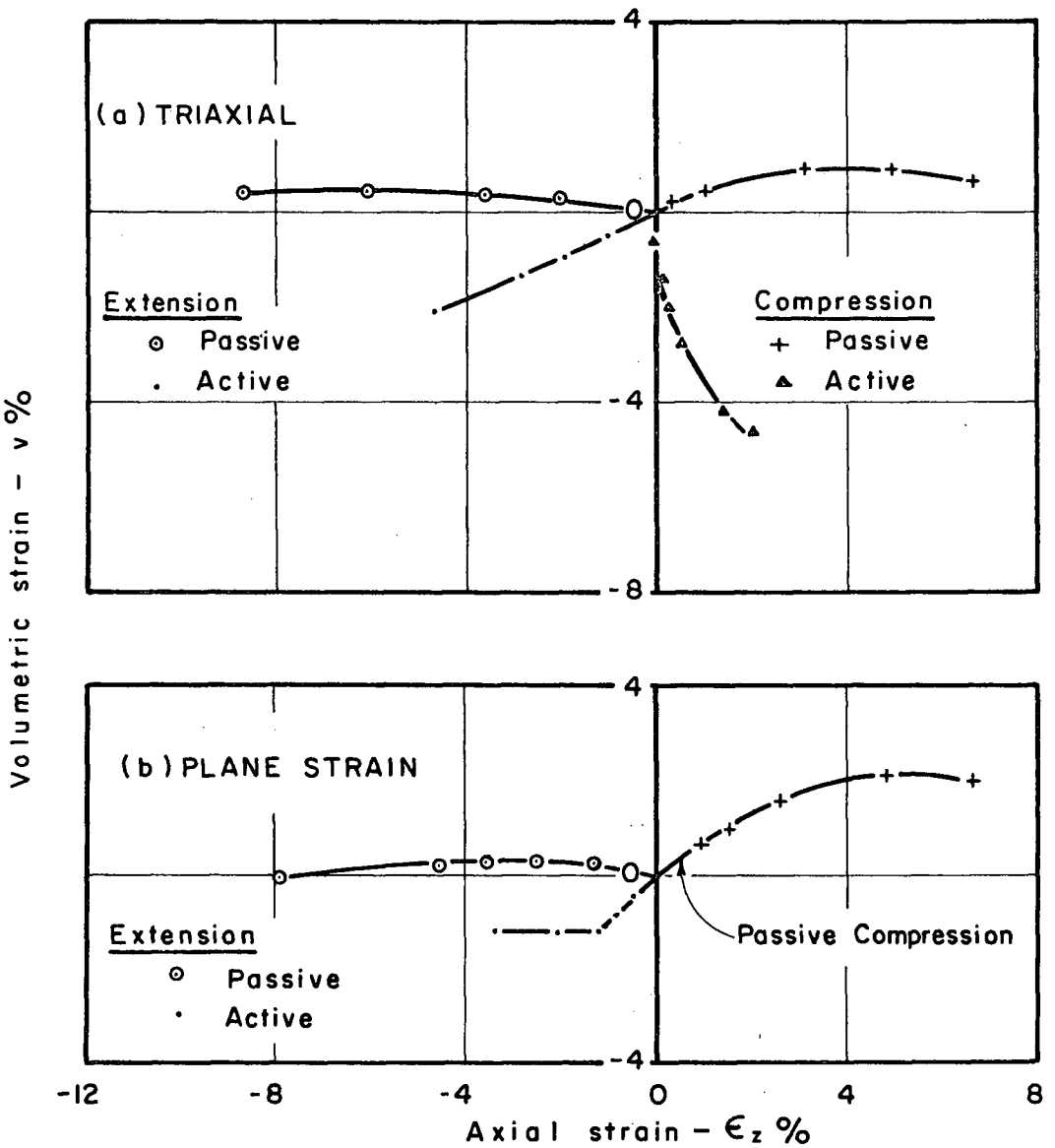

Fig. 8·5 - VOLUMETRIC STRAIN - AXIAL STRAIN RELATIONSHIPS DURING DRAINED TRIAXIAL AND PLANE STRAIN SHEAR - O.C. HANEY CLAY.

tests with pore pressures generated in the corresponding undrained tests.

For the same applied stress path, the undrained deviator stress-strain response was stiffer than the corresponding drained response. The strain to peak deviator stress was essentially equal for active and passive undrained and drained passive stress paths (see Tables VIII, IX). Fig. 8.6 shows that the deviator stress-strain response was essentially identical for drained and undrained passive extension stress paths. As pointed out earlier, this was due to negligible volumetric strains during drained shear, thus rendering the drained test virtually undrained.

Due to volume contraction during passive compression, drained strength, $(\sigma_1-\sigma_3)_{max}/2$, was higher than the undrained (Tables VIII, IX). Due to negligible volume changes during drained passive extension, drained and undrained strengths were essentially the same. Drained active stress paths, due to volume expansion at failure, resulted in lower drained strength compared to the undrained.

There is no immediate significance in the effective stress ratios, σ_1'/σ_3', at failure. This would be expected, since the use of an effective stress ratio is associated with linear failure envelopes passing

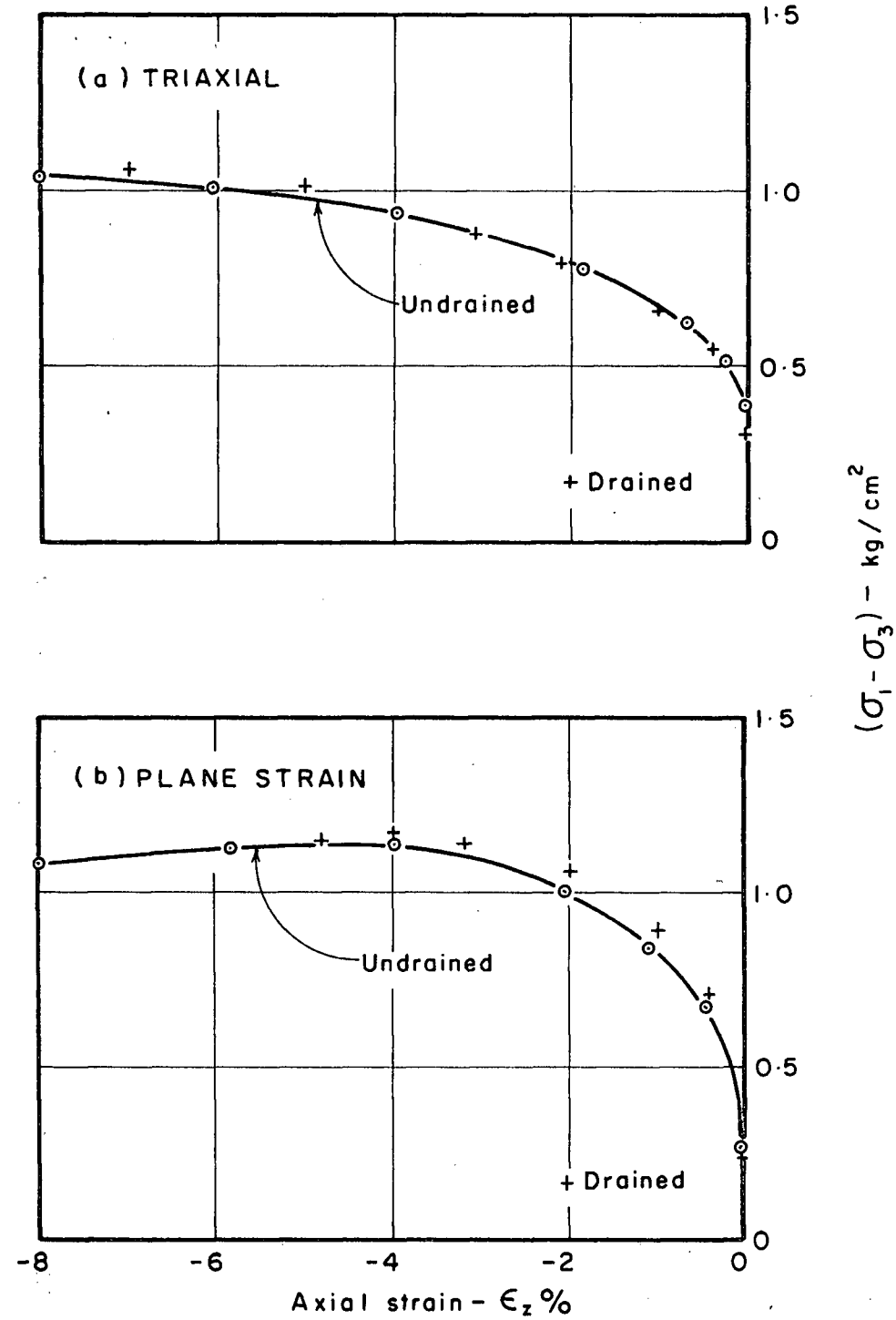

Fig.8.6 – COMPARISON OF SHEAR STRESS STRAIN BEHAVIOUR DURING DRAINED AND UNDRAINED PASSIVE EXTENSION IN TRIAXIAL AND PLANE STRAIN – O.C. HANEY CLAY.

through the origin, which is certainly not the case for a heavily overconsolidated clay. However, if $(\sigma_1'/\sigma_3')_{max}$ is plotted as a function of $(p_c)_{max}/p_f$, then the results of drained and undrained, normally and overconsolidated tests lie on a common envelope (Fig. 8.7). Here $(p_c)_{max}$ is the maximum mean normal consolidation stress and p_f is the mean normal effective stress at $(\sigma_1'/\sigma_3')_{max}$. The results given in Fig. 8.7 are simply a more general expression of the fact that the effective stress Mohr envelopes for drained and undrained tests are identical. However, different failure envelopes are obtained for compression and extension shear. Similar envelopes were used by Henkel (1960) and Simons (1960) to express triaxial failure of isotropically consolidated clays.

8.1.4 σ_y-Stress in Plane Strain

The variation of effective stresses during undrained shear is shown in Fig. 8.8. During extension shear, σ_y, the principal stress associated with the direction of zero strain, had a value intermediate between the other two principal stresses. However, compression shear involved initial unloading of shear stresses and σ_y was the major and not the intermediate principal stress during early stages of compression. It is a common

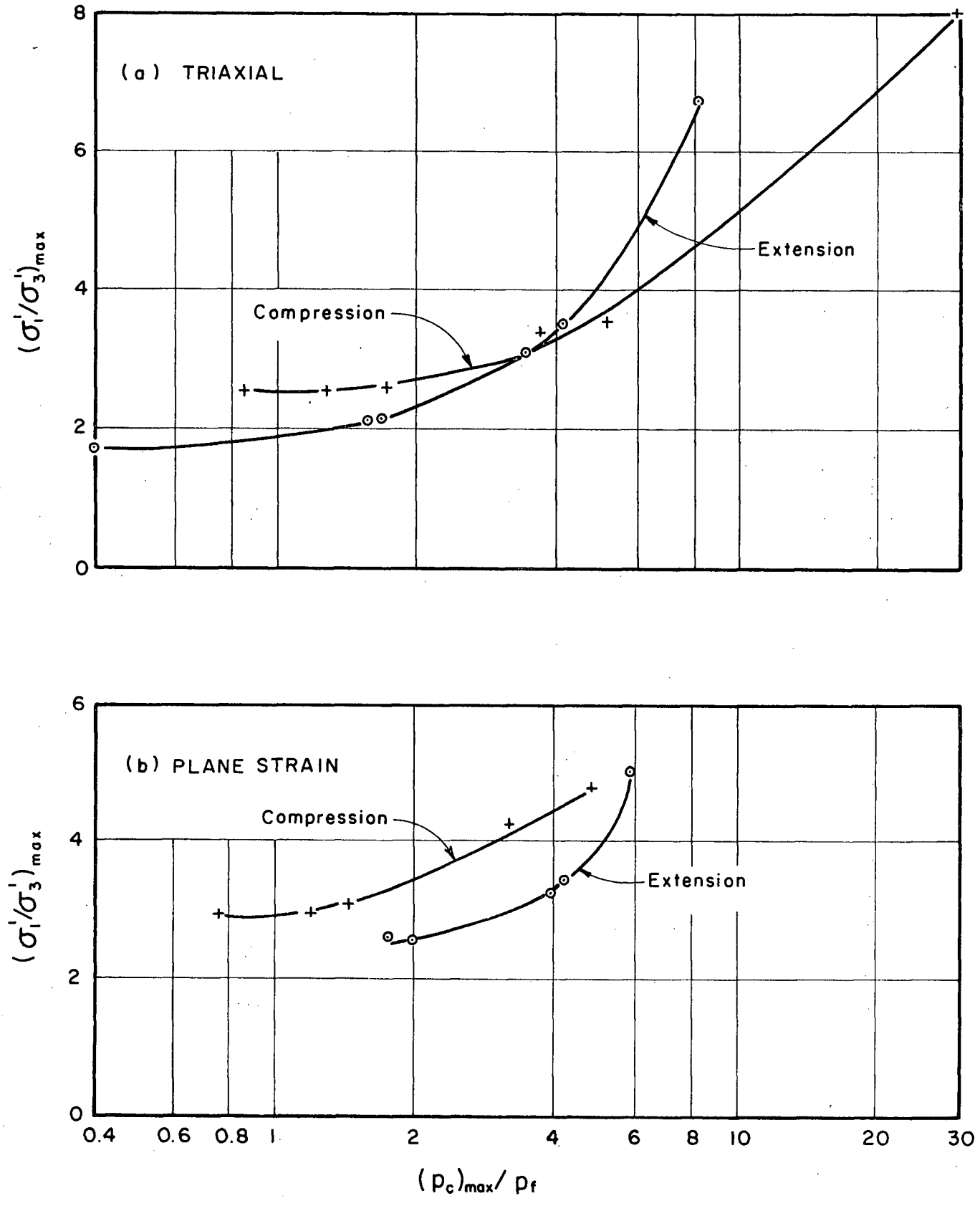

Fig.8.7 — TRIAXIAL AND PLANE STRAIN FAILURE ENVELOPES-N.C. AND O.C. HANEY CLAY.

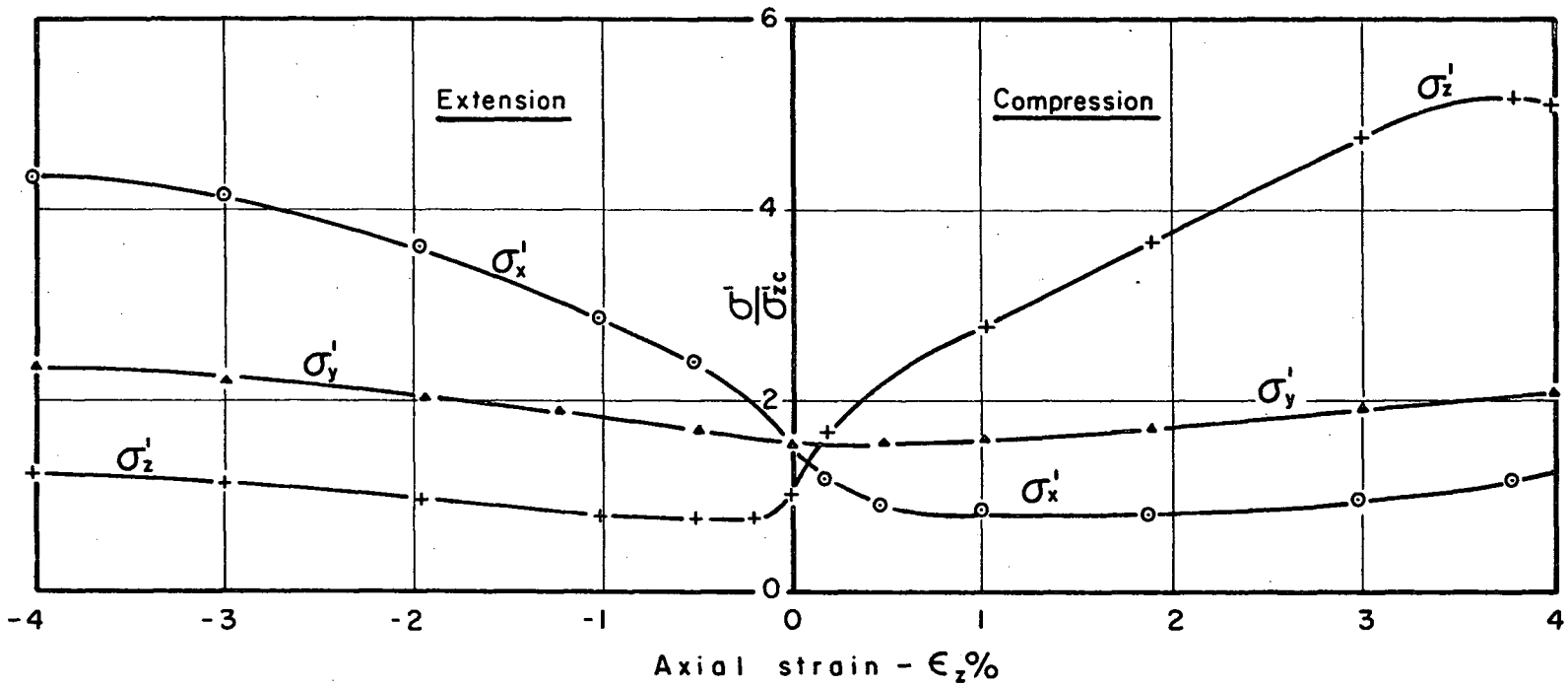

Fig. 8.8 – EFFECTIVE STRESS-STRAIN RELATIONSHIPS DURING UNDRAINED PLANE STRAIN SHEAR-O.C.HANEY CLAY.

practice to regard σ_y in plane strain as the intermediate principal stress. That this assumption is not always true is clearly indicated in Fig. 8.8 (and also in Fig. 5.3 for normally consolidated extension shear). The explanation offered for σ_y not assuming an intermediate value in normally consolidated extension shear applies to overconsolidated compression shear also.

The variation of stress ratio, $\sigma_y'/(\sigma_x'+\sigma_z')$, with axial strain was generally similar under drained or undrained, compression or extension types of shear (Fig. 8.9). Except for some scatter during drained passive extension, the average value of this ratio at failure $((\sigma_1-\sigma_3)_{max})$ was around 0.43 and was practically independent of the stress path. The corresponding value for normally consolidated clay was 0.37 $\pm$ 0.02.

8.2.0 Comparison of Triaxial and Plane Strain Results

An evaluation of the comparative triaxial and plane strain behaviour, under the same stress path, will be made with reference to Figs. 8.1 to 8.7, in which triaxial and plane strain results were presented side by side. A summary of the comparison is contained in Table X. Drained active compression and extension stress paths did not cause failure of either the triaxial

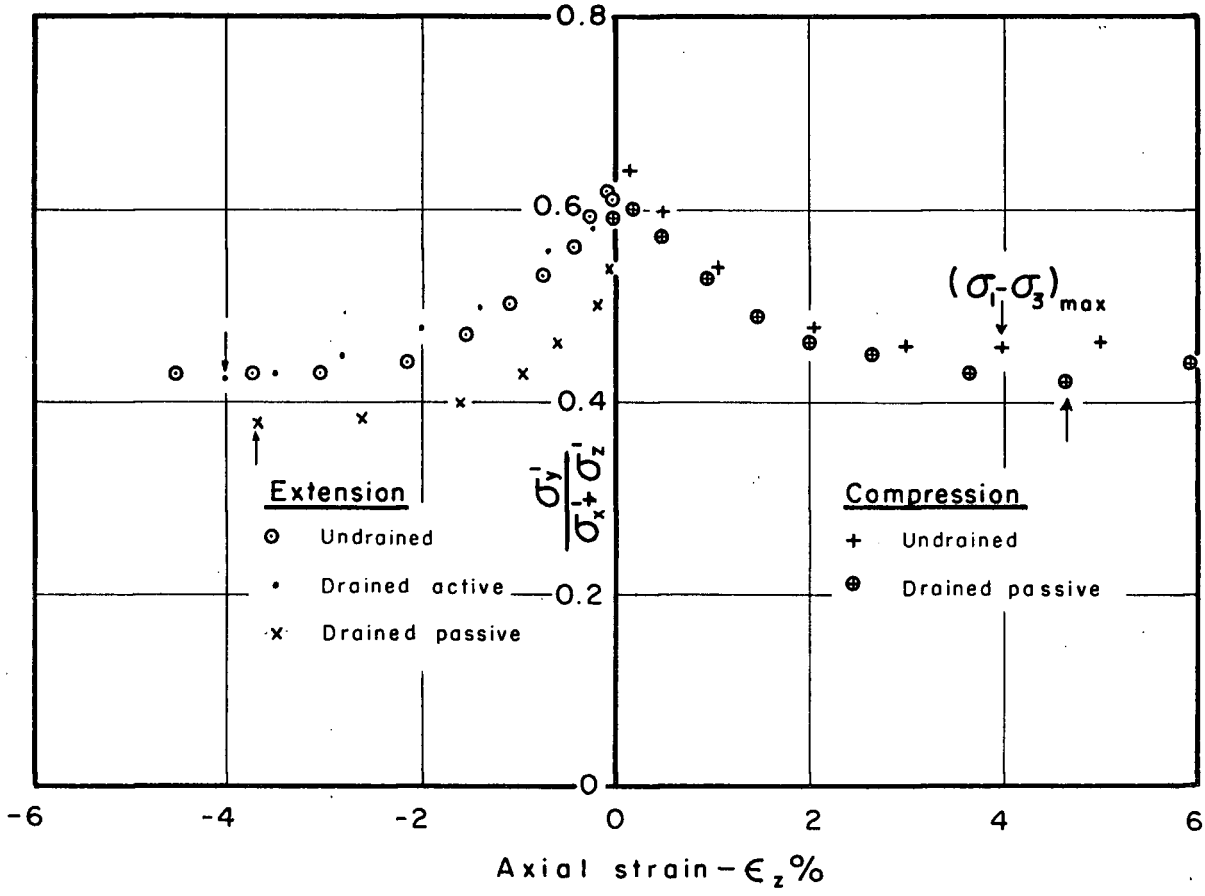

Fig. 8.9 – VARIATION OF STRESS RATIO, $\sigma_y'/(\sigma_x'+\sigma_z')$ WITH AXIAL STRAIN DURING PLANE STRAIN SHEAR O.C. HANEY CLAY.

TABLE X

Comparison of Triaxial and Plane Strain Test Results on O.C. Haney Clay

	End of Consolidation					Failure Condition									
				O.C.R.		$(\sigma_1-\sigma_3)_{max}$					$(\sigma'_1/\sigma'_3)_{max}$				
	σ'_{zc}	K_o	p_c	$\frac{(\sigma'_z)_{max}}{\sigma'_{zc}}$	$\frac{(p_c)_{max}}{p_c}$	ε_z%	$\sigma_1-\sigma_3$	σ'_1/σ'_3	v%	a	ε_z%	$\sigma_1-\sigma_3$	σ'_1/σ'_3	v%	a
Undrained Compression															
Triaxial	0.32	2.11	0.56	18.6	7.4	7.8	1.30	3.05	0	-0.62	3.50	1.06	3.45	0	-0.36
Plane Strain	0.35	1.64	0.50	17.3	8.1	3.8	1.42	4.5	0	-0.48	2.50	1.16	4.8	0	-0.30
Undrained Extension															
Triaxial	0.31	2.20	0.55	19.2	7.6	-7.8	1.05	3.10	0	-1.9	-3.0	0.88	3.45	0	-1.68
Plane Strain	0.38	1.68	0.56	15.6	7.6	-4.0	1.14	3.10	0	-1.26	-2.1	1.01	3.3	0	-1.05
Drained Passive Compression															
Triaxial	0.33	1.74	0.50	18.1	8.3	6.0	1.48	3.35	0.7	—	6.0	1.48	3.35	0.7	—
Plane Strain	0.35	1.59	0.56	16.6	8.5	4.8	1.66	4.2	2.2	—	4.8	1.66	4.2	2.2	—
Drained Passive Extension															
Triaxial	0.31	1.98	0.52	19.1	8.0	-8.0	1.06	3.2	0.4	—	-8.0	1.06	3.2	0.4	—
Plane Strain	0.38	1.58	0.53	15.4	7.7	-4.0	1.18	3.4	0.2	—	-4.0	1.18	3.4	0.2	—

Stresses in Kg/cm^2

or plane strain samples, and hence are not considered for comparison in Table X.

Unfortunately, the end of consolidation stresses in triaxial and plane strain samples, tested under the same applied stress path, were not strictly identical. A precise control of the rebound vertical stress in plane strain samples could not be exercised due to varying amounts of side friction from sample to sample. As a result, these samples, at the completion of rebound, ended up, in general, with slightly higher vertical effective stresses and lower K_o values than the corresponding triaxial samples. However, it is felt that the small differences in end of consolidation conditions are not likely to influence the comparative triaxial and plane strain stress-strain behaviour to any significant extent. In particular, the failure conditions should be the least affected.

Conventional comparison of the triaxial and plane strain behaviour is considered in this section. Octahedral stress-strain and failure relationships will be dealt with in a later section.

8.2.1 Stress-Strain Behaviour

For all the stress paths studied, plane strain deviator stress-strain behaviour was stiffer than the

corresponding triaxial behaviour. This can be easily seen in Figs. 8.1 and 8.4 where, for any given applied stress path, the plane strain curves occupy a higher location than the corresponding triaxial curves. In general, the axial strain to peak deviator stress in plane strain was about one-half the value for the triaxial conditions. This was true for undrained compression and extension and drained passive extension stress paths (Table X). During drained passive compression stress path the axial strain to failure in plane strain was about 75% of the triaxial value. Also, plane strain compression failure ($(\sigma_1-\sigma_3)_{max}$) occurred with a characteristic sharp peak which was not present in the case of triaxial failure (Figs. 8.1, 8.4).

Undrained compression strength, $(\sigma_1-\sigma_3)/2$, in plane strain was higher than the triaxial value by about 9%, corresponding to both, $(\sigma_1-\sigma_3)_{max}$ and $(\sigma_1'/\sigma_3')_{max}$ failure conditions (Table X). Similarly, plane strain extension undrained strength was higher than the triaxial by respectively 9% and 13% with respect to the same two failure conditions. It is concluded that during undrained shear of undisturbed heavily overconsolidated Haney clay, plane strain conditions give rise to higher strength and lower strain to failure than triaxial conditions.

Both compression and extension undrained effective stress paths on (σ_x', σ_z') plane were very similar for triaxial and plane strain conditions (Fig. 8.3). For both triaxial and plane strain conditions, during compression or extension shear, $(\sigma_1'/\sigma_3')_{max}$ occurred at a smaller strain than $(\sigma_1-\sigma_3)_{max}$. Axial strains in triaxial corresponding to $(\sigma_1'/\sigma_3')_{max}$ were about 1-1/2 times those under plane strain conditions. Also, strains were found to increase very rapidly as the effective stress failure envelopes were approached. This applied to both compression or extension shear in plane strain and triaxial.

8.2.2 Pore Pressures and Volume Changes

The dilating tendency during undrained triaxial extension was larger than that under plane strain conditions. This is seen in Fig. 8.2 where 'a' values in triaxial are more negative than the corresponding plane strain values. Thus, plane strain boundary conditions in overconsolidated clay lead to supressed dilatancy in comparison to axisymmetric stress conditions, as has been shown to be the case in sands (Cornforth, 1964; Finn et. al., 1967). Similarly, during undrained compression

'a' values at failure in triaxial were more negative than the corresponding failure values in plane strain (Table X).

Volume changes during drained shear are the combined effect of changes in mean normal stresses and the applied shear stresses. Passive compression in plane strain gave rise to larger volume compression than triaxial (Fig. 8.5), because of larger increases in mean normal stresses (due to higher (σ_1'/σ_3') at failure) and smaller dilatancy effects. Both triaxial and plane strain samples contracted until failure (Table X). As discussed earlier, this is not a familiar behaviour for heavily overconsolidated clays. Passive extension drained shear resulted in virtually little volume changes. This was apparently due to small changes in mean normal stresses to failure and the counteracting influence of shear dilatancy.

8.2.3 Failure Conditions

The triaxial and plane strain generalised failure envelopes are shown in Fig. 8.7. Considering the parts of the envelopes relevant to the overconsolidated soil only, it is seen that the plane strain compression failure envelope lies above the triaxial

compression envelope. Thus, triaxial test results would underpredict the plane strain strength. However, the overconsolidated triaxial and plane strain extension failure envelopes are virtually identical.

The failure $((\sigma_1'/\sigma_3')_{max})$ state of the overconsolidated samples on the familiar $(\sigma_1-\sigma_3)/2$ vs. $(\sigma_1'+\sigma_3')/2$ plot is shown in Fig. 8.10. It can again be seen that the plane strain compression envelope lies distinctly above the triaxial compression envelope. Extension failure envelopes for the two types of tests are comparatively much closer to each other.

8.3.0 Octahedral Stress-Strain Relations and Failure Conditions

8.3.1 Effective Stress Paths

In Chapter VII it was shown that during normally consolidated undrained compression tests, which did not involve unloading of consolidation shear stresses, common octahedral effective stress paths were followed under triaxial and plane strain conditions. In overconsolidated clay samples, extension and not compression testing corresponds to no initial unloading of shear stresses and, therefore, extension effective stress paths are expected to be common to triaxial and plane strain condition. Fig. 8.11 shows these effective stress paths.

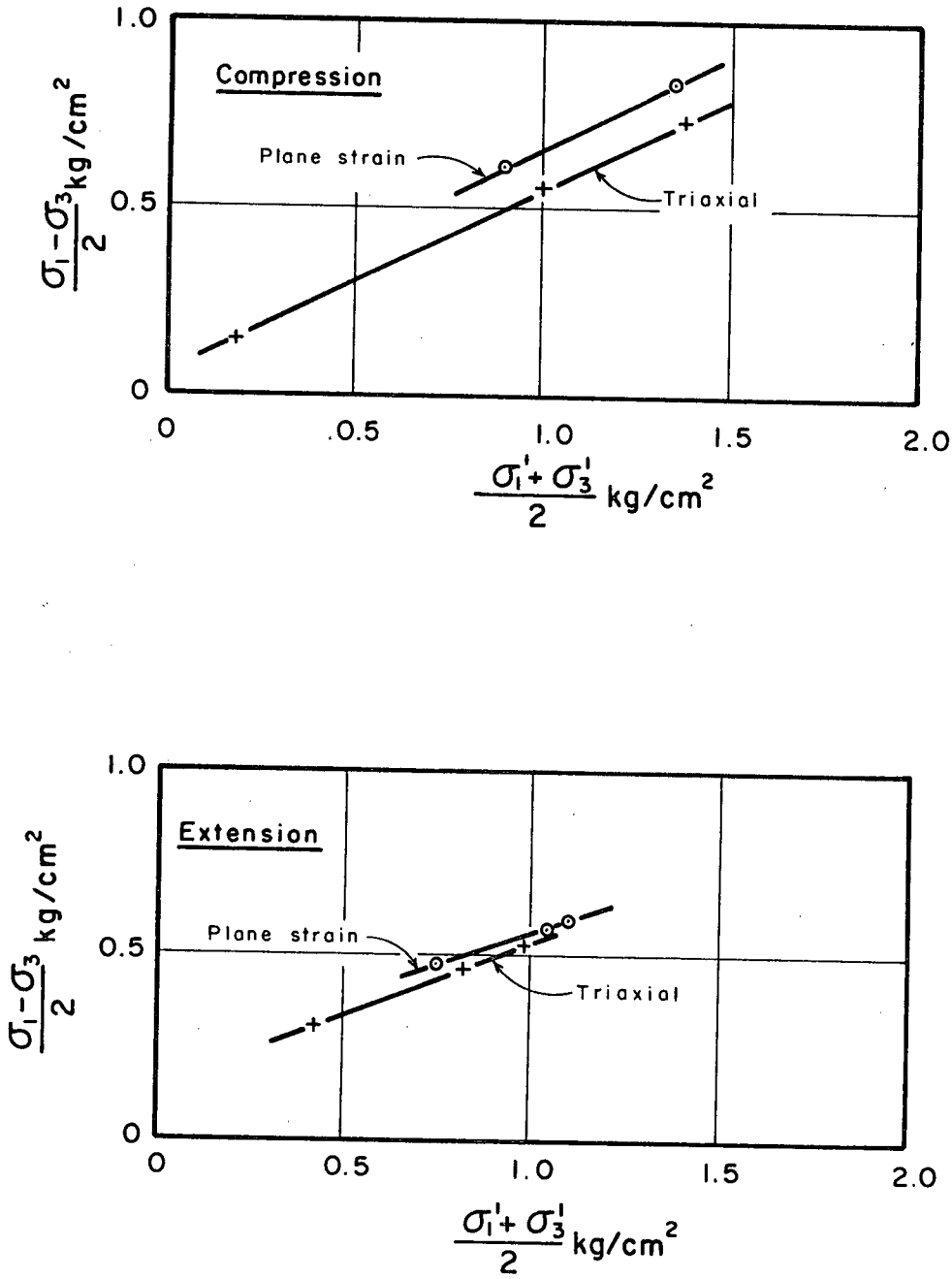

Fig. 8.10 – TRIAXIAL AND PLANE STRAIN FAILURE ENVELOPES – O.C. HANEY CLAY.

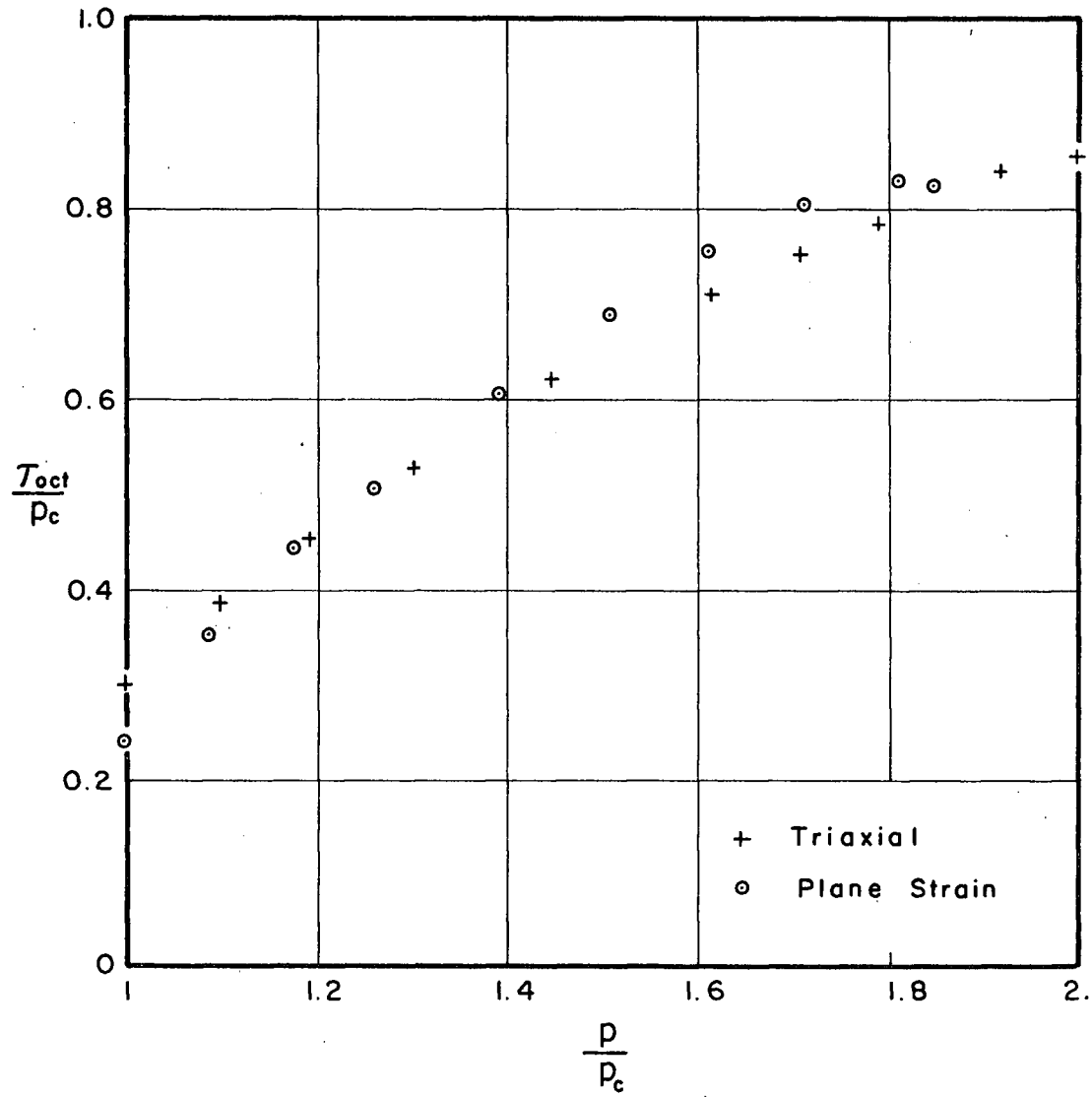

Fig. 8.11 – OCTAHEDRAL EFFECTIVE STRESS PATHS DURING UNDRAINED TRIAXIAL AND PLANE STRAIN EXTENSION – O.C. HANEY CLAY.

Except for some scatter near failure the stress paths may be considered unique.

8.3.2 Stress-Strain Comparisons

Undrained Extension

The uniqueness of effective stress paths in the octahedral plane during undrained extension suggests the existence of a common octahedral shear stress-strain relationship, similar to that found earlier (Chapter VII) for normally consolidated undrained compression tests. Fig. 8.12 shows the octahedral stress-strain relationship for overconsolidated clay in extension. There is a good agreement between triaxial and plane strain relationships, except near failure.

Undrained Compression

Compression stress paths involved initial unloading of τ_{oct}. Therefore, the octahedral stress-strain relation between $\Delta\tau_{oct}$ (defined in Eq. 7.6) and γ_{oct}, similar to that observed for normally consolidated extension tests, may be expected to be the same for plane strain and triaxial. The experimental relationships are shown in Fig. 8.13. Due to significant difference between consolidation mean normal stress, p_c,

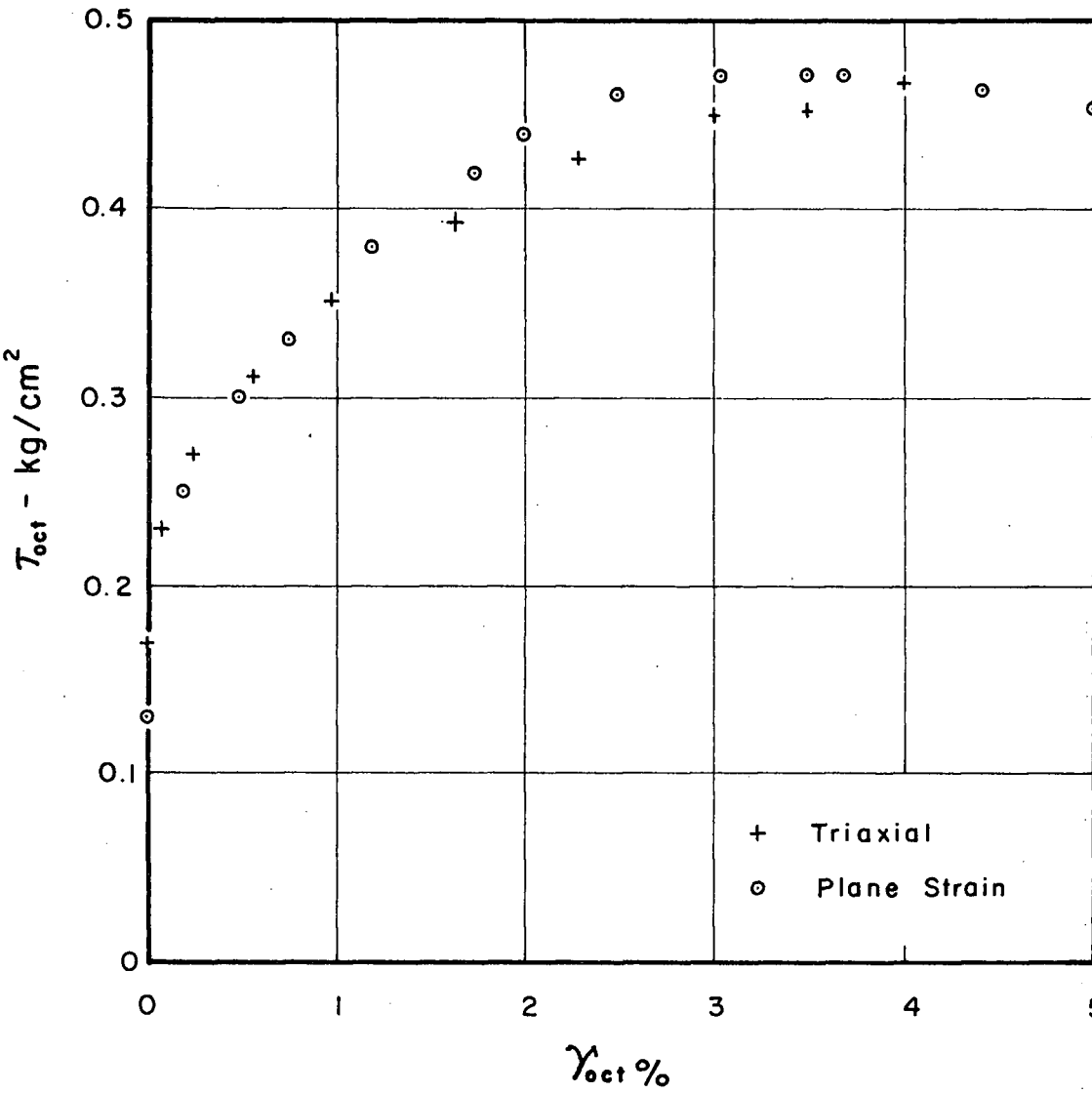

Fig.8.12 – OCTAHEDRAL SHEAR STRESS – STRAIN RELATIONSHIP DURING UNDRAINED TRIAXIAL AND PLANE STRAIN EXTENSION – O.C. HANEY CLAY.

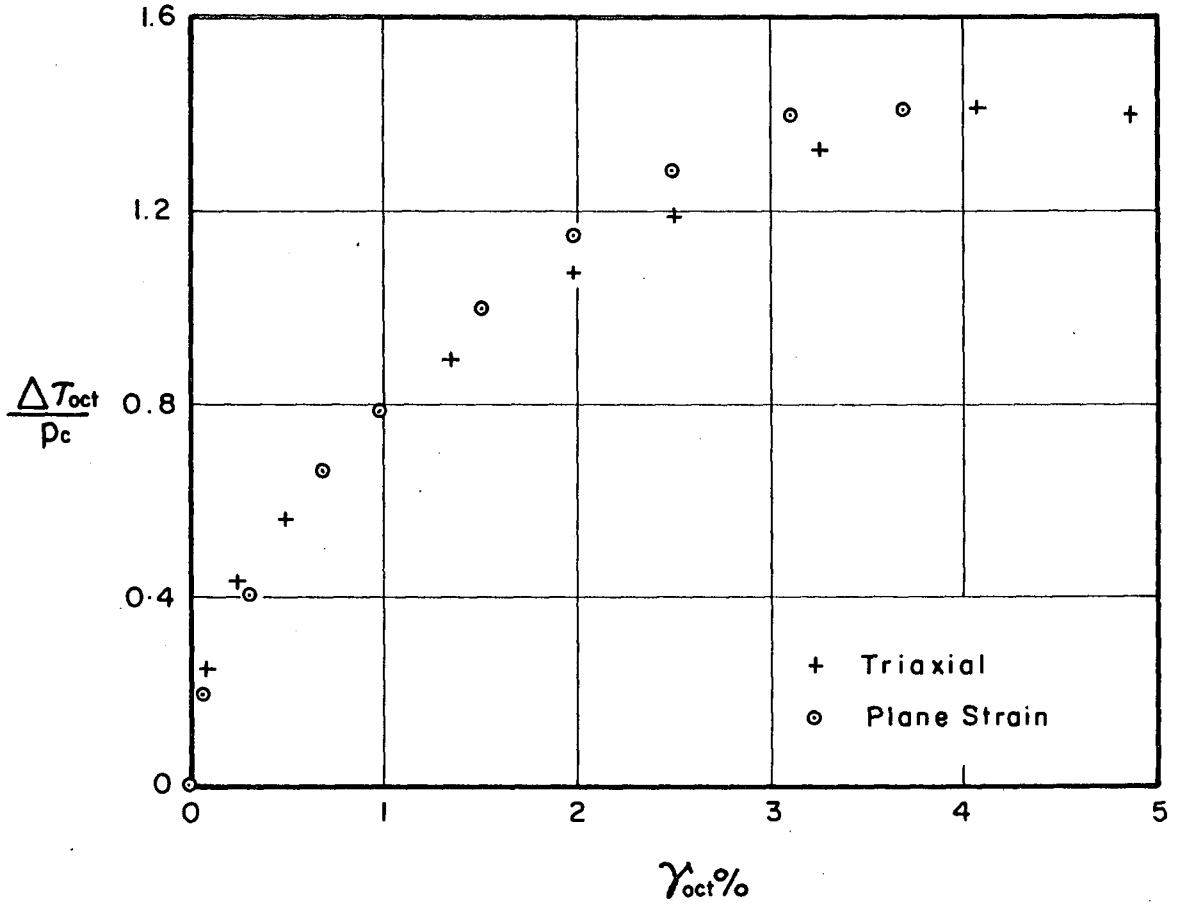

Fig. 8.13 - OCTAHEDRAL SHEAR STRESS - STRAIN RELATIONSHIP DURING UNDRAINED TRIAXIAL AND PLANE STRAIN COMPRESSION - O.C. HANEY CLAY .

on triaxial and plane strain samples (Table X), the ordinate in Fig. 8.13 has been divided by p_c. The agreement between the triaxial and plane strain results is seen to be fairly good.

Drained Tests

It was shown earlier that volume changes during passive extension drained tests were so small that these tests could virtually be regarded as undrained. This then implies that the octahedral shear stress-strain relationship which was found common to undrained triaxial and plane strain extension would also hold for drained passive extension. τ_{oct} vs. γ_{oct} relationships observed during drained passive extension are shown in Fig. 8.14. The agreement between triaxial and plane strain relationships seems good at small strain ($\leq$ 1%).

Octahedral stress ratio-strain relations during drained triaxial and plane strain passive compression are shown in Fig. 8.15. Similar to the case of normally consolidated clay, reasonable agreement between triaxial and plane strain result was obtained at small shear strains for (generally 1% or less) overconsolidated clay. At larger values of shear strains triaxial results corresponded to higher τ_{oct}/p ratio for a given value of strain.

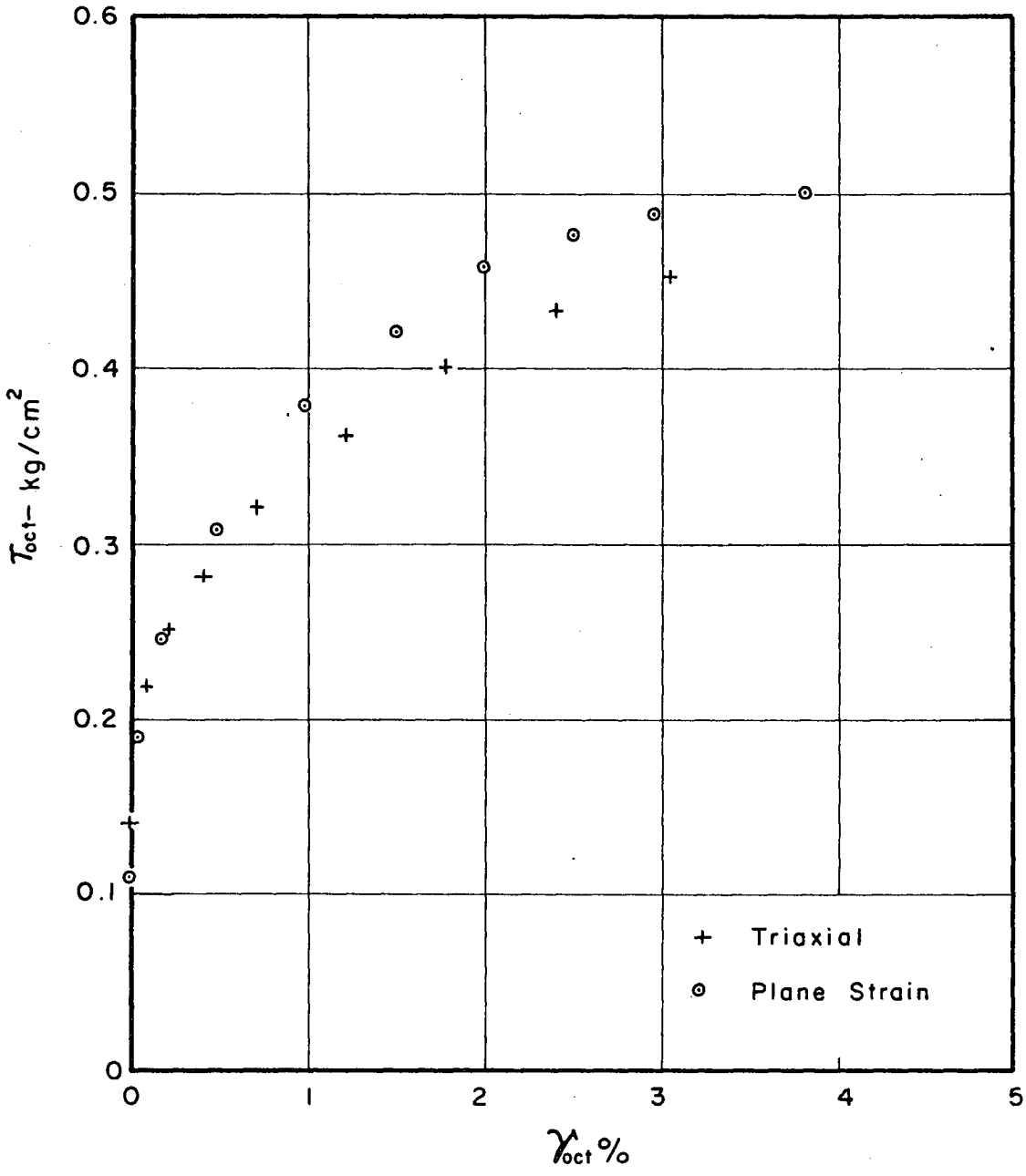

Fig. 8.14 - OCTAHEDRAL SHEAR STRESS-STRAIN RELATIONSHIP DURING DRAINED TRIAXIAL AND PLANE STRAIN PASSIVE EXTENSION - O.C. HANEY CLAY.

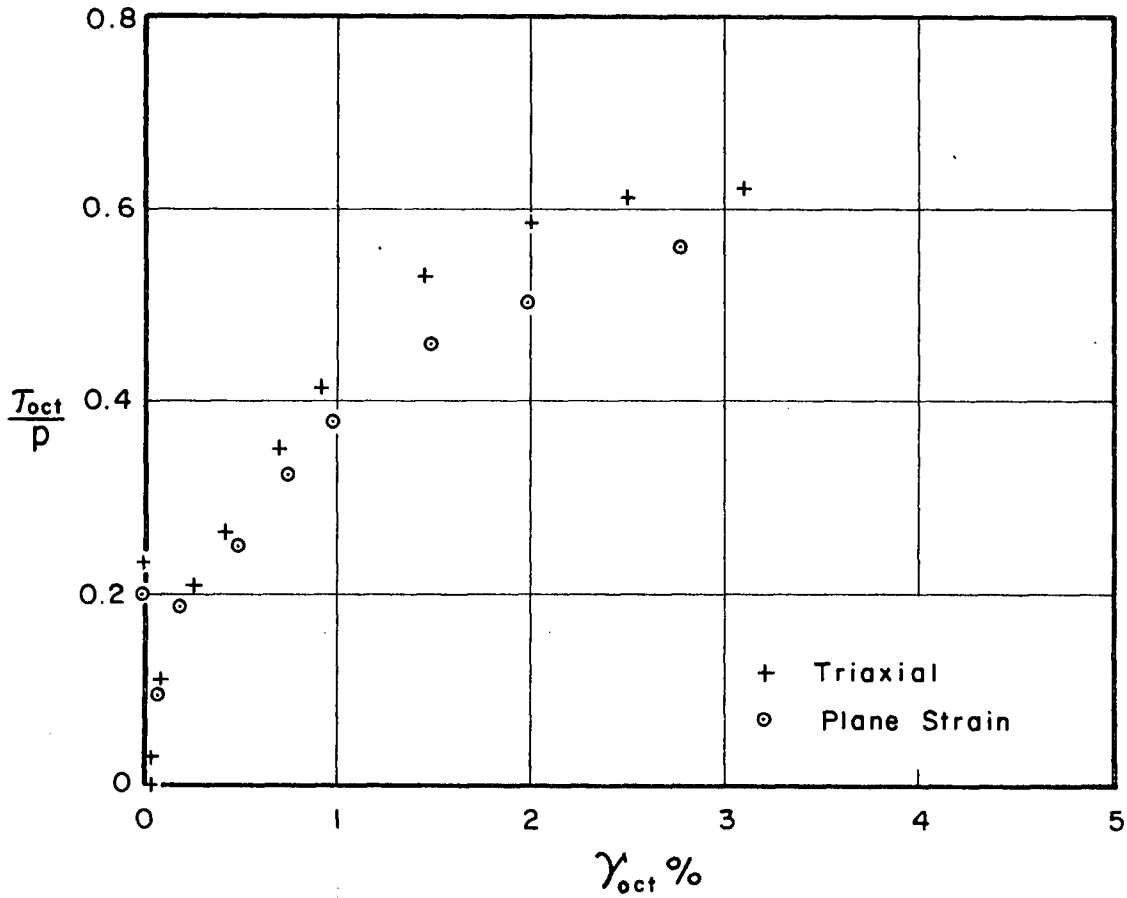

Fig. 8.15 – OCTAHEDRAL STRESS RATIO- SHEAR STRAIN RELATION DURING DRAINED TRIAXIAL AND PLANE STRAIN PASSIVE COMPRESSION – O. C. HANEY CLAY.

8.3.3 Failure Conditions

Undrained Strength

The conventional measure of the undrained strength, $(\sigma_1-\sigma_3)/2$, was shown to be smaller under triaxial than under plane strain conditions. The conclusion was valid for both compression and extension stress paths and at both $(\sigma_1-\sigma_3)_{max}$ or $(\sigma_1'/\sigma_3')_{max}$ failure conditions. These apparent differences were explained for normally consolidated clays when undrained strength was characterised by $(\tau_{oct})_{max}$. Similar comparisons for overconsolidated samples are presented in Table XI. It can be seen that the triaxial and plane strain undrained extension failure occurs at essentially the same values of τ_{oct}. In axial compression, however, the ratio $\Delta\tau_{oct}/p_c$ was found to be the critical parameter, which was essentially equal under triaxial and plane strain conditions. The reason for this was explained earlier while discussing normally consolidated undrained extension failure (Chapter VII).

Failure Criteria

During conventional comparison of overconsolidated triaxial and plane strain results, it was shown that overconsolidated Mohr envelopes were higher for plane

TABLE XI

Co-relation of Undrained Strength Under Triaxial and Plane Strain Conditions — O.C. Haney Clay

	Failure Condition			
	$(\sigma_1-\sigma_3)_{max}$ or $(\tau_{oct})_{max}$		$(\sigma_1'/\sigma_3')_{max}$ or $(\tau_{oct}/p)_{max}$	
Undrained Extension	$(\sigma_1-\sigma_3)$	τ_{oct}	$(\sigma_1-\sigma_3)$	τ_{oct}
Triaxial	1.05	0.48	0.88	0.44
Plane strain	1.14	0.47	1.01	0.43
Undrained Compression	$(\sigma_1-\sigma_3)$	$\Delta\tau_{oct}/p_c$	$(\sigma_1-\sigma_3)$	$\Delta\tau_{oct}/p_c$
Triaxial	1.30	1.39	1.06	1.21
Plane strain	1.42	1.41	1.16	1.25

Stresses in kg/cm^2

strain than for the triaxial conditions, though the extension envelopes differed only to a small extent (Fig. 8.10). This implies that plane strain strength will be underestimated by Mohr-Coulomb failure criterion. Enough overconsolidated tests were not performed in either triaxial or plane strain groups to enable the overconsolidated Mohr failure envelopes to be accurately defined. In the absence of appropriate values of c' and ϕ' for overconsolidated Haney clay, examination of the validity of other failure criteria (i.e. Tresca and von Mises) was not attempted.

CHAPTER IX

SUMMARY AND CONCLUSIONS

The results of triaxial and plane strain tests have been described in which undisturbed Haney clay was initially consolidated to 'identical' K_o-stresses. Not only the conventional passive compression but also a number of other stress paths were imposed to induce compression or extension, drained or undrained failure. Test results were analysed in order to:

1. Compare and correlate results under different stress paths for the same stress system (triaxial or plane strain), and

2. Compare and correlate triaxial and plane strain behaviour under identical stress paths to failure.

The study reported herein is believed to be the first of its kind, in which the behaviour of a natural clay has been compared and correlated under triaxial and plane strain conditions, using a variety of stress paths during

shear. In addition, both normally and heavily overconsolidated preshear conditions have been considered.

The response of Haney clay to a variation in applied stress path to failure was similar for both groups (triaxial and plane strain) of tests. On the basis of the results on normally consolidated Haney clay, the following conclusions were derived with regard to the influence of stress path to failure:

1. There was no similarity between undrained stress-strain behaviour in compression and extension; e.g., for the clay tested, the axial strain to peak deviator stress in extension was 15 times larger than in compression. Furthermore, the axial strain to peak deviator stress in drained shear was a function of the applied compression or extension stress path; e.g., unloading stress paths were associated with smaller failure strain than similar loading stress paths.

2. Undrained strength in extension was considerably smaller than that in compression. For the clay tested, this was associated with larger shear induced pore pressures and smaller ϕ' in extension when compared to that under compression.

3. For a given type of shear (compression or extension), the angle of shear resistance, ϕ', was independent of the stress path and drainage conditions when $(\sigma_1'-\sigma_3')_{max}$ was used as the failure condition and drained test results were corrected for volume change rates. However, for the sensitive Haney clay, ϕ' in undrained compression corresponding to $(\sigma_1-\sigma_3)_{max}$ failure condition was 5° smaller than ϕ' at $(\sigma_1'/\sigma_3')_{max}$ failure condition. In addition, ϕ' in extension was smaller than ϕ' in compression at $(\sigma_1'/\sigma_3')_{max}$. This result for Haney clay, in which ϕ' in extension was 5° smaller than in compression, is contrary to the results published earlier on remolded clays (Ladd 1967; Hambly and Roscoe, 1969), where compression and extension ϕ''s were reported as being either equal or extension ϕ' several degrees larger than compression.

The measured ϕ' (no volume change rate corrections) in drained passive extension can be several degrees smaller than ϕ' corrected for volume change rates. This was, for the clay tested, due to significant part of input energy being expended in doing work against the relatively high confining pressure in such a test.

4. The stress ratio $\sigma_y'/(\sigma_x'+\sigma_z')$ in plane strain was found essentially constant and independent of the

stress path or drainage conditions. This is similar to earlier results of Hambly and Roscoe (1969) on a remolded clay.

5. It was shown that Rendulic's hypothesis can be used to estimate volume changes in conventional drained passive compression tests from the results of similar undrained tests, provided samples considered have the same initial consolidation history. The stress parameters used to express Rendulic's uniqueness of void ratio-effective stress hypothesis were the octahedral mean normal effective stress, p, and octahedral shear stress τ_{oct}. Also, increments of volume change during drained passive extension were successfully estimated from the corresponding undrained tests, for that part of the stress path where the stress ratio, τ_{oct}/p, was increasing. It would be of interest to verify Rendulic's hypothesis for other load increasing drained stress paths.

Comparison of triaxial and plane strain results on normally consolidated Haney clay, under identical stress paths, led to the following conclusions:

1. The axial strain to failure in undrained shear was the same under triaxial and plane strain conditions which included both compression and extension stress paths.

This result for Haney clay is somewhat contrary to those published earlier for remolded clays (Henkel and Wade, 1966), where axial strain to undrained compression failure in plane strain was considerably smaller than that under triaxial conditions. However, during drained shear of Haney clay, irrespective of the stress path, axial strain to failure in plane strain was about 75% of that under triaxial conditions. Also, compression failure in plane strain was always accompanied by a sharp post peak drop in shear resistance, which was not present in the triaxial tests. This suggests that progressive action in plane strain can be more severe than under triaxial conditions.

2. Undrained strength was larger under plane strain than under triaxial conditions. For the clay tested, C_u/σ'_{1c} in plane strain compression was 0.293 compared to the triaxial value of 0.263. The corresponding values in extension were 0.193 and 0.130. In compression, higher C_u/σ'_{1c} in plane strain was associated with higher ϕ' in plane strain, as the pore pressures generated in the two types of tests were essentially same. In extension excessively larger C_u/σ'_{1c} in plane strain was associated with both, higher ϕ' and lower pore pressures in plane strain compared to those under triaxial conditions.

3. At both failure conditions, $(\sigma_1-\sigma_3)_{max}$ and $(\sigma_1'/\sigma_3')_{max}$, plane strain ϕ' was higher than triaxial ϕ' by 4° to 5° for all the stress paths investigated. Thus, a confirmation of the general picture, that the angles of shearing resistance of soils under plane strain conditions are higher, has been demonstrated for a natural clay.

4. Octahedral effective stress paths in terms of p and τ_{oct} were found to be the same for triaxial and plane strain undrained compression. However, in undrained extension, which involves a decrease in the stress ratio τ_{oct}/p and consequential reorientation of principal stresses during shear, common octahedral effective stress paths were found in terms of p and $\Delta\tau_{oct}$ (Eq. 7.6), where $\Delta\tau_{oct}$ represents cumulative change in octahedral component of shear stress. This correspondence of octahedral stress paths is of great importance in the development of stress-strain relationships for complex stress fields.

5. A unique octahedral shear stress-strain relation common to undrained triaxial and plane strain shear was found to exist. The compression relationship was between τ_{oct} and γ_{oct} whereas, the extension relationship was between $\Delta\tau_{oct}$ and γ_{oct}. For the clay tested, the compression

stress-strain relationship was valid even until strain levels which were several times larger than at which undrained failure ($(\tau_{oct})_{max}$) occurred. In other words, the uniqueness of the relationships existed even in the unstable post failure range. (In this range τ_{oct} decreased but τ_{oct}/p was increasing.) The extension stress-strain relationship was unique for the entire stress path until failure. (τ_{oct} and τ_{oct}/p reached peak values at the same strain in extension.)

6. The uniqueness of octahedral effective stress paths in undrained triaxial and plane strain compression permits Rendulic's hypothesis to be used to estimate volume changes in drained plane strain passive compression from the results of undrained triaxial compression tests. It has been further shown that the volume changes in unloading type plane strain active compression can be estimated from a similar triaxial test. For this type of test, a surface in (p, τ_{oct}, e) space common to triaxial and plane strain conditions could be assumed to exist. Further loading and unloading compression tests are required to substantiate these conclusions, which were derived from only a few tests on a specific clay.

7. Octahedral shear stress-strain relations during drained compression were found common to triaxial and plane strain conditions in terms of τ_{oct}/p vs. γ_{oct}. For the clay tested, the unique stress strain relationship in active compression was valid for all strains until failure in plane strain. In passive compression the uniqueness was restricted to strains which were less than 60% of the failure value in plane strain.

8. For undisturbed Haney clay, it has been shown that the Cambridge stress-strain theory results in large overprediction of strains during drained plane strain shear under conventional passive compression.

9. Although the undrained strength, as characterised by $C_u = (\sigma_1-\sigma_3)_{max}/2$, was larger in plane strain, the octahedral strength was the same for triaxial and plane strain conditions, when $(\tau_{oct})_{max}$ was used for compression and $(\Delta\tau_{oct})_{max}$ used for extension failure.

10. For undisturbed Haney clay, the plane strain compression ϕ' was underestimated by the Mohr-Coulomb failure criterion with respect to both $(\sigma_1-\sigma_3)_{max}$ and $(\sigma_1'/\sigma_3')_{max}$ failure conditions. The observed plane strain compression ϕ' at $(\sigma_1-\sigma_3)_{max}$ was closest to that predicted

by extended von Mises failure criterion, whereas at $(\sigma_1'/\sigma_3')_{max}$, the observed ϕ' was closest to that implied by extended Tresca failure criterion. In extension shear, plane strain ϕ' was underestimated by all three failure criteria. It was concluded that none of the failure criteria, in the present form, can account for failure under all stress paths and stress systems.

Test results on 'heavily' overconsolidated Haney clay led to the following conclusions with regard to the response under different applied stress paths:

1. Undrained compression and extension behaviour was very similar and the axial strain to peak deviator stress in either mode of shear was essentially the same. However, the axial strain to failure in drained shear depended on the applied stress path, as was the case for the normally consolidated clay.

2. Undrained strength in compression was still larger than in extension, but the difference was much smaller than in the normally consolidated clay. An approach towards equal undrained strength in compression and extension seems to be indicated as the overconsolidation ratio (O.C.R.) increases.

3. A very misleading picture of overconsolidated behaviour is obtained if O.C.R. in K_o-consolidated clays is defined as the ratio of maximum to rebounded vertical consolidation stresses. For the clay tested, even though the O.C.R. was between 16 to 19, no dilation occurred during the conventional passive compression drained shear. It is proposed that a more rational definition of O.C.R. for anisotropic consolidation conditions is the ratio of maximum to rebounded mean principal effective stresses. In terms of mean stresses the O.C.R. was between 7 to 8, which suggests that the clay was not very heavily over-consolidated.

4. Mohr's effective stress envelopes for overcon-solidated Haney clay corresponding to compression failure were higher than the extension envelopes. This, along with similar results on normally consolidated clay, suggests that natural clays may be inherently anisotropic in their effective strength parameters.

From the comparison of triaxial and plane strain behaviour of overconsolidated Haney clay, under identical stress paths, the following conclusions were derived:

1. Irrespective of the stress path, the axial strain to peak deviator stress was smaller in plane strain than

under triaxial conditions. A sharp peak was always associated with plane strain compression failure while a similar peak was not present under triaxial conditions. This was also seen in normally consolidated behaviour.

2. Undrained strength was larger in plane strain than triaxial under both compression and extension stress paths. The higher values in plane strain, for the clay tested, were again associated with higher σ_1'/σ_3' and lower pore pressures in plane strain.

3. Mohr's effective stress envelopes for plane strain failure were higher than the corresponding envelopes for triaxial failure. This difference was larger in compression than in extension. Thus, it can be stated that a general confirmation has been obtained of the fact that plane strain effective strength parameters are larger than triaxial for overconsolidated as well as normally consolidated undisturbed Haney clay.

4. Octahedral stress-strain relations and undrained effective stress paths were found common to triaxial and plane strain conditions for the overconsolidated soil also. However, the relationships which were found common to compression of normally consolidated clay were applicable

to extension shear of 'heavily' overconsolidated clay. This is because, compression and not extension stress paths in overconsolidated clay are associated with decreasing τ_{oct}/p and consequent reorientation of principal stresses at failure. Similarly, conclusions regarding extension shear of normally consolidated clay were valid for compression shear of overconsolidated clay.

Octahedral undrained strength was the same for triaxial and plane strain shear with respect to both failure conditions, $(\sigma_1-\sigma_3)_{max}$ and $(\sigma_1'/\sigma_3')_{max}$, when the strength was characterised by τ_{oct} in extension and $\Delta\tau_{oct}$ in compression.

BIBLIOGRAPHY

Armstrong, J.E. (1957) "Surficial Geology of New-Westminster Map - area, British Columbia," Geological Survey of Canada, pp. 57-5.

Baker, W.H. and Krizek, R.J. (1969) "Pore Pressure Equations for Arisotropic Clays," Journal of the Soil Mechanics and Foundation Division, ASCE, Vol. 95, No. SM2, pp. 719-723.

Bishop, A.W. (1964) "Correspondence," Geotechnique, Vol. 14.

Bishop, A.W. (1966) "The Strength of Soils as Engineering Materials," 6th Rakine Lecture, Geotechnique, Vol. 16, pp, 91-128.

Bishop, A.W. and Eldin, A.K. (1953) "The Effect of Stress History on Relation Between ϕ and Porosity in Sand," Proceedings, 3rd International Conference on Soil Mechanics and Foundation Engineering, Zurich, Vol. 1, pp. 100-105.

Bishop, A.W. and Henkel, D.J. (1962) "The Measurement of Soil Properties in the Triaxial Test," Edwin Arnold Ltd., London.

Bjerrum, L. and Kenny, T.C. (1967) "Effect of Structure on Shear Behaviour of Normally Consolidated Quick Clays," Proceedings of the Geotechnical Conference, Oslo, Vol. 2, pp. 19-27.

Bjerrum, L. and Landva, A. (1966) "Direct Simple Shear Tests on a Norwegian Quick Clay," Geotechnique, Vol. 16, pp. 1-20.

Bjerrum, L. and Simons, N.E. (1960) "Comparison of Shear Strength Characteristics of Normally Consolidated Clays," ASCE Research Conference on Shear Strength of Cohesive Soils, Boulder, Colorado, pp. 711-726.

Blight, G.E. (1963) "The Effect of Nonuniform Pore Pressures on Laboratory Measurement of Shear Strength of Soils," ASTM, STP. No. 361, pp. 173-184.

Byrne, P.M. (1966) "Effective Stress Paths in a Sensitive Clay," M.A.Sc. Thesis, U.B.C., Vancouver.

Campanella, R.G. and Vaid, Y.P. (1971) "K_o-Triaxial Apparatus," U.B.C. Soil Mechanics Series No. 15.

Clough, R.W. and Woodward, R.J. (1967) "Analysis of Embankment Stresses and Deformations," Journal of the Soil Mechanics and Foundation Division, ASCE, Vol. 93, No. SM4, pp. 529-549.

Conlon, R.J., Tanner, R.G. and Coldwell, K.L. (1970) "The Geotechnical Design of the Townline Road/Rail Tunnel, Welland, Ontario," Proceedings, 23rd Canadian Geotechnical Conference, Banff, Alberta.

Cornforth, D.H. (1964) "Some Experiments on the Influence of Strain Conditions on the Strength of Sand," Geotechnique, Vol. 14, pp. 143-166.

Crawford, C.B. (1959) "The Influence of Rate of Strain on Effective Stresses in a Sensitive Clay," Papers on Soils, ASTM, STP. No. 254, pp. 36-61.

Dickey, J.W., Ladd, C.C. and Rixner, J.J. (1968) "A Plane Strain Shear Device for Testing Clays," Quoted by Henkel, D.J. in ASCE Speciality Conference on Lateral Stresses in the Ground, Cornel University, 1970.

Duncan, J.M. and Seed, H.B. (1966) "Anisotropy and Stress Reorientation in Clay," Journal of the Soil Mechanics and Foundation Divison, ASCE, Vol. 92, No. SM5, pp. 21-50.

Duncan, J.M. and Seed, H.B. (1966a) "Strength Variation Along Failure Surfaces in Clay," Journal of the Soil Mechanics and Foundation Division, ASCE, Vol. 92, No. SM6, pp. 81-104.

Finn, W.D.L., Wade, N.H. and Lee, K.L. (1967) "Volume Change in Triaxial and Plane Strain Tests," Journal of Soil Mechanics and Foundation Division, ASCE, Vol. 93, No. SM6, pp. 297-308.

Hambly, E.C. and Roscoe, K.H. (1969) "Observations and Predictions of Stresses and Strains During Plane Strain of 'Wet' Clays," Proceedings, 7th International Conference on Soil Mechanics and Foundation Engineering, Mexico City, Vol. 1, pp. 173-181.

Hanson, J.B. and Gibson, R.E. (1949) "Undrained Shear Strength of Anisotropically Consolidated Clays," Geotechnique, Vol. 1, pp. 189-204.

Henkel, D.J. (1960) "The Shear Strength of Saturated Remolded Clays," ASCE Research Conference on Shear Strength of Cohesive Soils, Boulder, Colorado, pp. 533-554.

Henkel, D.J. (1970) "Geotechnical Considerations of Lateral Stresses," ASCE Speciality Conference on Lateral Stresses in the Ground, Cornell University, pp. 1-50.

Henkel, D.J. and Sowa, V.A. (1963) "The Influence of Stress History on Stress Paths in Undrained Triaxial Tests in Clay," Laboratory Shear Testing of Soils, ASTM, STP. No. 361, pp. 280-291.

Henkel, D.J. and Wade, N.H. (1966) "Plane Strain Tests on a Saturated Remolded Clay," Journal of Soil Mechanics and Foundation Division, ASCE, Vol. 92, No. SM6, pp. 67-80.

Hvorslev, M.J. (1960) "Physical Components of the Shear Strength of Saturated Clays," ASCE Research Conference on Shear Strength of Cohesive Soils, Bolder, Colorado, pp. 169-273.

Khera, R.P. and Krizek, R.J. (1967) "Strength Behaviour of Anisotropically Consolidated Remolded Clay," H.R.B. Highway Research Record, No. 190, pp. 8-18.

Ladanyi, B. (1967) "Discussion," Journal of Soil Mechanics and Foundation Division, ASCE, Vol. 93, No. SM5, pp. 322-325.

Ladd, C.C. (1964) "Stress-Strain Modulus of Clay in Undrained Shear," ASCE Conference on Design of Foundations for Control of Settlement, Evanston, Ill., pp. 127-154.

Ladd, C.C. (1965) "Stress-Strain Behaviour of Anistropically Consolidated Clays during Undrained Shear," Proceedings, 6th International Conference on Soil Mechanics and Foundation Engineering, Montreal, Vol. 1, pp. 282-286.

Ladd, C.C. (1967) "Discussion on Session 1," Geotechnical Conference, Oslo, Vol. 2, pp. 112-114.

Ladd, C.C. and Bailey (1964) "Correspondence," Geotechnique, Vol. 14.

Ladd, C.C. and Lambe, T.W. (1963) "The Strength of 'Undisturbed' Clay Determined from Undrained Tests," Laboratory Shear Testing of Soils, ASTM, STP No. 361, pp. 342-371.

Lambe, T.W. (1964) "Methods of Estimating Settlements," ASCE Conference on Design of Foundations for Control of Settlement, Evanston, Ill., pp. 47-70.

Lambe, T.W. (1967) "Stress Path Method," Journal of Soil Mechanics and Foundation Division, ASCE, Vol. 93, No. SM6, pp. 309-332.

Lewin, P.I. and Burland, J.B. (1970) "Stress-Probe Experiments on Saturated Normally Consolidated Clay," Geotechnique, Vol. 20, pp. 38-56.

Lo, K.Y. (1965) "Stability of Slopes in Anisotropic Soils," Journal of Soil Mechanics and Foundation Division, ASCE, Vol. 91, No. SM4, pp. 85-106.

Lo, K.Y. and Milligan, V. (1967) "Shear Strength Properties of two Stratified Clays," Journal of Soil Mechanics and Foundation Division, ASCE, Vol. 93, No. SM1, pp. 1-16.

Mitchell, J.K. (1969) "Discussion on Session 1," Proceedings, 7th International Conference on Soil Mechanics and Foundation Engineering, Mexico City, Vol. 3, pp. 159-168.

Newmark, N.M. (1960) "Failure Hypotheses for Soils," ASCE Research Conference on Shear Strength of Cohesive Soils, Boulder, Colorado, pp. 17-32.

Noorany, I. and Seed, H.B. (1965) "In-Situ Strength Characteristics of Soft Clays," Journal of Soil Mechanics and Foundation Division, ASCE, Vol. 91, No. SM2, pp. 49-80.

Poulos, S.J. (1964) "Control of Leakage in the Triaxial Test," Harvard Soil Mechanics Series No. 71.

Rendulic, L. (1936) "Relation between void ratio and Effective Principal Stresses for a Remolded Silty Clay," Proceedings of 1st International Conference on Soil Mechanics and Foundation Engineering, Cambridge, Mass., Vol. 3, pp. 48-51.

Rendulic, L. (1937) "Ein Grundgesetz der Tonmechanik und sin experimenteller Beweiss," Der Bauingenieur, Vol. 18, pp. 459-467.

Roscoe, K.H. and Burland, J.B. (1968) "On the Generalised Behaviour of 'Wet' Clays," Engineering Plasticity, J. Heyman and F.A. Leckie, ed., Cambridge, pp. 535-609.

Roscoe, K.H. and Poorooshasb, H.B. (1963) "A Theoretical and Experimental Study of Strains in Triaxial Tests on Normally Consolidated Clays," Geotechnique, Vol. 13, pp. 12.

Roscoe, K.H. and Schofield, A.N. (1963) "Mechanical Behaviour of an Idealised 'Wet Clay,'" European Conference on Soil Mechanics and Foundation Engineering, Vol. 1, pp. 47-54.

Roscoe, K.H., Schofield, A.N. and Wroth, P.W. (1958) "On the Yielding of Soils," Geotechnique, Vol. 8, pp. 22-53.

Scott, R.F. (1963) "Principles of Soil Mechanics," Addison Wesley Publishing Co.

Shibata, T. and Karube, D. (1967) "Discussion," Journal of Soil Mechanics and Foundation Division, ASCE, Vol. 93, No. SM5, pp. 325-327.

Simons, N.E. (1960) "The Effect of Overconsolidation on the Shear Strength Characteristics of an Undisturbed Oslo Clay," ASCE Research Conference on Shear Strength of Cohesive Soils, Boulder, Colorado, pp. 747-763.

Simons, N.E. (1963) "The Influence of Stress Path on Triaxial Test Results," Laboratory Shear Testing of Soils, ASTM, STP. No. 361, pp. 270-278.

Smith, R. E. and Wahls, H. E. (1969) "Consolidation Under Constant Rates of Strain," Journal of Soil Mechanics and Foundation Division, ASCE, Vol. 95, No. SM2, pp. 519-540.

Skempton, A.W. (1954) "The Pore Pressure Coefficients A and B," Geotechnique, Vol. 4, pp. 143-147.

Skempton, A.W. and Sowa, V.A. (1963) "The Behaviour of Saturated Clays During Sampling and Testing," Geotechnique, Vol. 13, pp. 269-290.

Vaid, Y.P. (1968) "A Plane Strain Apparatus for Soils," M.A.Sc. Thesis, U.B.C., Vancouver.

Ward, W.H. (1956) "Discussion," Proceedings of the 4th International Conference on Soil Mechanics and Foundation Engineering, London, Vol. 3, pp. 123-124.

Ward, W.H., Samuels, S.G., and Butler, M.E. (1959) "Further Studies of the Properties of London Clay," Geotechnique, Vol. 9, pp. 33-58.

Whitman, R.V., Ladd, C.C. and Cruz, P. da (1960) "Discussion on Session 3," ASCE Research Conference on Shear Strength of Cohesive Soils, Boulder, Colorado, pp. 1049-1056.

APPENDIX A

FRICTION CORRECTION TO MEASURED AXIAL STRESS IN PLANE STRAIN TESTS

Referring to Fig. A-1, let at any stage of the test

F_t = The measured axial force on the loading cap.

F_b = The measured axial force transmitted to the sample bottom.

L,B,H = Respectively the length, width and height of the sample.

h = Height of the loading cap surface (shown shaded in Fig. A-1) in contact with lateral pressure diaphrams.

σ_x = Stress in lateral pressure diaphrams.

σ_y = Stress on rigid end plates.

Then the total normal force, N, contributing to friction

$$N = 2\{L(H+h)\sigma_x + B.H.\ \sigma_y\}$$

Total friction force

$$F_f = F_t - F_b$$

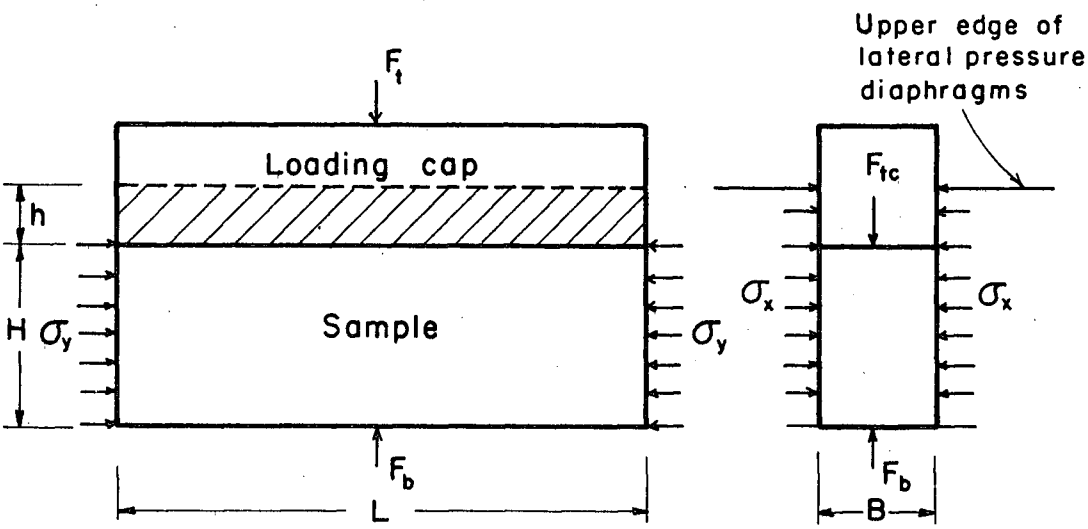

Fig. A-1 — NORMAL STRESSES BETWEEN VERTICAL SURFACES ON WHICH FRICTION ACTS.

Hence, an average coefficient of friction

$$\mu_a = F_f/N$$

Now the frictional force, F_c, acting on the vertical surface of the loading cap

$$F_c = \mu_a \cdot 2 \cdot L \cdot H \cdot \sigma_x$$

Therefore, the axial force, F_{tc}, actually transmitted to the sample top

$$F_{tc} = F_t - F_c$$

The average vertical force, F_a, on the sample was then taken as the mean of F_{tc} and F_b, i.e.,

$$F_a = 1/2\left(F_b + F_{tc}\right)$$

If the area of the sample was A then the vertical stress, σ_z, corrected for side friction effect was

$$\sigma_z = \frac{F_a}{A}$$